uOttawa

L'Université canadienne
Canada's university

FACULTÉ DES ÉTUDES SUPÉRIEURES ET POSTOCTORALES

uOttawa

L'Université canadienne
Canada's university

FACULTY OF GRADUATE AND POSDOCTORAL STUDIES

Patrick Brisson

AUTEUR DE LA THÈSE / AUTHOR OF THESIS

M.A.Sc. (Civil Engineering)

GRADE / DEGREE

Department of Civil Engineering

FACULTÉ, ÉCOLE, DÉPARTEMENT / FACULTY, SCHOOL, DEPARTMENT

Unsaturated Flow in Tailings

TITRE DE LA THÈSE / TITLE OF THESIS

Dr. Sai Vanapalli

DIRECTEUR (DIRECTRICE) DE LA THÈSE / THESIS SUPERVISOR

Dr. Vinod Garga

CO-DIRECTEUR (CO-DIRECTRICE) DE LA THÈSE / THESIS CO-SUPERVISOR

EXAMINATEURS (EXAMINATRICES) DE LA THÈSE / THESIS EXAMINERS

Dr. Paul Simms

Dr. Mamadou Fall

Dr. I. Nistor

Gary W. Slater

Le Doyen de la Faculté des études supérieures et postdoctorales / Dean of the Faculty of Graduate and Postdoctoral Studies

# UNSATURATED FLOW IN TAILINGS

by

Patrick Brisson

A thesis

submitted under the supervision of

Dr. Vinod K. Garga

Dr. Sai K. Vanapalli

in partial fulfillment of the

requirements for the degree of

Master of Applied Science

in

Civil Engineering

Department of Civil Engineering

University of Ottawa

Ottawa, Canada

K1N 6N5

April, 2006

*Your file Votre référence*
*ISBN: 978-0-494-18402-8*
*Our file Notre référence*
*ISBN: 978-0-494-18402-8*

**ACKNOWLEDGEMENT**

First and foremost, I would like to thank both of my thesis supervisors, Dr. Vinod Garga and Dr. Sai Vanapalli, for their ongoing support and guidance throughout this research program.

I would also, like to thank John, Istemi, Kenton, Cevat and Jules for pointing out mistakes, or highlighting the lighter side of things whenever an occasion presented itself, or even when it didn't. Also, many thanks are directed to Mr. Richard "Dick" Moore and Mr. Brent Cotter, since their abilities and contributions made the laboratory work possible.

Finally, I could not have accomplished the work described in this document without relentless support and encouragement from my family… merci Mom, Dad et Dani!

## SUMMARY

The work presented in this document is two-fold. The major part of the work described herein, involved designing and building an apparatus to determine the unsaturated coefficient of permeability of mine tailings in a laboratory environment. The Modified Permeameter was built based on a permeameter used by Meerdink et al (1996) which was used with compacted clay samples.

The modifications include using a large size sample; the ability to accommodate mobile sensors to alleviate the problems associated with the formation of water pockets and to use the same test specimen and determine the SWCC and unsaturated coefficient of permeability of the tailings over a large range of saturation.

Mobility of the sensors was achieved with a system of counterweights, which also retained the water-tightness of the apparatus. Although Time Domain Reflectometry (TDR) sensors did not yield any results during this research program, the Modified Permeameter includes counterweight system to provide mobility for three TDR probes to measure volumetric water content. During the experimental work, water content was measured with sampling tools developed and built for use in the Modified Permeameter. Negative pore water pressures were measured with tensiometers.

Two gradations of tailings were tested with the Modified Permeameter. The two gradations were the overflow (fine) and the underflow (coarse) samples. Prior to laboratory experimentation with the tailings, numerical predictions of soil-water characteristic curves (SWCC) and conductivity curves were computed. These predictions were obtained using the SoilVision software package.

The predicted curves were compared with the laboratory values. The estimated SWCC for both tailings gradations and the laboratory results show good agreement. In regards to the conductivity curves, insufficient laboratory data was gathered to compute the

unsaturated coefficient of permeability of the coarse underflow sample. The laboratory results for the overflow sample show important scatter around the predicted conductivity curve.

Due to the differences observed between the laboratory results and the predicted conductivity curve, the numerical modeling portion of this research, which constitutes the second portion of this research, was conducted using typical permeability values.

The modeling portion consisted of producing a generic model of an upstream tailings dam on which individual factors were analysed. The factors considered were as follows:

- Effect of beach length;
- Effect of pervious foundation;
- Effect of blanket drain;
- Effect of segregation along the beach;
- Effect of anisotropy;
- Combined effect of segregation along the beach and blanket drain.

The numerical analysis showed that maintaining a good beach length throughout the construction period of the upstream dam helps to prevent saturation of the fine tailings underlying the shell. The addition of a blanket drain to a good beach length provided the desired effect, which was to lower the phreatic surface away from the fines closest to the dam's shell.

## TABLE OF CONTENTS

**CHAPTER 4 – DETAILS OF THE MODIFIED PERMEAMETER**

## CHAPTER 5 – LABORATORY PROGRAM AND RESULTS



## CHAPTER 6 – MODELING FLOW THROUGH TAILINGS DAMS

## LIST OF TABLES

## LIST OF FIGURES

# CHAPTER 1 - INTRODUCTION

## 1.1 PROBLEM STATEMENT

Tailings dams are typically constructed according to one of three main construction methods. They are the downstream construction method, the centreline construction method, and the upstream construction method. Of the three methods, upstream tailings dams are believed to be more susceptible to liquefaction failures because of the presence of large quantities of loose, saturated material underlying the structural component of the dam. More failures are commonly reported in tailings dam that are constructed using the upstream method of construction than in the other methods of construction. Although high risks are associated with the upstream dams, they are still commonly used by mining companies due to their lower construction cost.

The history of the (upstream) method of dam construction, as reported by Klohn (1979) is plagued with failures, some of them catastrophic. The majority of failures that occur in the upstream tailings dam are due to factors such as high phreatic line, piping, and liquefaction. In a study of six different seismic events, Conlin (1987) reported that many active tailings impoundments suffered no major damage or no damage at all. Furthermore, the study showed that the inactive impoundments with lower phreatic levels had suffered little or insignificant damage. This study also shows that the location of the phreatic level and its movements in both tailings dams and impoundments is critical to the longevity of the structure. Other studies by Vick (1983) show that the seepage conditions within the embankment exert a controlling influence on tailings dam or impoundment stability.

It is therefore of interest and value to evaluate the location of the phreatic surface and the seepage conditions in tailings dams constructed using the upstream construction method.

## 1.2 OBJECTIVE

The coefficient of permeability, $k$, is one of the key design parameters in tailings dams. The coefficient of permeability is required to assess pore water pressures, phreatic

surface fluctuations, and discharge quantities. Typically, the saturated coefficient of permeability in tailings can vary by three to six orders of magnitude. Under unsaturated conditions, the range is greatly increased.

Current laboratory and field methods used to determine the unsaturated coefficient of permeability require elaborate testing equipment and are time consuming and costly.

The objective of this research program was two-fold:

- To design and build a simple and versatile laboratory apparatus to determine the unsaturated coefficient of permeability of tailings.
- To demonstrate the "advantage" of maintaining a long beach length in tailings dams by using the laboratory results in a finite element type software.

## 1.3 SCOPE OF WORK

The saturated coefficient of permeability can be reliably determined using conventional testing procedures. On the other hand, it is a challenging exercise to determine the variation of the coefficient of permeability with respect to suction. In order to determine the unsaturated coefficient of permeability of tailings over a large suction range, a Modified Permeameter is designed as a part of the present research study. The equipment is an improvement over the original design proposed by Hamilton et al. (1979) that uses the Instantaneous Profile Method (IPM) to determine the coefficient of permeability. The designed apparatus is capable of simultaneously measuring the suction and water content at different locations along the length of large size specimen. The unsaturated coefficient of permeability is determined from water content and pore water pressure measurements taken during the drainage of the sample.

The study presented in this thesis focuses on understanding the flow behaviour in tailings dams constructed using the upstream construction method. Particular emphasis is placed on evaluating fluctuations of the phreatic surface due to such physical constraints as:

(i) The influence of increasing the tailings beach length,

(ii) The influence of man-made drainage conditions.

It is conventionally believed that by increasing the length of the tailings beach, the phreatic level in the dam is lowered, which makes the dam less susceptible to liquefaction failure. Various scenarios in which the phreatic level can be lowered are simulated using SEEP/W from Geo-Slope International Ltd.

The seepage analysis is performed on a given cross-section of a dam, and as such the model must be fitted with the correct properties for each of the different components of the evaluated cross-section. To complete an analysis, the SEEP/W model requires the "conductivity curve" of various soil types used in the tailings dam construction. The "conductivity curve" is the relationship between the coefficient of permeability and the suction measured in the soil.

## 1.4 ORGANIZATION

This thesis is divided into seven chapters to present all the aspects of this research program. Chapters 2 and 3 provide details of the basic properties of tailings dams, the laboratory methods used in determining unsaturated coefficients of permeability. Chapter 4 presents the design details of the modified permeameter developed during this research. The laboratory results are then presented in Chapter 5. Chapter 6 presents the finite element analyses and Chapter 7 presents the conclusions ensuing from this research.

Appendix A includes all the shop drawings for the various pieces of equipment built throughout this research program.

# CHAPTER 2 – TAILINGS DAMS: A BRIEF BACKGROUND OF THE CONSTRUCTION METHODS

## 2.1 INTRODUCTION

The generic term "tailings" is used to describe the crushed rock and water discarded at the end of the mining process. The disposal of tailings is commonly identified as the most important negative environmental impact due to mining activities. Several concerns have been raised with respect to the methods used in the disposal of massive quantities of tailings. For example, a mine operation described as small, typically discards 3,000 tonnes of dry tailings with 4,500 tonnes of water. A large mine may discard 60,000 tonnes of dry tailings with 90,000 tonnes of water per day (Robinsky 1999).

Tailings are disposed either mechanically, by means of conveyor belts or trucks, or hydraulically through pipelines. When disposed mechanically, the tailings are dry and can be placed and compacted into large heaps or reintroduced in the mining pit. However, the mechanical method is not always feasible especially in the case where a contaminated fluid is produced during processing, or if long distances separate the processing plant and the disposal area. In most cases, hydraulic disposal of tailings is seen as the preferred method. A disposal area is created by enclosing the tailings slurry by means of a tailings dam. The focus of this research was placed on hydraulically deposited tailings.

Vick (1983) defined the tailings dam as surface impoundment structures most commonly consisting of raised embankments, where the construction of the embankment is staged over the life of the impoundment. In the past, tailings dams were seen as simple embankments and no engineering principles were used either in designing or constructing them. Massive failures of such tailings dams as El Cobre, Buffalo Creek, and Aberfan brought forward public awareness and governmental legislation (Morgenstern 1985, Conlin 1987, Krause 1997).

## 2.2 TYPES OF TAILINGS DAMS

Three basic types of dams are constructed to create tailings reservoirs. The dams are classified based on the construction method employed in elevating the crest. The dam crest can be raised in an upstream, downstream or centreline fashion. Some details of tailings deposition are presented prior to providing information about the various construction techniques and their respective advantages and disadvantages.

## 2.3 TAILINGS DEPOSITION

Two different methods of tailings deposition are used to accommodate the different dam configurations and various tailings properties. The first method is the simplest form of deposition and is done by using a single discharge line. In this case, the tailings produced at the mill are discharged at a single location. When the beach at the point of discharge has built up to the desired height, the pipe is moved along the crest of the dam in such a manner to build up the beach parallel to the crest. This discharge method requires more effort from the mine operators since the discharge line is required to be moved periodically.

The second method is called "spigotting". In this method, a single pipe with multiple discharge points is laid along the crest of the dam. Spigots can be used with or without cyclones. The cyclones are simple devices that function on a centrifugal separation principle to separate the coarse and fine material from the slurry produced at the mill (Vick 1983).

The cyclone (Figure 2.1), receives the discharge of the mill, or feed, at entry point (A). From there, the tailings spiral up or down according to their weight. Essentially, the larger, heavier particles fall out to the bottom (B) of the cyclone, and the finer particles are pushed upwards as slime through the upper discharge point (C). The name underflow and overflow are given to the material falling out and being pushed up respectively. The material that is produced by the mill is consistent, with known gradation, unit weight, shear strength, and saturated coefficient of permeability. The coarse fraction (the

underflow) can be used in the structural portion of the dam since the physical properties and characteristics are often similar to those of angular fine to medium sands.

There are typically four components to a tailings dam. Figure 2.2 shows a generic profile of both an upstream and a downstream dam configuration, with the four components. The structural shell (1) is constructed with the coarser size material and is elevated throughout the lifespan of the mine. The slurry is discharged from the crest of the dam. As the slurry travels down the inner slope of the reservoir, segregation occurs. The larger, heavier particles within the slurry fall out of the slurry sooner than the smaller and lighter particles. The inner slope of the reservoir, where segregation occurs, is called the beach (2). The portion of the tailings dam labelled (3) is composed of fine material, known as the slimes. These slimes remain saturated and are in an underconsolidated state for long periods of time. The decant pond (4) is the fourth component of a tailings dam. The pond is the accumulation of the process water from which the suspended solids have fallen out.

## 2.4 TAILINGS CHARACTERISTICS

The slurry material transported in the pipelines is composed of crushed rock and water. The solids represent anywhere from 15 to 55 percent of the slurry (Vick 1983). Tailings are difficult to describe under general terms since they are site specific and vary according to the different ore extraction methods. However, as a general rule, tailings particles are angular and can exhibit higher shear strength than comparatively sized naturally occurring materials. Also, some tailings may show an increase in shear strength over time due to cementation of particles (Troncosco 1988, 1990).

## 2.5 UPSTREAM CONSTRUCTION

Upstream dams have been built around the world since the beginning of the 20$^{th}$ century (Martin and McRoberts 1999). As the name implies, the crest of the dam moves upstream into the reservoir as the dam is raised. They remain the most common type of tailings dam construction technique due to its lower cost compared to other construction techniques (Davies and Martin, 2000).

Martin and McRoberts (1999) suggest that there are no fundamental flaws associated with upstream tailings dams as long as the design and operating fundamentals are addressed. There are several investigators who favour upstream construction method to other methods (Klohn 1979; Vick 1983; Krause 1997; Szymanski 1999; and Davies and Martin 2000).

Several key design and operating fundamentals are found in literature for the upstream tailings dams. For example, Davies and Martin (2000) present a set of rules for appropriate dam design, construction, and stewardship. Other sources of guidelines include Klohn (1979), Vick (1983), and Martin and McRoberts (1999).

The need for a wide beach between the pond and the dam is well established as one of the key requirements for a good design. According to the USEPA (1994), the single most important criteria for the application of the upstream construction method are related to the tailings beach, which must form a competent foundation for the support of the next dike. The beach forms a crucial part of the tailings dam and in certain cases, failures have been attributed to its poor quality (Lighthall, et al. 2002). A large number of failures of upstream embankments can be attributed to inadequate separation distance between the pond and the embankment crest (Vick 1983). Improper beach sizing or pond management can result in encroachment of the beach, which can lead to unsafe conditions such as insufficient freeboard, and high pore water pressures.

The decant pond has to be designed to accept precipitation and runoff from surrounding areas. As well, the rate at which the dam is raised has to be slow enough to allow dissipation of excess pore water pressures. Also, a good underdrainage layer must be provided to lower the pore water pressure or increase the distance between the phreatic surface and the structural shell. This drainage layer could be naturally occurring or a man-made layer should be provided to allow good drainage.

A wide beach, slow rate of rise with respect to construction, and proper underdrainage will contribute to minimise water outflow at the dam face and reduce the probability of failure of the upstream dam.

Apart from its high susceptibility to liquefaction, the upstream type dam also has one important disadvantage in that pond water location is the only main factor influencing the phreatic surface that can be controlled during operation (Vick 1983). However, there is evidence to demonstrate that damages associated with seismic loading are minimal if the upstream dams are properly constructed (Vick 1983, Conlin 1987, and Martin and McRoberts 1999).

The upstream method of construction remains a popular construction method as it requires only limited quantity of material to raise the crest. The upstream dam is typically raised into the reservoir in such a way that the dam's footprint does not progress downstream using up more land. Another reason for the wide adoption of this type of dam in spite of its failure potential lies in its ease of construction. In fact, once the starter dam is complete, mining personnel only have to relocate the discharge line at given time intervals to elevate the crest of the dam. If all design factors are taken as equal and the choice of construction method relies solely on the cost of raising the embankment. The upstream dam is likely to be chosen more often since it requires less material.

## 2.6 DOWNSTREAM CONSTRUCTION

The downstream method of construction sees the crest of the dam move downstream, away from the reservoir as the dam is raised. This construction method is believed to be safer than the upstream method since this method uses a sound, engineered foundation upon which the crest is raised. In this type of construction sequence, each lift is constructed with material placed and compacted with heavy equipment unlike the upstream dam where the underlying layer is neither placed nor compacted. The downstream method almost entirely eliminates the possibility of seismically induced liquefaction of the structural shell material, upon the proper design and construction of the dam (Davies and Martin 2000; Davies et al. 2000).

The main disadvantage of the downstream construction when compared to other types of tailings dams lies in the amount of material required to raise the crest. Figure 2.3 shows an idealized cross-section of the three types of tailings dams discussed in this research. Figure 2.3(b) shows that for an equivalent increase in crest elevation, the downstream method of construction requires three times as much fill as the upstream construction. This implies that more labour and equipment is required on site to place and compact the extra material.

## 2.7 CENTRELINE CONSTRUCTION

The centreline method of construction incorporates features of both the upstream and downstream construction methods. In the centreline method, the newly added section has a portion of its foundation consisting of loose slimes, and the other portion made of compacted sand. Unlike the upstream dam, the centreline technique is not as susceptible to damage if the pond water encroaches the beach since drainage is usually provided in the design. The centreline type dam is less likely than the upstream method to suffer liquefaction damage. However, this construction method will require more fill than the upstream method to elevate the crest. Figure 2.3(c) shows that the centreline method requires one-third less material than the downstream method but twice as much as the upstream dam.

In spite of many features that may enhance the safety of the dam, the centreline and downstream methods are not always the preferred choices, due to either economics or material and production requirements. It is for these reasons that upstream tailings dams, although generally seen as risky or unsafe when compared to other types of tailings dams, are still commonly used.

## 2.8 TAILINGS DAMS FAILURES

Several failures over the last decade have outlined the importance of designing and constructing tailings dams using engineering principles, knowledge and practical experience. Table 2.1 lists some of the key recorded failures involving tailings dams over

the last 10 years. Table 2.1 shows failures regardless of the type of construction technique, type of ore mined, failure mechanism and activity of the mine.

Davies and Martin (2000) reported that two-thirds of the failures in dams were observed in dams that were constructed using upstream methods (Figure 2.4). These numbers are to some extent biased considering that the majority of tailings dams built during the early periods of mining were of the upstream type. It should also be noted that in this early period of mining, tailings dams were constructed based on empirical procedures and limited experience. Davies and Martin (2000) also reported that an estimated 3,500 tailings dams exist worldwide. Of these, approximately half are constructed using the upstream method.

## 2.9 UNSATURATED PROPERTIES OF TAILINGS AND TAILINGS DAMS

Figure 2.5 shows the main failure modes associated with the upstream tailings dams. It can be seen that over two thirds of reported failures are due to seismic, slope and seepage failures. The common trait with these failure modes lies in the saturation levels of the beach and shell as well as the location of the decant pond. Yoshimi *et al.* (1989) laboratory studies showed that liquefaction was induced in material with degrees of saturation levels as low as 80%. With so many failures attributed to the position of water in the tailings reservoir, designers have to understand the flow behaviour to determine critical information such as pore water pressure and effective shear strength.

There is a general consensus among researchers that an unsaturated condition of the tailings beach provides many advantages for the dam. However, there is only limited data available for designers to clearly understand the influence of unsaturated conditions. To undertake modeling exercises, the unsaturated properties of tailings are required. For example, two soils with different gradations may have similar coefficients of permeability under fully saturated conditions, but may differ considerably under unsaturated conditions (i.e., with different negative pore pressures or suction values). In other words, the storage characteristics and hence the engineering behaviour of tailings can significantly differ under unsaturated conditions. Modelling water flow under both

the saturated and unsaturated conditions remains difficult even with the numerous codes available for that purpose. Martin (1999) provided good insight in the problem when he suggested that predicting and modelling of unsaturated flow is complex, since the simple range of parameters alone can significantly influence the flow behaviour in saturated and unsaturated soils.

## 2.10 SUMMARY

Modern designers and practitioners continue building tailings dams using the upstream construction method since it has significant economic advantages in comparison to other methods. However, there is some concern with the upstream construction method since a large number of reported failures are associated with this method of construction.

Several investigators state that tailings dams failures have for the most part been the result of human errors (Davies and Martin 2000, Fourie et al. 2001, Martin and McRoberts 1999). However, if standards or guidelines are developed to better understand the grey area with respect to design, construction and maintenance measures, the upstream dam construction technique can be considered to be a safe alternative. To provide practitioners with guidelines or standards, research on the saturated and unsaturated movement of water within the tailings dams and reservoirs is required. The importance of a firm minimal distance separating the decant pond and the crest of the dam should be among these standards as opposed to being only recognised as an important consideration when evaluating a tailings dam design.

| Date | Location | Type of Incident | Release |
|---|---|---|---|
| 03/10/2003 | Chile | tailings dam failure | 50,000 tonnes of copper tailings |
| 27/09/2002 | San Marcelino, Philippines | overflow and spillway failure of two abandoned tailings dams after heavy rain | unavailable |
| 22/06/2001 | Minas Gerais, Brazil | mine waste dam failure | unavailable |
| 08/09/2000 | Gällivare, Sweden | tailings dam failure from insufficient perviousness of filter drain | 2.5 million $m^3$ of liquid, subsequent release of 1.5 milllion $m^3$ of water with slurry |
| 26/04/1999 | Placer, Philippines | tailings spill from a damaged concrete pipe | 700,000 tonnes of cyanide tailings |
| 31/12/1998 | Huelva, Spain | dam failure during storm | 50,000 $m^3$ of acid and toxic water |
| 22/10/1997 | Printo Valley, USA | tailings dam slope failure | 230,000 $m^3$ of tailings and mine rock |
| 12/11/1996 | Nazca, Peru | liquefaction of upstream dam during earthquake | >300,000 $m^3$ of tailings |
| 19/08/1995 | Omai, Gyana | tailings dam failure | 4.2 million $m^3$ of cyanide slurry |
| 22/02/1994 | Merriespruit, South Africa | dam wall breach following heavy rain | 600,000 $m^3$ |

**Table 2.1: Recorded Tailings Dam Failures (source: WISE 2002)**

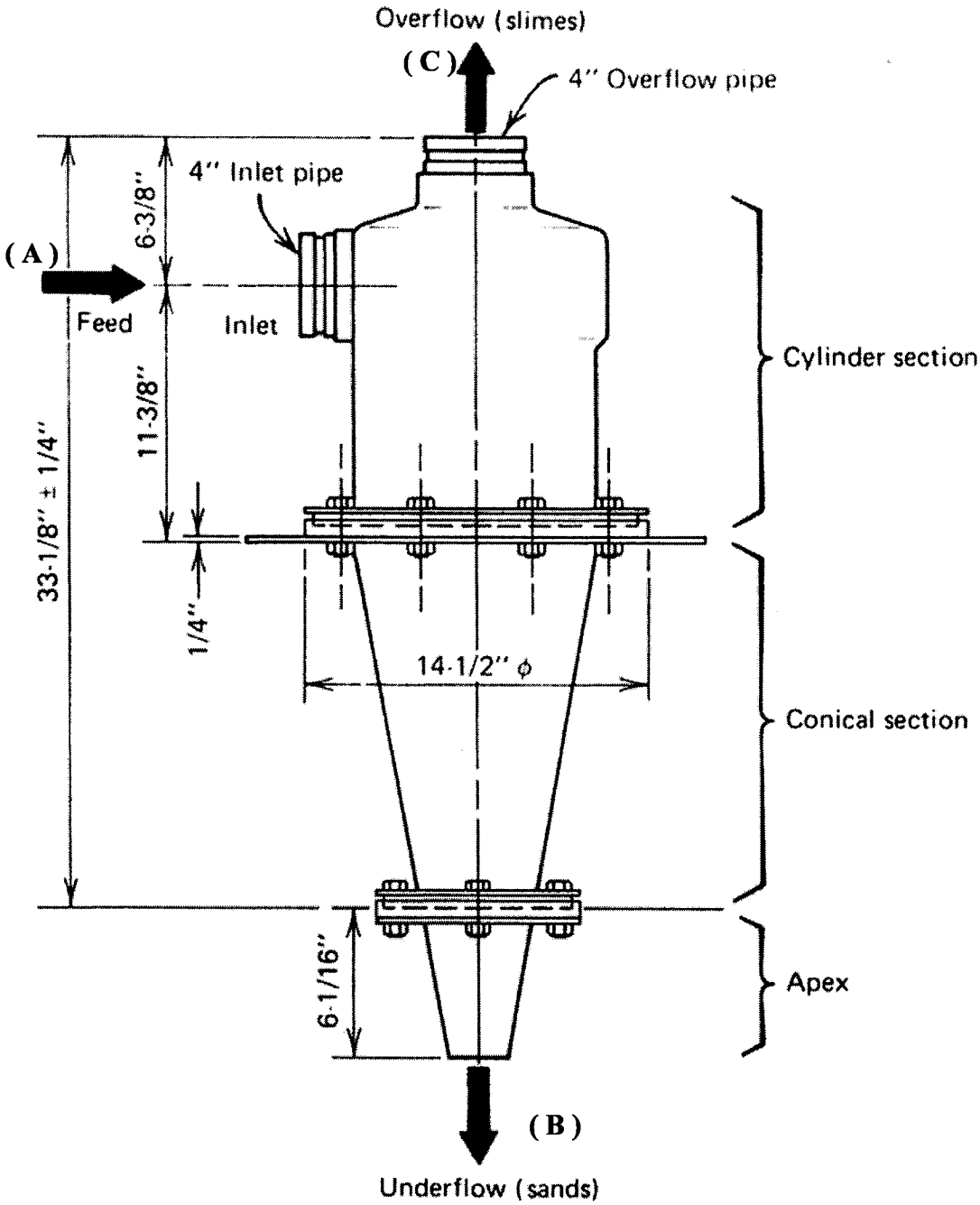


**Figure 2.1: Cyclone (after Vick 1983)**

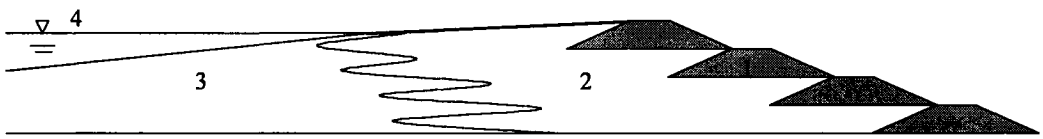


(a) Upstream

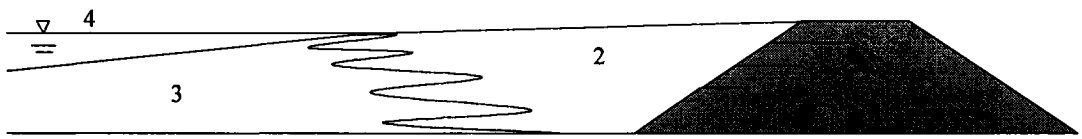


(b) Downstream

**Figure 2.2: Components of tailings dams (after Vick, 1983)**

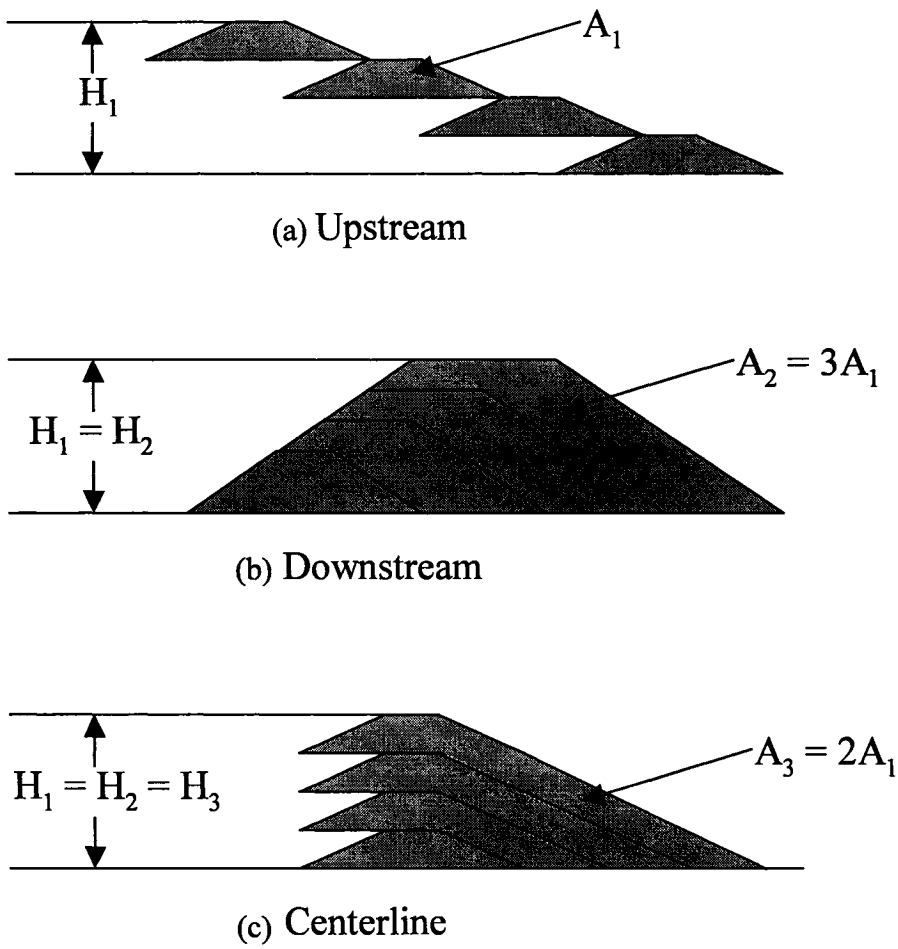


**Figure 2.3: Types of Tailings Dams with Fill Volumes Comparison (after Vick 1983)**

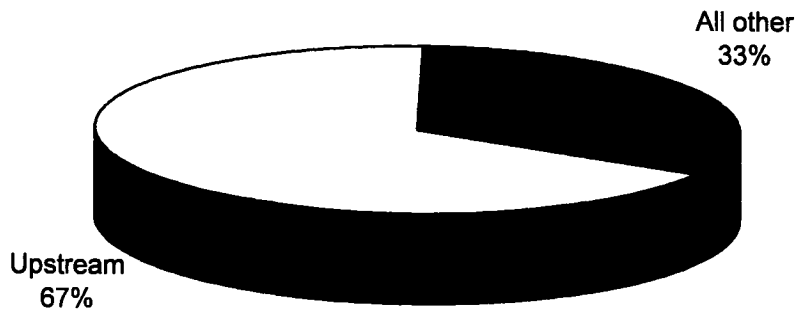


**Figure 2.4: Failure of tailings dams by construction type (Davies and Martin 2000)**

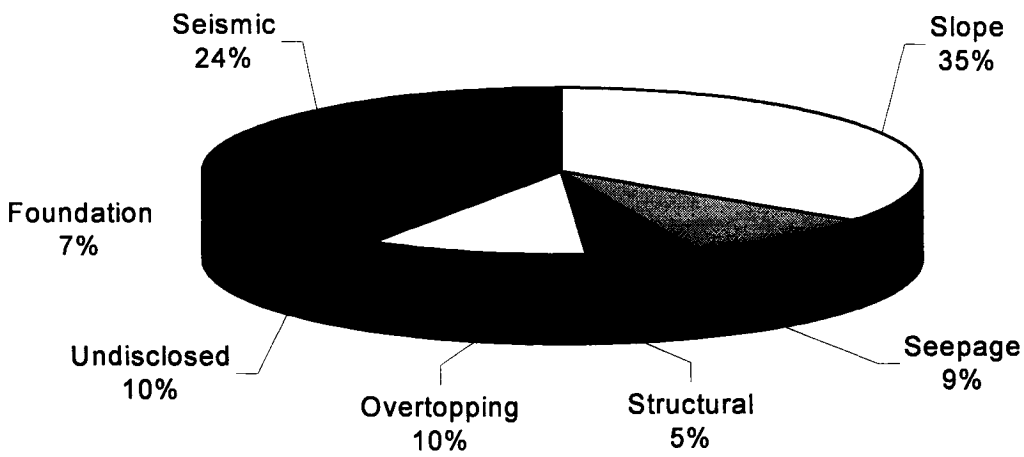


**Figure 2.5: Main failure modes for upstream tailings dams (op. cit.)**

# CHAPTER 3 – LABORATORY METHODS

## 3.1 INTRODUCTION

Several experimental methods are available to determine the flow behaviour in unsaturated soils and tailings. However, the unsaturated flow conditions are commonly predicted and not measured. This has become conventional engineering practice since the direct measurements of unsaturated flow properties require elaborate equipment and qualified personnel, which prove to be time consuming and expensive. Several researchers have proposed simplifications in the prediction of unsaturated flow behaviour of soils and tailings based on conventional soil properties such as grain size distribution, and index properties of soils (Gupta and Larson 1979; Aubertin et al. 1998; Fredlund et al. 1997; Vanapalli and Lobbezoo 2002).

The unsaturated coefficient of permeability, $k_{unsat}$, and the Soil-Water Characteristic Curve (SWCC) are used to predict the flow behaviour in most prediction methods found in literature. Several investigators have shown that the predicted values provide reasonably good comparisons between the measured and predicted values of the unsaturated coefficient of permeability, $k_{unsat}$. These comparisons have been mainly provided between the predicted results and the laboratory test data determined on small size specimens. Conventionally, small size specimens are used in laboratory testing for determining engineering properties of unsaturated soils mainly to reduce the testing time. Several factors such as the density, soil structure, compaction water content, stress state, mineralogy, and hysteresis influence the SWCC behaviour (Vanapalli et al. 1999, Zapata et al. 2000). The parameters that influence the SWCC behaviour also influence the flow behaviour in unsaturated conditions.

A number of studies have shown significant differences between the predicted and field measured unsaturated flow behaviour (Meerdink et al. 1996; Amraoui et al. 1998; Holland et al. 2000). The differences between the predicted and measured flow behaviour can be attributed to the influence of various parameters that govern the unsaturated flow behaviour. One of the key parameters may be associated with the non-

representative size of the specimen used in the laboratory to measure the SWCC, which in turn is used to predict the field behaviour.

Research suggests that the macro and micro features of an *in-situ* soil must be adequately represented in laboratory specimens for proper assessment of the flow behaviour in soils. Various investigators have demonstrated that the field flow properties in saturated conditions can vary by several orders of magnitude in comparison to laboratory test specimens, which are typically smaller (Daniel 1984; Elsbury et al. 1990). Other investigators recommend using large size specimens in the laboratory for determining the flow properties to represent the field flow behaviour (Elsbury et al. 1990; Benson et al. 1994). While these investigations are related to the flow behaviour in saturated soils, they should also be valid for the interpretation or prediction of unsaturated flow behaviour of both soils and tailings. Many researchers recommend relying on field measurements rather than laboratory measurements due mostly to the inaccurate representation of the flow behaviour when using smaller laboratory specimens (Benson and Gribb 1997; Houston and Houston 1995; Fredlund and Rahardjo 1993).

Preliminary investigations have shown that there are significant differences between the measured and predicted flow behaviour of tailings using the presently available empirical methods. Due to this reason, more studies are necessary towards development of experimental techniques using large tailings specimens to better understand the influence of numerous parameters that govern the flow behaviour of tailings. The experimental methods presently used to determine the unsaturated coefficient of permeability, and/or the SWCC are briefly summarized in this chapter.

## 3.2 LABORATOY METHODS

The unsaturated coefficient of permeability can be measured in the laboratory under either steady state or transient state conditions. Under steady state conditions, the unsaturated coefficient of permeability is determined by applying a fixed flux at one end of the sample until equilibrium is reached, at which point, physical measurements are taken on the sample. The coefficient of permeability is then computed from the collected

data. Under transient state, the water or air flux is varied during testing to produce different suctions or water content profiles.

### 3.2.1 Traditional steady state method

A constant head of water is maintained in this method with either a vertically or horizontally positioned sample. Figure 3.1 shows a schematic of the apparatus from Klute and Dirksen, 1986. The approach is to provide a one-dimensional measurable flow of water to the specimen (Klute, 1972). The specimen is also subjected to a constant air supply to create a measurable suction. Once steady state conditions are reached, the gradient is measured, and a sample is retrieved from the specimen for water content measurement. A series of tests have to be performed to obtain the variation of the coefficient of permeability with suction. This method is time consuming since numerous tests have to be performed in order to collect SWCC data.

### 3.2.2 Centrifuge method

The Centrifuge method is similar to the traditional steady state method. The main difference is that the flow of water is accelerated with the use of a commercial centrifuge. This is advantageous when testing soils with low coefficient of permeability since testing time is greatly reduced (Nimmo et al., 1992). The soil is kept unsaturated through the test sequence by applying a constant head over the sample. Figure 3.2 shows a sample container used for centrifuge testing from Nimmo et al. (1992). To compute the unsaturated coefficient of permeability, the distance travelled by the sample and its angular velocity are measured, and Darcy's Equation takes the form of Equation 3.1.

$$q_{s,\psi} = -K_{\psi}\left(\frac{d\psi}{dr} - \rho_w \omega^2 r\right)A \qquad (3.1)$$

where:

$q_{s,\psi}$ is the steady state volumetric water flux at applied water suction ($\psi$)

$r$ is the radial distance

$\omega$ is the angular velocity

$\rho_w$ is the density of water

$K_\psi$ is the unsaturated coefficient of permeability for the applied suction ($\psi$)

Dismantling of the supports and container to reach the sample complicate measuring the water content. Once the container and porous plates have been removed from the centrifuge, the components have to be individually weighed to obtain the gravimetric water content of the sample. Suction in the sample is controlled by the choice of porous ceramic plates, and the pressure head applied to them. Other than the high cost associated with a commercial centrifuge, the material tested has to be sufficiently dense to be able to resist the high stresses induced by the centrifuge.

### 3.2.3 Bruce-Klute absorption method

This unsteady state method as described by Benson and Gribb (1997) is based on the diffusivity ($D_\theta$) and its relation to the coefficient of permeability as given by Equation 3.2:

$$D_\theta = k_\psi \left( \frac{d\theta}{d\psi} \right) \tag{3.2}$$

The diffusivity ($D_\theta$) is computed using Equation 3.3 once water content measurements have been taken along the long, thin cylindrical sample:

$$D_\theta = -\frac{1}{2} \frac{d\lambda_\theta}{d\theta} \int_{\theta_n}^{\theta_s} \lambda_\theta d\theta \tag{3.3}$$

where:

$\lambda_\theta$ is a parameter relating distance and time

$\theta_s$ is the saturated water content

$\theta_n$ is the initial water content

The coefficient of permeability of the unsaturated soil sample is calculated using Equation 3.2, after determining the diffusivity from Equation 3.3. The Bruce-Klute absorption method is performed horizontally and necessitates that the SWCC be obtained from and independent sample. Figure 3.3 shows the apparatus used to perform the Bruce-Klute absorption test. The small sections of glass containing the soil sample have to be dismantled and weighed to determine the gravimetric water content of the sample under different suction values.

### 3.2.4 Sorptivity method

The Sorptivity method, described by Benson and Gribb (1997), involves measuring the diffusity as well as the sorptivity and subsequently, the coefficient of permeability can be determined from Equation 3.2. Similarly to the Bruce-Klute method, the sorptivity method also requires determination of the SWCC using a different sample.

For the Sorptivity method, a cylindrical specimen with a known water content is prepared. The infiltration rate in the specimen can be determined using a pre-programmed pump to deliver a time dependant flow. The infiltration rate ($I$) can then be used to find the sorptivity of the material. Subsequently, the sorptivity is used to determine the diffusity. The coefficient of permeability is then determined from the relationship shown in Equation 3.2. The sorptivity ($S_\theta$) is given by:

$$S_\theta = \frac{I}{\sqrt{t}} \tag{3.4}$$

Sorptivity is then used in Equation 3.5 to obtain the diffusity ($D_\theta$).

$$D_\theta = \frac{\pi S_\theta^2}{4(\theta_i - \theta_o)^2}\left\{\left[\frac{(\theta_i - \theta_o)}{(1+\varepsilon)\log e}\right]\left[\frac{d\log S_\theta^2}{d\,\theta_i}\right] - \left[\frac{1-\varepsilon}{1+\varepsilon}\right]\right\} \tag{3.5}$$

where:

$S_\theta$ is the sorptivity at a given water content

$\theta_i$ is an incremental water content

$\theta_o$ is the initial water content

$\varepsilon$ is a constant that varies between 0.5 and 0.67

### 3.2.5 Outflow methods

The Outflow methods regroup a number of procedures where the rate and the amount of water flowing out of the sample are measured (Klute 1972, Abu-Hejleh et al. 1993, Benson and Gribb 1997). The flow out of the sample is then used to compute the coefficient of permeability either directly or indirectly. The outflow methods are typically performed with laboratory equipment used to determine the SWCC. Such apparatuses include the hanging column and the pressure plate extractor. Figure 3.4 shows the hanging column apparatus from Benson et al. 1993. Figure 3.5 shows a pressure plate extractor (from Tinjum et al. 1997).

#### 3.2.5.1 Multi-step outflow method

This method consists of subjecting a soil specimen to small incremental steps in matric suction ($\Delta\psi$) and measuring the rate of outflow as well as the total outflow during each suction step. The diffusion function $D_\theta$ and corresponding water content can be determined from the outflow data and the increment in matric suction applied. Once the diffusion function is known, the coefficient of permeability can be obtained using Equation 3.2.

The following six assumptions are made in the Multi-step outflow method ;

- $K_\psi$ is constant over each $\Delta\psi$
- $\psi$ is linearly related to water content for water contents corresponding to the step $\Delta\psi$
- The pressure plate provides no impedance to flow
- Flow is one-dimensional
- Gravity gradients are negligible

- The specimen is homogeneous and rigid (i.e. water is expelled only by hydrodynamic flow induced by the hydraulic gradient imposed by $\Delta\psi$)

3.2.5.2 One-step outflow method

The One-step method differs in the way that matric suction is applied. Instead of applying several small incremental steps, one large step in matric suction is applied and outflow monitored. The outflow data is then analysed to obtain the diffusivity function ($D_\theta$). Unlike the Multi-step method, the One-step method requires that the SWCC be obtained independently because not enough matric suction increments are applied to generate a complete curve. Furthermore, the hydraulic gradient is much larger in the One-step method, which means that inaccuracies are introduced in soils responsive to the hydraulic gradient, or to soils exhibiting large variances due to stress change. Another weakness of this method lies in the assumption that the diffusivity, $D_\theta$ is assumed to remain constant throughout the specimen at any given time.

3.2.5.3 Multi-step direct outflow method

The Multi-step direct outflow method is a variation of the Multi-step outflow method. The direct outflow method is based on the assumption that $\theta$ only varies significantly near the soil-plate interface of the apparatus. As a result, the matric suction is reasonably constant and Darcy's law can be used to calculate the unsaturated coefficient of permeability, provided small increments in suction are applied over short time intervals.

The shortcomings associated with the Multi-step direct outflow method are the difficulties in measuring the total heads when dealing with small gradients, and accurately measuring the saturated coefficient of permeability of the porous plate.

3.2.5.4 Continuous outflow method

The Continuous outflow method is also a variation of the Multi-step method. In this method, the matric suction continuously varies throughout the test. Small specimens are used to minimise the variation of saturation in the direction of the flow. The Continuous

outflow method results in large scatter in the unsaturated coefficient of permeability values at low suctions or high degrees of saturation.

### 3.2.6 Thermal method

The Thermal method consists of applying a temperature gradient across an insulated horizontal column of soil having a known initial water content (Benson and Gribb 1997). The application of the thermal gradient induces water flow towards the cool end of the column. Simultaneously, a gradient in matric suction develops due to the changes in water content induced by the thermal gradient. The matric suction gradient induces flow towards the warm end of the specimen. Once equilibrium in temperature and water content is reached, the distribution of temperature and water content throughout the sample is obtained. The coefficient of permeability is computed using Equation 3.6.

$$k_{\psi} = \frac{5x10^{-11}}{S_{\psi}} \tag{3.6}$$

where:

$S_{\psi}$ is the thermogradient coefficient given by:

$$S_{\psi} = \frac{d\psi}{dx}\left(\frac{dt}{dx}\right)^{-1} \tag{3.7}$$

Once equilibrium has been reached, the gravimetric water content distribution is obtained by separating the sample and weighing the pieces. Discrepancies are found in the results if the test is stopped prior to attaining equilibrium since there are no defined procedures to determine when equilibrium is attained.

The drawbacks of this method include obtaining the SWCC on an independent test samples, and the destructive means used to get the water content distribution.

### 3.2.7 Instantaneous profile method

The Instantaneous profile method (IPM) is performed by introducing a wetting or drying front in a vertical sample and measuring the suction and volumetric water content to determine the unsaturated coefficients of permeability. (Klute 1972, Hamilton et al. 1979, Olsen and Daniel 1981, Meerdink et al. 1996, Amraoui et al. 1998) The coefficient of permeability of the sample is then computed from the known relationships between water content and flow, and suction with hydraulic gradient given in Equation 3.8.

One of the advantages of this method is that contrary to other previously described methods, it can be performed on larger samples. Also, by introducing a wetting front and subsequently allowing the sample to dry, both the wetting and the drying cycles can be measured in a single test. Furthermore, this procedure does not require the SWCC to be determined on a separate sample since the required parameters are measured on the test sample during the procedure.

The IPM was originally described by Richards and Weeks (1953) and several other investigators have used this technique since then (Klute 1972, Hamilton et al. 1979, Meerdink et al. 1996, Amraoui et al. 1998). Figure 3.6 shows the permeameter used by Meerdink et al. 1996 to determine the unsaturated coefficient of permeability using the IPM.

The unsaturated coefficient of permeability is computed from Equation 3.8.

$$k_{unsat} = -\frac{\Delta V}{A\Delta t}\left(\frac{1}{dh/dz}\right) \tag{3.8}$$

where:

$\Delta V$ is the volume of water flowing past a specific depth

$A$ is the cross-sectional area of the specimen

$\Delta t$ is a given time increment

*dh/dz* is the hydraulic gradient

The volume of water flowing through a given location is obtained from Equation 3.9.

$$\Delta V = A\int_{z_o}^{z_i}(\Delta\theta)dz \tag{3.9}$$

where:

$z_o$ and $z_i$ are two consecutive depths

Equation 3.10 relates the hydraulic gradient, *dh/dz,* to the change in matric suction, $\delta\psi$, over two successive depths at which volumetric water contents, $\theta$, are also measured.

$$-\left(\frac{dh}{dz}\right) = 1 + \left(\frac{\delta\psi}{\delta z}\right) \tag{3.10}$$

Some of the main advantages of the IPM include such items as measuring the SWCC during both the drying and wetting stages, using a single specimen. Large and more representative size specimens can be used with this method contrary to other transient methods. For this reason, several uncertainties associated with using small specimens can be eliminated when applying IPM results to actual field conditions. Furthermore, the IPM requires significantly less time to obtain the flow characteristics, especially when dealing with coarse-grained soil specimens.

## 3.3 SUMMARY

Preliminary investigation of laboratory methods used to determine the unsaturated coefficient of permeability of soil samples yielded numerous results. The methods listed above are the most common in literature and were considered for the present research. The main objective during this literature investigation was to find a method that could be used with a soil that would range from a slurry to an essentially dry sample. It was

deemed preferable to conduct non-destructive testing on a single sample, from which sufficient data could be collected to compute the SWCC and the conductivity curve.

The Instantaneous Profile method was chosen because it better satisfied the above requirements. This method also provided the opportunity of developing an apparatus specifically designed for tailings.

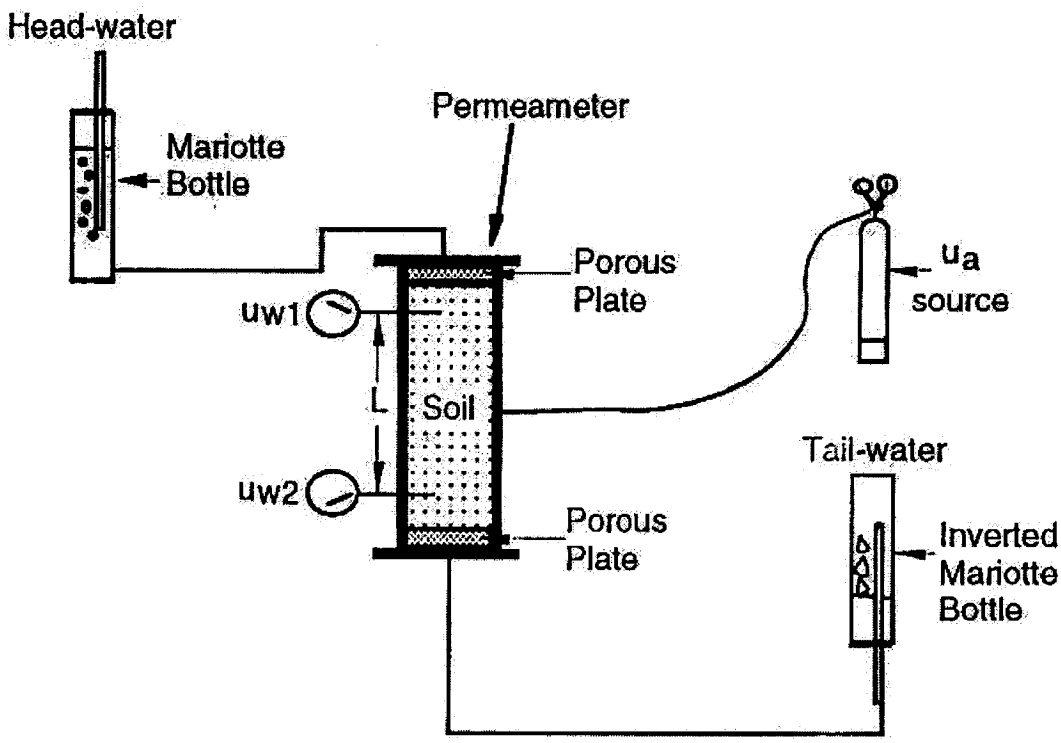


**Figure 3.1: Traditional Steady-State Method Apparatus (Klute and Dirksen, 1986)**

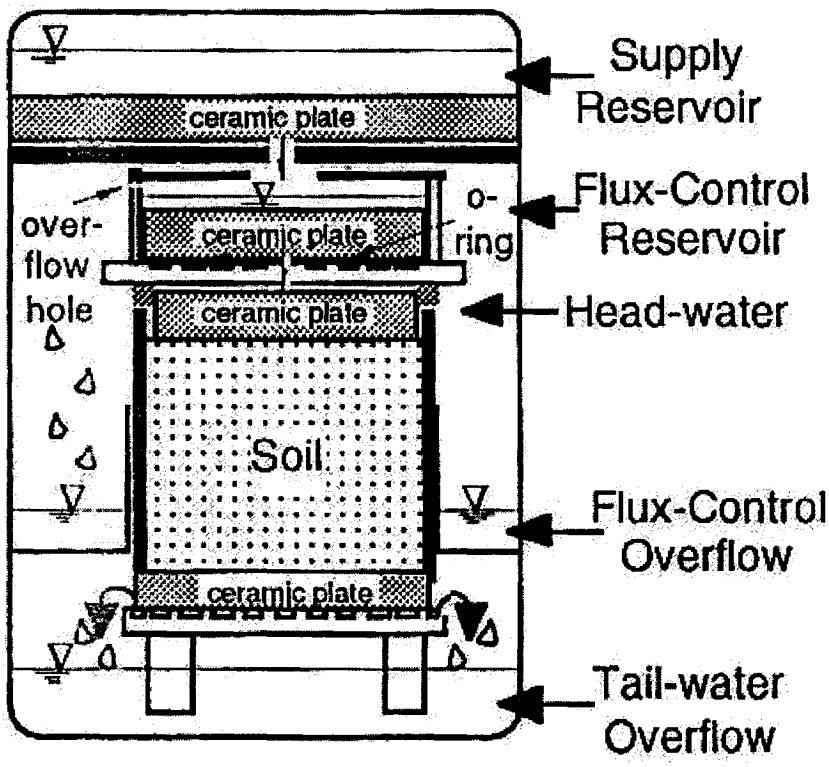


**Figure 3.2: Centrifuge Sample Container (Nimmo *et al.* 1992)**

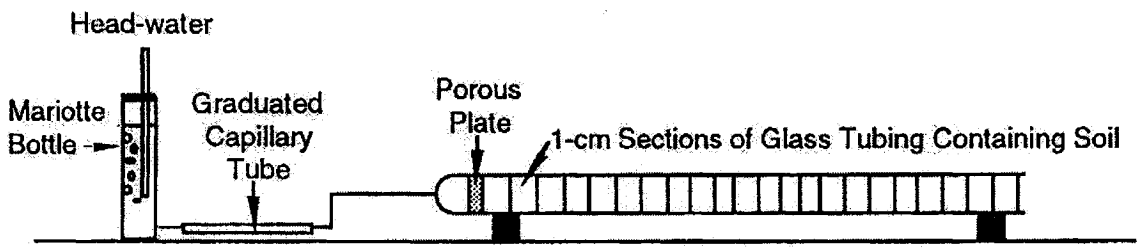


**Figure 3.3: Bruce-Klute Absorption Apparatus**

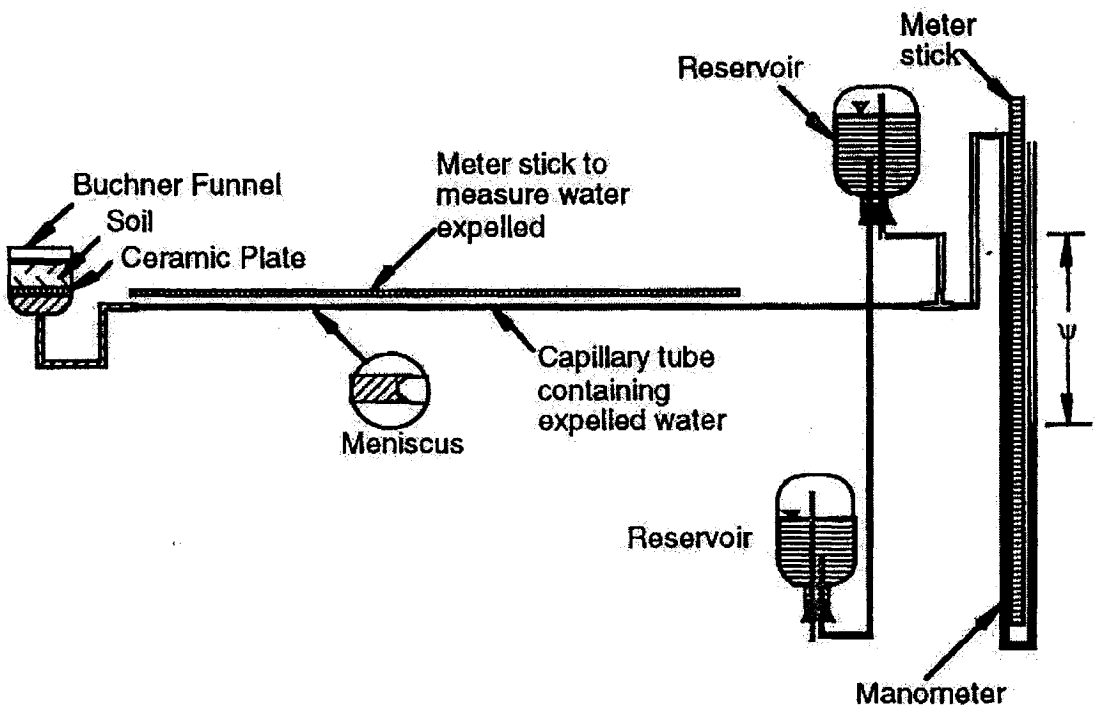


**Figure 3.4: Hanging Column Apparatus**

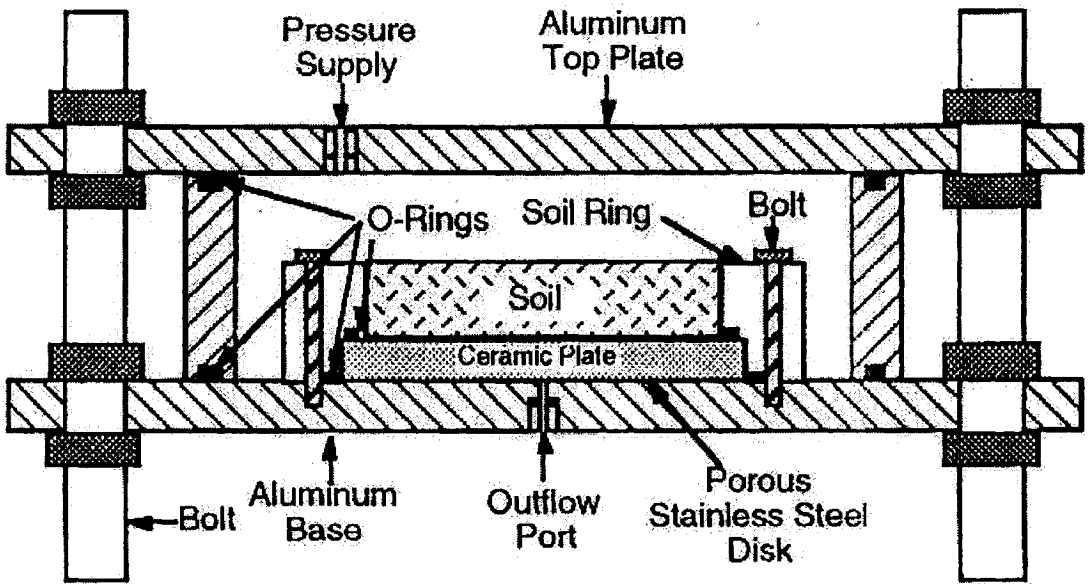


**Figure 3.5: Pressure Plate Extractor**

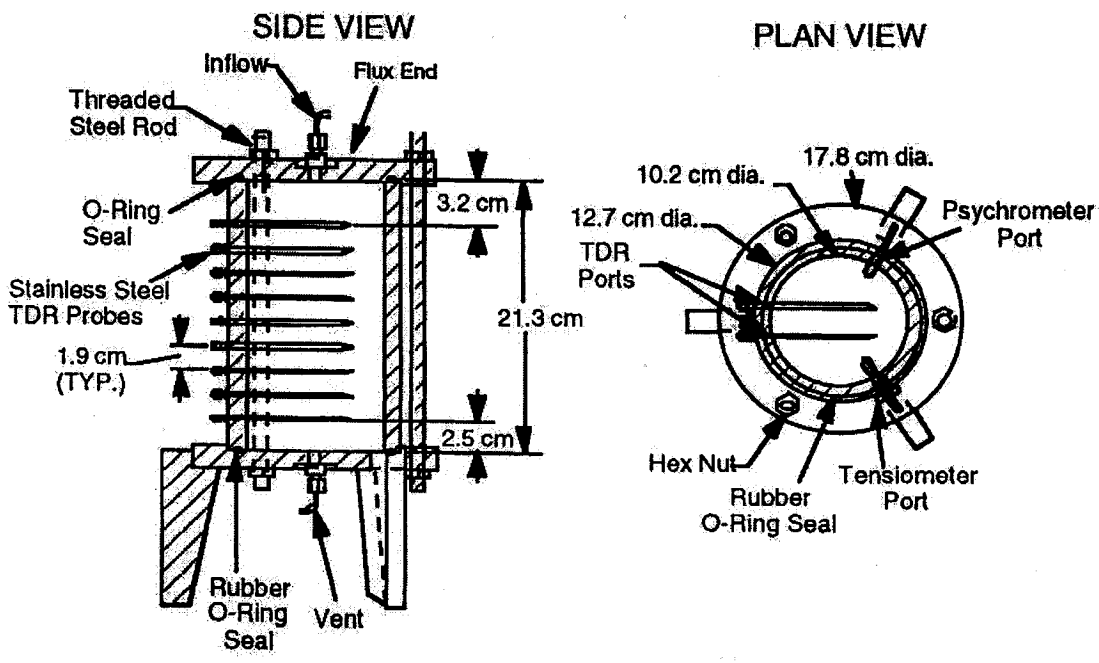


**Figure 3.6: Permeameter used by Meerdink et al. (1996)**

# CHAPTER 4 – DETAILS OF THE MODIFIED PERMEAMETER

## 4.1 INTRODUCTION

Different laboratory methods that are available to determine the unsaturated coefficient of permeability of soil samples are summarised in Chapter 3. The instantaneous profile method was chosen over methods such as the steady-state method, the centrifuge method, or the absorption method, mainly due to the versatility that it offered. A new piece of testing equipment was developed to determine the SWCC and the unsaturated coefficient of permeability, taking into account constraints such as sample size, testing time, and apparatus requirements.

The apparatus, which is referred to as the Modified Permeameter through the remainder of this thesis, was designed and built in the Geotechnical Engineering Laboratory of the University of Ottawa. This apparatus is used to determine the flow behaviour of unsaturated tailings using the instantaneous profile method.

## 4.2 PERMEAMETER

Meerdink et al. (1996) used a permeameter to determine the flow behaviour of compacted clays under unsaturated conditions. The key objective for the apparatus was to determine the unsaturated coefficient of permeability of a compacted clay specimen in the laboratory.

### 4.2.1 Description of testing equipment

Figure 4.1 shows a schematic of the permeameter used by Meerdink et al. (1996). The clay sample was directly compacted in the 102 mm diameter plastic tube of this apparatus. To measure water content and suction, the investigators used Time Domain Reflectometry (TDR) probes (described later), tensiometers, and psychrometers. The investigators used nine equidistant TDR probes, psychrometers, and tensiometers to measure the suction along the length of the tube. Flow in the sample was achieved through an inflow port located at the top and an outflow port located at bottom of the apparatus. A small water supply was provided at the top port (for wetting curves) and

evacuated through the bottom port. Meerdink and al. (1996) reported adjusting their apparatus for drying curves. To provide a drying front, the top cover of the apparatus was removed, and a continuous flux of air was applied at the top of the sample.

### 4.2.2 Drawbacks

The permeameter designed by Meerdink et al. (1996) cannot be directly used to determine the flow characteristics of tailings under unsaturated conditions. Tailings are an industry by-product and have characteristics that are different from naturally occurring soils or compacted soils. It is difficult to duplicate the depositional conditions of natural tailings and drainage conditions that are typically found at the tailings storage area using the permeameter.

## 4.3 THE MODIFIED PERMEAMETER

The Modified Permeameter shown in Figures 4.2a and schematically in 4.2b, was designed and constructed to suit the specific requirement of testing tailings. Some of the key features include the use of a large sample; accommodate mobile sensors and use the same test specimen to determine the SWCC and flow characteristics of tailings over a large range of saturation.

### 4.3.1 Dimensions

The Modified Permeameter accommodates a larger sample compared to conventional laboratory sizes. The apparatus has a square base measuring 200 mm x 200 mm (Figure 4.3). The Modified Permeameter can hold a 400 mm high sample, which is necessary when dealing with soils that exhibit large consolidation.

A number of studies have shown significant differences between the predicted unsaturated flow behaviour using the SWCC and the field measured unsaturated flow behaviour (Meerdink et al. 1996, Amraoui et al. 1998, Holland et al. 2000). The differences between the predicted and measured flow behaviour can be attributed to the influence of various parameters that govern the unsaturated flow behaviour. One of the key parameters is the

non-representative size of the specimen used in the laboratory to measure the SWCC to predict the field behaviour. For this reason, large size specimens were used in this study.

### 4.3.2 Counterweight system

The water content of the sample in the Modified Permeameter was designed to determine with the use of Time Domain Reflectometry (TDR). TDR works by sending an electro-magnetic pulse through a conductor of known length. The time interval for the pulse to travel the length of the conductor (a steel rod in this case) is proportional to the resistance surrounding the rod. The steel rod is inserted in the soil where soil grains, air, and water are present. Since soil water offers different resistance than either air or soil grains, the water content can be estimated in the soil sample based on the resistance values. Accordingly, air pockets surrounding the rods can significantly influence the travel time of the electromagnetic pulse. More details of TDR technology will be described later in the chapter.

Since the tailings slurry would consolidate with drainage of the sample, it was feared that voids would form around the TDR rods and introduce errors in the measured water content values. To prevent voids from forming around the probe's rods, the Modified Permeameter was designed to allow mobility of the TDR sensors. A counterweight system was used to provide mobility to the sensors during the testing period. With the counterweight system, the TDR probes essentially became buoyant in the sample. Due to prevailing buoyant conditions only a small vertical pressure was required to move the probe's rods. This pressure was provided by the consolidating tailings

Figure 4.4 shows a cross-section of the Modified Permeameter highlighting the details of the counterweight system. A TDR probe is inserted in the tailings sample through a rubber seal. The counterweight arm is slid in an opening in the sliding arm and attached to the permeameter at the pivot point. The counterweight arm is then free to pivot unrestricted for any movement of the TDR probe. At the extremity of the counterweight arm is a brass counterweight (which is identical to the weight as the TDR probe) that can be slid horizontally to finely adjust the vertical force acting at the TDR sensor's location.

A second counterweight system was designed to achieve water-tightness in the Modified Permeameter. The bottom counterweight system (Figure 4.4) applies a horizontal force against the sliding arm to balance the hydrostatic pressure of water found in the sample, which is applied at the opening in the wall of the permeameter.

Leaks were feared at the interface between the sliding arm, holding the TDR probe, and the permeameter itself (see Arrow 4 of Figure 4.4). Different types of materials were tested at the interface in order to provide a waterproof seal between the sliding arm and the permeameter's external face. Combinations of Teflon®, various foam tapes, and numerous types of greases were evaluated before the current arrangement proved to be suitable. Water-tightness and mobility were both achieved with a bead of a graphite-based grease. The graphite-based grease does not creep when applied on a vertical surface, and unlike other types of grease tested, is not excessively viscous as to reduce mobility of the sliding arm.

### 4.3.3 Porous ceramic

A high air-entry porous ceramic (1 bar) was used in the Modified Permeameter in order to evaluate the flow behaviour of tailings over a large range of saturation. To maintain flexibility in the design of Modified Permeameter, the porous ceramic was fitted to a removable aluminium collar (Figure 4.5, Arrow 1). This aspect of the design facilitates to independently remove the ceramic and saturate it by boiling prior to testing. The aluminium collar also facilitates changing the ceramic in case it was damaged, or in the event other soils would have to be tested. The ceramic was fastened in the aluminium collar with all weather silicon (Arrow 2). The all-weather silicon was chosen instead of commonly used epoxy such that the ceramic could be easily removed and replaced if needed.

The aluminium collar with the porous ceramic shown in Figure 4.5, is fastened with screws to the base of the permeameter through a permanently fixed aluminium base plate. The permanent aluminium base plate has the same dimensions as the aluminium collar,

with the exception that the machined opening in its centre is slightly smaller. The smaller opening in the aluminium base plate creates a lip for the porous ceramic such that the load of the sample above is not exclusively supported by the silicon holding the ceramic to the aluminium collar.

The thickness of the aluminium base plate also creates a small reservoir below the porous ceramic, which is useful to sight air bubbles that form.

### 4.3.4 Flushing system

To determine the unsaturated coefficient of permeability using the Instantaneous Profile method with the Modified Permeameter, the total volume of water that drains from the sample is not required. For this reason, a simple technique for removing air coming out of solution was used.

This was achieved with the aid of tubing, valves, and hypodermic syringes to flush the air bubbles out from under the porous ceramic. Figure 4.6 shows a schematic of the ceramic's aluminium collar with the tubes and syringes at the corners. On the underside of the collar, at each corner, small grooves were machined to create openings. The assumption was that air coming out of solution under the ceramic would find its way to the highest point (i.e., the machined openings), from there the air could be removed. Small Teflon® tubes were attached to the aluminium collar at the groove's location. The other extremity was connected to syringes. Between the aluminium plate and the syringes, plug valves were connected to allow dismantling of the syringes for refilling or emptying. The flushing system proved to be successful in the removal of air bubbles located below the porous ceramic.

## 4.4 SENSORS

To determine the coefficient of permeability of unsaturated soils using the instantaneous profile method, the soil suction and volumetric water content values are required. Different sensors are commercially available that can be used to measure these parameters. Due to the larger size of the apparatus, the use of various types of sensors

was investigated. These included thermal conductivity matric suction sensors, gypsum blocks, psychrometers, and different arrangements of TDR sensors. After several trial tests Time Domain Reflectometry (TDR) and tensiometers were selected to measure water content and suction respectively.

### 4.4.1 Tensiometers

Tensiometers consist of a porous ceramic cup connected to a vacuum gauge. The porous ceramic cup, which is inserted in the soil, reacts to the fluctuations of the water content in the soil. As water flows between the porous ceramic and the soil, the negative pore pressure acting at the porous ceramic is displayed by the vacuum gauge.

From a theoretical point of view, tensiometers are capable of directly measuring the matric suction of a soil in the range of 0 to 101.3 kPa (or 1 atm). At the suction value of 101.3 kPa, the pore water pressure is equal to the atmospheric pressure and cavitation can initiate. However, researchers reported cavitation effects at pressure values around 90 kPa Fredlund and Rahardjo (1993). The tensiometer used in this research, shown in Figure 4.7, were all graduated from 0 to 100 centibars (approximately 0 to 100 kPa) and recommended for used in the 0-85 centibars range, or approximately 0 to 8 meters of water.

### 4.4.2 Time domain reflectometry

Time Domain Reflectometry (TDR) technology was first developed during the 1950's to locate and identify cable faults in the power and telecommunications industries (O'Connor and Dowding 1999). The distance to the fault could be calculated since the pulse travels at the speed of light.

TDR technology works by sending an electromagnetic pulse down a conductor and measuring the time it takes for the reflection of the pulse to come back to its point of origin. However, in soil science applications, the pulse is given a path of known length to travel. TDR, in soil science applications, is not used to find the length of the conductor, but rather the impedance of the conductor on the electromagnetic pulse.

In other words, cables coated with insulating material inhibit external factors from impeding the pulse's travel speed. And if this insulating material is removed, materials with different dielectric constants will affect the travel speed of the pulse. If a parallel can be made between soils and electrostatics, the dielectric constant of a material can be compared to a soil's coefficient of permeability. In other words, the greater the value of the coefficient or constant, the greater will be the influence on the travel speed of the material moving in the conductor. The dielectric constant, ($K = \epsilon/\epsilon_0$), of air is 1, ranges from 3 to 5 for most soil mineral grains, and is approximately 81 for water (at 20°C). Thus, a small change in moisture content of unsaturated soils will have a significant effect on the bulk dielectric constant of the air-soil-water medium (O'Connor and Dowding 1999).

The TDR sensors in Figure 4.8 show the parallel rod probe required to measure volumetric water content. Baker and Lascano (1989) found that the sensitivity of parallel rod probes was largely confined to an area of 20 mm by 65 mm surrounding the two-rod probe. Figure 4.9 shows typical contours of dimensionless electrical field distribution normal to a two-rod probe in a material of uniform dielectric constant (Zegelin et al. 1989).

The TDR equipment used for this research program was Moisture Point's MP-917 model. Moisture Point's SDRC020 two-rod probes with removable rods of 200 mm were used since this type of probe is better suited for laboratory work (Figure 4.8).

### 4.4.3 The sampling tool

During preliminary testing, there was large fluctuation in the measured water content values using TDR. For this reason, a method was developed to directly measure the water content values and compare with the water content measurements obtained from the TDR sensors. This was achieved by developing the sampling tool.

The sampling tool shown in Figures 4.10 and 4.11 is a simple device that provides easy determination of the gravimetric water content of the test sample at different elevations and for different time intervals during testing. The water content can be determined using this technique without dismantling the soil sample. In other words, the water content can be determined without terminating the test. One of the advantages of the sampling tools lies in their ability to allow tailings to consolidate in and around it, even though the sampling tool is fixed to the permeameter's wall. This feature minimises void formation around obstacles in the specimen during testing.

In Figure 4.11, Arrow 1 shows the exterior wall of the permeameter, through which a support (Arrow 5) is introduced to hold the sampling tool in a horizontal position while preventing air and water from existing the system by means of O-rings (Arrow 6). The sampling tool is composed of two cylinders. The outer cylinder acts as a sleeve for the inner cylinder. An opening is provided at the same location along both cylinders, which allows the slurry sample to flow through the sampling tool during testing. When a small sample is collected, the knob connected to the inner cylinder is rotated by 90 degrees to trap a small sample in the opening of the interior cylinder. The O-rings located just besides the opening (see Arrow 4) seal the sample in the outer sleeve, preventing changes in the water content.

## 4.5 TRIAL TESTS

The Modified Permeameter was subjected to a number of changes during preliminary testing. The following sections highlight the most important modifications and observations.

### 4.5.1 Time Domain Reflectometry

Preliminary calibration testing of the TDR equipment provided widely scattered results. The results plotted in Figure 4.12 show significant differences between the theoretical volumetric water content ($\theta$) and experimental measurements using TDR. It should be noted that some scatter was expected due to the intrinsic software of the MP-917

(programmed for 300 mm long probes) since the length of the probes used in the laboratory was 200 mm.

However, this difference should have given a constant error in the readings since the travel time of the electromagnetic wave along the probes is directly proportional to the length of the probe, as seen in Equation 4.1 (Davis and Chudobiac 1975).

$$t = \frac{2l_p}{V_p} \tag{4.1}$$

where:
$l_p$ is the length of the probe
$V_p$ is the velocity of the propagation wave

In turn, the propagation velocity of the wave (Topp et al. 1980) is given by:

$$V_p = \frac{c}{\sqrt{\epsilon}} \tag{4.2}$$

where:
$c$ is the speed of an electromagnetic wave in free space
$\epsilon$ is the permitivity of the medium

From Equation 4.3 it can be seen that if a shorter probe is used, the apparent dielectric constant, $K_a$, measured with TDR, increases if both $c$ and $\epsilon$ are assumed constant.

$$K_a = \left[\frac{ct}{2l_p}\right]^2 \tag{4.3}$$

In an attempt to explain the discrepancies between the laboratory results and the theoretical curve, the tailings were tested for electrical conductivity and magnetism. The

nickel tailings proved to be highly conductive to an electrical current and magnetic field (most likely due to iron found in the pyrite and pyrrhotite). Robinson et al. (1994) studies also show that the iron minerals could significantly affect the determination of water content using TDR.

### 4.5.2 The sampling tool

Early trials showed that the sampling tools trapped excess water between the O-rings and the piston if no precautions were taken during removal of the internal piston from its copper casing. Subsequent testing showed that simple precautions could minimise the occurrence of this situation, resulting in more precise measurements of water content.

## 4.6 APPARATUS ASSEMBLY AND PREPARATION

The assembly of the Modified Permeameter forms the first step of the testing since it is disassembled after all test sequences to clean and maintain. The next step was to make sure that the high air-entry porous ceramic was saturated. This achieved by boiling the stone. The bottom plate of the Modified Permeameter is seated on its support, and the bottom valve is screwed in place. Then, the valve is closed and the area within the seal is filled with water as shown in Figure 4.13.

The saturated ceramic stone is placed on the seal ensuring that no air is entrapped between the collar and the seal. The collar is then fastened to the seal, as shown in Figure 4.14, eliminating the possibility of leaks. The Teflon® tubes of the flushing system are then connected to the ceramic plate's collar and threaded through the top of the permeameter as shown in Figure 4.15. A rubber gasket is then positioned around the seal and the side-walls of the Modified Permeameter are fastened to the bottom plate by 32 screws. The Modified Permeameter is then ready to be fitted with the sliding arms as shown in Figure 4.16. These measures ensure that the bottom of the Modified Permeameter is air and watertight.

The sliding arms are then slid in place, along with the counterweight system as shown in Figure 4.17. Once all the side-mounted parts are in place, a bead of graphite-based

grease is caulked around the TDR opening in the side-walls. The counterweights are then adjusted to ensure a uniform bead of grease around the opening.

The sampling tools are then inserted in pre-numbered ports to assure that no errors occur during the removal and drying of the devices for the gravimetric water content determination. A precautionary measure to be performed prior to placing the sample includes the removal of air from the tubes of the flushing system. The Modified Permeameter is now essentially ready to receive the sample (Figure 4.18).

## 4.7 TESTING PROCEDURE

All samples were thoroughly mixed in their storage containers to achieve a homogeneous slurry conditions prior to being placed in the Modified Permeameter. This was done using a paint stirrer that was attached to a drill and put in the sample until visual and manual inspections were satisfactory (i.e., no more lumps in the tailings could be seen or felt). The homogeneous tailings slurry was poured in the Modified Permeameter in a consistent manner. The sample was then left in place over a period of 12 hours to allow the fines to settle. The excess free-standing water was removed and the tensiometers inserted to the same depths as the sampling tools. Once all the instrumentation is put in place the test was initiated by opening the valve to allow drainage.

At this point, the sample requires a period of time for water to drain out of the permeameter, and suction values be displayed by the tensiometers. Periodically, a reading was taken from the tensiometers, and simultaneously a sample retrieved with a sampling tool located at the corresponding depth. Once all the sampling tools contain a sample, the test is stopped.

## 4.7 SUMMARY

As outlined in this chapter, the Modified Permeameter was built to provide a versatile research equipment used to evaluate the flow behaviour of large samples of unsaturated soil samples. However, to use this equipment with reliability it is essential to provide mobile, frictionless sensors and that no air voids form during a testing period over a

suction range. This challenge was achieved with a reasonable degree of accuracy using the procedures detailed in this chapter.

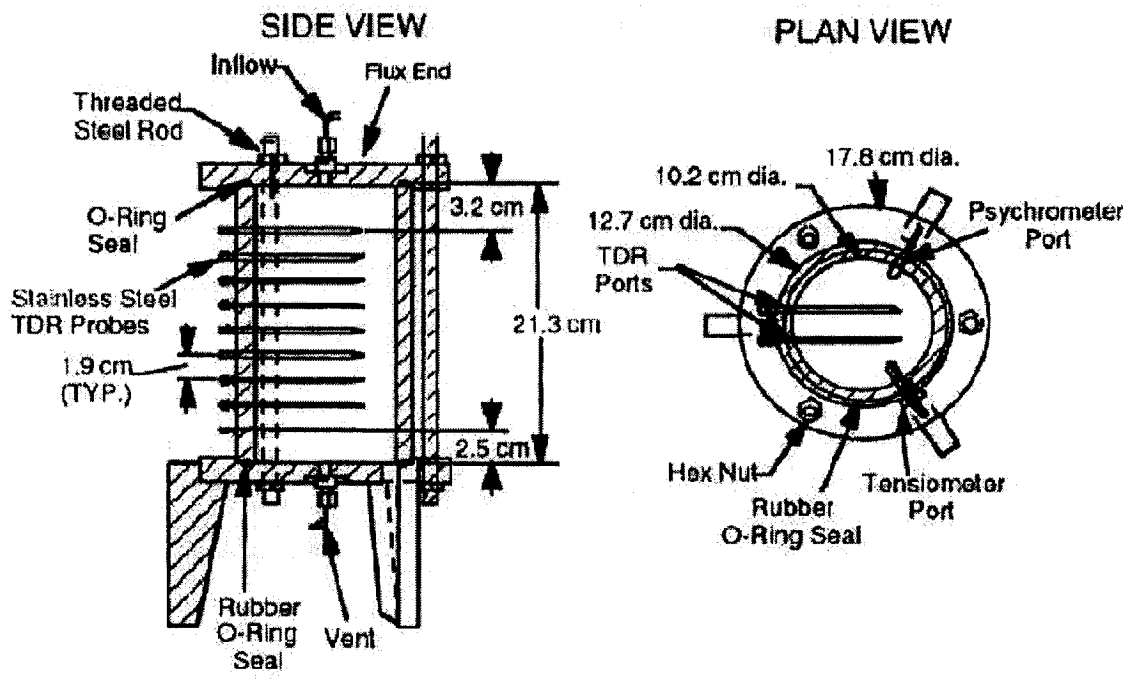


**Figure 4.1: Permeameter used by Meerdink et al. (1996)**

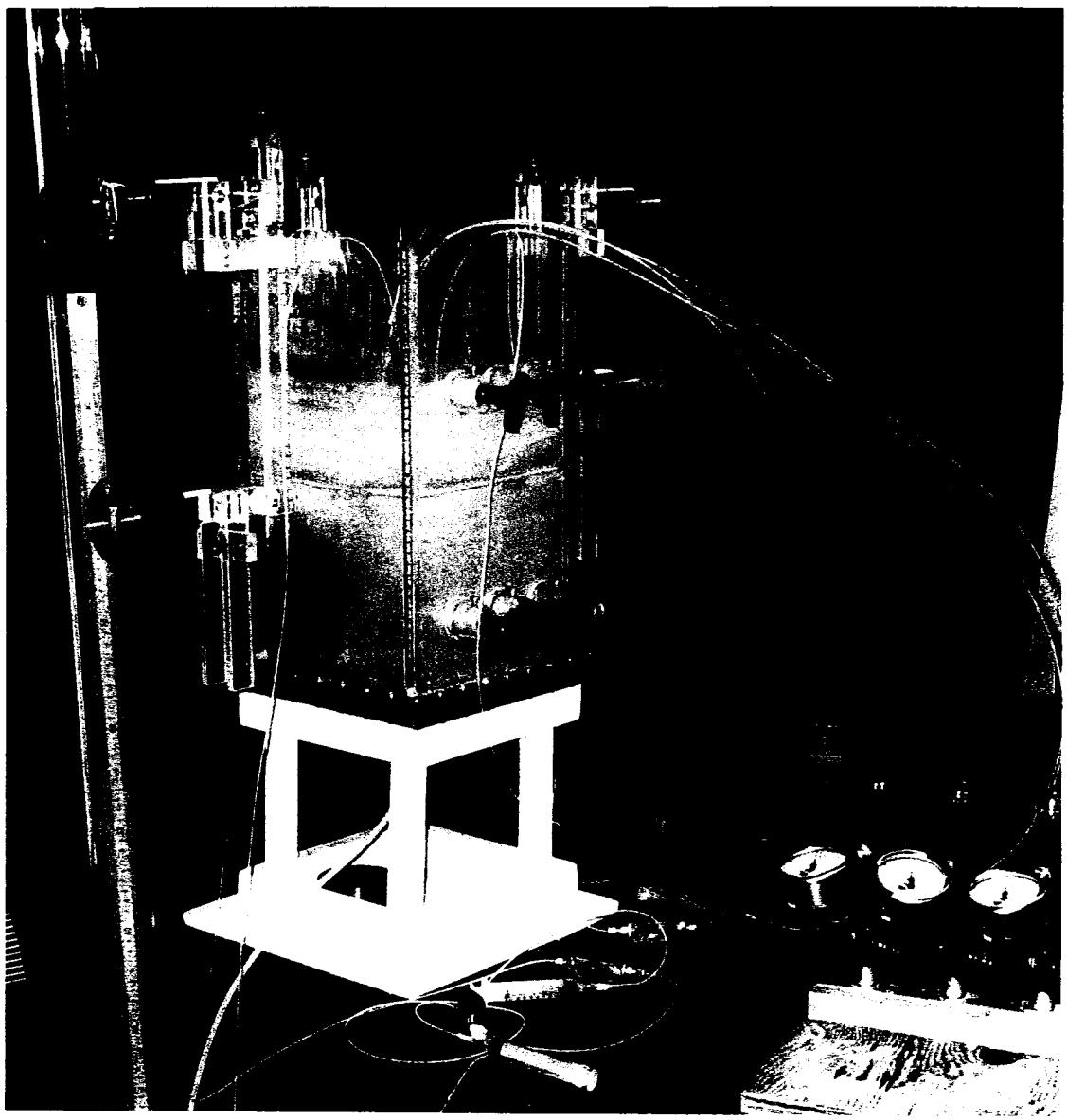

**Figure 4.2(a): The Modified Permeameter**

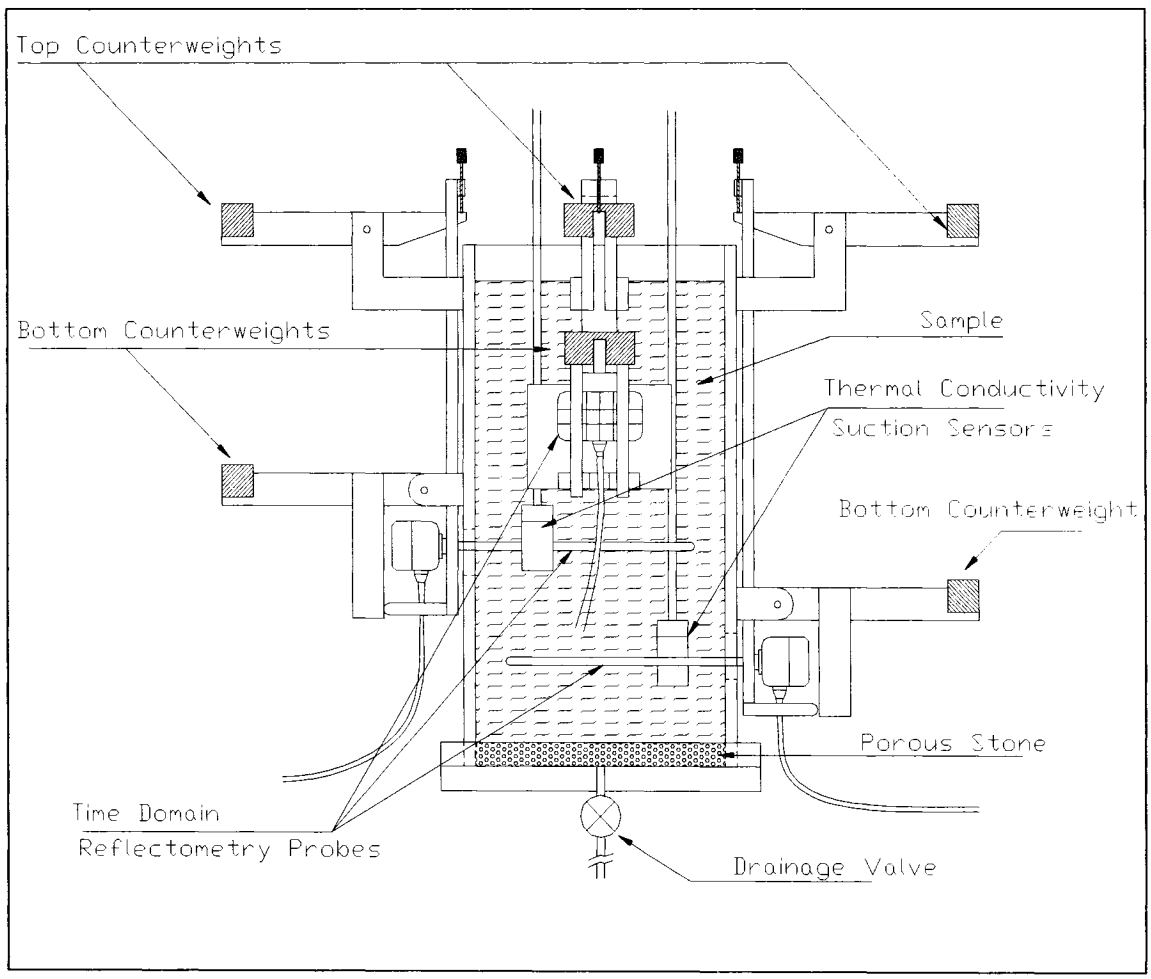


**Figure 4.2(b): The Modified Permeameter - schematic**

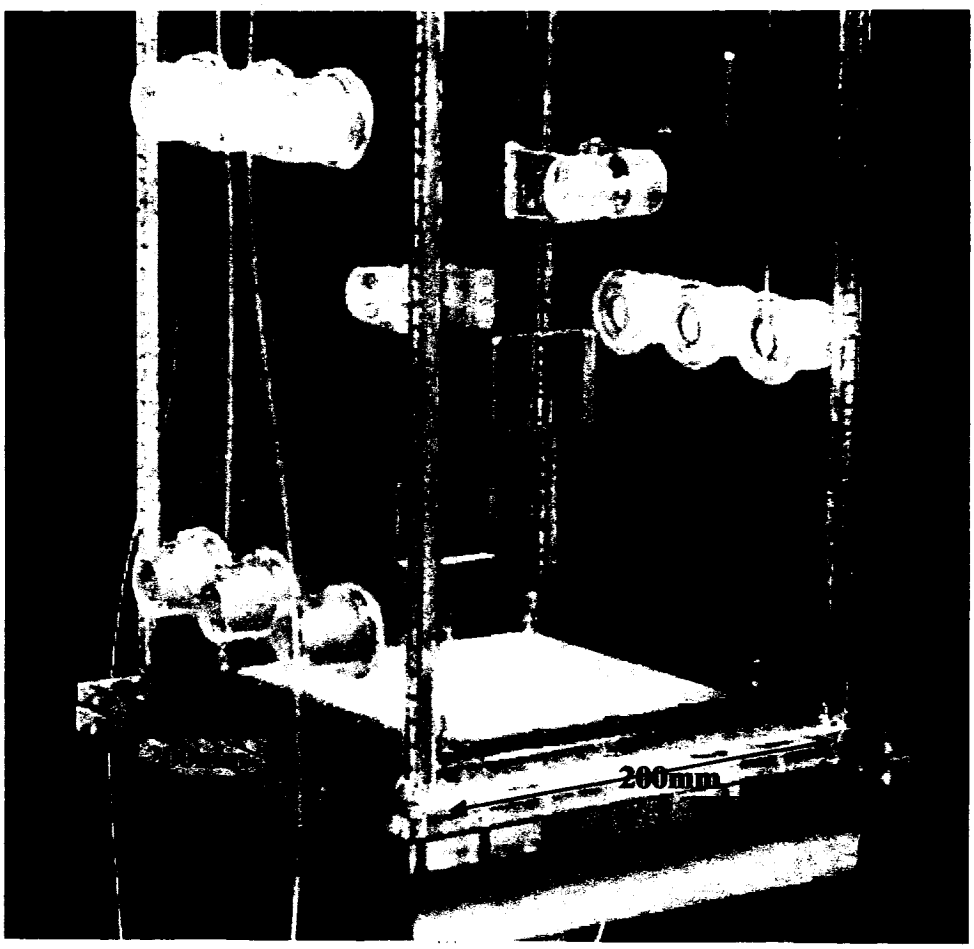


**Figure 4.3: The Modified Permeameter's dimensions**

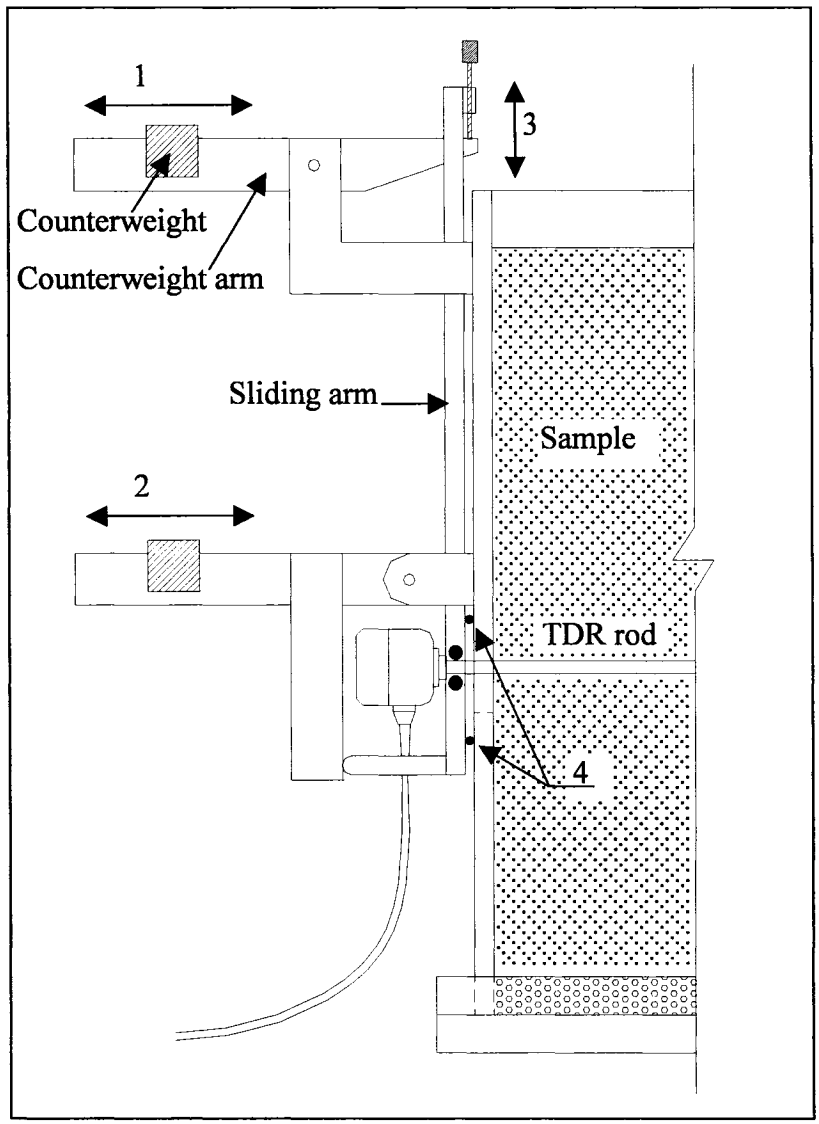


**Figure 4.4: Schematic of the Modified Permeameter's counterweight system**

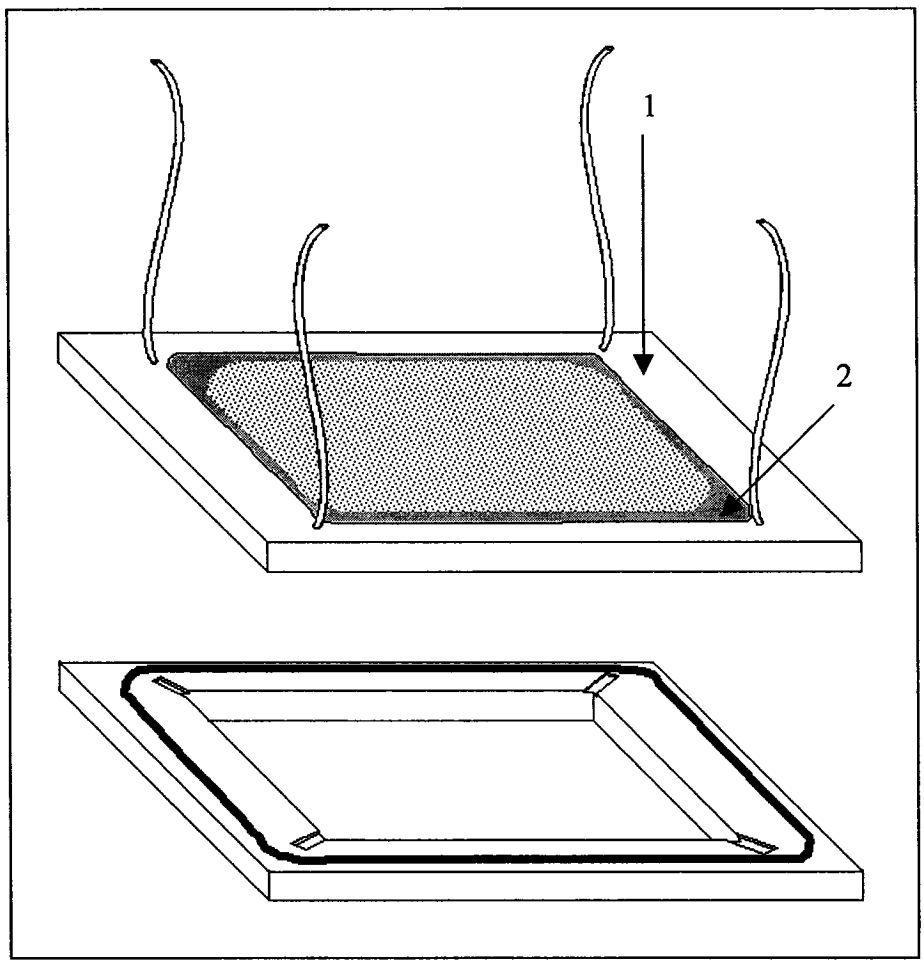


**Figure 4.5: Porous ceramic collar and seal plates**

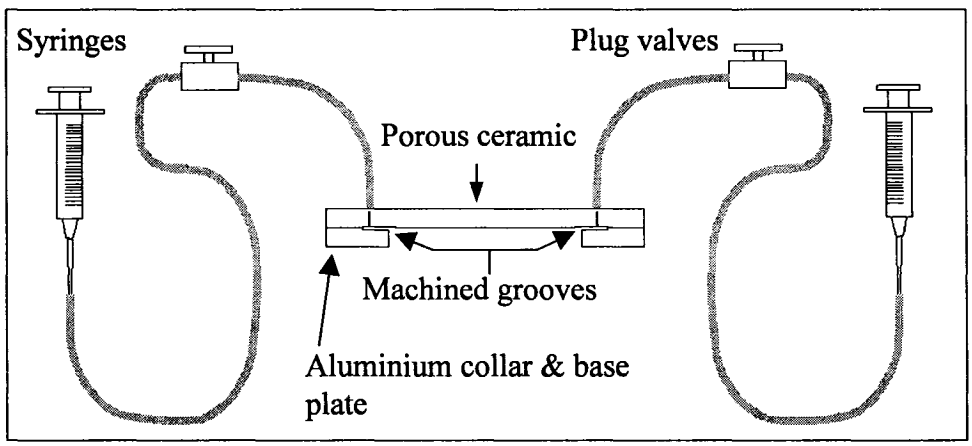


**Figure 4.6: Schematic of the flushing system**

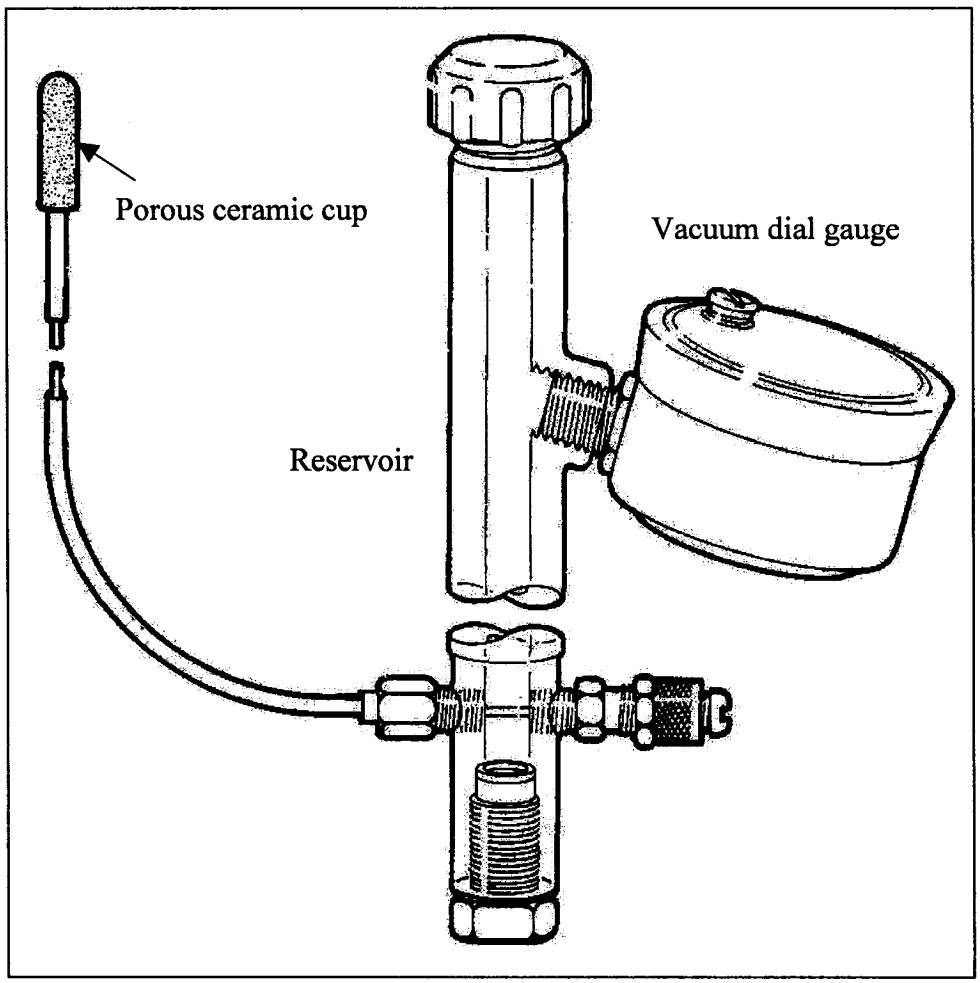


**Figure 4.7: The tensiometer (Soilmoisture Equipment Corp.)**

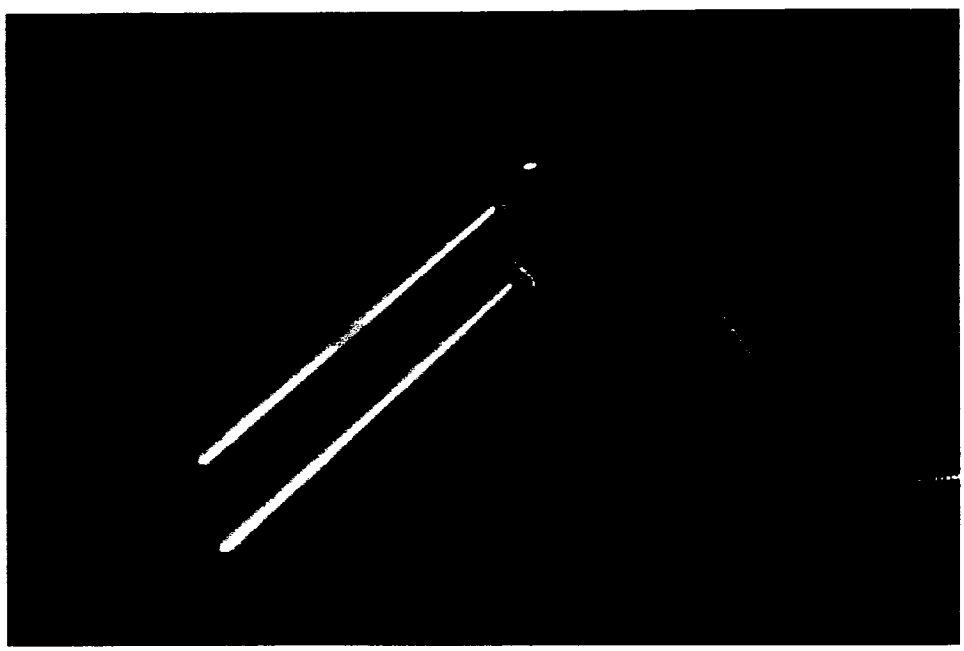

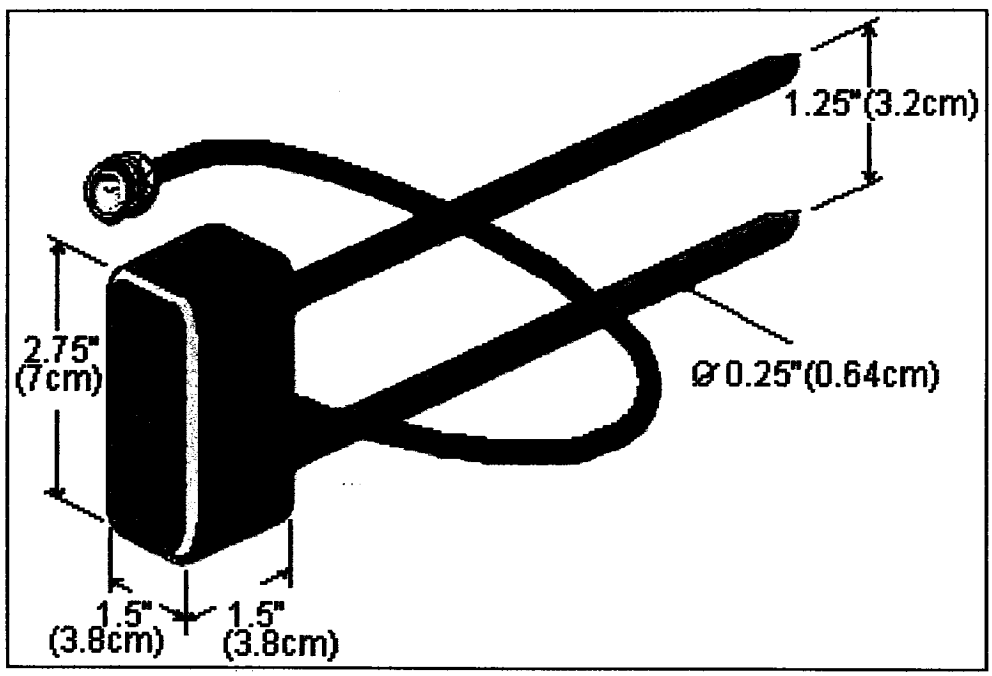


**Figure 4.8: Moisture Point's two-rod TDR probe**

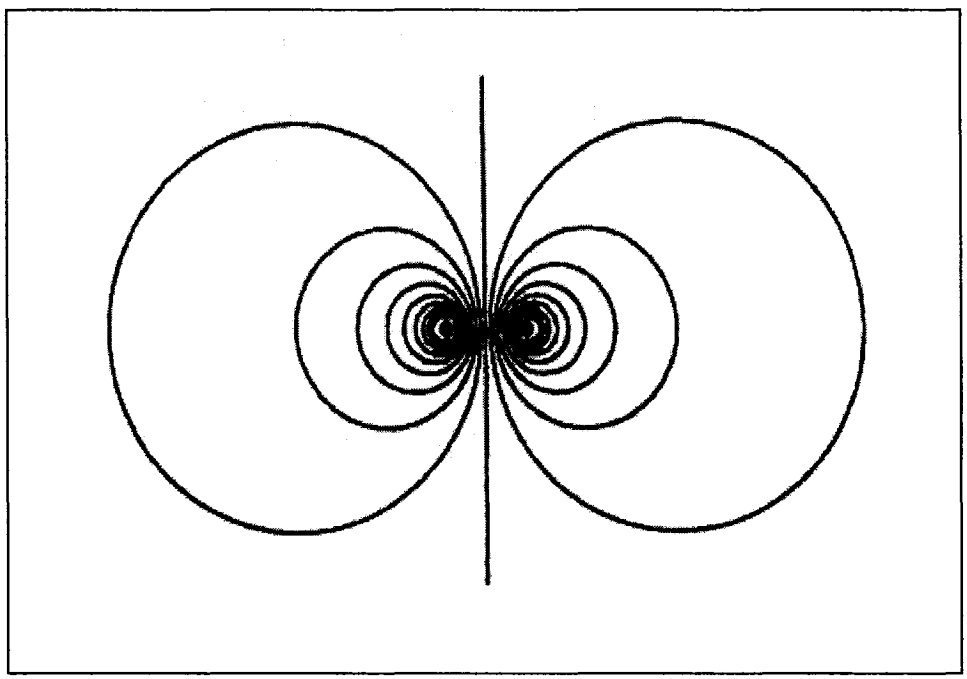

**Figure 4.9: Contours of electric field distribution normal to direction of two-rod parallel probe in material of a uniform dielectric constant (Zegelin et al. 1989)**

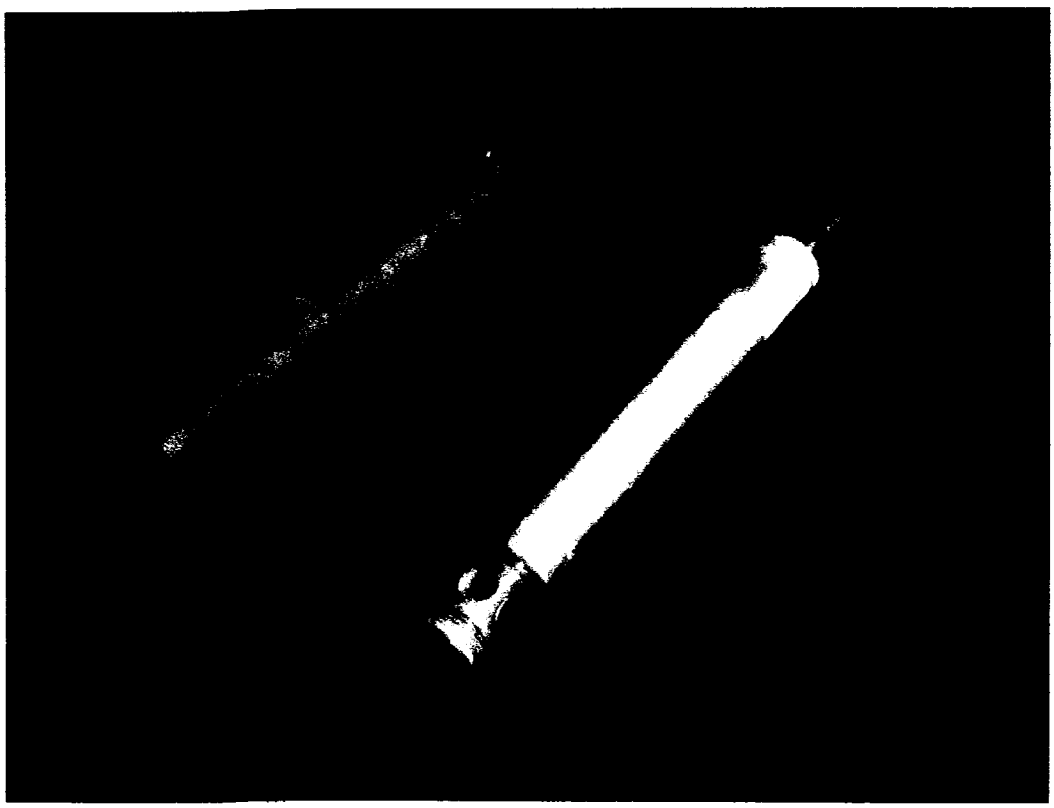

**Figure 4.10: The sampling tool**

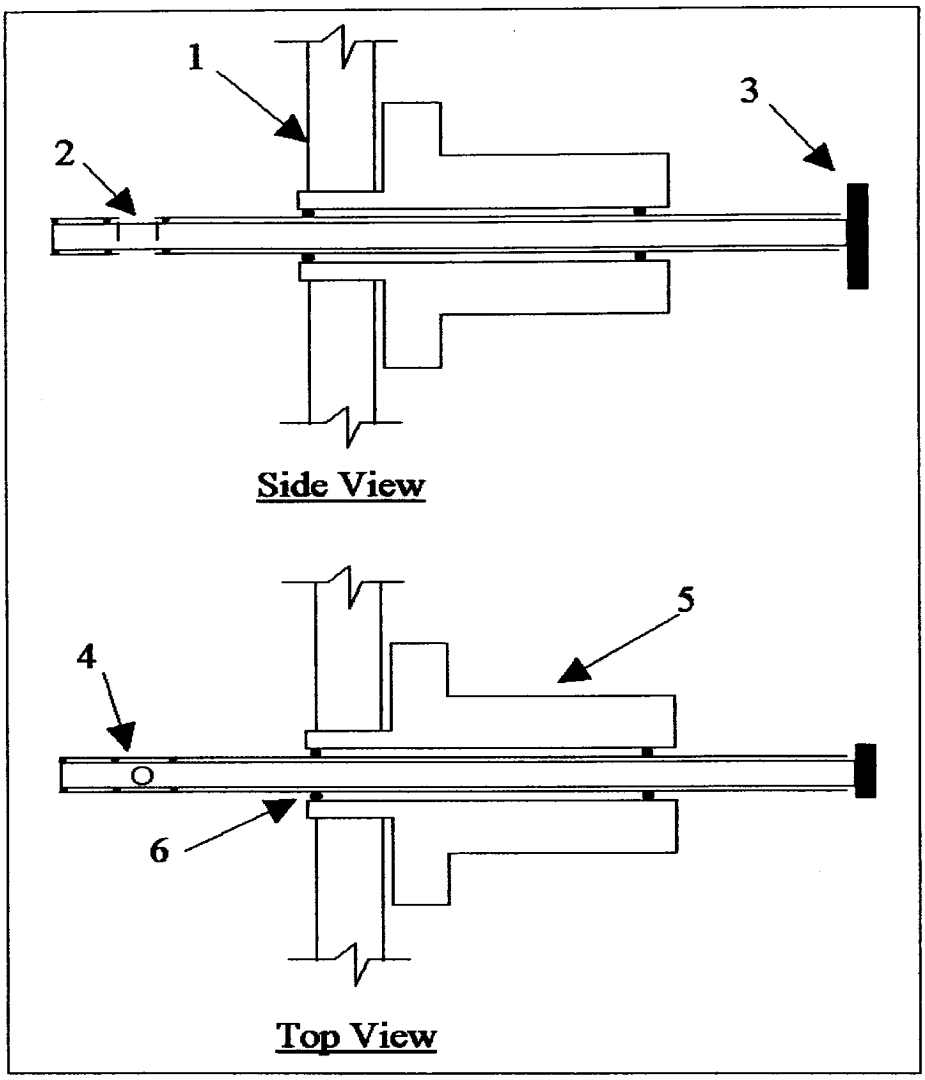


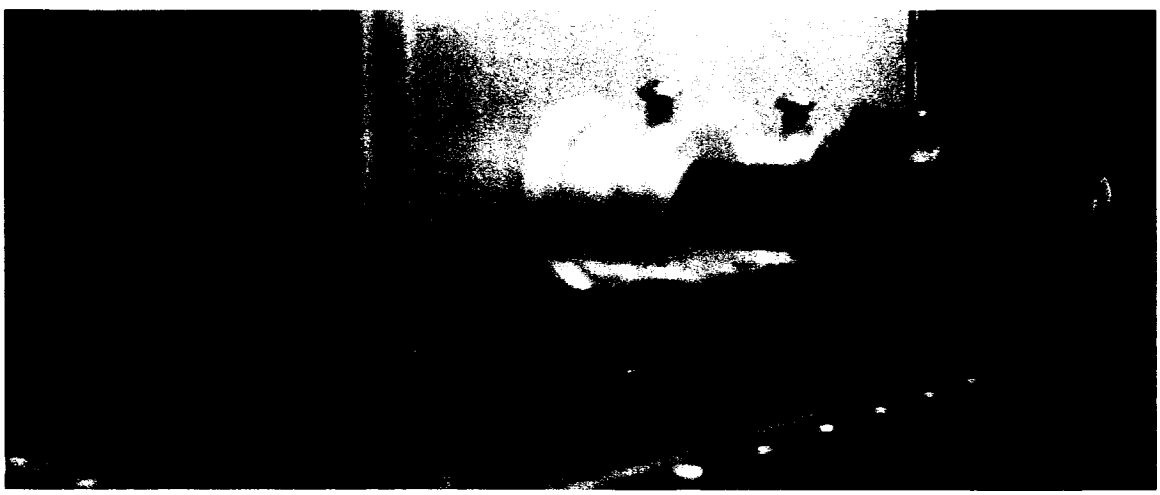

**Figure 4.11: The sampling tool**

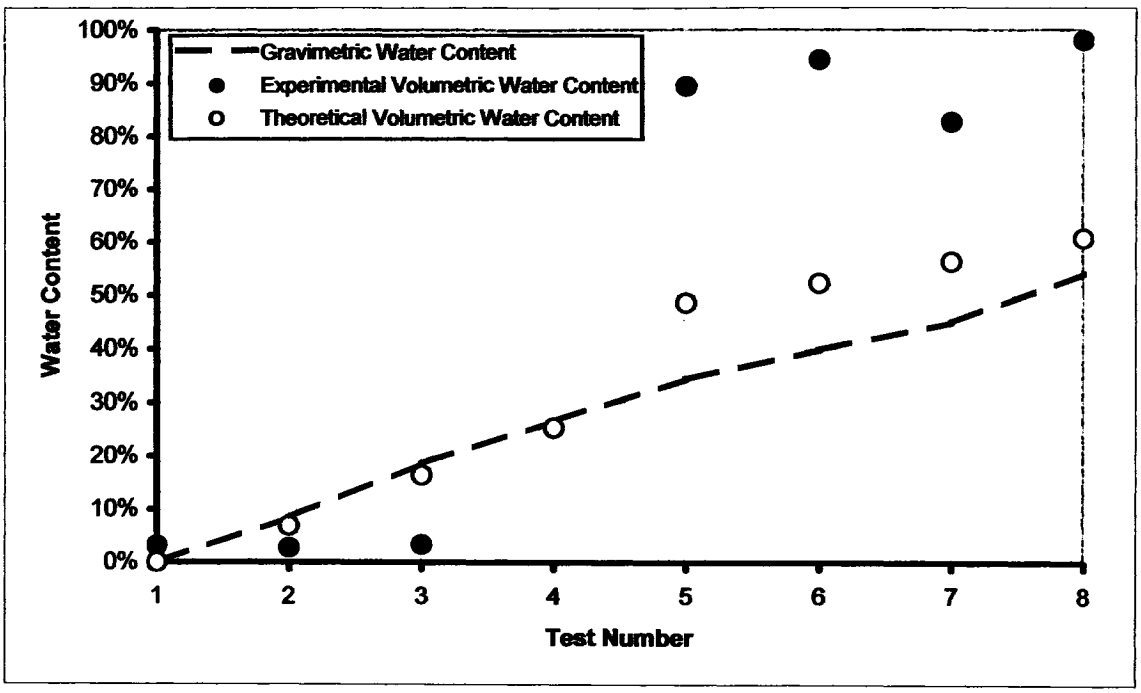


**Figure 4.12: TDR Calibration results**

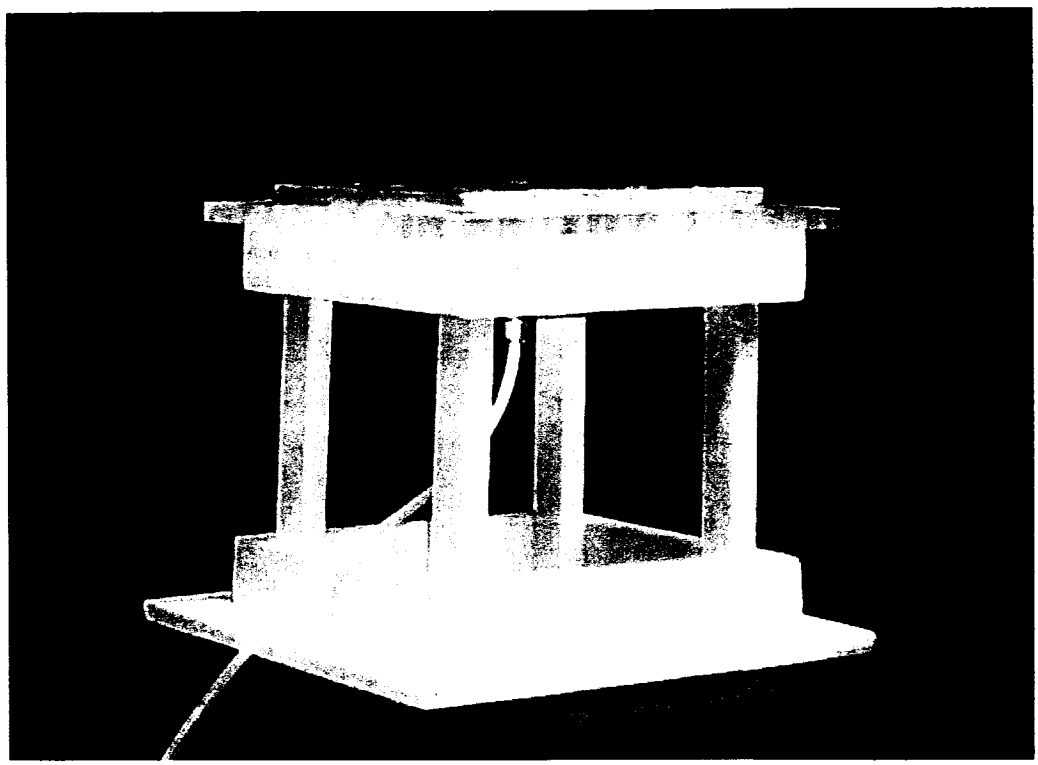

**Figure 4.13: The Modified Permeameter's stand with the seal plate**

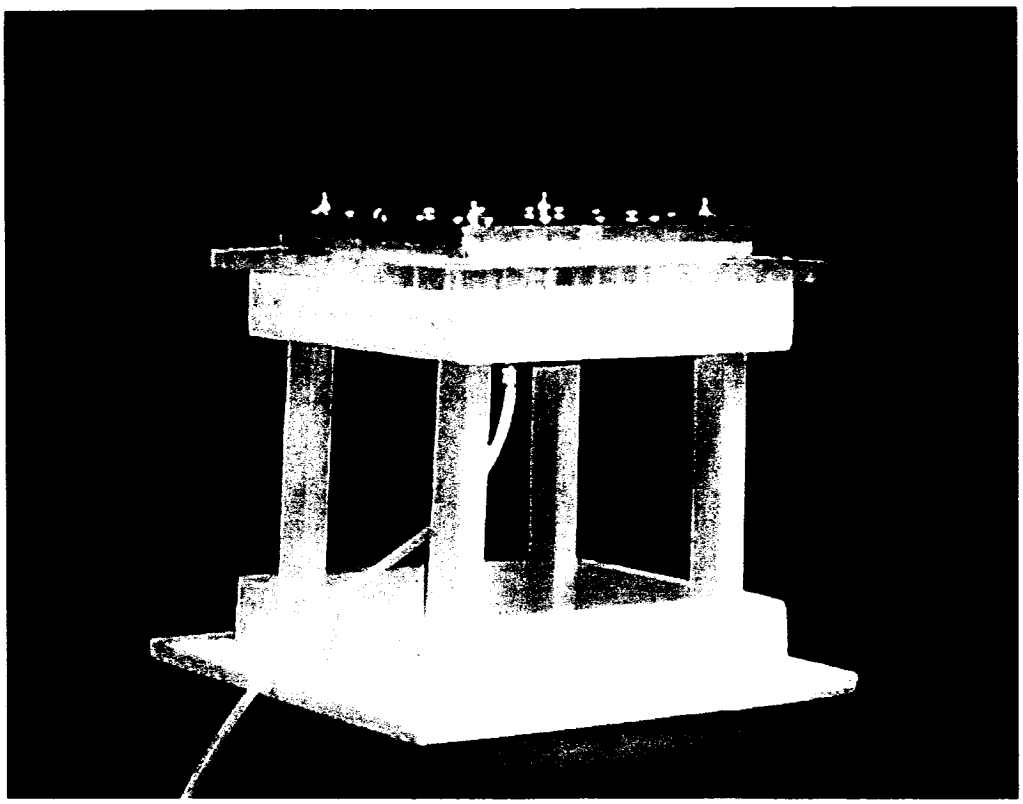

**Figure 4.14: Assembly of the porous ceramic's collar plate with the flushing system's connections**

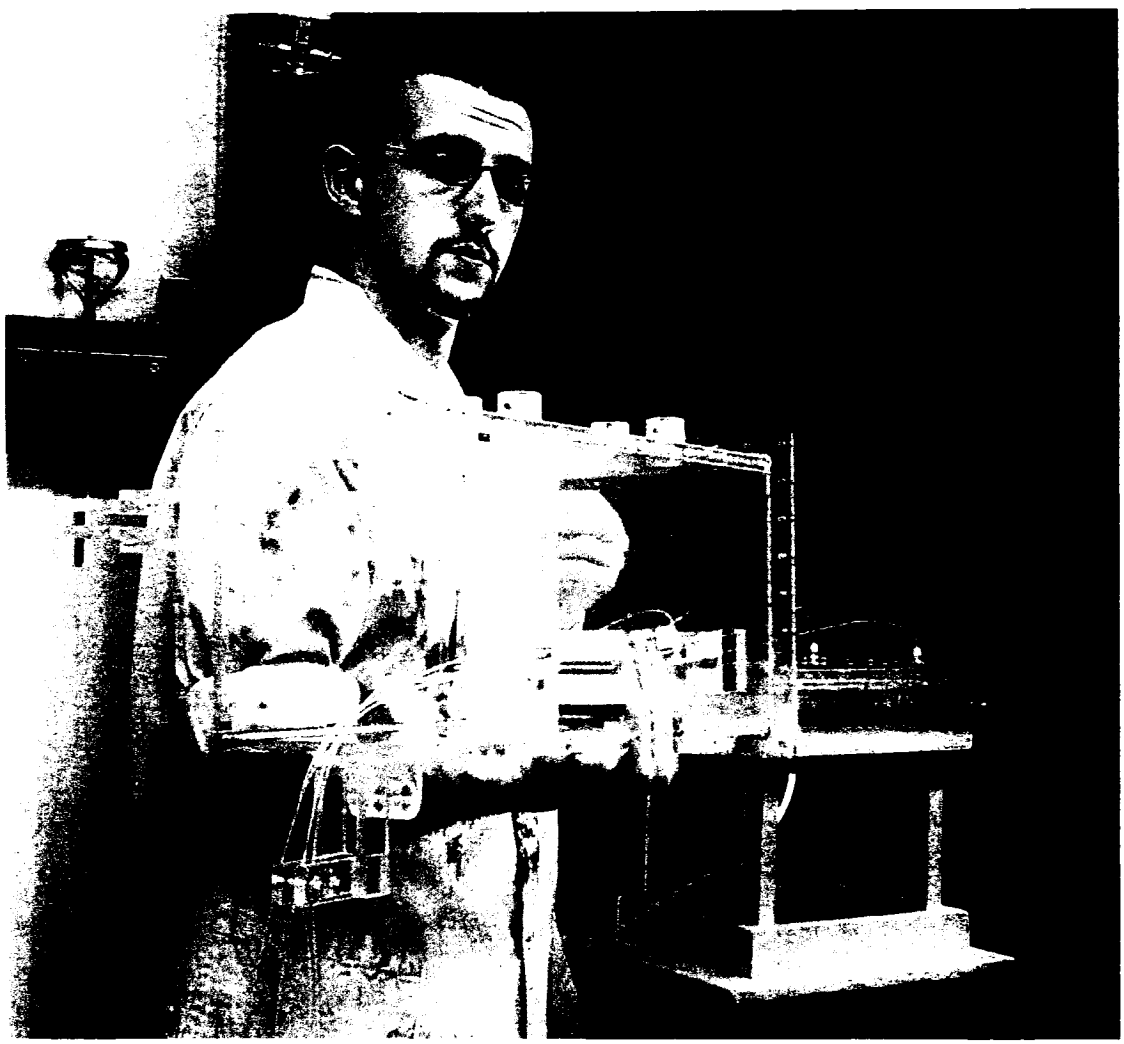

**Figure 4.15: Assembly of the Modified Permeameter with the flushing system**

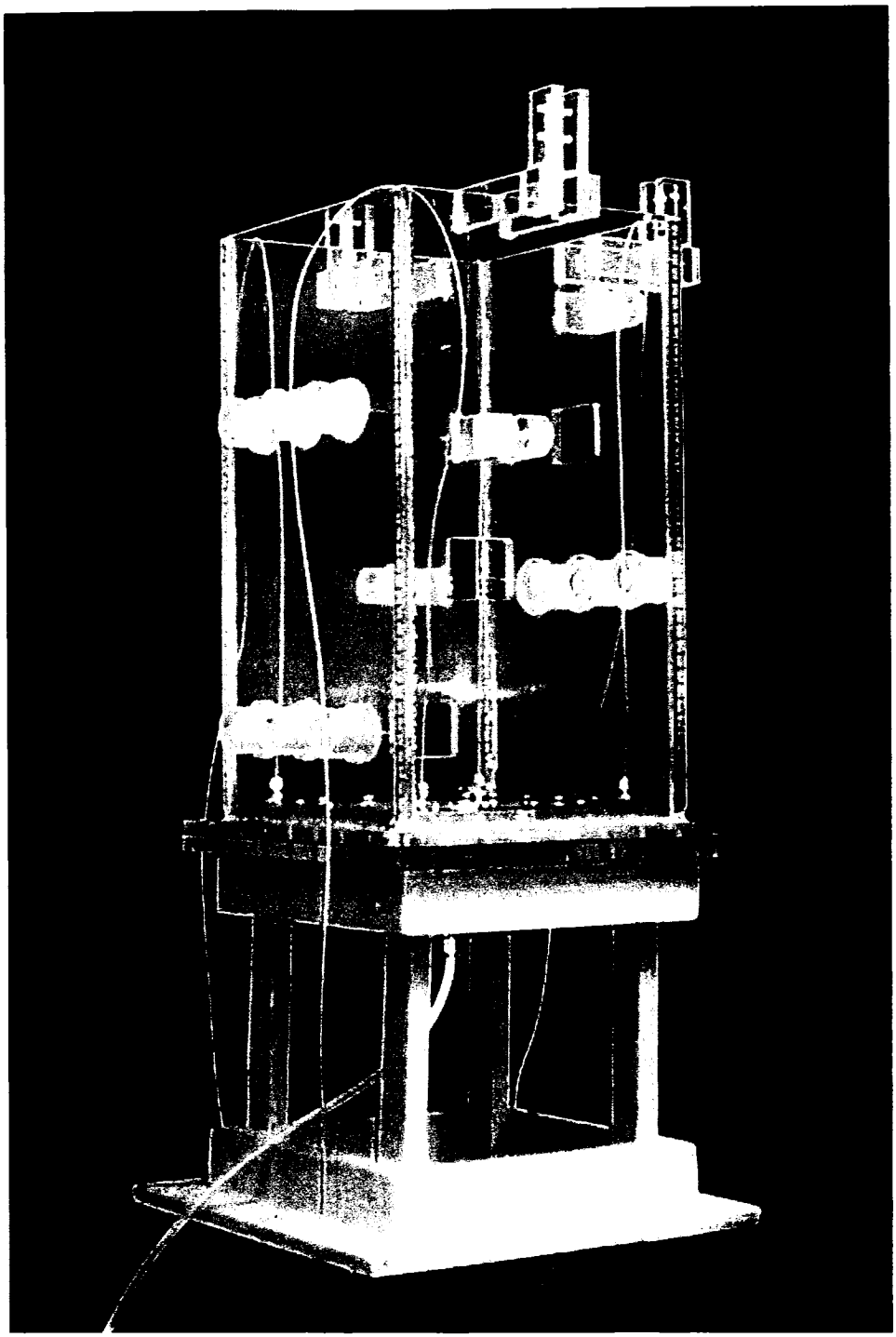

**Figure 4.16: The Modified Permeameter ready for counterweight system**

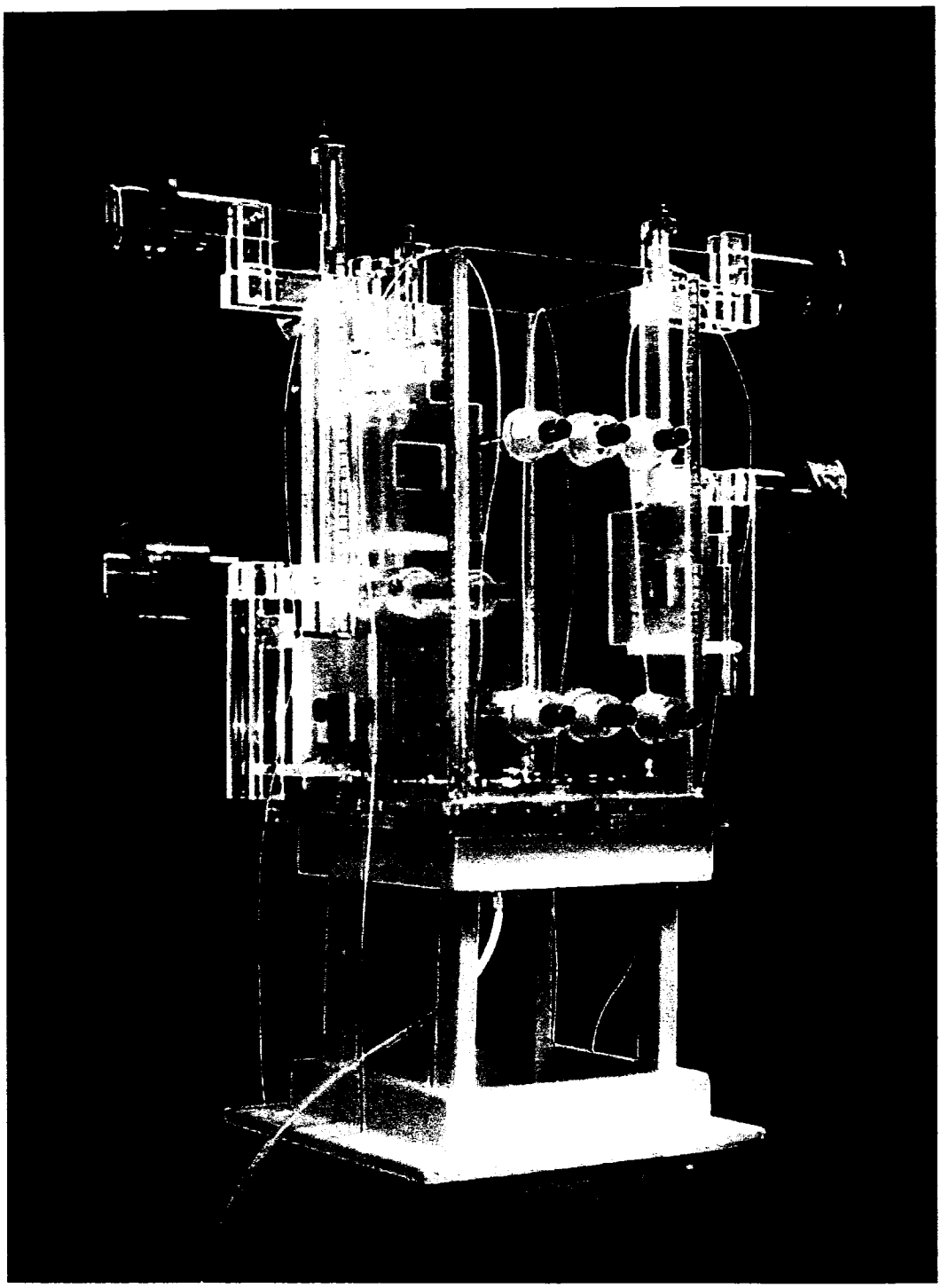

**Figure 4.17: The Modified Permeameter's counterweight system**

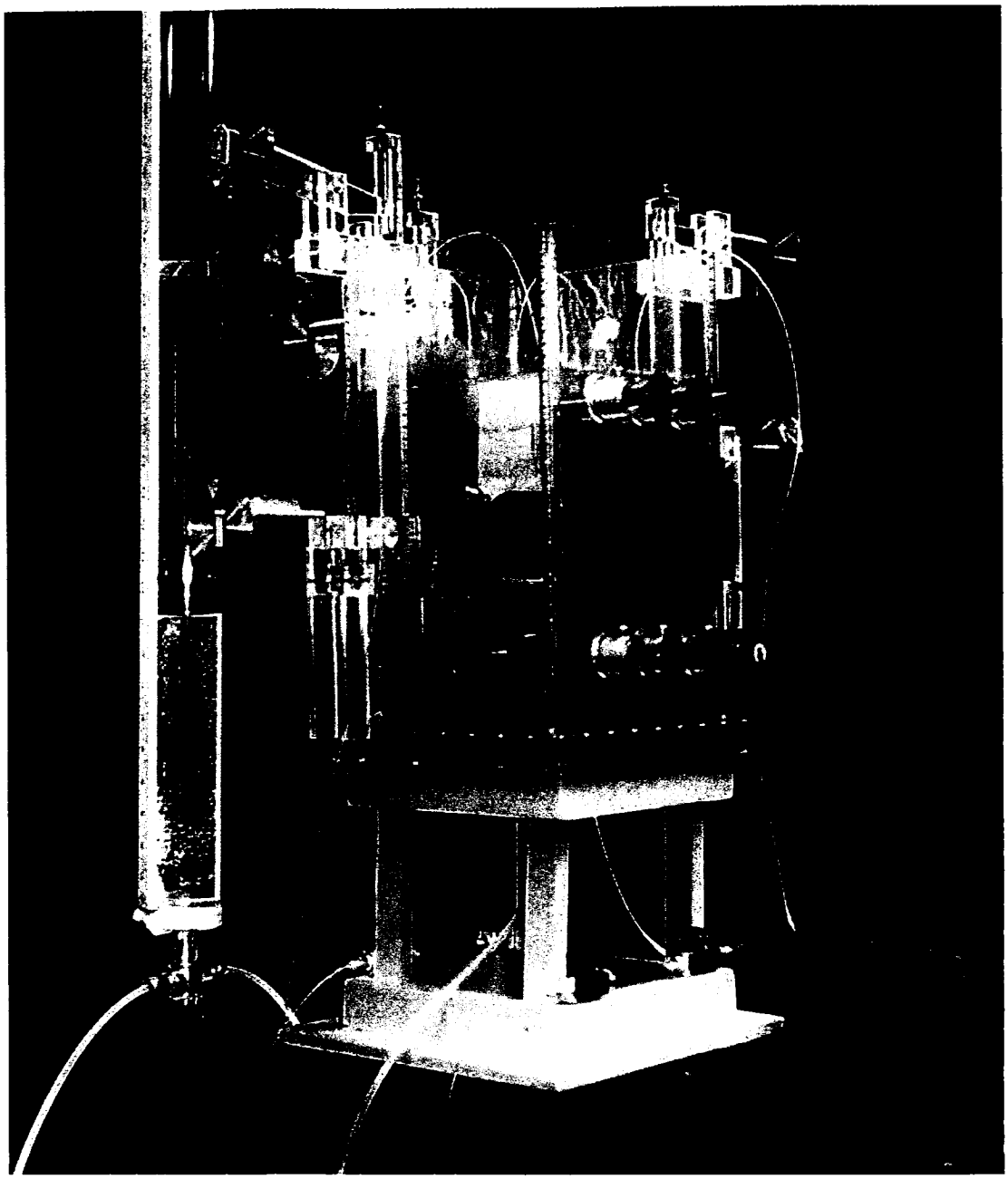

**Figure 4.18: The Modified Permeameter with a tailings sample**

# CHAPTER 5 – LABORATORY PROGRAM AND RESULTS

## 5.1 INTRODUCTION

A major portion of this research program was directed towards designing and building the Modified Permeameter, described in Chapter 4, to simultaneously determine the soil-water characteristic curve (SWCC) and the coefficient of permeability of unsaturated tailings.

In this chapter, the properties of tailings and the results associated with the unsaturated flow characteristics of the underflow and overflow tailings specimens are presented. Comparisons are provided between the measured and predicted values of coefficient of permeability variation with respect to suction for tailings specimens. The measured values of coefficient of permeability were obtained using the Modified Permeameter. The coefficient of permeability function (i.e., variation of the coefficient permeability with respect to suction) was predicted using the commercial software SoilVision.

## 5.2 TAILINGS PROPERTIES

The laboratory studies of this research program were undertaken on nickel tailings obtained from the mining operations of Falconbridge Ltd, Sudbury. According to the information provided on the Falconbridge wesite, the nickel-copper ore deposits of Falconbridge Ltd. in Sudbury are associated with a large body of igneous rock known as the Sudbury Igneous Complex (SIC). The mineralization in the deposits consists of zones of massive, inclusion-bearing massive, stringer and disseminated sulphides associated with brecciated host rocks located in footwall troughs or embayments around the outer, lower edge of the SIC. The minerals pyrrhotite, pentlandite, chalcopyrite and pyrite are the major sulphides in the Sudbury ores. Magnetite is a common oxide mineral. Pentlandite is the main nickel-bearing sulphide with a nickel content of 33 to 35 weight percent.

Various specimens were collected from the Sudbury mine site to properly represent the different gradations that are commonly found in tailings dams and reservoirs. The tailings

specimens collected at different locations along the discharge line (i.e., feed, overflow and underflow) were stored in sealed pails before they were used for testing.

The nickel tailings under dry conditions are dark grey in colour. The same tailings under wet conditions are black in colour. They also release a very particular odour, most likely due to the presence of sulphur in the host rock.

The grain size distribution of underflow and overflow tailings was determined using the dry sieve and hydrometer methods (ASTM D 422-63). The grain size distributions of both the specimens (see Chapter 2 for a description of overflow and underflow) are provided in Figure 5.1. The underflow (coarse) sample predominantly has particle sizes that fall in the range of fine sand and the overflow (fine) sample has a silt size fraction. The gradation properties of both tailings specimens are summarised Table 5.1.

The coefficient of uniformity is low for both the specimens tested, indicating a poorly graded material with a uniform grain size. Relatively low coefficients of curvature, $C_c$ also suggests that the nickel tailings are uniform.

The specific gravity, $G_s$, was measured for both specimens using ASTM D 854-92. The Atterberg limits for both samples were determined using ASTM D 4318-84. Both the specimens were not plastic in nature. Table 5.2 summarises the above properties along with the saturated coefficient of permeability ($k_{sat}$). The saturated coefficient of permeability was determined in the laboratory using the constant head method.

### 5.2.1 The saturated coefficient of permeability ($k_{sat}$)

A series of permeameters were built to simultaneously determine the saturated coefficient of permeability $k_{sat}$ of five tailings samples in the laboratory. These permeameters were built with sections of ABS piping that can cheaply be replaced when worn or damaged.

A schematic of the permeameter system built and used to determine the laboratory $k_{sat}$ of the various tailings samples is shown in Figure 5.2. The schematic shows how the

desired value of hydraulic head ($H$) can be provided to the sample by changing the height of the reservoir.

The saturated coefficient of permeability is required as an input parameter in SoilVision to predict the coefficient of permeability of unsaturated tailings. The predicted permeability curves are also useful to decide on target suction values that can be used to collect data using the instrumentation from the Modified Permeameter.

## 5.3 SOILVISION SYSTEMS LTD, 2001

SoilVision is a commercial software package that can be used to predict the flow behaviour in unsaturated soils using several methods (Fredlund et al. 1994, van Genuchten 1980, Brooks and Corey 1964, Gardner 1956).

Several investigators have provided mathematical functions to predict the SWCC based on the information related to the physical properties of the soils or the grain size distribution data (Gupta and Larson 1979, Arya and Paris 1981, Fredlund et al. 1997).

The SoilVision software package allows the user to predict a SWCC from the grain size distribution. The software requires any three of the following four parameters to compute an estimated SWCC; the volumetric water content, $\theta$; the gravimetric water content, $w$; the dry density, $\rho_d$; and/or the specific gravity, $G_s$, along with the saturated coefficient of permeability, $k_{sat}$.

## 5.4 COARSE TAILINGS SAMPLE

### 5.4.1 Empirical results

To act as a guide during laboratory work, a SWCC and an unsaturated coefficient of permeability versus suction curve were estimated using the SoilVision software package.

5.4.1.1 Estimation of the SWCC for coarse tailings sample

A number of methods are available for predicting the SWCC using the grain size distribution data with the aid of SoilVision software (Gupta and Larson 1979, Arya and Paris 1981, Rawls and Brakensiek 1985, Vereecken et al. 1989, Tyler and Wheatcraft 1989, Scheinost et al. 1996, Fredlund et al. 1997). In several of these methods, in addition to grain size distribution data, other information such as the volumetric water content, gravimetric water content and specific gravity information are required. Table 5.3 summarises the input parameters used for estimating the SWCC of the underflow sample.

Various methods investigated for estimating the SWCC for the underflow sample provided similar estimates. The method described by Fredlund et al. (1997), was chosen for estimating the sample's SWCC in this research program.

Fredlund et al. (1997) method is found under the "Fredlund and Wilson PTF" heading in the SoilVision Software. Using the equation below the algorithm can predict the SWCC based on a soil's grain size distribution.

$$P_p(d) = \frac{1}{\ln\left[\exp(1) + \left(\frac{g_a}{d}\right)^{g_n}\right]^{g_m}} \left\{1 - \left[\frac{\ln\left(1 + \frac{d_r}{d}\right)}{\ln\left(1 + \frac{d_r}{d_m}\right)}\right]^7\right\} \qquad (5.1)$$

where:

$P_p(d)$ is the percent passing a particular grain size d.

$g_a$ is a fitting parameter corresponding to the initial break in the grain size curve.

$g_n$ is a fitting parameter corresponding to the maximum slope of the grain size curve.

$g_m$ is a fitting parameter corresponding to the curvature of the grain size curve.

$d$ is the particle diameter (mm)

$d_r$ is the residual particle diameter (mm)

$d_m$ is the minimum particle diameter (mm).

The SoilVision software allows the user to choose between a unimodal fit and a bimodal fit of the grain size distribution. The coarse tailings grain size distribution was fitted using a bimodal fit. Fredlund et al. (1997) studies show that the SWCC can be reasonably predicted for sands and silts. The accuracy is shown to be highest for coarse grained soils in comparison to fine grained soils.

The predicted SWCC for the underflow (coarse) sample is shown in Figure 5.3. The curve is plotted only for a suction range of 0.1 to 1000 kPa. The estimated air-entry value is approximately 1.5 kPa for the underflow sample.

5.4.1.2 Prediction of the conductivity curve for the coarse tailings sample

Several methods are available in the literature to predict the coefficient of permeability using the SWCC and the saturated coefficient of permeability (Gardner 1958, Brooks and Corey 1964, Mualem 1976, van Ganuchten 1980, Fredlund et al. 1994).

Brooks and Corey (1964) equation is used for predicting the coefficient of permeability function using the estimated SWCC for the underflow sample (Equation 5.2). This equation is useful for predicting the coefficient of permeability of coarse-grained soils such as the underflow sample.

$$k_{\psi} = k_{sat} \left\{ 1 \quad for\ (\psi \le \psi_b) \quad ; \quad \left( \frac{\psi_b}{\psi} \right)^{2+\left(\frac{5\lambda}{2}\right)} \quad for\ (\psi > \psi_b) \right\} \tag{5.2}$$

where:

$k_{\psi}$ is the coefficient of permeability for a given suction $\psi$

$k_{sat}$ is the saturated coefficient of permeability

$\psi_b$ is the air-entry pressure

$\psi$ is the measured suction

$\lambda$ is a fitting parameter

The predicted coefficient of permeability function of the coarse tailings sample, computed using Equation 5.2, is shown in Figure 5.4. The function characteristics are consistent with the SWCC behaviour of underflow sample showing a very steep curve (Figure 5.3). The rapid decrease in the coefficient of permeability over a relatively small change in suction agrees with the SWCC behaviour that clearly demonstrates a rapid drop in water content once the air-entry value is attained. The unsaturated coefficient of permeability decreases by approximately four orders of magnitude when suction increases from 0 to 10 kPa.

### 5.4.2 Coarse tailings experimental results

Using the Modified Permeameter, the unsaturated behaviour of a coarse tailings sample was observed within the suction range of 0 kPa to 10 kPa.

#### 5.4.2.1 Coarse tailings experimental SWCC results

Figure 5.5 shows the measured water content values plotted against the measured suction values. The experimental values show good agreement with the estimated SWCC.

#### 5.4.2.2 Coarse tailings experimental conductivity curve results

The unsaturated coefficient of permeability can be computed provided that a minimum of two locations along the axis of flow are instrumented to measure water content and suction.

Figure 5.6 shows the middle sampling tools barely covered by the underflow sample immediately after the initial settlement of the slurry, before drainage of the excess water. The dashed line in Figure 5.6 indicates the top of the sample. As the sample started to drain, the tailings consolidated and cracking occurred, exposing the sampling tools. Figure 5.7 shows typical cracking observed at the top surface of the tailings due to consolidation that initiated around the sampling tools.

Due to consolidation, insufficient data were gathered to enable computation of the conductivity curve of the coarse underflow sample.

## 5.5 FINE TAILINGS SAMPLE

The overflow is the finer material separated by the cyclones. The overflow, also known as the slimes, exhibits a much lower saturated coefficient of permeability than the coarser underflow material. The saturated coefficient of permeability of the slimes was measured to be $1x10^{-6}$ cm/sec.

### 5.5.1 Fine tailings empirical results

The input parameters used to estimate the SWCC are given in Table 5.4. The SWCC was estimated with the SoilVision software, using the Fredlund et al. (1997) approach.

#### 5.5.1.1 Estimation of the SWCC for fine tailings sample

The estimated SWCC for the overflow sample is shown in Figure 5.8. The estimated air-entry value of the overflow sample is approximately 10 kPa, compared to 1.5 kPa for the underflow sample.

#### 5.5.1.2 Prediction of the conductivity curve for the fine tailings sample

The predicted conductivity curve for the fine tailings, shown in Figure 5.9, was obtained with the SoilVision software. The coefficient of permeability function was predicted using the Brooks and Corey (1964) method.

According to the estimated conductivity curve, the finer overflow sample would remain at an approximately constant coefficient of permeability until a suction of at least 10 kPa would be reached (i.e., until the air-entry value was attained) at which point, the coefficient of permeability would decrease sharply.

### 5.5.2 Fine tailings experimental results

The experimental portion of this research program dealing with the fine tailings was also conducted in the laboratory using the Modified Permeameter.

5.5.2.1 Fine tailings experimental SWCC results

Figure 5.10 shows the water content plotted against the suction values, along with the predicted curve obtained using the SoilVision software.

5.5.2.2 Fine tailings experimental conductivity results

The suction and water content values measured during testing were plotted in relation to their respective depths and time intervals. The unsaturated coefficient of permeability can be computed using this information.

Figure 5.11 shows the volumetric water content values measured at each sensor depth, for three different time periods. Equation 5.3 was used to calculate the volume of water flowing out of the sample.

$$\Delta V = A \int_{z_o}^{z_1} (\Delta\theta) dz \tag{5.3}$$

where:

$A$ is the cross-sectional area of the sample

$z_o$, $z_1$ are two consecutive sensor depths

$\Delta\theta$ is the volumetric water content difference between $z_o$, $z_1$

Figure 5.12 shows the suction values measured at each sensor location for the same three time periods shown in Figure 5.11. The hydraulic gradient is determined according to Equation 5.4.

$$-\left(\frac{dh}{dz}\right) = 1 + \left(\frac{\delta\psi}{\delta z}\right) \tag{5.4}$$

The volume of water flowing out of the sample, along with the hydraulic gradient acting at the given time interval are then used in Equation 5.5 to determine the unsaturated coefficient of permeability.

$$k_{unsat} = -\frac{\Delta V}{A\Delta t}\left(\frac{1}{dh/dz}\right) \tag{5.5}$$

where:

$\frac{\Delta V}{A}$ is the volume of water flowing out of the sample during the selected time increment

$-\left(\frac{dh}{dz}\right)$ is the hydraulic gradient acting during the selected time increment

The results obtained using Equation 5.5, are plotted in Figure 5.13. A significant difference exists between the predicted curve and the experimental results.

Previous researchers who used the Instantaneous Profile method have reported significant scatter in experimental results. Hamilton et al. (1979) reported variability of up to one order of magnitude. Meerdink et al. (1996) reported scatter in experimental results close to two orders of magnitude. Barbour et al. (2002) reported experimental unsaturated coefficients of permeability with up to six orders of magnitude difference.

## 5.6 SUMMARY

Although the unsaturated coefficients of permeability obtained with the Modified Permeameter using the Instantaneous Profile method appear scattered, the experimental portion of this research program has proven successful.

The Modified Permeameter designed and built for investigating the behaviour of tailings throughout the entire transition from a saturated to an unsaturated phase, yielded data throughout the transition. For the two tailings samples used in this research (fine and coarse samples), sufficient data was amassed to compare experimental values with the theoretical SWCC.

Using the Instantaneous Profile method, experimental unsaturated coefficient of permeability values were determined for the fine, overflow tailings sample. Due to problems

with the coarse, underflow tailings sample, insufficient data were measured to determine unsaturated coefficient of permeability values.

Laboratory determination of the unsaturated coefficient of permeability is difficult. In order to improve the quality of the results, it is this researcher's opinion that continuous, automated data-gathering equipment must be used in combination with the Modified Permeameter.

The benefit of software packages such as SoilVision became obvious during the laboratory portion of this research program. Prediction of properties such as the SWCC from the grain size distribution curve provides a fast and inexpensive means of obtaining valuable results. From a practical point of view, preliminary designs can easily be achieved from the theoretical curves produced using the algorithms found in such softwares as SoilVision.

| Parameter | Overflow | Underflow |
|---|---|---|
| | | |
| Clay fraction | 0.0% | 3.5% |
| Slit fraction | 100.0% | 27.4% |
| Sand fraction | 0.0% | 69.1% |
| $C_c$ | 1 | 1.5 |
| $C_u$ | 1.3 | 5.2 |
| | | |

**Table 5.1: Gradation properties**

| Parameter | Overflow | Underflow |
|---|---|---|
| | | |
| $G_s$ | 2.91 | 2.99 |
| *LL* | 31.1% | 8.4% |
| *PL* | N/A | N/A |
| *PI* | N/A | N/A |
| $k_{sat}$ (cm/sec) | 1.0e-6 | 2.4e-3 |
| | | |

**Table 5.2: Physical properties**

| Parameter | Value | Units |
|---|---|---|
| | | |
| Volumetric Water Content, | 0.47 | $m^3/m^3$ |
| *Gravimetric Water Content, w* | 35.00 | kg/kg |
| *Specific Gravity, $G_s$* | 2.99 | |
| | | |

**Table 5.3: Underflow input parameters**

| Parameter | Value | Units |
|---|---|---|
| | | |
| Volumetric Water Content, | 0.60 | $m^3/m^3$ |
| *Gravimetric Water Content, w* | 50.50 | kg/kg |
| *Specific Gravity, $G_s$* | 2.91 | |
| | | |

**Table 5.4: Overflow input parameters**

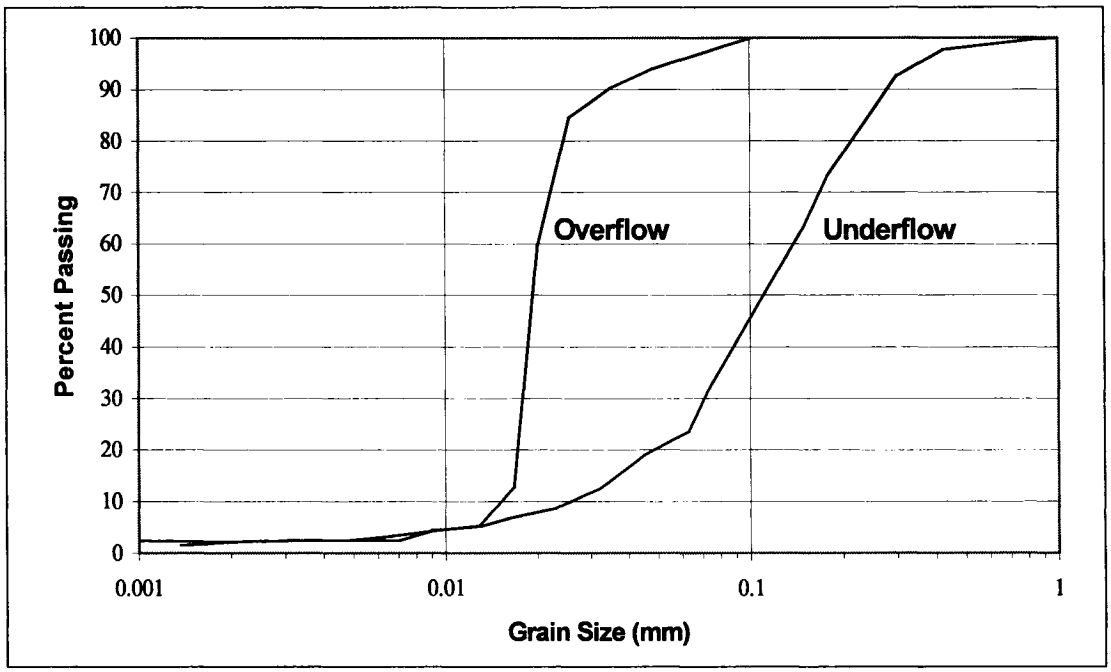


**Figure 5.1: Nickel tailings grain size distribution curve**

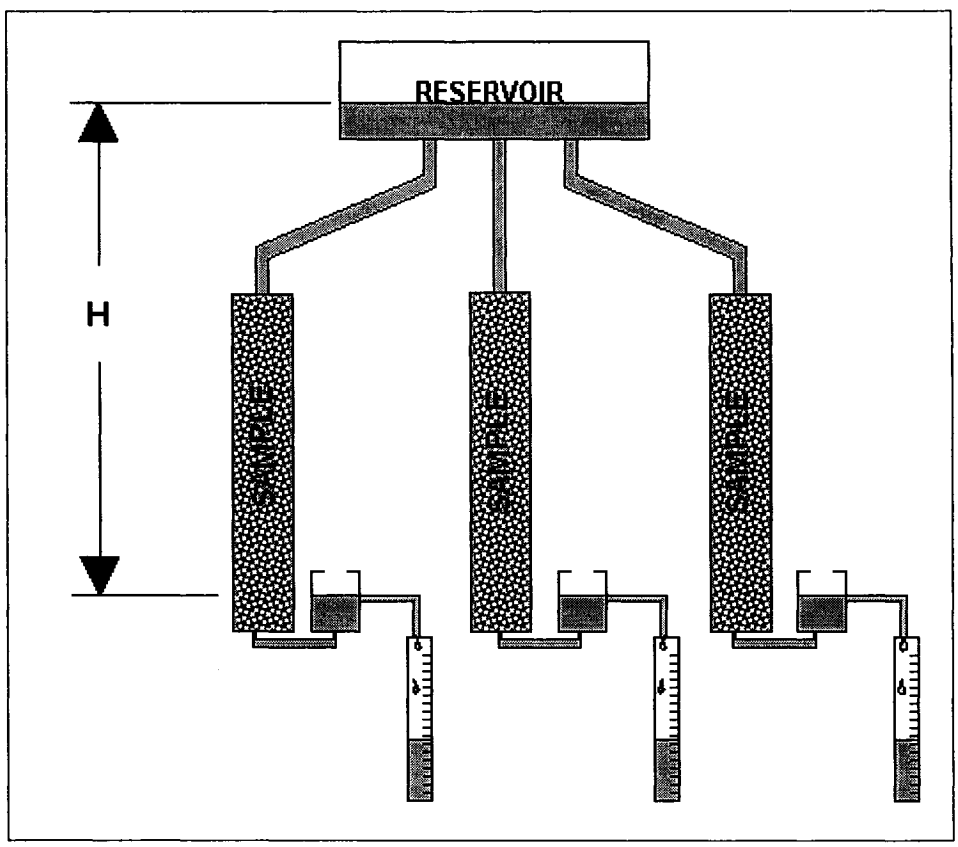


**Figure 5. 2: Schematic diagram of permeameter used to determine $k_{sat}$**

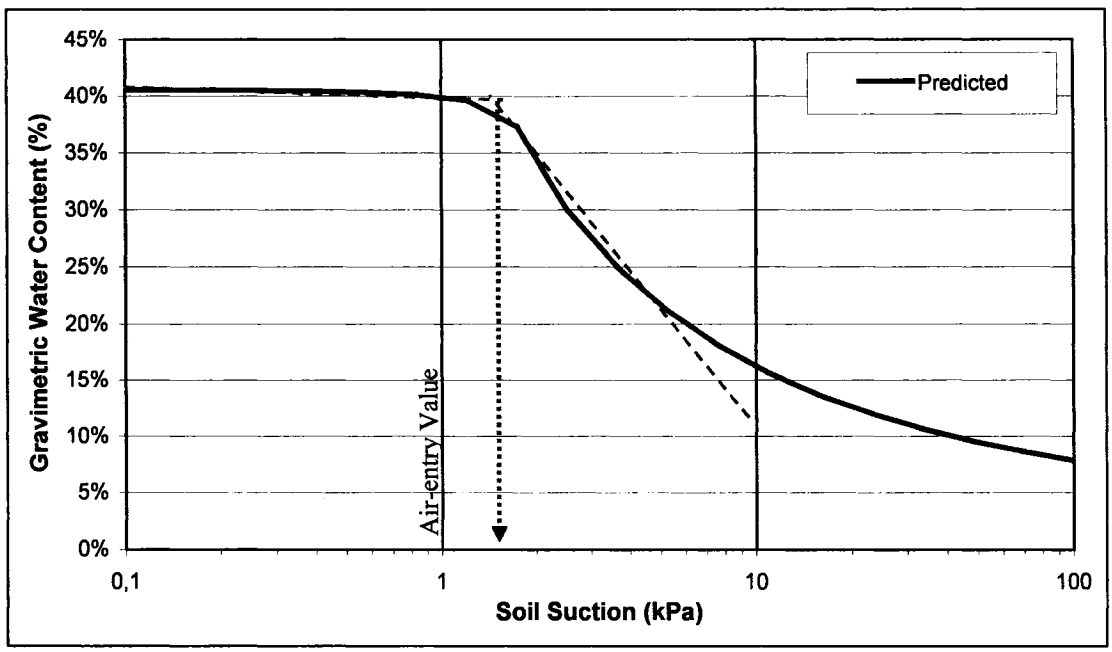


**Figure 5.3: Predicted SWCC for underflow tailings**

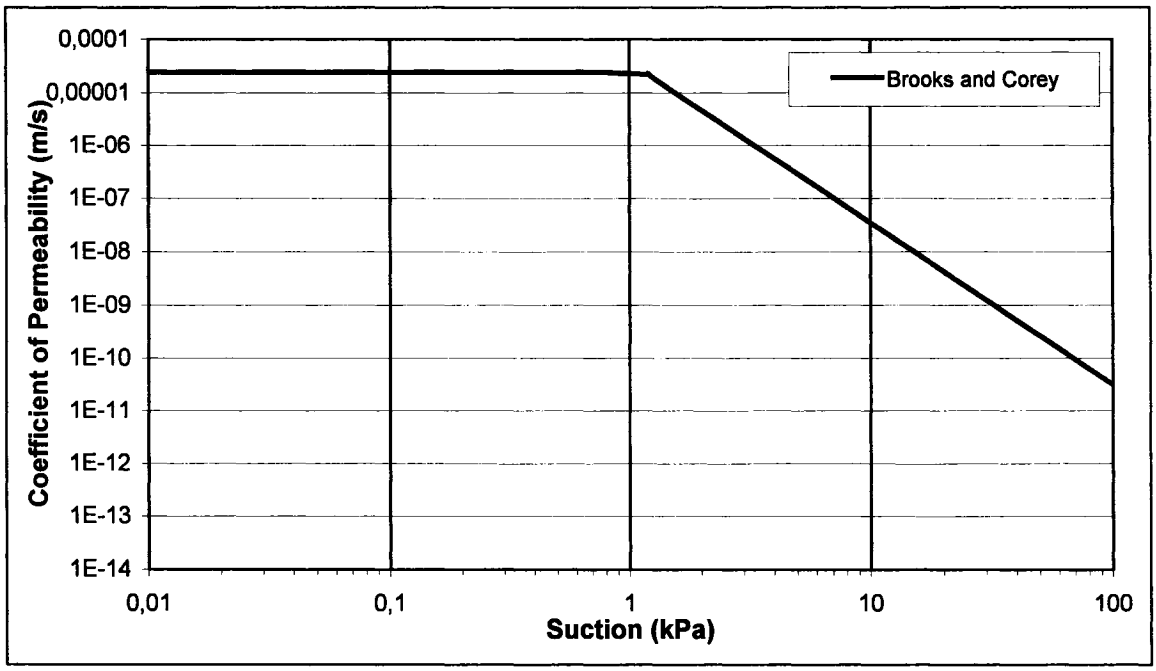


**Figure 5.4: Predicted conductivity curve for underflow tailings using Brooks and Corey (1964) model**

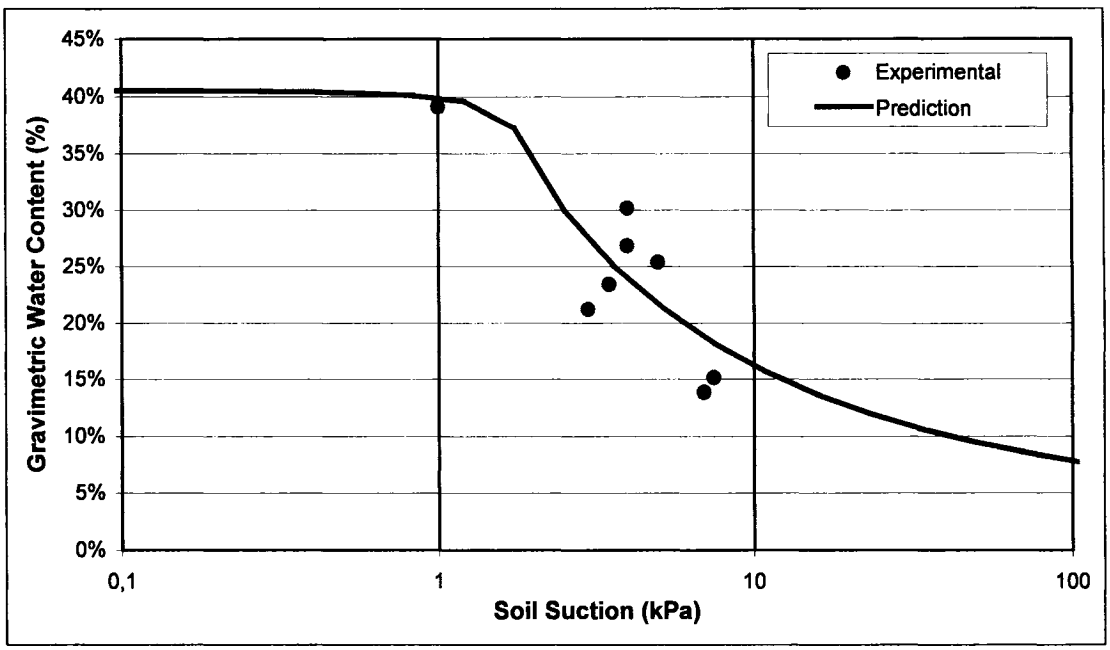


**Figure 5.5: Experimental SWCC for underflow tailings**

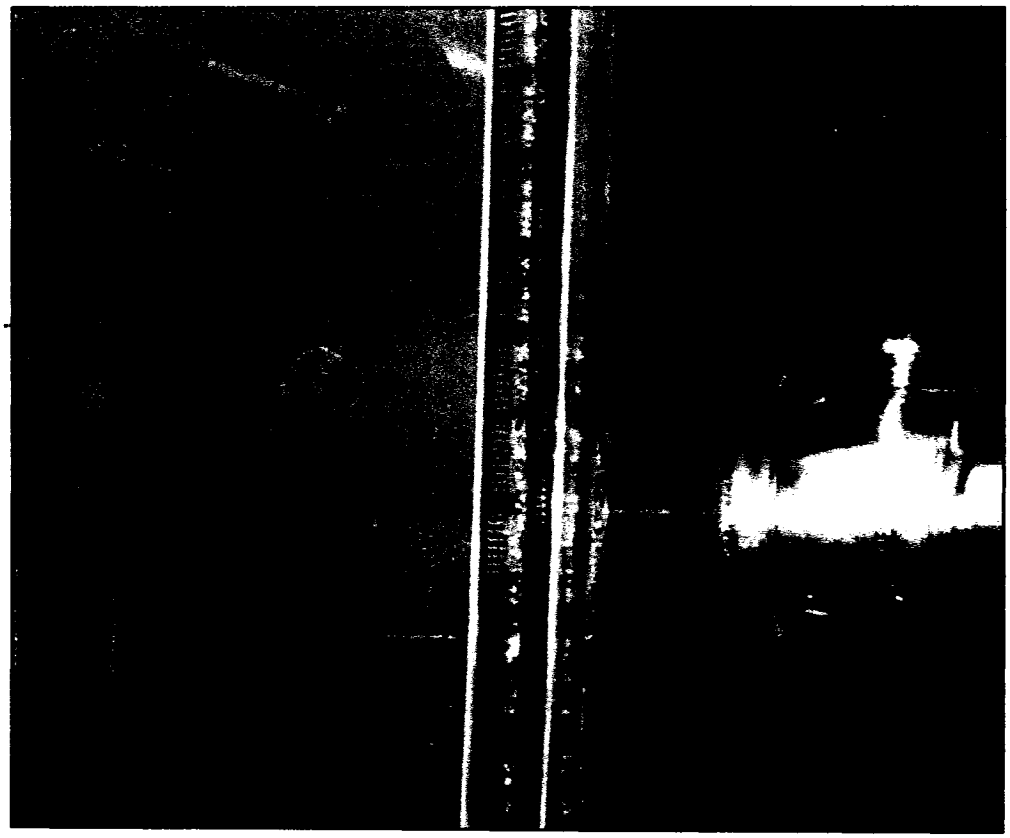

**Figure 5.6: Close-up of underflow sample at sampling tools location**

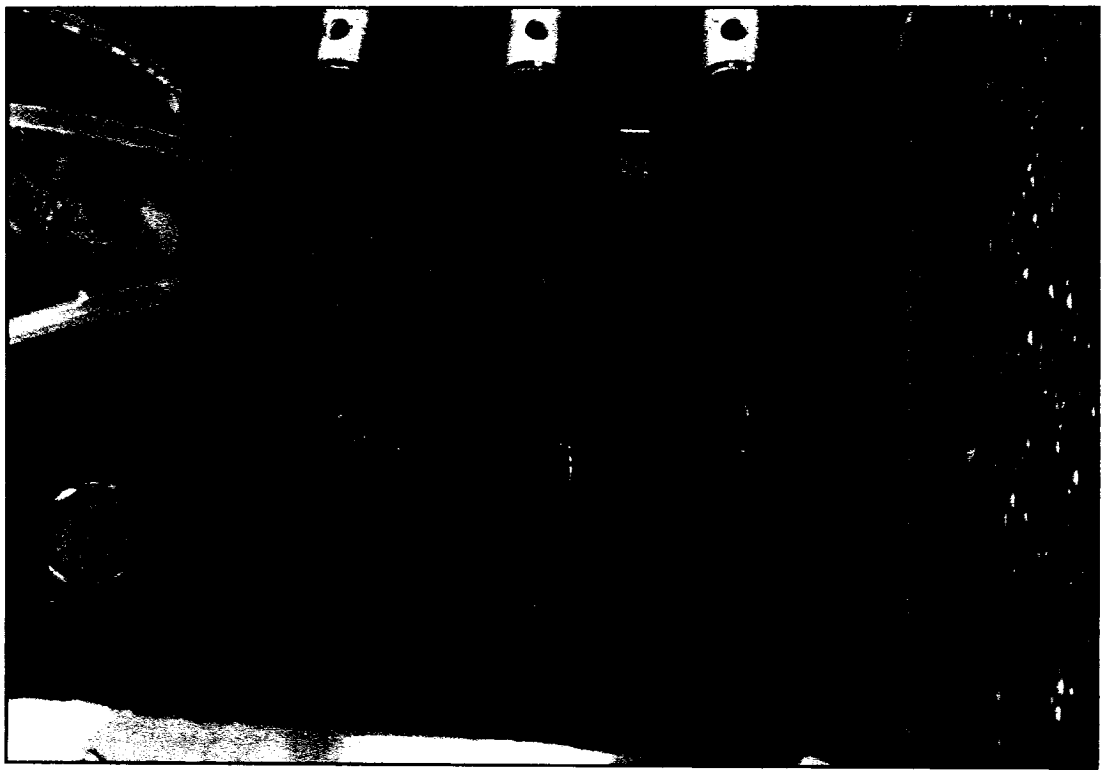

**Figure 5.7: View of cracking due to consolidation of the coarse tailings**

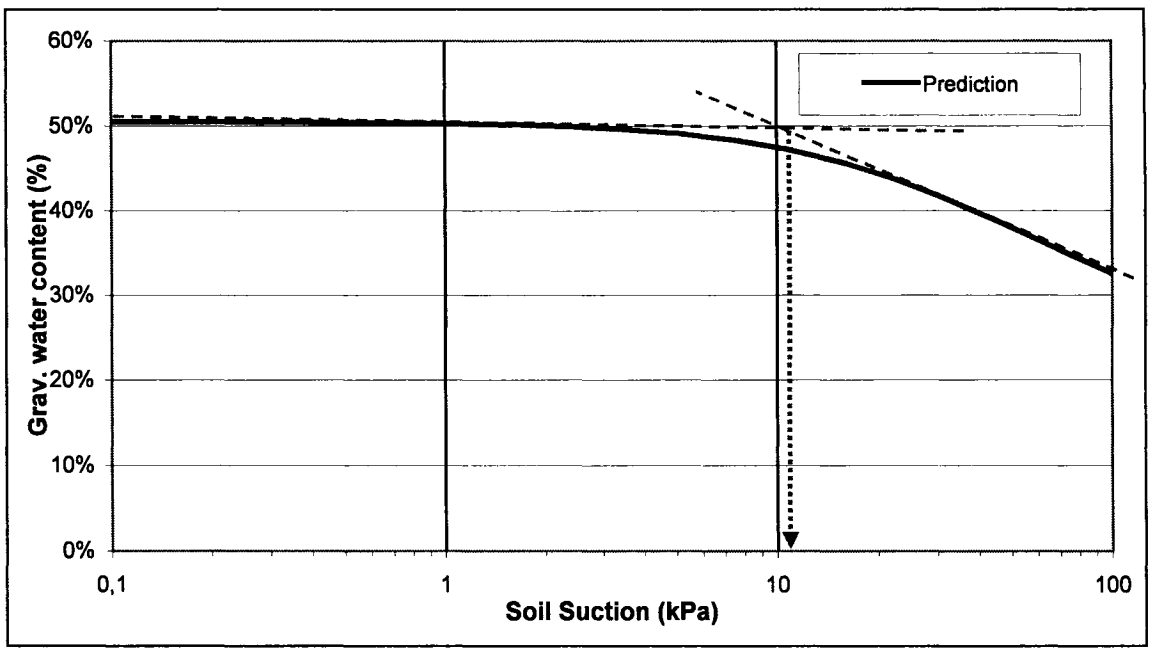


**Figure 5.8: Predicted SWCC for overflow tailings**

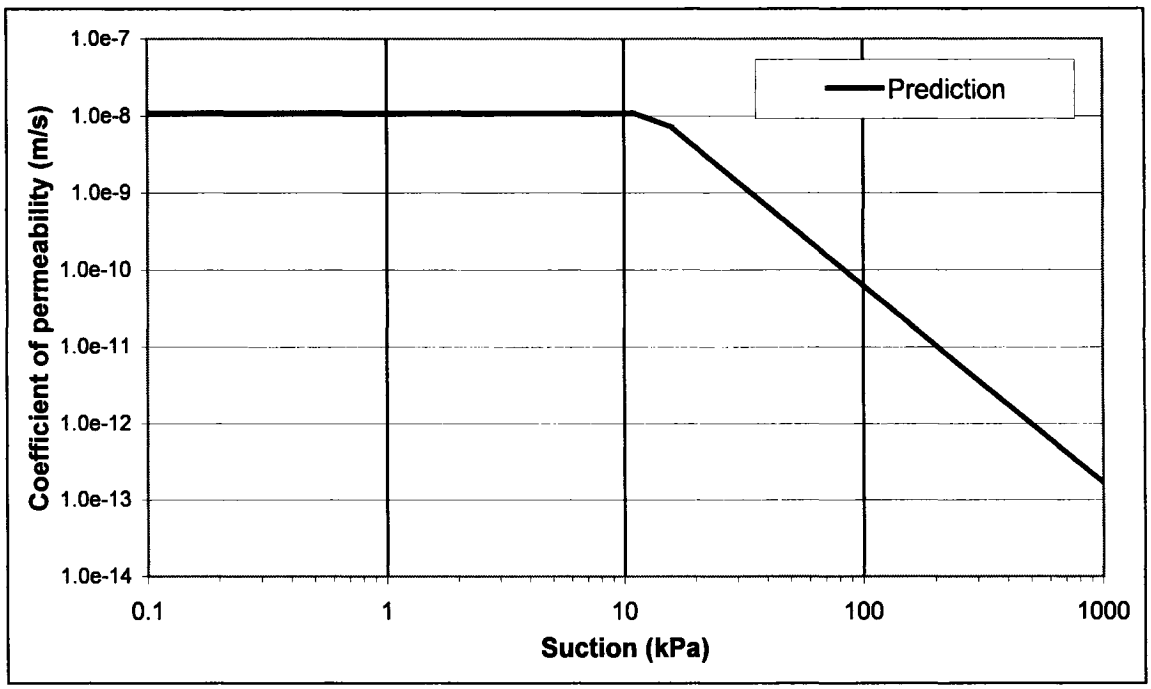


**Figure 5.9: Predicted conductivity curve for overflow tailings using Brooks and Corey (1964) model**

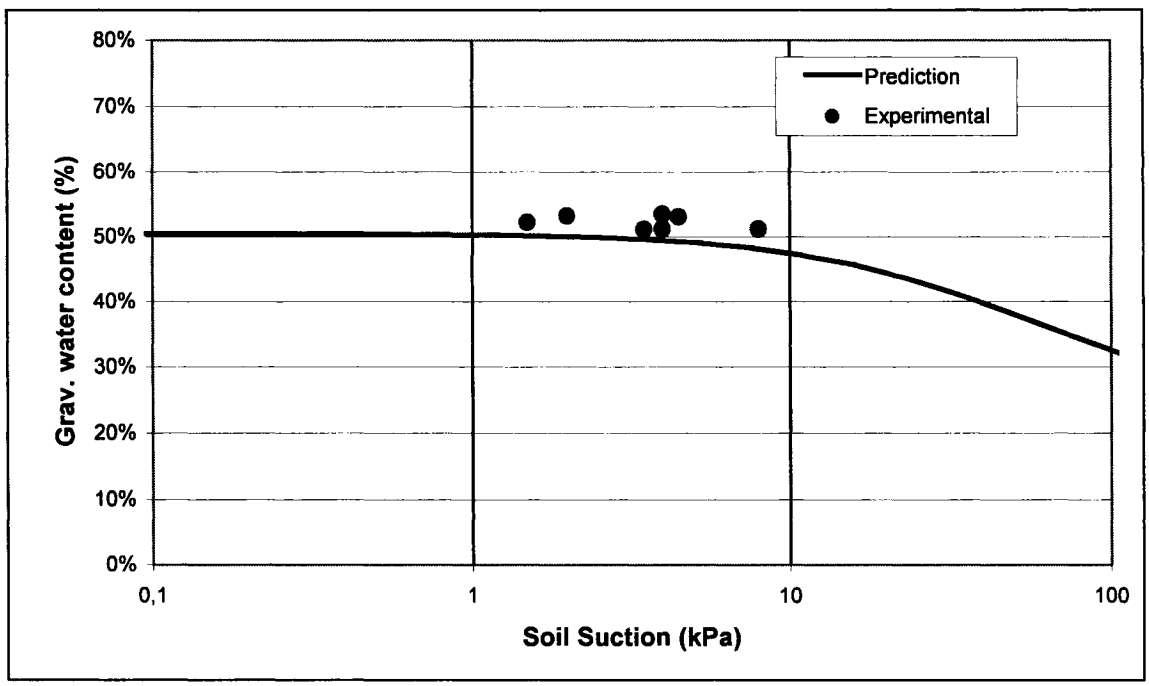


**Figure 5.10: Experimental SWCC for overflow tailings**

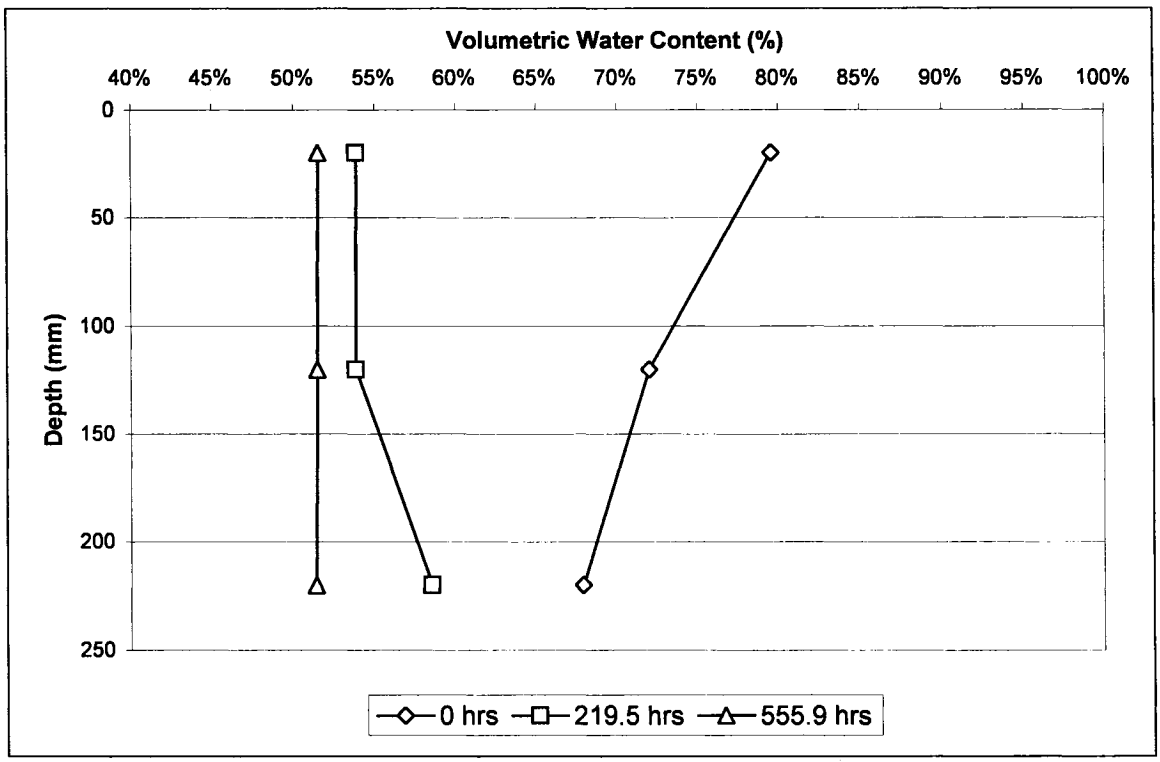


**Figure 5.11: Volumetric water content against depth for three time intervals**

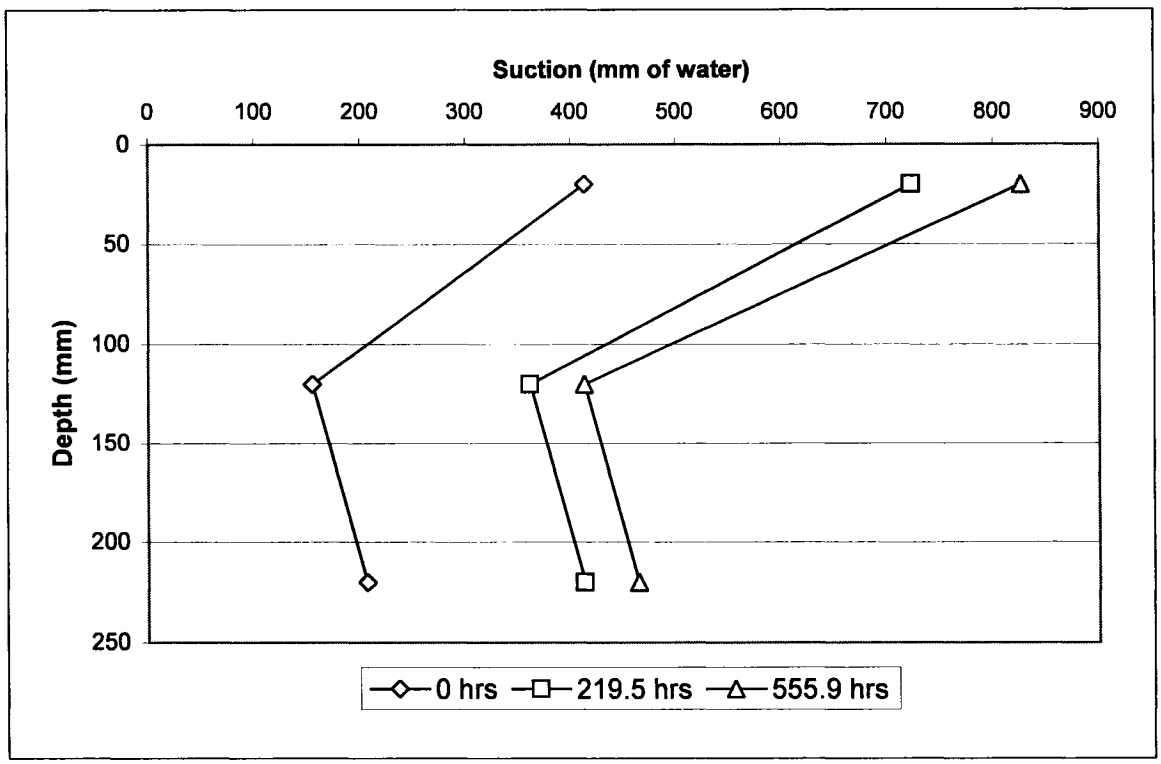


**Figure 5.12: Suction against depth for three time intervals**

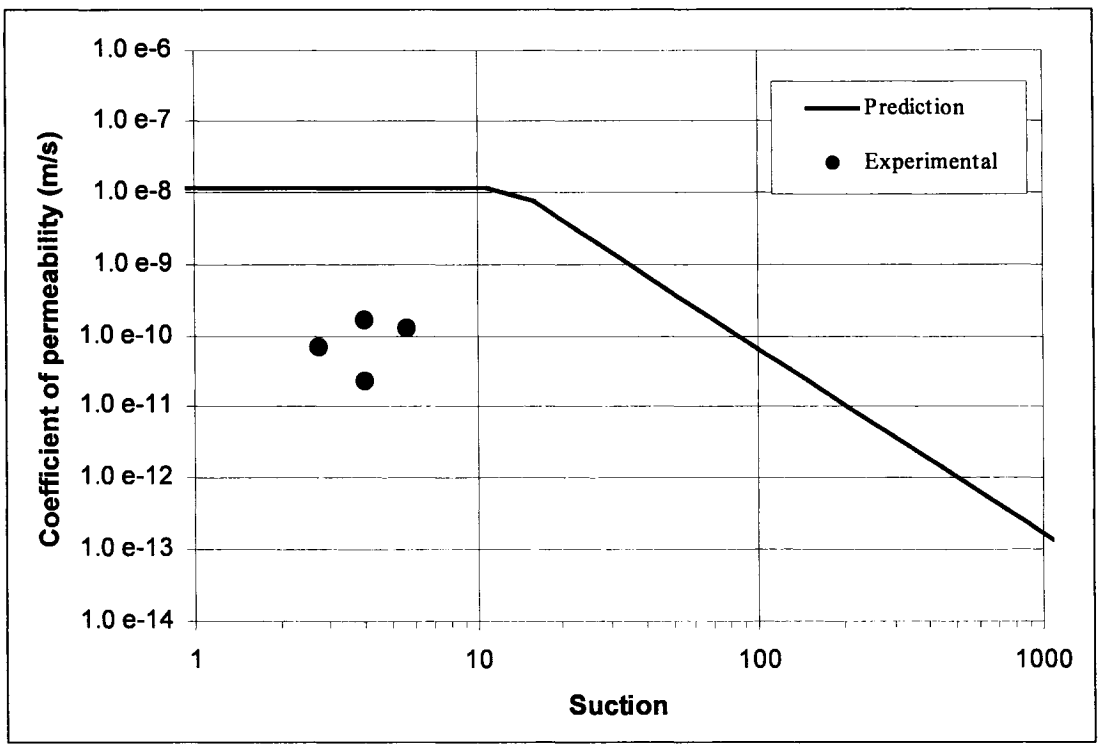


**Figure 5.13: Experimental conductivity curve for overflow tailings**

# CHAPTER 6 – MODELING FLOW THROUGH TAILINGS DAMS

## 6.1 INTRODUCTION

The objective of the modeling portion of this research is to demonstrate the importance of maintaining a lengthy beach, throughout the entire operational life of the dam. To illustrate the benefits of a long and well-maintained beach, seepage in a tailings dam is simulated with the SEEP/W software from by Geo-Slope Inc.

Although several subcategories of upstream tailings dams exist, the focus of this modeling portion is place on upstream dams that are raised with the cycloning process.

## 6.2 UPSTREAM TAILINGS DAM

The upstream tailings dam is built on a footprint that typically does not increase outwards as the dam is raised. The crest of the dam is raised in such a way to move in the upstream direction, away from the centreline of the starter dam. The main advantage of this type of dam is the small amount of material that is required to raise the crest and increase the reservoir's capacity (see Chapter 2 for more details). The main disadvantage of the upstream dam is that the dam is raised by placing material on saturated, unconsolidated, liquefiable material. For many years, the advantages outweighed the disadvantages, because as it is shown in Chapter 2, more than half of all tailings dams built in the world were built using one form or another of the upstream dam.

Several researchers and regulatory bodies (Davies and Martin 2000, Klohn 1986, ICOLD 1994) have investigated the reasons behind the good performance of some upstream dams as opposed to poor performance in others. Some items are common in their findings:

- A low phreatic line;
  - Typically, dams that performed better had a lower phreatic surface than dams that failed either locally or catastrophically, allowing less saturated material to be close to the shell.

- Good beach length;
    - The term good beach length is used loosely. Few researchers have defined what a good beach length should be. In general terms, good beach lengths (i. e., where a significant distance was maintained between the crest and the pond) had been maintained when the dam a good performance. Vick (1983), pointed out that once the mine is operational and the tailings dams is functional, maintaining a long beach remains the only manner in which the location of the phreatic surface can be controlled.

When considering the performance of a dam, the dam may perform well structurally, but may have a poor environmental performance. It should be clarified that the scope of work of this research program did not include the evaluation of environmental performances of dams.

The structural and environmental performances may or may not be linked. For instance, seepage of a contaminant in the environment may represent a poor performance with regards to the environmental capacities of the dam, but could result in a lower phreatic surface, lower pore pressures, and lower hydraulic gradients resulting in a good structural performance. Therefore, environmental factors were not considered for the modelling portion of this research program.

With the environmental factors removed, a poor performance with regards to the structural component may occur due to the following mechanisms:

- Low shear strengths;
    - Low shear strength of the tailings occurs with a decrease in effective stress, which is caused by an increase in pore water pressure. This increase may occur intentionally, such as raising of the dam crest, or unintentionally during loading of the reservoir, such as during a seismic event.

- Elevated hydraulic gradients;
  - The hydraulic gradient is defined as the change in hydraulic head ($\Delta H$) over a length ($\Delta L$). In silty, sandy soils, a hydraulic gradient value greater than 1 can indicate degradation in the soil structure, possibly leading to localized failure.

- Piping;
  - Piping occurs when fine soil particles migrate along the flow path of the water. The problem associated with piping occurs when sufficient fines migrate to create "pipes" or channels along which water can travel with less resistance. In turn, the increasing velocity of the flowing water may induce a greater migration of particles. The escalating effect leading to a more generalized failure.

- Overtopping of the beach;
  - Unlike water retention dams, where overtopping can be controlled, and permitted, the same does not occur with tailings dams. In the case of tailings dams, water flowing over the crest of the dam erodes the structural shell and cause failure. Overtopping can occur when a sufficiently long beach is not maintained, and/or greater precipitation and runoff are collected in the reservoir.

- High phreatic surface;
  - The high phreatic surface in itself is not a failure mechanism, but it may trigger some of the mechanisms listed previously. The main drawback associated with the high phreatic surface is that it introduces a greater amount of saturated material closer to the structural shell.

Since most of the poor performance items are related to the location of the phreatic surface, knowledge on its location is important if a good structural performance is to be achieved.

## 6.3 SEEP/W SOFTWARE

SEEP/W from Geo-Slope is a finite element software that can solve saturated and unsaturated seepage problems. The software has been used in the past to solve unsaturated problems dealing with multilayered covers, and aquifer pumping tests (Chapuis and Aubertin 2001, Leoni et al. 2004, Rodgers and Mulqueen 2006). Chapuis and Aubertin (2001) further demonstrated the applicability of the SEEP/W software to analyze the flow through small dykes in both saturated and unsaturated conditions. The use of an earlier version of SEEP/W was also used to evaluate seepage in small dykes, with some success (Crespo, 1993).

Chapuis et al. (1993, 2001) also evaluated the SEEP/W software for its ability and reliability to solve two-dimensional seepage problems. In 2001, the authors reported that SEEP/W correctly solved "the 2D seepage problems in a vertical plane where both conditions $u_w > 0$ and $u_w < 0$ are encountered."

## 6.4 MODELLING CONSIDERATIONS

During the preliminary design phase of the tailings dam and of the tailings reservoir, several items have to be considered. The list below shows some of the more significant items:

a) General considerations:
   - i. Geography (seismically active region);
   - ii. Geology (foundation materials, available local borrow)
   - iii. Available construction area (footprint);
   - iv. Distance from the plant;
   - v. Effluent contamination;
   - vi. Construction cost;
   - vii. Maintenance Cost;
   - viii. Life expectancy;
   - ix. Decommissioning requirements.

b) Design specific considerations:

i. Engineering properties of materials;

ii. Permeability of foundation;

iii. Annual precipitation, runoff;

iv. Storage requirements (sub-aqueous, sub-aerial);

v. Oxidation of tailings.

For modeling purposes, some of the items listed above have to be eliminated in order to observe the influence of specific factors on the location of the phreatic line. Most of the general factors are assumed to be non-controlling, difficult to control or reproduce and are disregarded in this analysis.

With regards to the design specific considerations, listed earlier, some items are taken as constant to provide proper means of comparison. As such, some of the engineering properties of the different materials chosen for the model were homogenized. Further details are provided later in the text.

## 6.5 EFFECT OF BEACH LENGTH

The upstream construction method for tailings dam is not inherently flawed as a construction method. Researchers have found that upstream tailings dams have survived seismic activity. For instance, Conlin (1987) compared active tailings dams with decommissioned dams. He found that inactive dams had sustained little or no damage following earthquakes of substantial magnitude. He suggested that the lower phreatic surface and lower saturation in the tailings close to the shell were contributing factors for the good performance of the dams during the earthquakes.

Martin and McRoberts (1999) provided the three following statements to explain the increase in stability of tailings impoundments with time once their operational life came to an end.

- "Surface water is usually absent, particularly for impoundments regraded to shed runoff, allowing levels of saturation within the outer shell (and possibly the slimes) to gradually reduce."
- "Excess pore pressures induced by the raising of the impoundment will gradually dissipate, resulting in an increase in strength in the tailings slimes."
- "Capping of impoundments for closure reduces infiltration and allows for further reduction in saturation levels, particularly in dry climates."

Since the position of the phreatic surface during the decommissioned stage has such an impact on the stability of the tailings dam, control of the phreatic surface during the operational stage of the tailings impoundment is critical.

Davies and Martin (2000) stated that the upstream tailings dam remains a sound alternative provided good stewardship is maintained throughout the life of he structure. Their main recommendations included maintaining a good beach length separating the crest and the decant pond. Davies and Martin (2000) do not suggest what a good beach length may be. However, in reporting the properties of an existing structure where "the rules are followed", the upstream dam had a beach-length-to-dam-height ratio of 3.3. This ratio is further detailed later in the text.

## 6.6 NUMERICAL MODELING

The following section describes the analysed models and presents observations on the six different scenarios that were evaluated. The analysis consisted of the following scenarios:

- Variation in beach length;
- Introduction of a permeable foundation;
- Introduction of a blanket drain;
- Addition of a transition zone between the shell and the slimes;
- Introduction of anisotropic conditions (with regards to the permeability);
- Combination of the blanket drain and the transition zone.

For each of the above-listed scenarios, three cases were analysed. The three cases analysed represent the three beach lengths considered. The short beach has a beach-length-to-dam-height ratio of 0.5, such that the beach separating the crest and the decant pond is half as long as the dam's height. The medium beach model has a beach-length-to-dam-height ratio of 1.0, and the long beach model has a beach-length-to-dam-height ratio of 2.0.

For the purpose of this portion of the research, the beach-length-to-dam-height ratio is defined as the ratio between the height of the dam, measured from the toe of the starter dyke, to the top of the crest at the time of interest, (not at the proposed completion elevation), and the length of the beach, measured from the point inside the reservoir where the change of slope occurs and softens to the edge of the decant pond.

### 6.6.1 Analysed models

Cases 1 through 3 were introduced as a starting point to directly compare the effects of the beach length on the location of the phreatic surface. Case 1 has a short beach of half the height of the dam, an impervious foundation and is analysed under isotropic conditions. Cases 2 and 3 are similar to Case 1 except that the beach length is increased. In Case 2, the beach length is the same as the height of the dam, whereas in Case 3, the beach length is twice as long as the dam's height.

Cases 4 through 6 are replicas of cases 1 through 3 respectively with the addition of a 5 m thick pervious foundation. The addition of a pervious foundation was introduced in the modeling analysis to examine the effect of the beach length, when a subsoil was more permeable.

Cases 7, 8, and 9 include a blanket drain to replicate a man made drainage layer. The blanket drain is a 2 m thick permeable material, positioned at the base of the dam. A saturated coefficient of permeability of $6.3 \times 10^{-5}$ m/sec was attributed to the blanket drain.

Cases 10, 11, and 12 include a transitional layer that separates the shell and the fines in the reservoir. The model remains isotropic with an impervious foundation.

Cases 13, 14, and 15 have anisotropy added as the new variable. Case 13 is a duplicate of Case 1 with a horizontal anisotropy factor of 10:1 applied to the coefficient of permeability. Case 14 introduces the same anisotropic factor to a duplicate section of Case 7, which has a short beach and a blanket drain. Case 15 is a replica of Case 10, which includes a short beach, and the transition layer. Cases 16, 17, and 18 model the combination of the blanket drain with the transition layer.

### 6.6.2 Existing upstream tailings dam

An existing upstream tailings dam was reproduced to complete the numerical modelling section. The existing upstream dam is located in South America, and only minimal information was available for the analysis (information obtained from Garga personal contacts).

The geometry of the dam was obtained from site investigation results. Figure 6.23 shows the cross-section of the dam, along with the location where two borehole investigations were carried out.

The SPT N-values obtained during the field investigation are shown in Figure 6.23. The fingering effect due to sequential layering of fine and coarse material can be observed from the blow count variations. Also, where the slimes were closer to the structural shell, low SPT N-values were obtained in the coarser material.

In Figure 6.23, the light coloured material represents the coarse underflow material ($k_{sat}$ = $1x10^{-3}$ m/sec). The dark coloured material represents the fines ($k_{sat}$ = $1x10^{-6}$ m/sec) in the reservoir, which was created along the side of a mountain.

The objective of the analysis on the existing dam was to examine the location of the phreatic surface due to a change in the slime's location under the shell. To verify the

assumption that maintaining a long beach length helps keep water away from the shell, the case study model was reproduced following the initial analysis, The reproduced section was modified to improve the geometry. Figure 6.25(a) shows the new arrangement given to the slimes. This was accomplished by repositioning the slimes away from the shell, simulating proper maintenance during operations. The existing conditions, analysed initially are outlined with a solid line in the light coloured material.

## 6.7 MODELING PARAMETERS

The geometry of the cases analysed was based on an idealised cross-section of an upstream tailings dam. The generic model shown in Figure 6.1a, was generated from typical small to medium-sized cross-sections of dams found in literature.

Figure 6.1 (a) shows the configuration of the typical section used throughout the analysis. The dam is composed of 3.0 m high dykes with a downstream face at a 2.5H:1V slope. The crest of the dam is limited to a 7.0 m width. The total height of the modelled dam is 18 m, which makes the structure a small to medium sized dam. This size of dam was chosen for the analysis since most dam failures occur in dams ranging between 11 m and 20 m according to Martins (year unavailable).

Figure 6.1 (b) shows the four major components found in the models. The term "shell" refers to the structural shell, which is constructed of cycloned coarse underflow material. For some analysed sections, a transitional layer was introduced between the shell and the reservoir. The transitional layer represent the material that is naturally segregated between the discharge point and the decant pond (Lipinski and Golebiewska, 2000). The transitional layer was attributed properties of an intermediate nature between the coarse underflow material, and the fine overflow material. The slimes designate the fine overflow material that is stored in the reservoir.

The input requirements for the modeling process includes defining properties such as the conductivity curves (the coefficient of permeability plotted against the suction), the water content curves (the soil-water characteristic curve *SWCC* or the volumetric water content

plotted against the suction), a grid pattern (or element mesh), and boundary conditions. The same materials were used throughout the modeling process.

By providing both a conductivity curve and a water content curve for a soil, the SEEP/W code can provide solutions for both saturated and unsaturated conditions.

### 6.7.1 Materials

Initially, the results of the laboratory portion of this research program were supposed to be entered as input for the numerical modelling. However, due to discrepancies found in the laboratory results (see Chapter 5 for experimental results), input for the finite element models came from the function library available with SEEP/W.

The coarse overflow tailings found in the shell have a saturated coefficient of permeability of $5.4 \times 10^{-5}$ m/sec. Figure 6.2 shows the conductivity curve for the material used in the shell. Under negative pore water pressure, the shell desaturates at a relatively fast rate as shown by the slope of the curve.

The material in the blanket drain (in cases 7, 8, 9, 14, 16, 17, and 18) is the same as the material used in the extended foundation (in cases 4, 5, and 6). These soils have a saturated coefficient of permeability of $6.3 \times 10^{-5}$ m/sec with a steep desaturation curve, as can be seen in Figure 6.2.

The tailings in the transitional layer between the shell and the slimes, have a saturated coefficient of permeability of $4.8 \times 10^{-7}$ m/sec. Under negative pore water pressures, the tailings in the transitional layer desaturate less rapidly than the coarse tailings found in the shell, but more rapidly than the slimes.

The slimes have a low saturated coefficient of permeability ($5.8 \times 10^{-8}$ m/sec) with a much more gradual decrease in permeability for an increase in suction, representative of finer grained soils.

Figure 6.3 shows the SWCC used for all materials used throughout the analysis. The beach is shown as the material with the highest porosity.

### 6.7.2 Element mesh

In order to keep results as consistent as possible from one case to another, all cases modelled were digitised in an identical manner. All elements in the SEEP/W cases were given consistent dimensions of 0.25 m by 0.25 m. Simple models were initially analysed with varying element meshes composed entirely of elements sized 1.0 m by 1.0 m, 0.5 m by 0,5 m, 0.25 m by 0.25 m, and 0.125 m by 0.125 m. Square elements of 0.25 m by 0.25 m were found to provide the greatest versatility while maintaining the number of elements sufficiently low to minimize computing time. Previous researchers typically used elements sized between 0.5 m to 2.0 m. (Chapuis et al. 2001)

### 6.7.3 Boundary conditions

The analysed models were assigned two types of boundary conditions. On the downstream portion of the dam, the element nodes were assigned unknown total flux values, with review possibilities. In doing so, the node's total flux was revised after each iteration of the program. The upstream end of the model was assigned a total head value. The two different types of nodal boundary conditions are shown in Figure 6-1 (c).

### 6.7.4 Flux section

In order to provide quantitative means with which to compare the analysed sections, a flux section was introduced in each model. In SEEP/W, the flux section measures the flow of water passing through the designated section. The flux sections were identically positioned in each model. In Figures 6.5 to 6.22, the flux section is shown as a vertical line with an arrowhead pointing upwards. The area chosen as the most representative is located vertically across the shell and penetrates into the slimes as can be seen in the analysed sections.

It should be noted that the flux computed during the analysis of a problem is computed from the specific discharge, which is computed from the total flux divided by the full

cross-sectional area. As defined in the software user's manual, the actual microscopic velocity (average linear velocity) is obtained by dividing the specific discharge by the porosity of the material.

### 6.7.5 Volumetric water content

Along with the quantitative results provided with the flux sections, a qualitative analysis is also completed for each case. The results of each case analysed are plotted as contour profiles. The contours have intervals of 0.11 $m^3/m^3$. Table 6.1 provides an approximate degree of saturation value (shown in *italic*) for every contour interval, for each case analysed.

### 6.7.6 Pressure head

The second contour profile plotted for each case analysed shows the pressure head. The pressure head contours were plotted with increments of 2 meters of head, starting at a value of 0 to better show the phreatic surface. Table 6.2 presents the convergence parameters used for each case modelled.

### 6.7.7 Hydraulic gradient

SEEP/W offers the user the possibility of examining hydraulic gradients computed during the analysis. The hydraulic gradients are computed according to Equation 6.1, as defined in the User's Manual.

$$\begin{Bmatrix} i_x \\ i_y \end{Bmatrix} = [B]\{H\} \tag{6.1}$$

where:

$i_x$ is the gradient in the $x$ direction.

$i_y$ is the gradient in the $y$ direction.

$[B]$ is the gradient matrix as defined in the Finite Element Equations (see User's Manual)

$\{H\}$ is the vector of total head at the nodes.

SEEP/W computes the hydraulic gradient at every node of the elements. The results can also be plotted with contours to better see the areas where larger values develop.

## 6.8 RESULTS

Figure 6.4 presents the flow values measured at each flux section for each case analysed. Cases 1, 2, and 3, were used as baseline models for comparison. They include no other variable than a different beach length from one to the other. The increase in beach length from Case 1 to Case 2 and again to Case 3 sees a decrease in flow values measured at the flux section as the beach length is increased.

As shown in Figure 6.4 there is a significant difference in the quantity of water flowing at the flux section, when comparing the medium and the long beach models for the three cases where a pervious foundation was modelled (i.e., Cases 4, 5, 6). Figures 6.5, 6.6, and 6.7 show a direct correlation between the beach length and the location of the phreatic surface. Cases 7, 8, and 9 show a decrease in flow at the flux section as the beach is lengthened. These three models include the blanket drain and show a lowering of the phreatic surface for an increase in beach length. The blanket drain has a significant impact on the location of the phreatic surface when the beach is longer. The effect is not as prominent with the short beach.

Cases 10, 11, and 12 incorporate the transitional layer between the shell and the slimes. Based on the flow values, it appears that an increase in beach length does not reduce the quantity of water flowing in the area of the flux section between the short and medium beach (Cases 10 and 11 respectively). Closer inspection of the phreatic surface and the volumetric water content contours of Case 11, (shown in Figure 6.15 (b), and (c) respectively) reveals that the increase in water flow is due to water movement in the unsaturated phase. According to the water content contours of Figure 6.15 (b), and Table 6.1, the saturation of the transition layer at the flux section varies between approximately 37 percent and 85 percent. Although Case 11 has a higher flow rate than Case 10, the

longer beach provides a larger region of unsaturated material, providing better protection against liquefaction.

Cases 13, 14, 15 include an anisotropic factor on the coefficient of permeability. In comparison to Case 1, Case 13 shows a decrease in the flow measured at the same location. The same observation is true when comparing Case 7 with Case 14, and Case 10 with Case 15. Increasing the horizontal coefficient of permeability to account for horizontal layering typically associated with tailings, reduce the amount of water flowing in the area depicted by the flux section.

The last three models analysed combine the blanket drain and the transitional layer. The values plotted in Figure 6.4 indicate that there is relatively no difference in the quantity of water flowing through the flux sections of Cases 16 and 17. The difference is likely due to the larger quantity of water flowing in the unsaturated tailings within the transitional layer. In Case 18, essentially no water flows in the area of interest. The combination of the long beach and a blanket drain in Case 18 provides the largest unsaturated area immediately behind the shell.

### 6.8.1 Existing upstream tailings dam

The advantage of proper maintenance is illustrated in Case 20, where the existing dam was slightly modified from its configuration shown in Figure 6.24. The fines closest to the downstream face were removed and replaced with coarse underflow material as shown in Figure 6.25. The lowering of the phreatic surface between elevations 25 m and 30 m is due to the increased distance between the slimes and the shell.

Although the volumetric contours could not be plotted for the existing tailings dam, it can be assumed that the modified dam would provide better resistance against liquefaction. Based on the previous cases, lowering of the phreatic surface provides a larger quantity of unsaturated material near the downstream face of the dam.

### 6.8.2 Hydraulic Gradient Results

The hydraulic gradients where computed for each analysis and plotted to see if any analysed scenario had developed high gradients. The plotted results showed some areas with high gradient values (i.e., values greater than 2) in areas that should not have shown high gradient values. Further investigation showed that the highest gradient values arose due to changes in the material properties at the junction of the fine tailings in the reservoir and the coarse tailings of the structural shell.

The overall analysis results are correct since the convergence criterion was reached, however, the differences in the pressure head at these locations are greater than surrounding differences, which produces large localized hydraulic gradients. The hydraulic gradient contours were not included in the results, since the main areas of interest of the dams (i.e., the general area of the downstream starter dam), could not be properly isolated and observed.

### 6.8.3 SEEP/W

The modeling portion of this work was completed with the SEEP/W software (version 4.0). As the work progressed, so did the appreciation of the capabilities and limitations of the software. The main advantage of working with SEEP/W lies in its "user-friendliness". The software is widely known, and help is generally available, from either previous users, or the software designers.

There are however constraints with the software. Some of the limitations include output capacities of the software. The version used during this research program did not allow the user to produce a colour scale to be plotted for results plotted with contour profiles. The software allows the user to produce output lists of velocities, gradients, etc., which are computed at the nodes, but does not allow the user to obtained a detailed list showing the node numbers and coordinates. This is a major drawback when users are trying to determine localized anomalies. Finally, the software cannot deal with abrupt changes in material properties, as is the case when filters are introduced, or when segregation is encountered.

## 6.9 CONCLUSION

The results of the analysis performed on the generic tailings dam, indicate that maintaining a long beach during the operational life of a tailings dam is beneficial. A long beach that sufficiently increases the distance between the structural shell and the decant pond may generate a greater area of unsaturated tailings in the reservoir. As such, the tailings closest to the shell may be sufficiently unsaturated to resist liquefaction.

Given the simplicity of the modeling exercise completed herein, the results clearly show that longer beaches are beneficial. The beach-length-to-dam-height ratio should be as large as possible at all times.

When possible, the addition of a blanket drain at the toe of the dam should be evaluated. A blanket drain alone cannot ensure that a significant distance will exist between the phreatic surface and the structural shell. The blanket drain will greatly contribute in draining excess water as well as controlling the phreatic surface.

The SEEP/W software provided a satisfactory tool to assess the influence of several design options, and maintenance scenarios on the location of the phreatic surface. Further investigation would be required to reduce convergence difficulties at junctions between different materials.

| Case | Maximum $\phi$ (from analysis) | $\phi$ Contour Increment Value | | | | |
|---|---|---|---|---|---|---|
| | | 0.055 | 0.165 | 0.275 | 0.385 | 0.495 |
| | | *Degree of Saturation* | | | | |
| 1 | 0.405 | *14 %* | *41 %* | *68 %* | *95 %* | *> 100 %* |
| 2 | 0.405 | *14 %* | *41 %* | *68 %* | *95 %* | *> 100 %* |
| 3 | 0.405 | *14 %* | *41 %* | *68 %* | *95 %* | *> 100 %* |
| 4 | 0.402 | *14 %* | *41 %* | *68 %* | *96 %* | *> 100 %* |
| 5 | 0.402 | *14 %* | *41 %* | *68 %* | *96 %* | *> 100 %* |
| 6 | 0.399 | *14 %* | *41 %* | *69 %* | *96 %* | *> 100 %* |
| 7 | 0.405 | *14 %* | *41 %* | *68 %* | *95 %* | *> 100 %* |
| 8 | 0.405 | *14 %* | *41 %* | *68 %* | *95 %* | *> 100 %* |
| 9 | 0.405 | *14 %* | *41 %* | *68 %* | *95 %* | *> 100 %* |
| 10 | 0.405 | *14 %* | *41 %* | *68 %* | *95 %* | *> 100 %* |
| 11 | 0.450 | *12 %* | *37 %* | *61 %* | *86 %* | *> 100 %* |
| 12 | 0.450 | *12 %* | *37 %* | *61 %* | *86 %* | *> 100 %* |
| 13 | 0.405 | *14 %* | *41 %* | *68 %* | *95 %* | *> 100 %* |
| 14 | 0.405 | *14 %* | *41 %* | *68 %* | *95 %* | *> 100 %* |
| 15 | 0.446 | *12 %* | *37 %* | *62 %* | *86 %* | *> 100 %* |
| 16 | 0.429 | *13 %* | *38 %* | *64 %* | *90 %* | *> 100 %* |
| 17 | 0.442 | *12 %* | *37 %* | *62 %* | *87 %* | *> 100 %* |
| 18 | 0.450 | *12 %* | *37 %* | *61 %* | *86 %* | *> 100 %* |
| Average Saturation | | *13 %* | *40 %* | *66 %* | *92 %* | *> 100 %* |

**Table 6.1: Volumetric water content ($\phi$) contour value to degree of saturation equivalency table**

| Case | Max. # of Iterations | Tolerance | Max. Change | Rate of Change | Min. Change | Max. Seepage Reviews | Direct Iteration | Iterations to Convergence |
|---|---|---|---|---|---|---|---|---|
| 1 | 1000 | 0.1 | 0.5 | 1.05 | 0.0001 | 10 | Yes | 719 |
| 2 | 1000 | 0.1 | 0.5 | 1.05 | 0.0001 | 10 | Yes | 644 |
| 3 | 1000 | 0.1 | 0.5 | 1.05 | 0.0001 | 10 | Yes | 367 |
| 4 | 1000 | 0.1 | 0.5 | 1.05 | 0.0001 | 10 | Yes | 415 |
| 5 | 1000 | 0.1 | 0.5 | 1.05 | 0.0001 | 10 | Yes | 113 |
| 6 | 1000 | 0.1 | 0.5 | 1.05 | 0.0001 | 10 | Yes | 75 |
| 7 | 1000 | 0.1 | 0.5 | 1.05 | 0.0001 | 10 | Yes | 750 |
| 8 | 1000 | 0.1 | 0.5 | 1.05 | 0.0001 | 10 | Yes | 94 |
| 9 | 1000 | 0.1 | 0.5 | 1.05 | 0.0001 | 10 | Yes | 72 |
| 10 | 1000 | 0.1 | 0.5 | 1.05 | 0.0001 | 10 | Yes | 1002 |
| 11 | 1000 | 0.1 | 0.5 | 1.05 | 0.0001 | 100 | Yes | 1169 |
| 12 | 1000 | 0.1 | 0.5 | 1.05 | 0.0001 | 100 | Yes | 1078 |
| 13 | 1000 | 0.1 | 0.5 | 1.05 | 0.0001 | 100 | Yes | 1315 |
| 14 | 1000 | 0.1 | 0.5 | 1.05 | 0.0001 | 100 | Yes | 1161 |
| 15 | 1000 | 0.1 | 0.5 | 1.05 | 0.0001 | 100 | Yes | 1125 |
| 16 | 1000 | 0.01 | 0.5 | 1.05 | 0.0001 | 100 | Yes | 1259 |
| 17 | 1000 | 0.01 | 0.5 | 1.05 | 0.0001 | 100 | Yes | 3284 |
| 18 | 1000 | 0.01 | 0.5 | 1.05 | 0.0001 | 100 | Yes | 4631 |

**Table 6.2: Modelling convergence parameters**

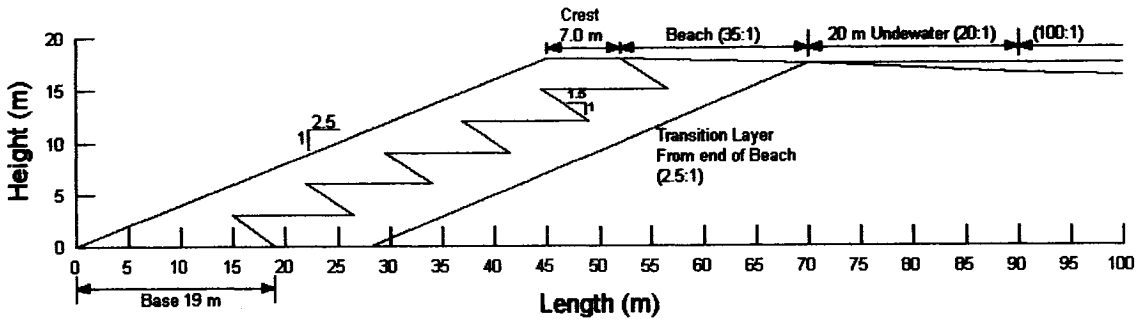


(a) Geometry

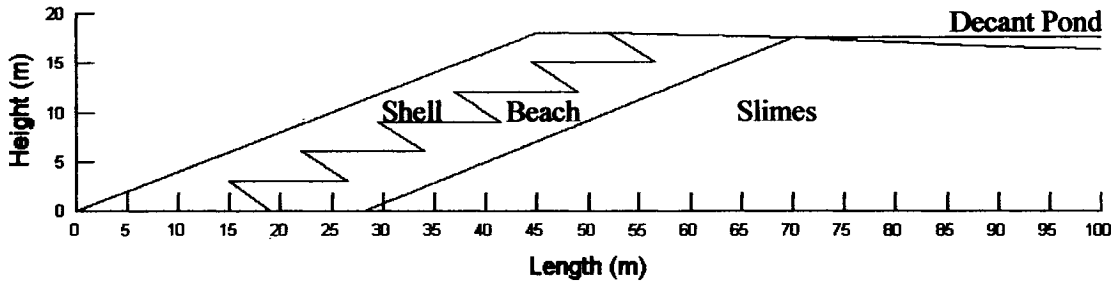


(b) Components

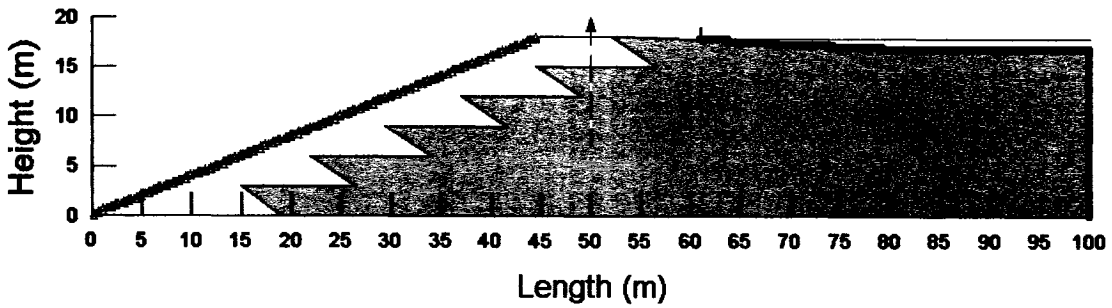


(c) Boundary Conditions

**Figure 6.1: Upstream tailings dam model**

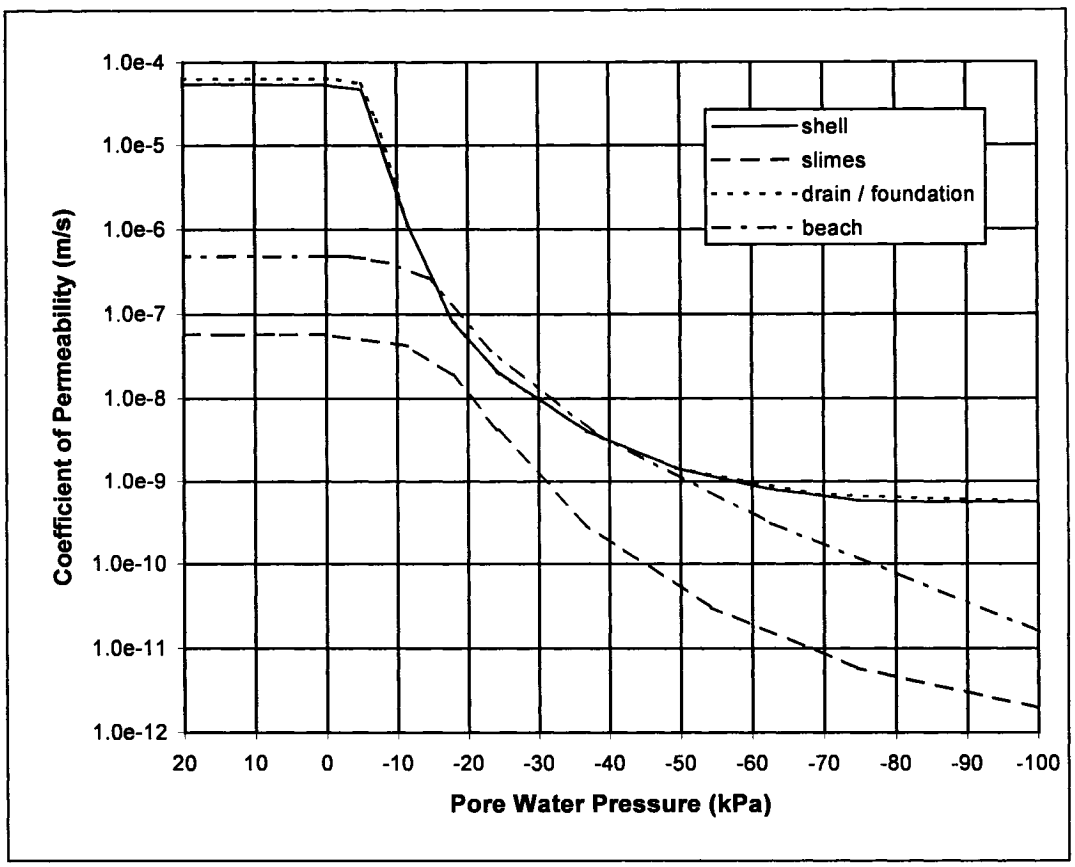


**Figure 6.2: Conductivity curves used for numerical modelling**

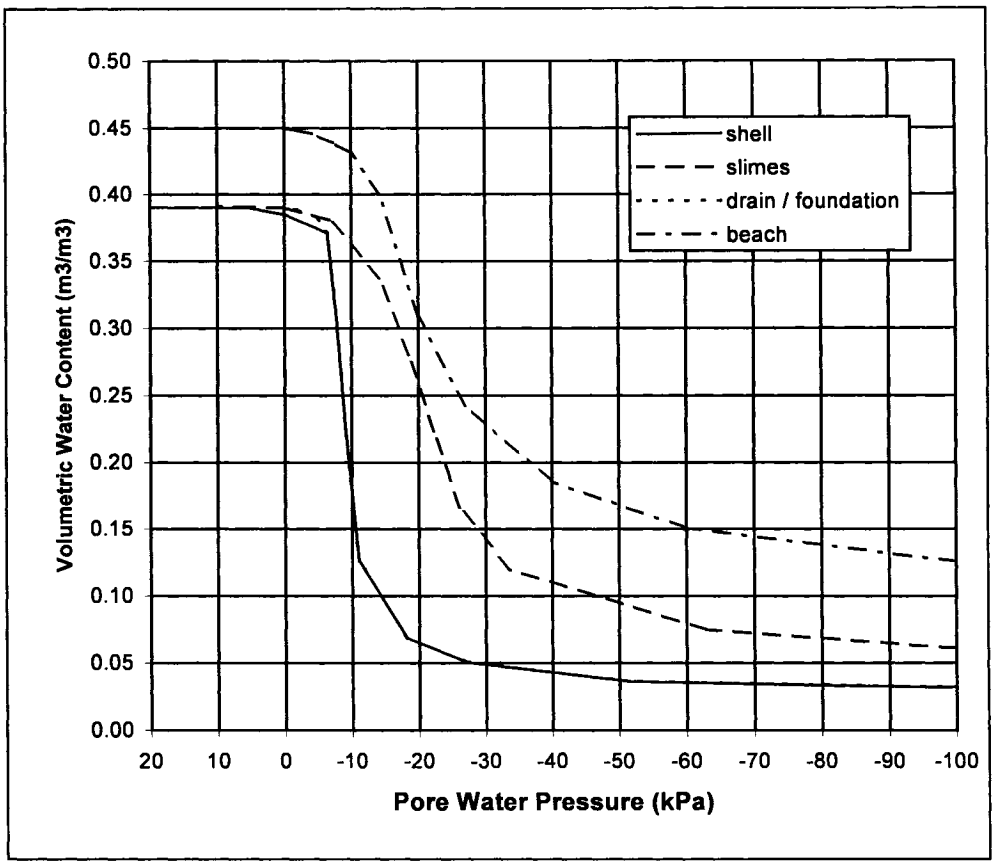


**Figure 6.3: SWCC used for numerical modelling**

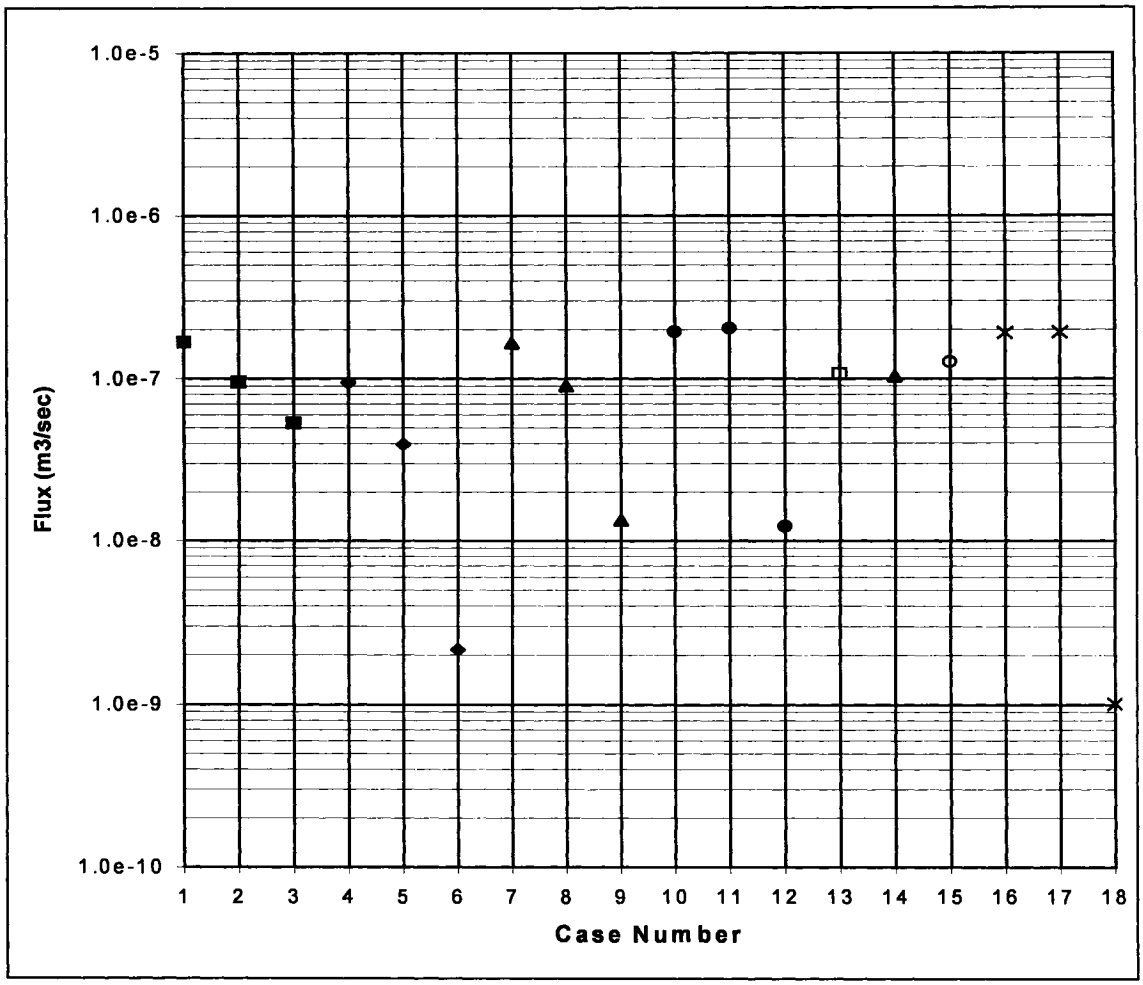


**Figure 6.4: Flow measured at flux section during modelling**

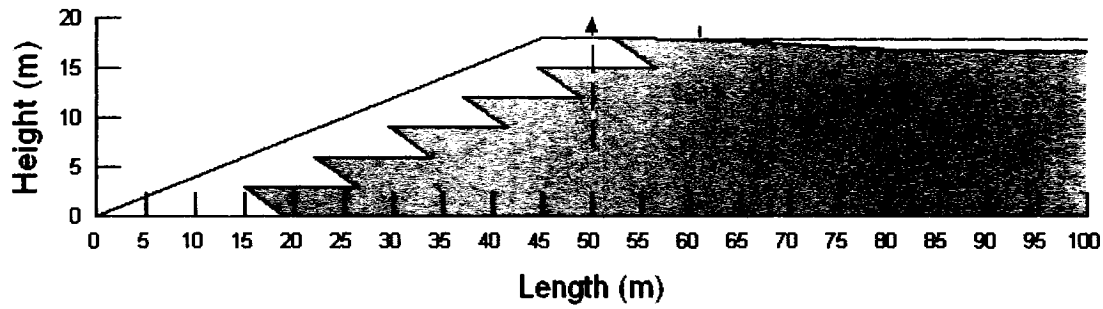


(a) Analysed Section

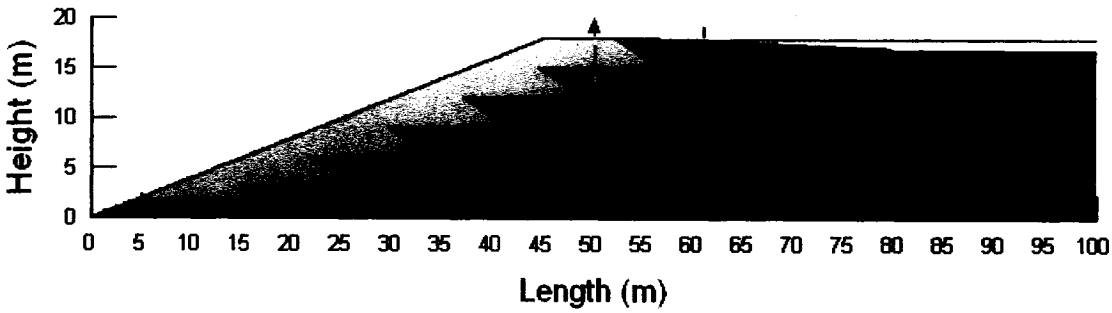


(b) Volumetric Water Content Result

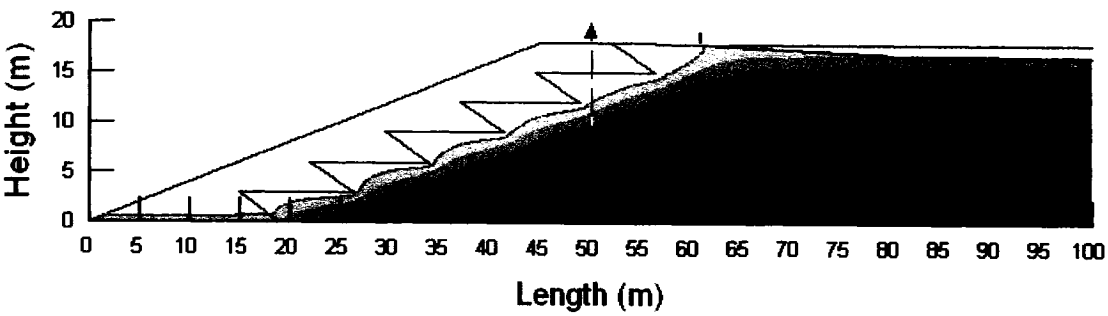


(c) Pressure Head Result

**Figure 6.5: Case 1 – Variation in beach length (short beach)**

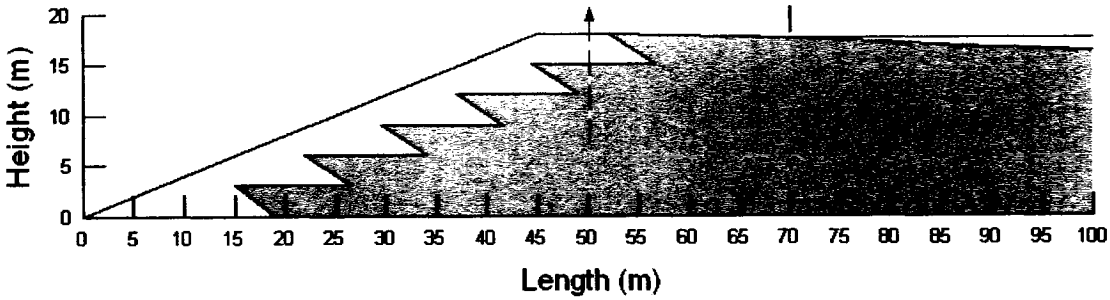


(a) Analysed Section

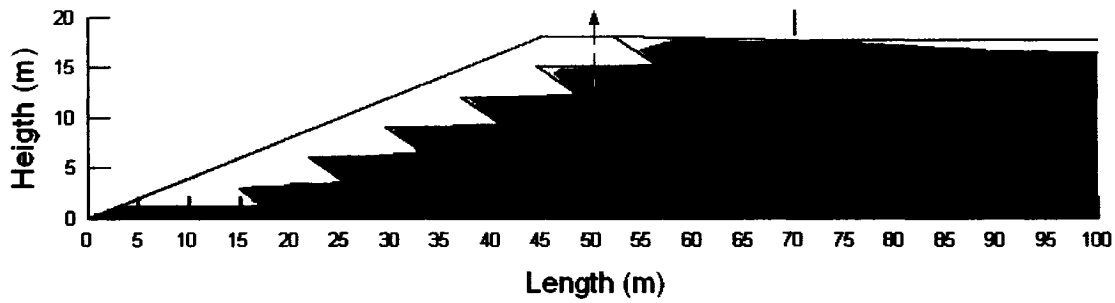


(b) Volumetric Water Content Result

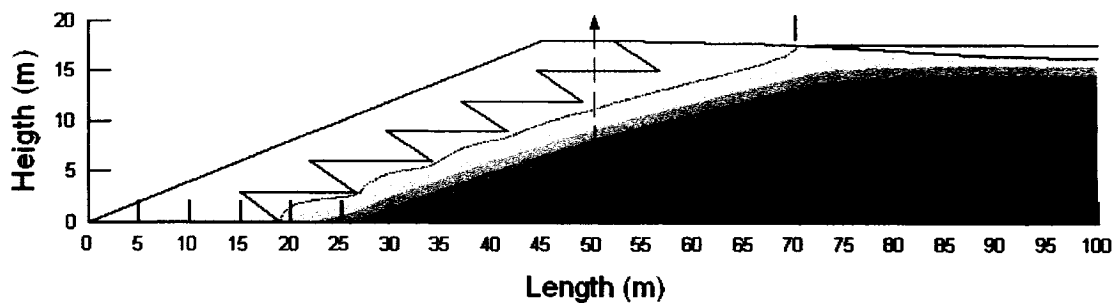


(c) Pressure Head Result

**Figure 6.6: Case 2 – Variation in beach length (medium beach)**

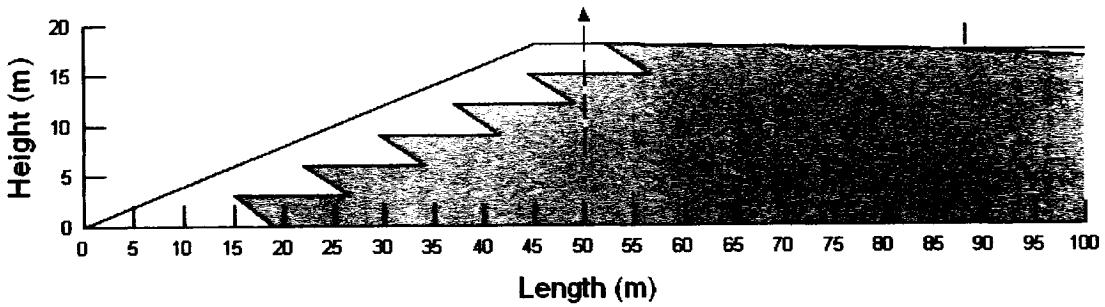


(a) Analysed Section

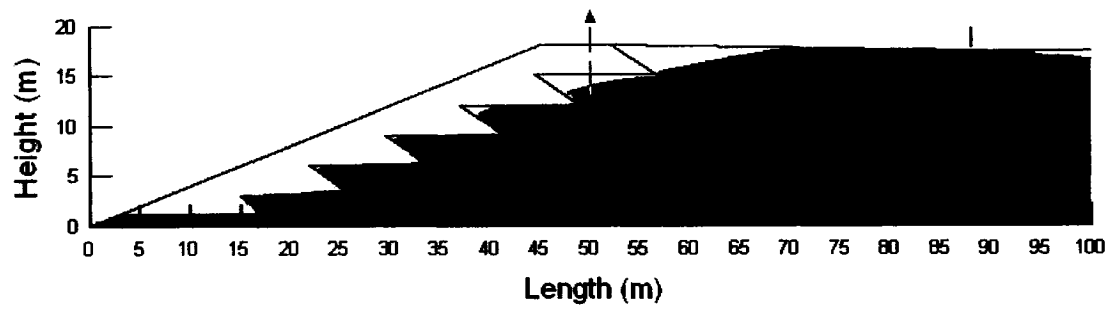


(b) Volumetric Water Content Result

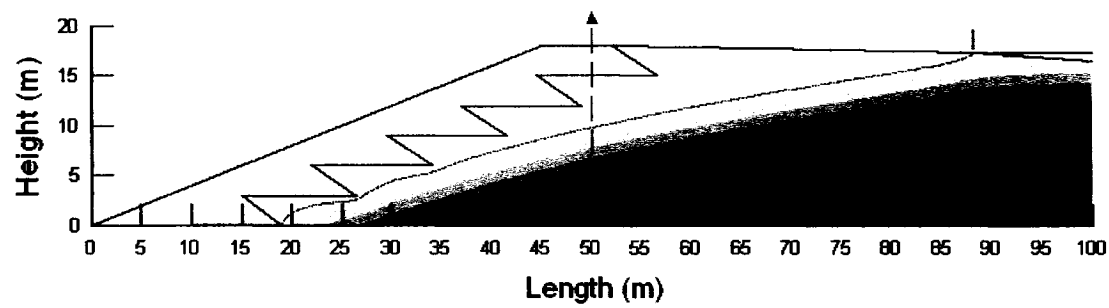


(c) Pressure Head Result

**Figure 6.7: Case 3 – Variation in beach length (long beach)**

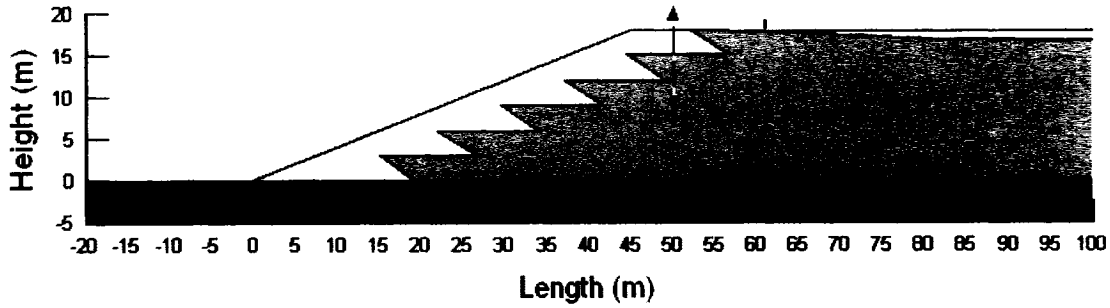


(a) Analysed Section

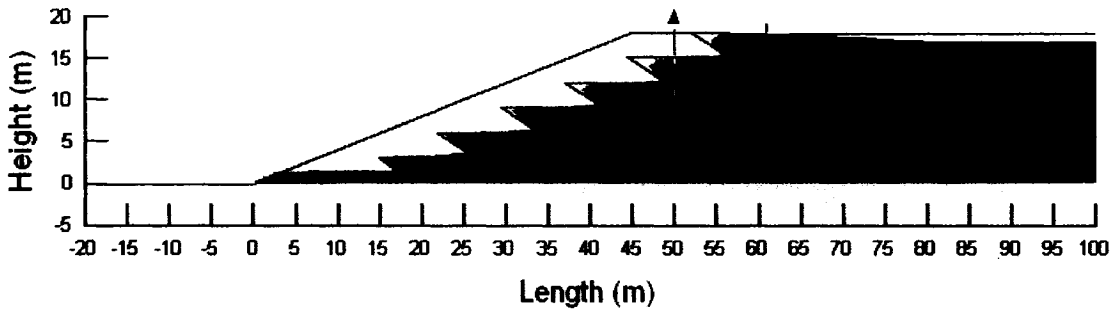


(b) Volumetric Water Content Result

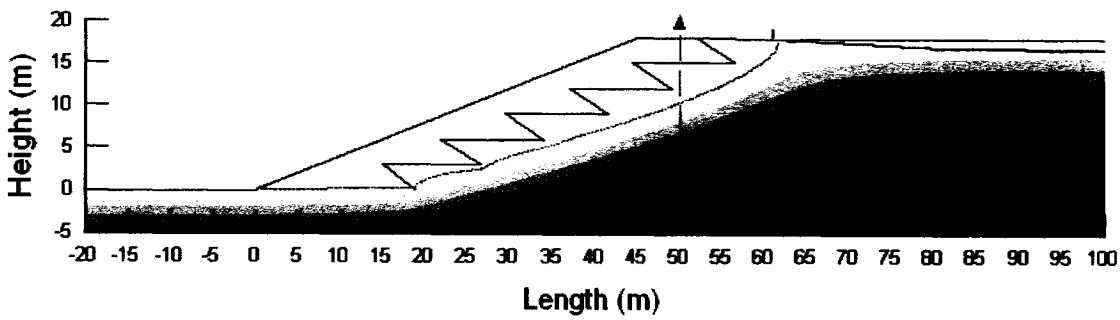


(c) Pressure Head Result

**Figure 6.8: Case 4 – Permeable foundation (short beach)**

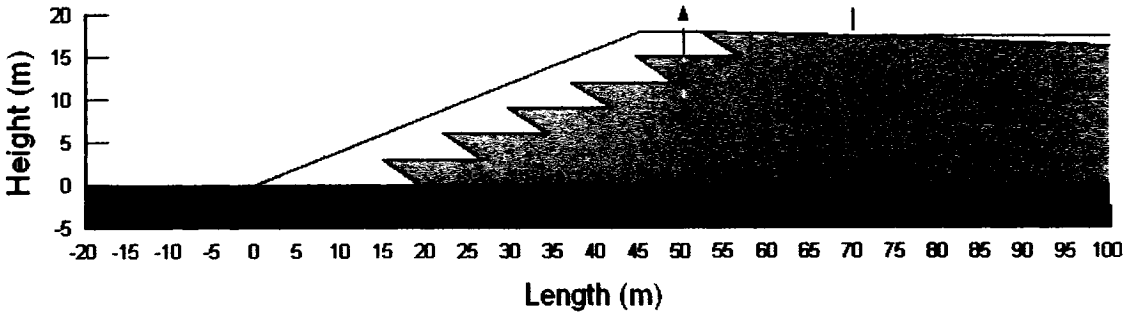


(a) Analysed Section

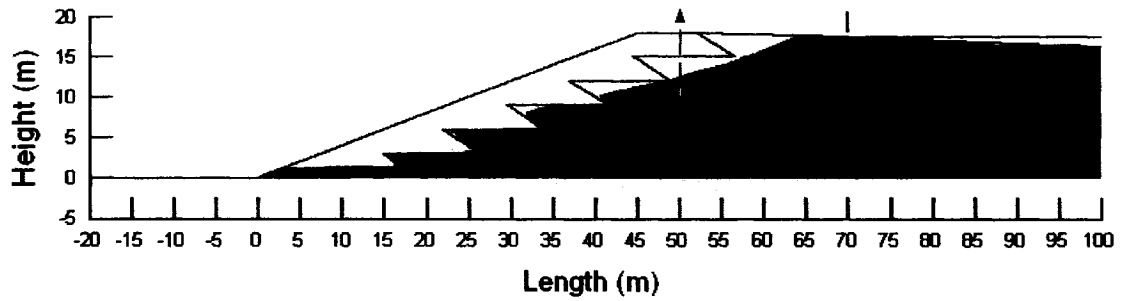


(b) Volumetric Water Content Result

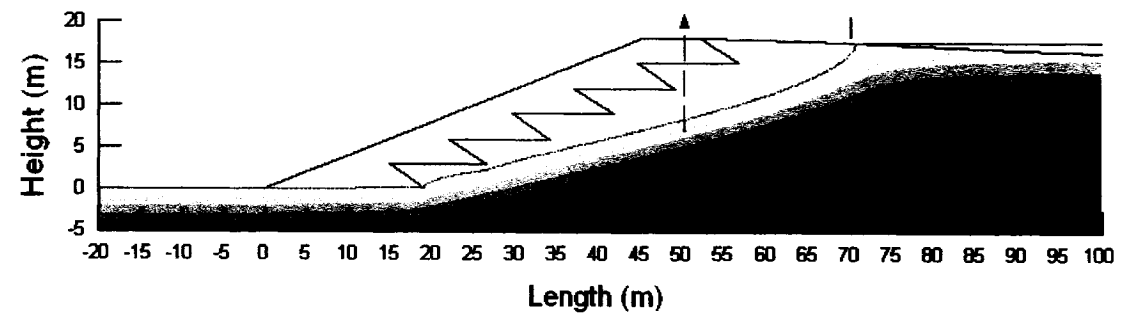


(c) Pressure Head Result

**Figure 6.9: Case 5 – Permeable foundation (medium beach)**

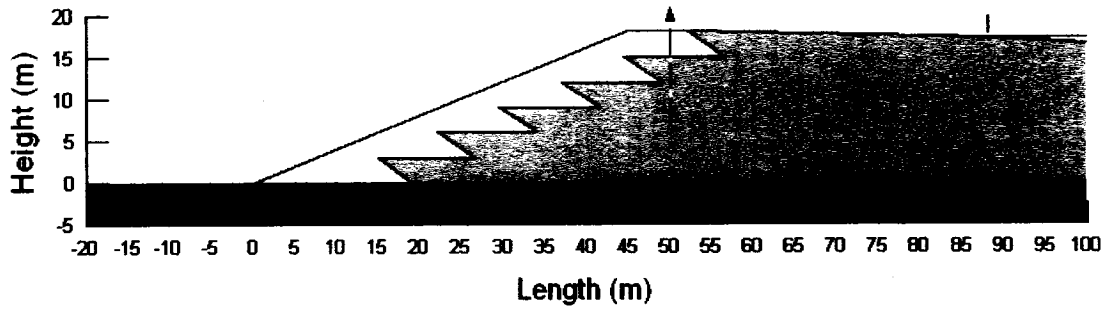


(a) Analysed Section

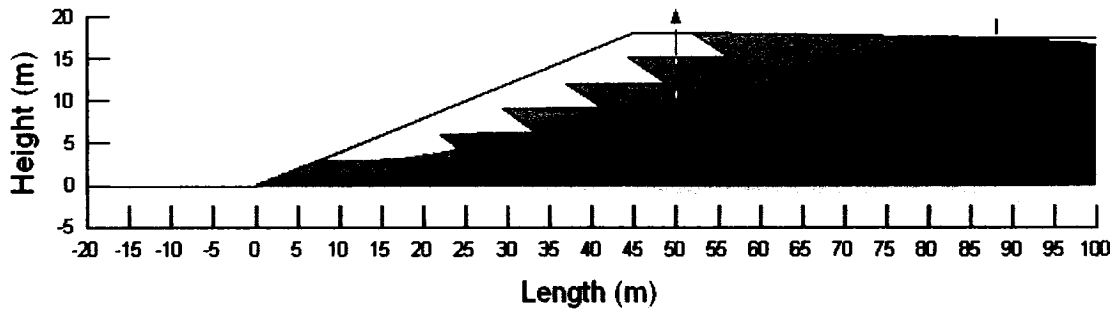


(b) Volumetric Water Content Result

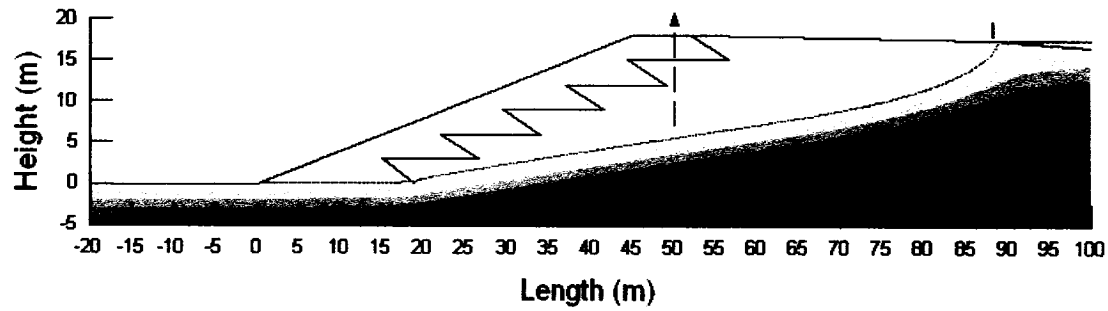


(c) Pressure Head Result

**Figure 6.10: Case 6 – Permeable foundation (long beach)**

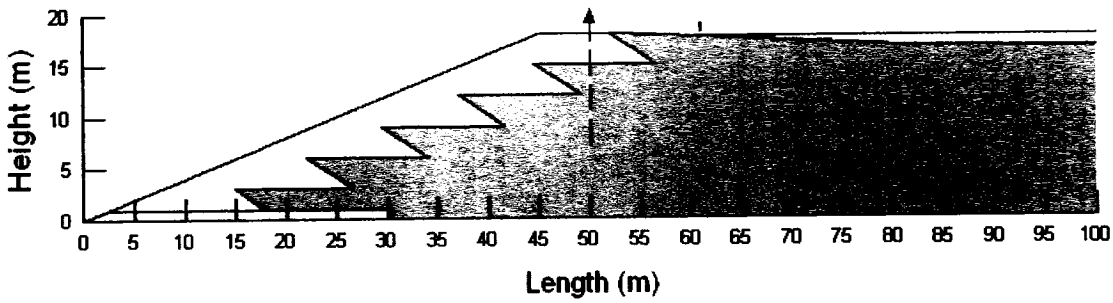


(a) Analysed Section

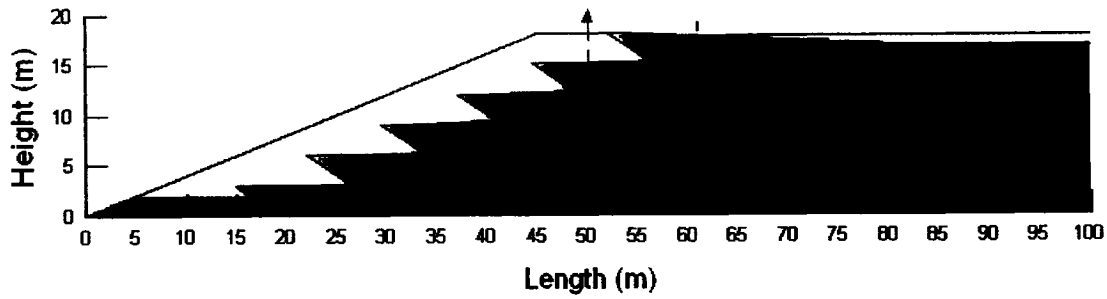


(b) Volumetric Water Content Result

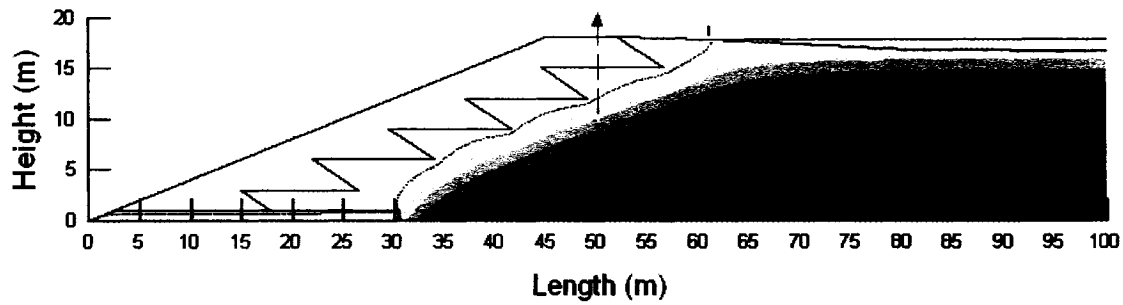


(c) Pressure Head Result

**Figure 6.11: Case 7 – Blanket drain (short beach)**

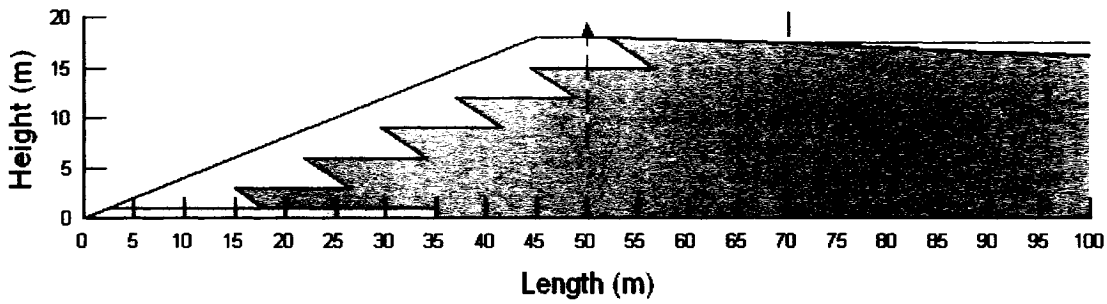


(a) Analysed Section

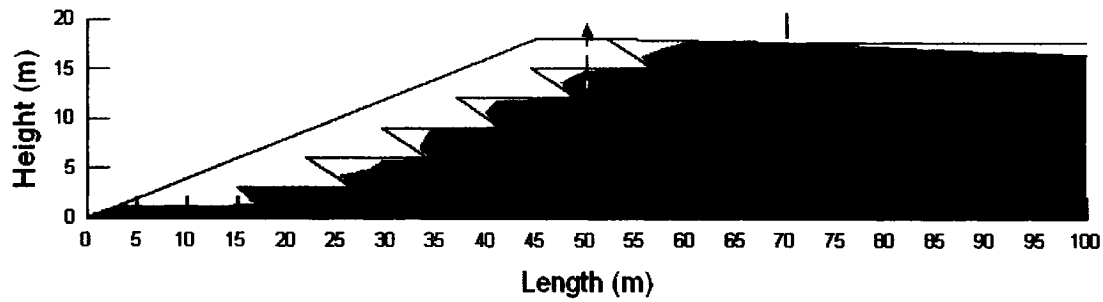


(b) Volumetric Water Content Result

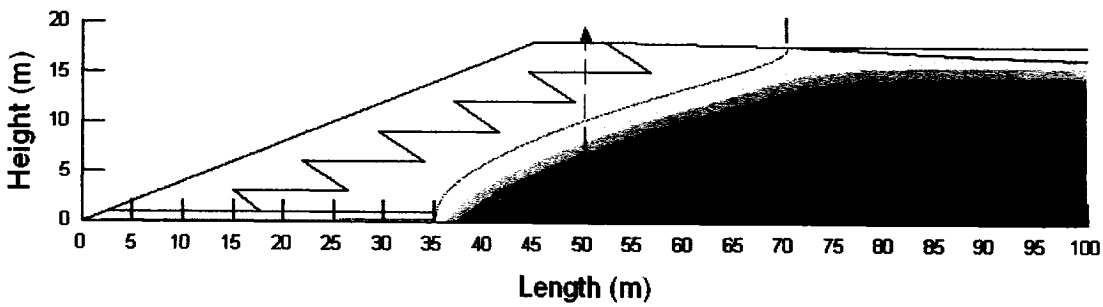


(c) Pressure Head Result

**Figure 6.12: Case 8 – Blanket drain (medium beach)**

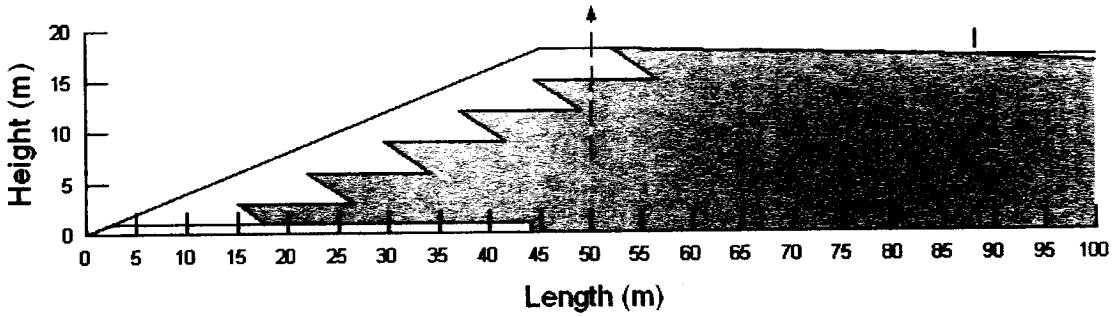


(a) Analysed Section

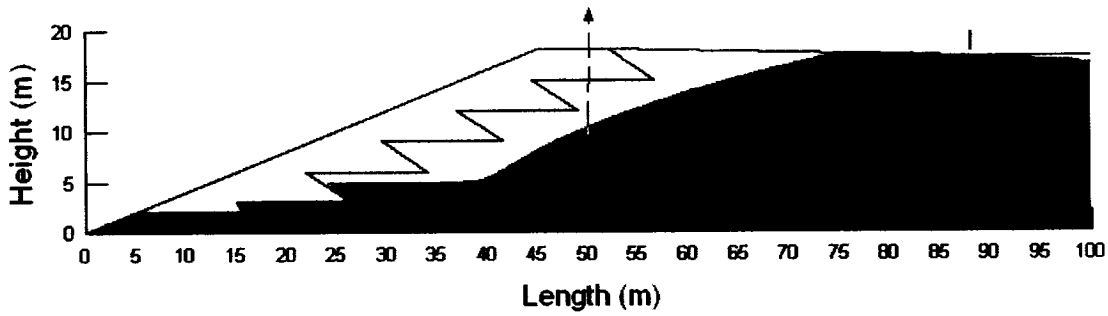


(b) Volumetric Water Content Result

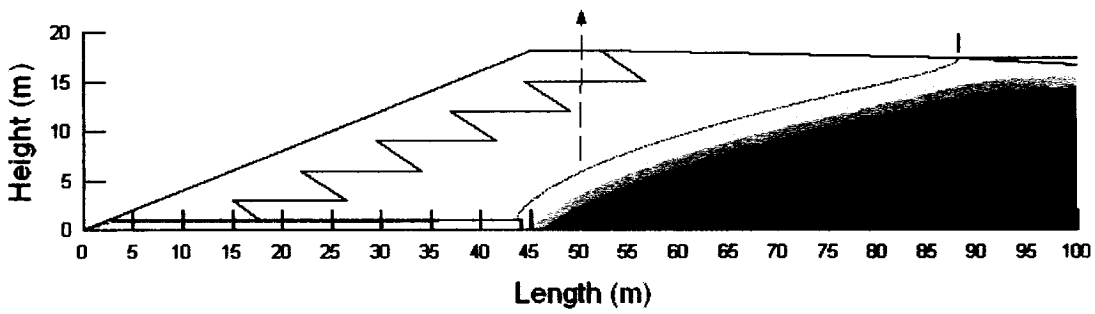


(c) Pressure Head Result

**Figure 6.13: Case 9 – Blanket drain (long beach)**

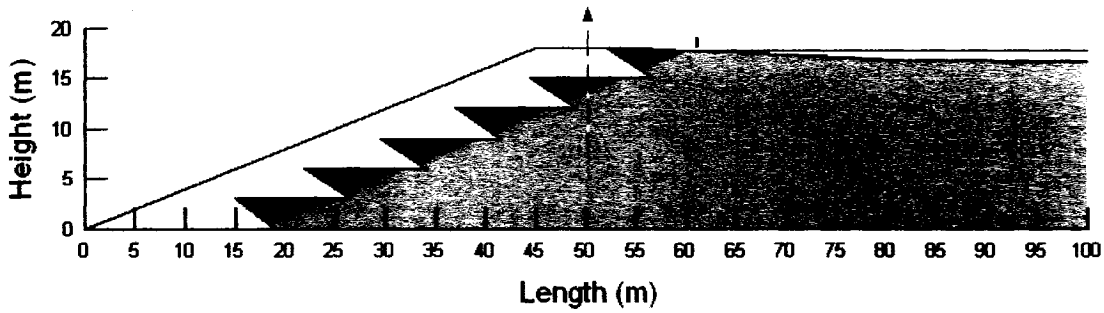


(a) Analysed Section

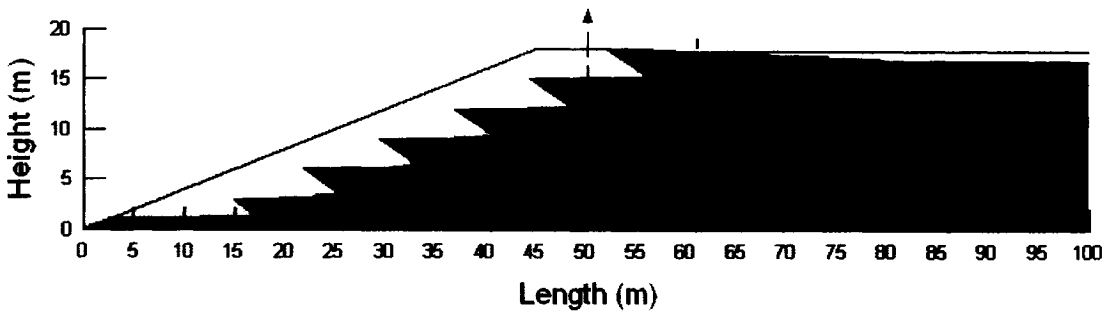


(b) Volumetric Water Content Result

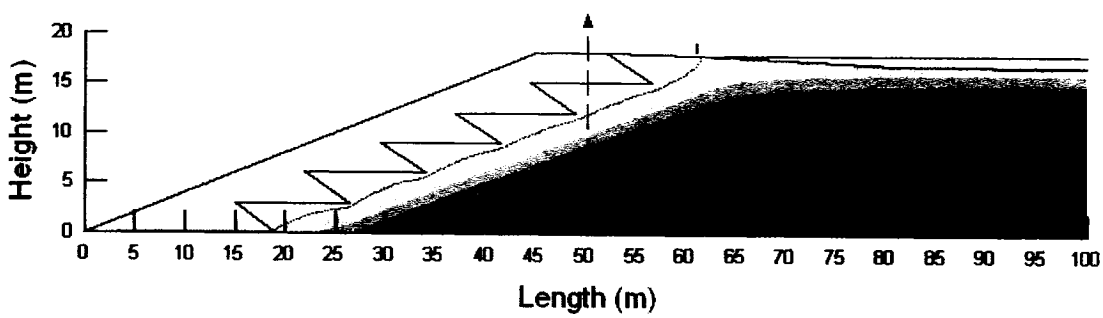


(c) Pressure Head Result

**Figure 6.14: Case 10 – Transition zone (short beach)**

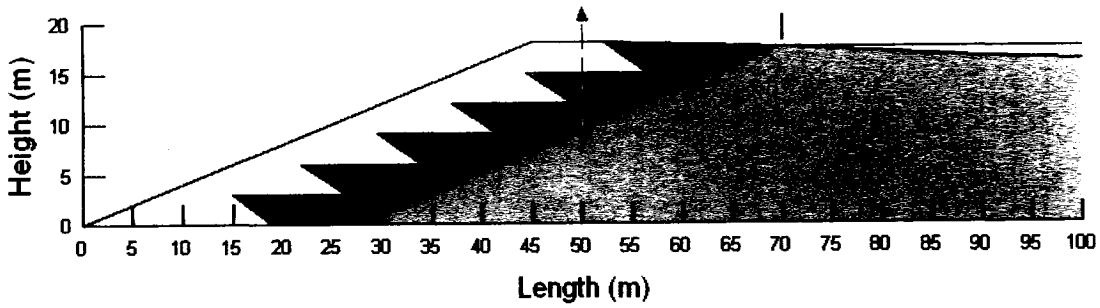


(a) Analysed Section

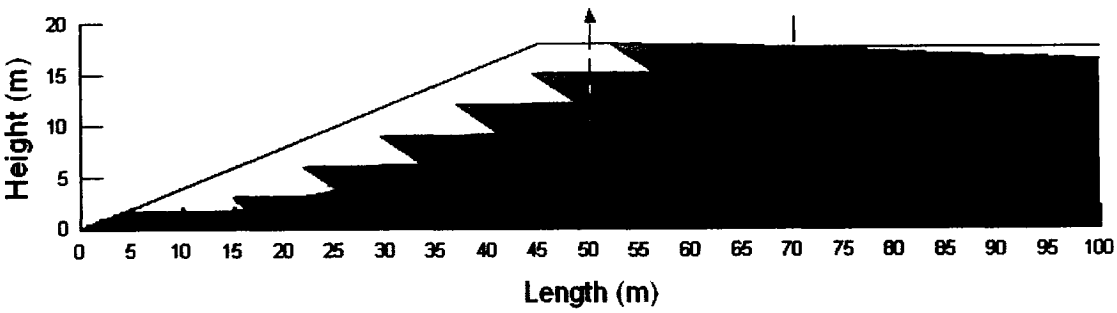


(b) Volumetric Water Content Result

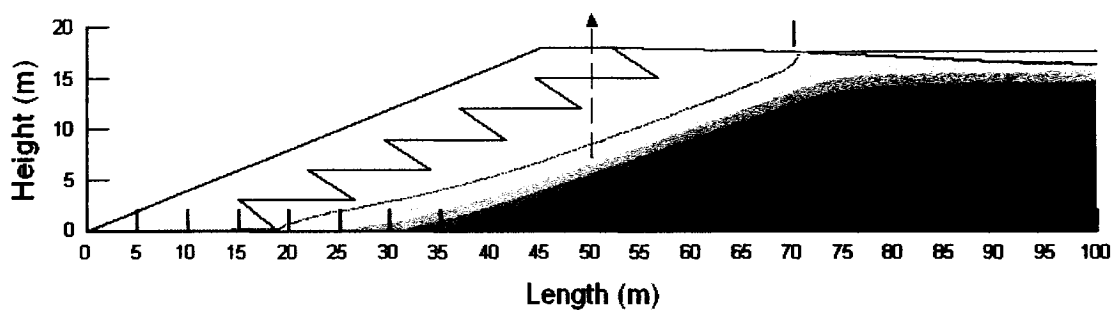


(c) Pressure Head Result

**Figure 6.15: Case 11 – Transition zone (medium beach)**

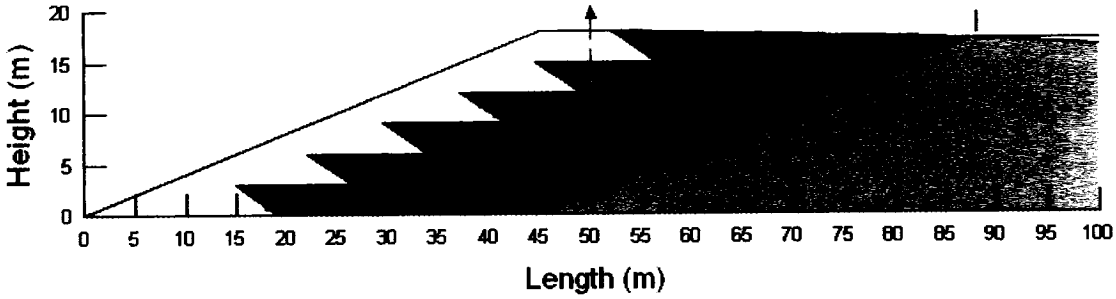


(a) Analysed Section

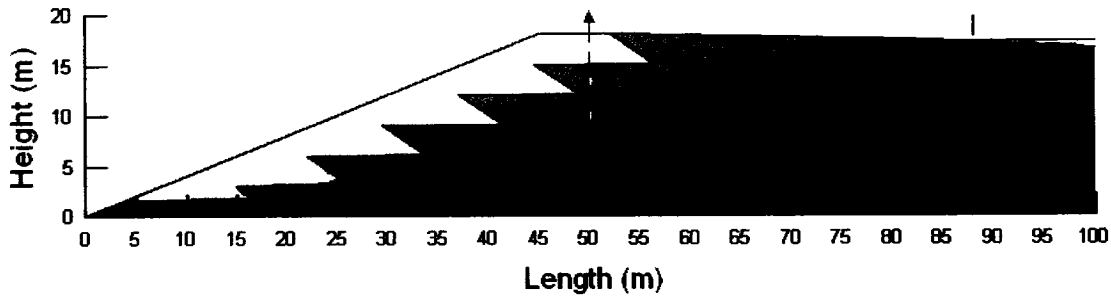


(b) Volumetric Water Content Result

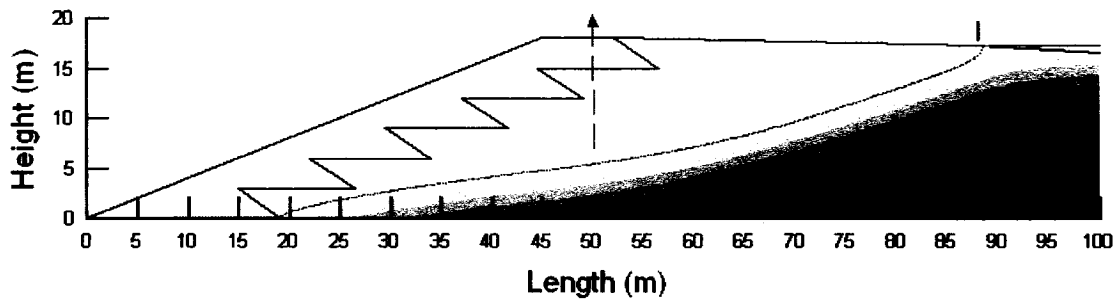


(c) Pressure Head Result

**Figure 6.16: Case 12 – Transition zone (long beach)**

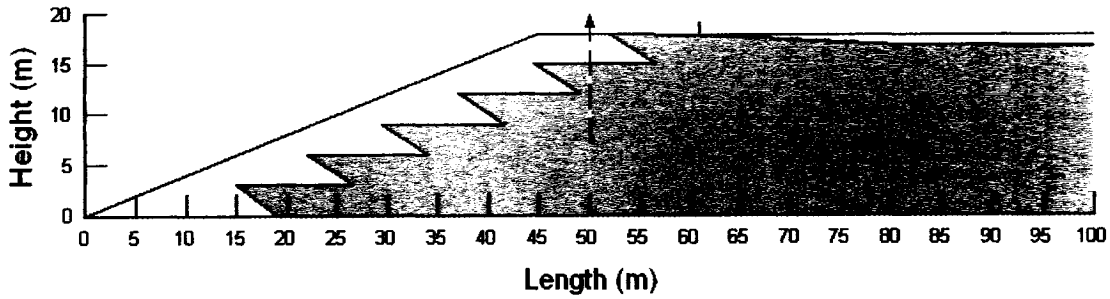


(a) Analysed Section

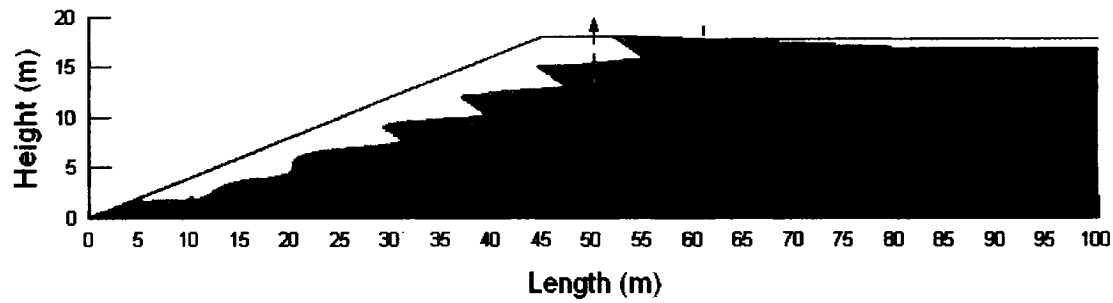


(b) Volumetric Water Content Result

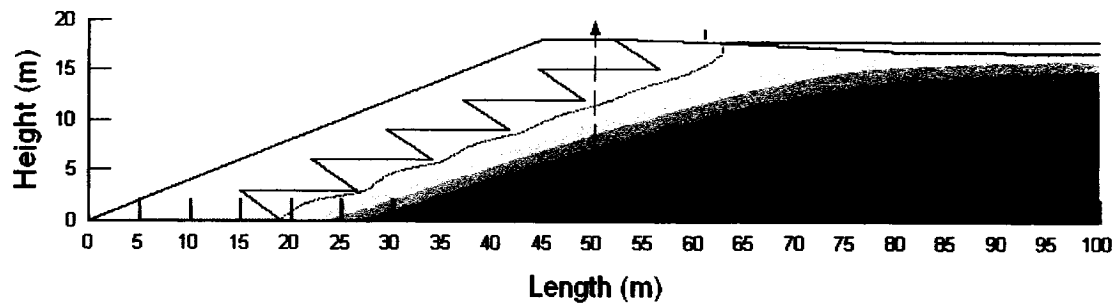


(c) Pressure Head Result

**Figure 6.17: Case 13 – Anisotropy (short beach)**

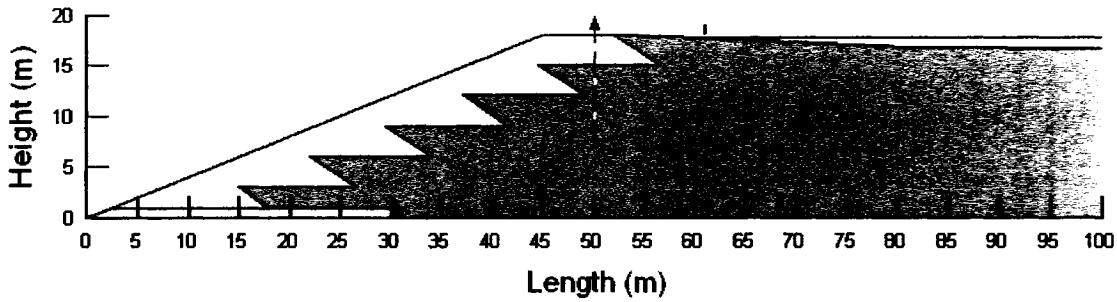


(a) Analysed Section

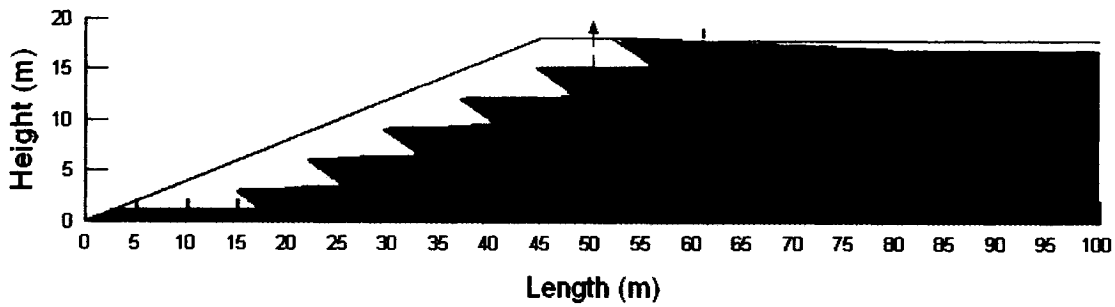


(b) Volumetric Water Content Result

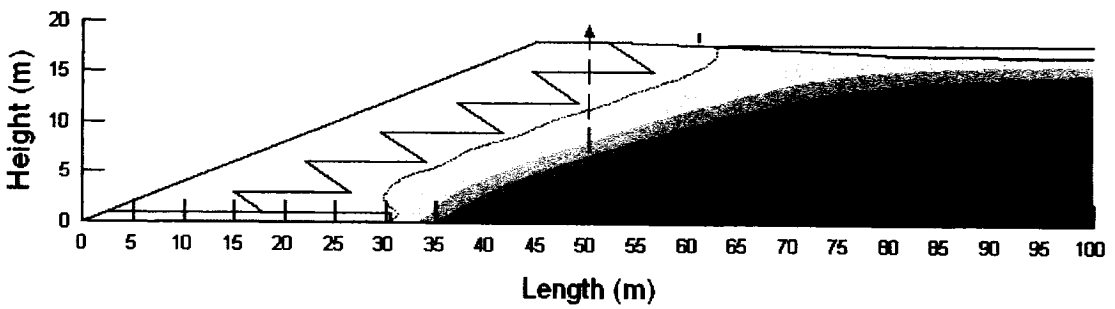


(c) Pressure Head Result

**Figure 6.18: Case 14 – Anisotropy with blanket drain (short beach)**

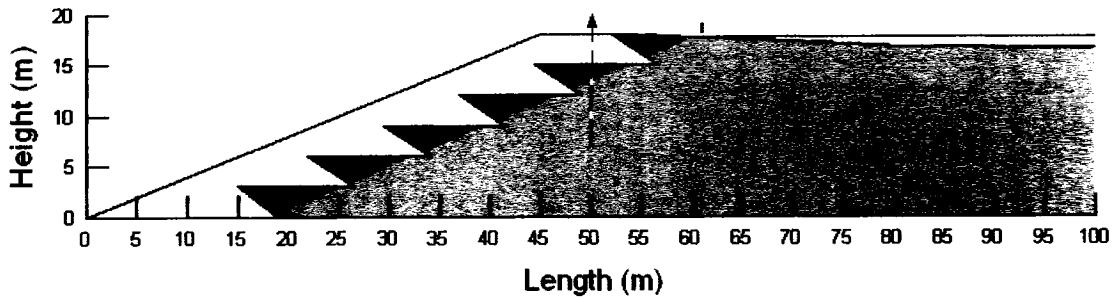


(a) Analysed Section

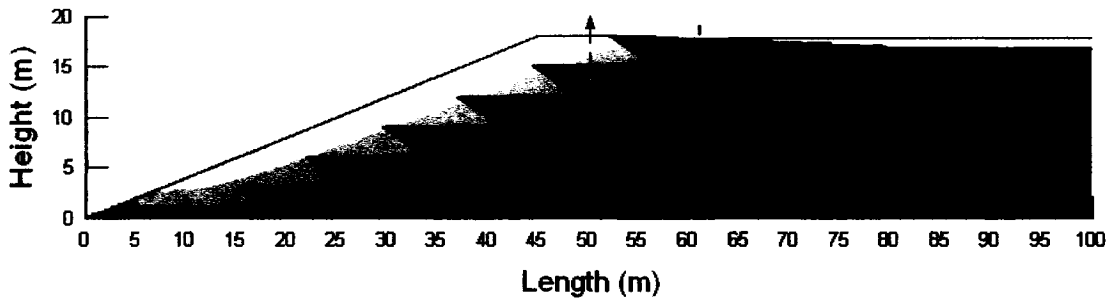


(b) Volumetric Water Content Result

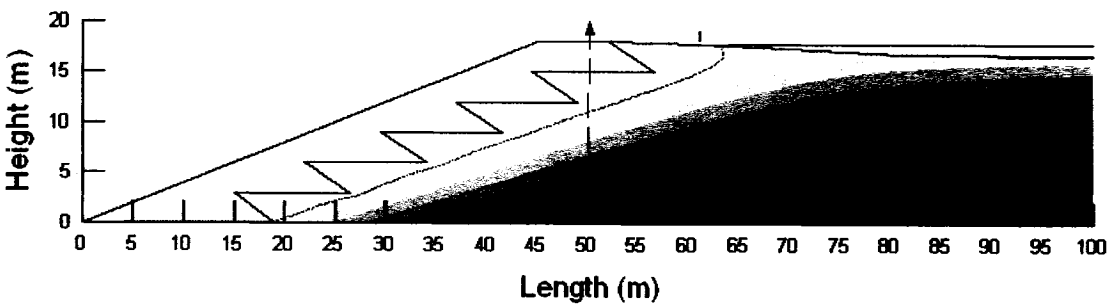


(c) Pressure Head Result

**Figure 6.19: Case 15 – Anisotropy with transition zone (short beach)**

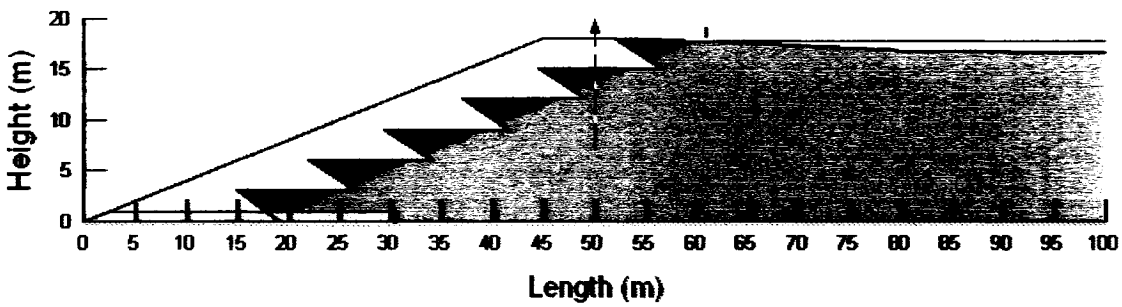


(a) Analysed Section

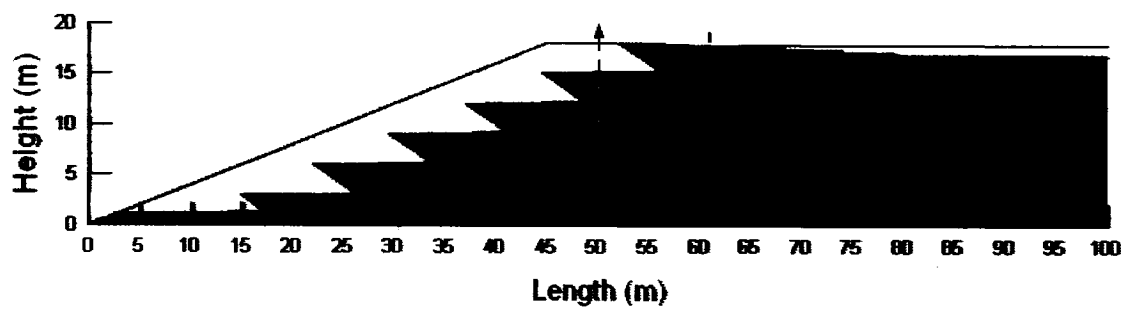


(b) Volumetric Water Content Result

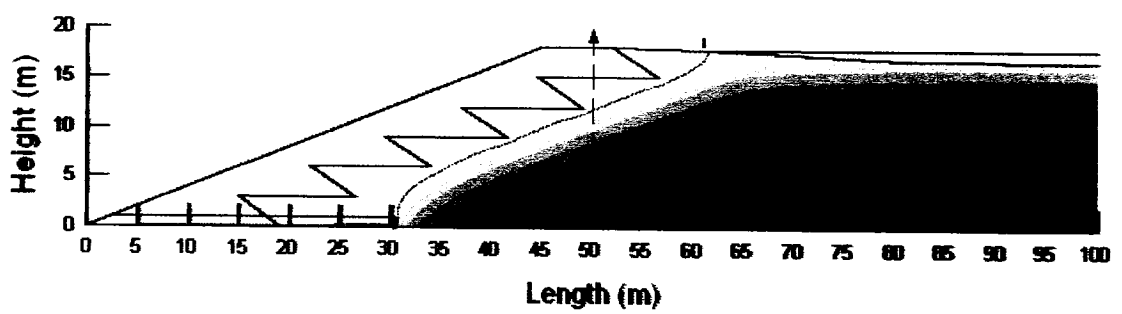


(c) Pressure Head Result

**Figure 6.20: Case 16 – Blanket drain and transition zone (short bench)**

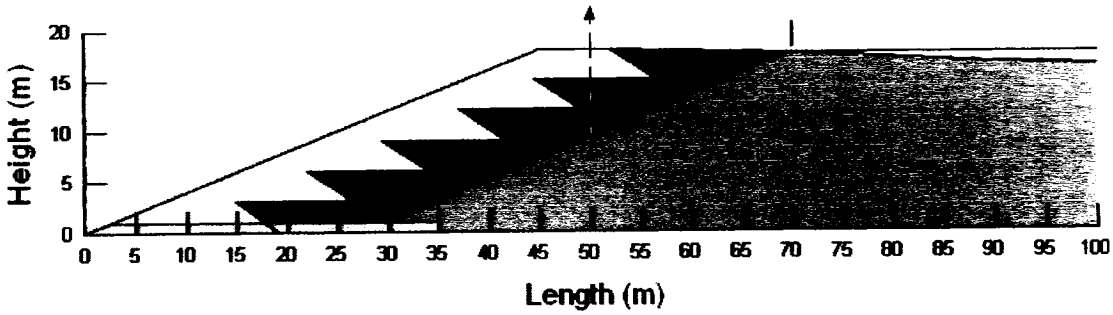


(a) Analysed Section

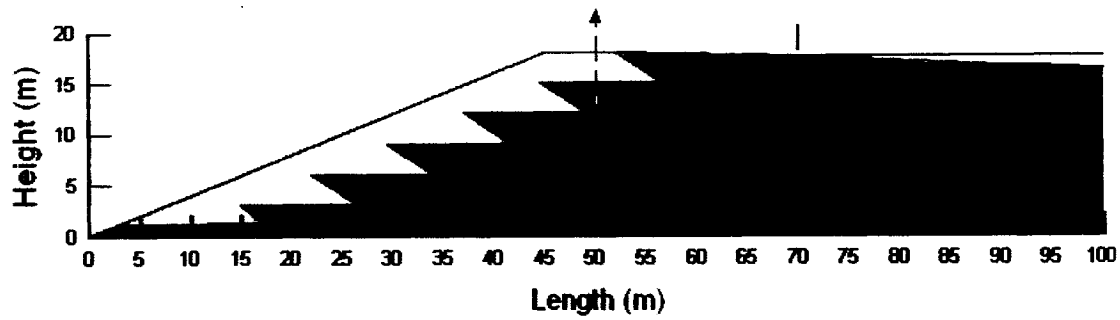


(b) Volumetric Water Content Result

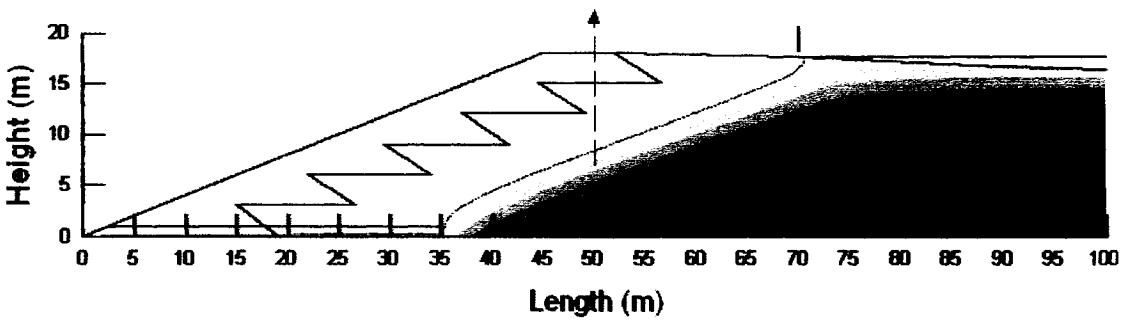


(c) Pressure Head Result

**Figure 6.21: Case 17 - Blanket drain and transition zone (medium beach)**

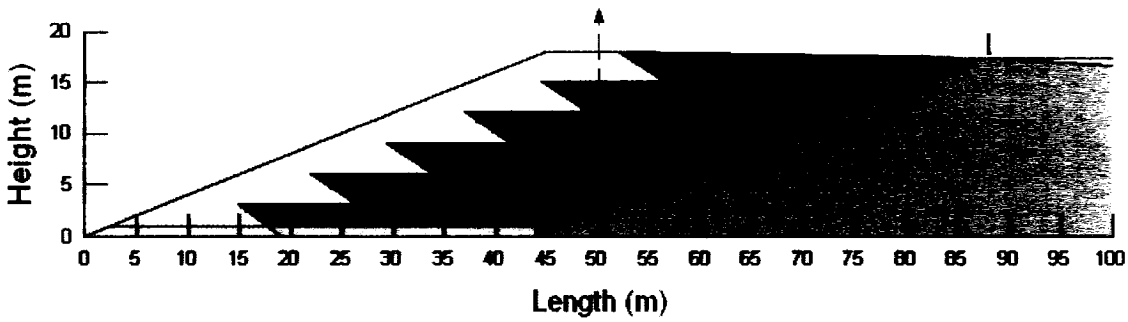


(a) Analysed Section

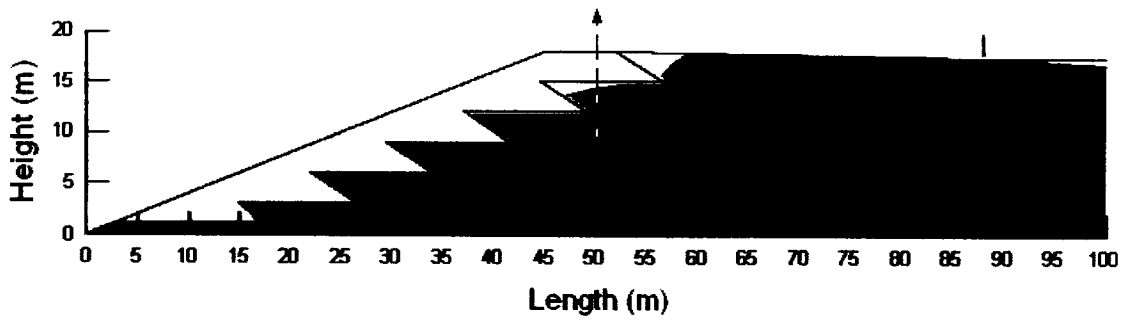


(b) Volumetric Water Content Result

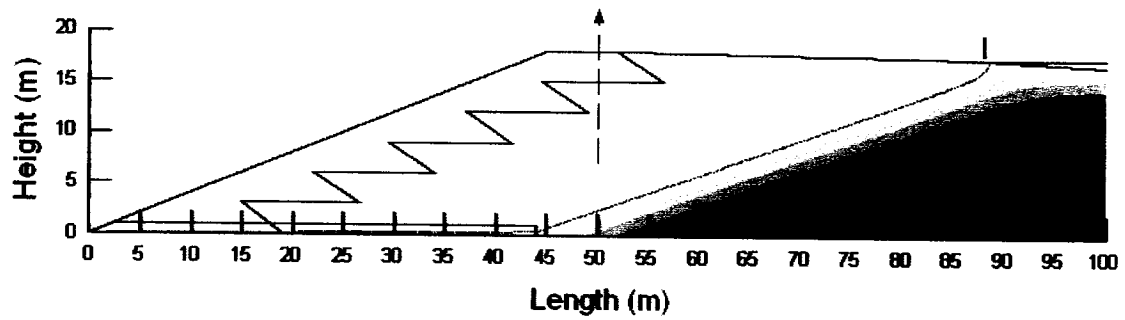


(c) Pressure Head Result

**Figure 6.22: Case 18 - Blanket drain and transition zone (long beach)**

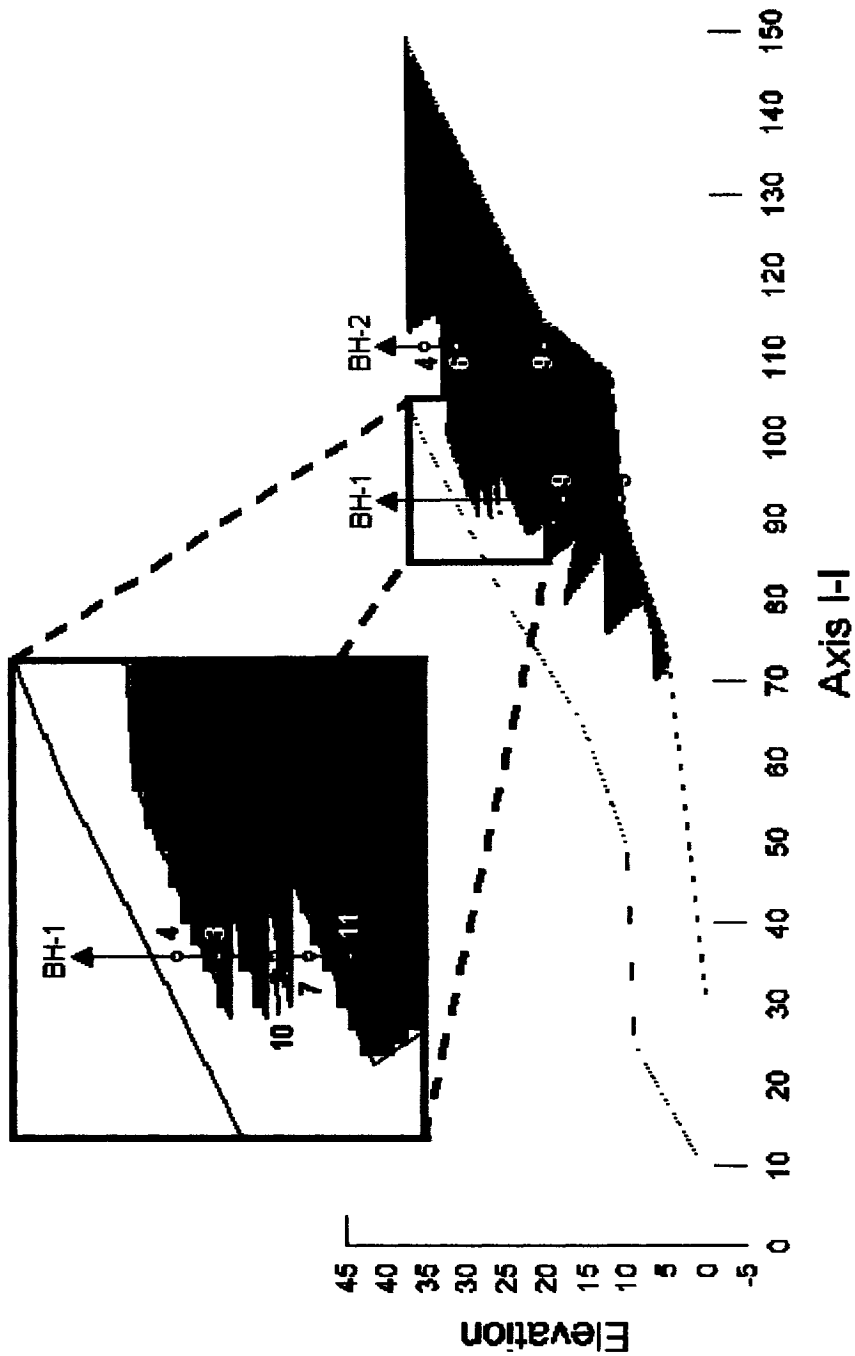


**Figure 6.23: Geometry of South American tailings dam with SPT N-values**

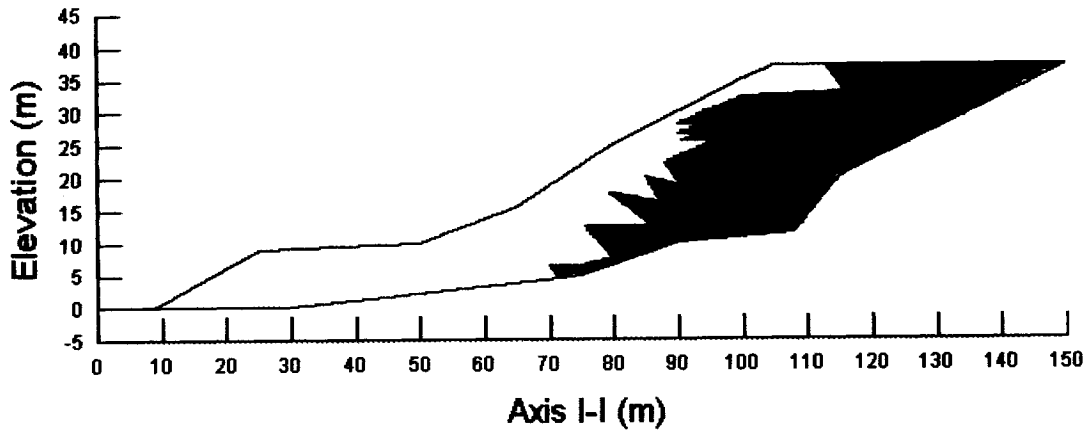


(a) Analysed Section

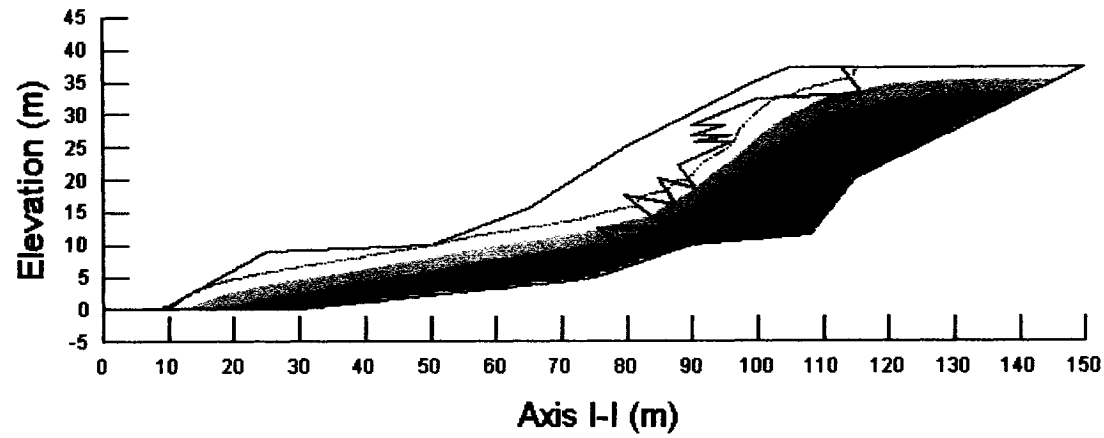


(b) Volumetric Water Content Result

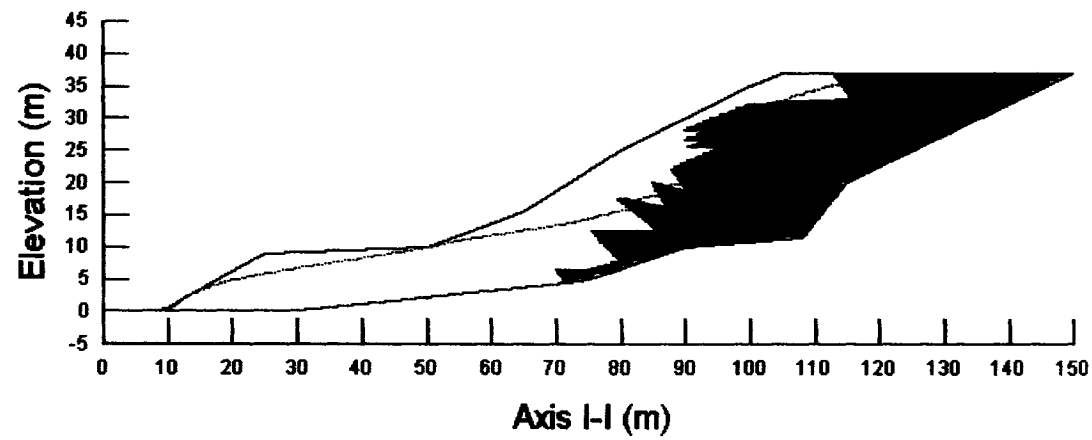


(c) Pressure Head Result

**Figure 6.24: Case 19 – Existing South American dam**

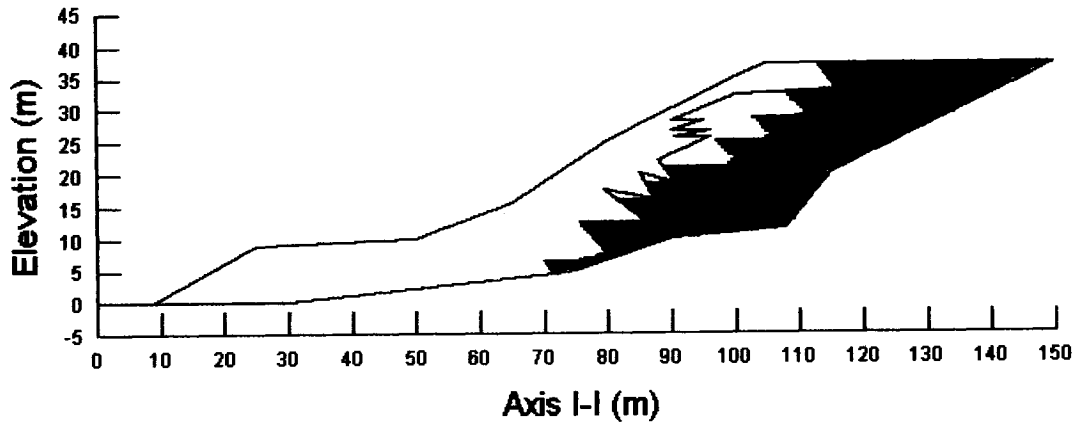


(a) Analysed Section

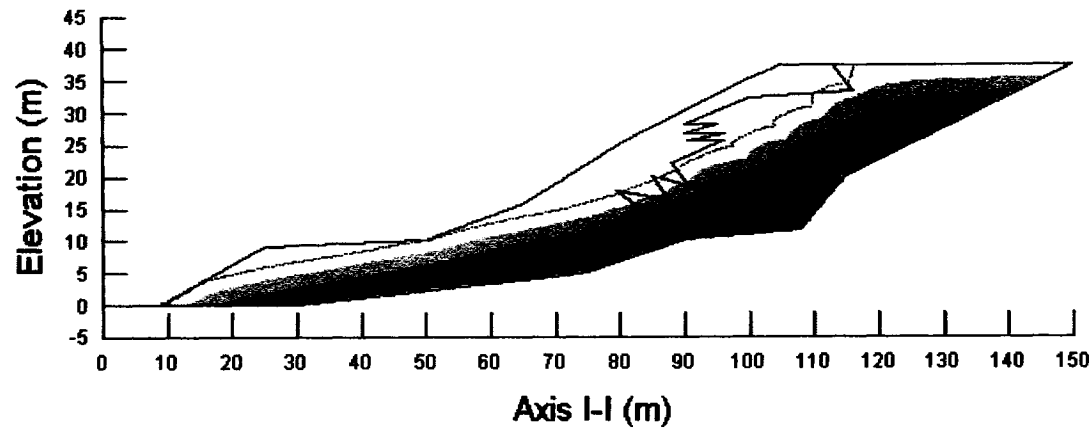


(b) Volumetric Water Content Result

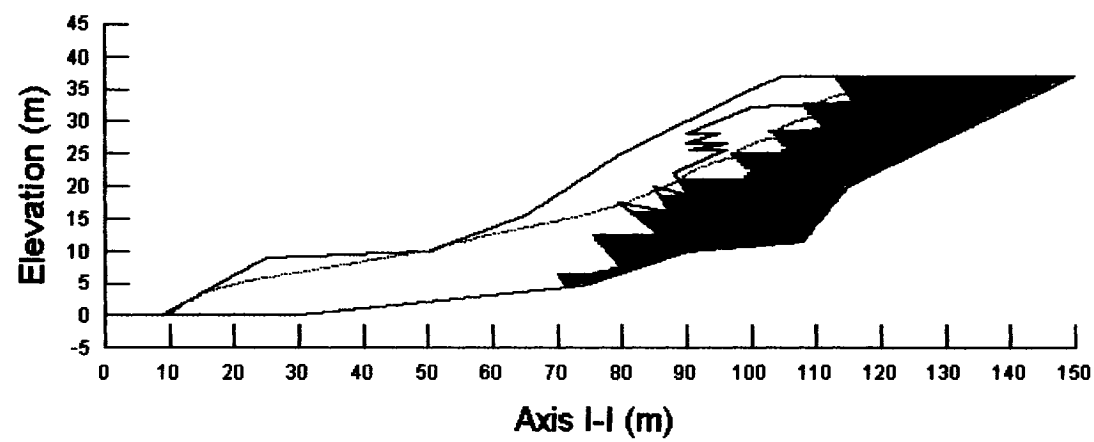


(c) Pressure Head Result

**Figure 6.25: Case 20 – Modified South American dam**

# CHAPTER 7 – CONCLUSIONS

## 7.1 CONCLUSIONS

The work in this research program consisted of two main components; experimental work and numerical modeling. The experimental work comprised of modifying an existing permeameter to determine the unsaturated coefficient of permeability of tailings.

The main constraints for the redesign of the permeameter were to permit the simultaneous measurement of water content and pore air pressures at different time intervals, while allowing the tailings to settle under their own weight during drainage.

The soil-water characteristic curve, SWCC, and the permeability curves were predicted with the SoilVision software. The predicted results and the experimental results were compared.

The conclusions that can be drawn from the experimental work of this research program are as follows:

- The Modified Permeameter, designed and built during this research program, provided sufficient data to compute the SWCC and the unsaturated coefficient of permeability for two different gradations of tailings.
- The Modified Permeameter allowed a single sample to be tested through the full transition from a slurry to a dry sample.
- The predicted SWCC and measured values for the coarse underflow tailings are similar at low pressures.
- The predicted SWCC and measured values for the fine overflow tailings are similar at low pressures.
- Insufficient data was gathered to compute the unsaturated coefficient of permeability for the coarse underflow sample.
- The unsaturated coefficient of permeability obtained from the experimental work with the fine overflow sample produced scattered data. The trend in data points and the predicted values are in agreement.

The objective of the modeling component of this research program was to demonstrate the benefit of maintaining a long beach for an upstream tailings dam.

A small to medium-sized generic upstream tailings dam was modelled and steady-state seepage was simulated under different beach lengths, and under various influences. The numerical analysis was completed with the finite element modeling software SEEP/W.

The main conclusions from the modeling portion of this thesis are as follows:

- Maintaining a long beach length throughout the construction of the upstream tailings dam will prevent saturation of the fine tailings immediately underlying the shell.
- The tailings closest to the shell may sufficiently desaturate to resist liquefaction, if an adequate distance separating the phreatic surface and the shell is provided, and maintained throughout the entire operational life of the dam.
- Proper drainage at the toe of the dam will help control the location of the phreatic surface. The use of a blanket drain can help increase to quantity of unsaturated material immediately underlying the downstream face of the dam.
- SEEP/W was a satisfactory software for the purpose of this work.

## BIBLIOGRAPHY

Abu-Hejleh, A.N., Znidarcic, D. and Illangasekare, T.H., (1993), "Permeability determination for unsaturated soils", Unsaturated Soils, Geotechnical Special Publication No. 39, Eds. Sandra Houston and Warren Wray, Texas, pp.163-174.

Abdelkabir, M., Bussière, B., and Aubertin, M., (2002), "L'hystérésis de sols non saturés utilisés dans les couvertures avec effets de barrière capillaire", Proceedings of the 55th Canadian Geotechnical and 3rd Joint IAH-CNC and CGS Groundwater Specialty Conferences, Niagara Falls, pp. 181-188.

Amraoui, N., Masrouri, F. and Tisot, J.-P., (1998), "Influence of initial conditions of the hydraulic conductivity of an unsaturated soil: Laboratory experimental results and statistical modelling", Proceedings of the Second International Conference on Unsaturated Soils - Beijing, International Academic Publishers, Vol. 1, pp. 549-556.

Arya, L.M. and Paris, J.F. (1981). A physicoempirical model to predict the soil moisture characteristic from particle-size distribution and bulk density data. Soil Science Society of America Journal, Vol. 45, pp. 1023-1030.

Aubertin, M., Ricard, J.-F., and Chapuis, R.P., (1998), "A predictive model for the water retention curve: application to tailings from hard-rock mines", Canadian Geotechnical Journal, Vol. 35, pp. 55-69.

Baker, J.M. and Lascano, R.J., (1989), "The spacial sensitivity of time domain reflectometry, Soil Science, Vol. 14, No. 5, pp.378-384.

Barbour, S.L., (1998), "Nineteenth Canadian Geotechnical Colloquium: The soil-water characteristic curve: a historical perspective", Canadian Geotechnical Journal, Vol. 35, pp. 873-894.

Bedel, P.R., Firlotte, F.W., and Atherton, K., (2002), "A case record of tailings dam construction using residual soils", Canadian Geotechnical Society, Vol. 39, pp. 409-416.

Been, K., (1999), "The critical state line and its application to soil liquefaction", Physics and Mechanics of Soil Liquefaction, Balkema, Rotterdam, pp.195-204.

Benson, C.H., Hardianto, F.S., and Motan, (1994), "Representative specimen size for the hydraulic conductivity assessment of compacted soil liners", ASTM STP 1142, Hydraulic conductivity and waste contaminant transport in soils, D.E. Daniel, and S.J. Trautewin, eds, ASTM, Philadelphia, pp. 3-29.

Benson, C.H. and Gribb, M.M., (1997), "Measuring unsaturated hydraulic conductivity in the laboratory and field", Unsaturated Soil Engineering Practice, Geo. Spec. Pub. No. 68, ASCE, New York, pp. 113-168.

Benson, C., Khire, M. and Bosscher, P., (1993), "Final cover hydrologic evaluation, Final Report – Phase II", Env. Geotechnics Report 93-4, University of Wisconsin-Madison.

Bishop, A.W. and Bjerrum, L., (1960), "The relevance of the triaxial test to the solution of stability problems", Norwegian Geotechnical Institute, Publication No.34, Oslo

Brooks, R.H. and Corey, A.T. (1964), "Hydraulic properties of porous media", Colorado State University Hydrology Paper, 3, 27p.

Burger, C.A. and Shackelford, C.D., (2001), "Soil-water characteristic curves and dual porosity of sand-diatomaceous earth mixtures", Journal of Geotechnical and Geoenvironmental Engineering, Vol. 127, No. 9, pp. 790-800.

Castro, G. and Poulos, S.J., (1977), "Factors affecting liquefaction and cyclic mobility", Journal of the Geotechnical Engineering Division, ASCE, Vol.103, No. GT6, pp. 501-516.

Cedergren, H.R., (1989), "Seepage, drainage, and flow nets - Third Edition", Wiley & Sons, Toronto

Chai, J-R., Li, S-Y., Li, K-H., He, M., D, X-H., (2005), "Numerical analysis of seepage field in Mijiangou tailings dam to be designed to increase the dam height", Yantu Lixue/Rock and Soil Mechanics, Vol. 26, No. 6, June 2005, pp. 973-977.

Chapuis, R.P. and Aubertin, M., (2001), "A simplified method to estimate saturated and unsaturated seepage through dikes under steady-state conditions", Canadian Geotechnical Journal, Vol.38, pp. 1321-1328.

Chapuis, R.P., Chenaf, D., Bussière, B., Aubertin, M., and Crespo, R., (2001), "A user's approach to assess numerical codes for saturated and unsaturated seepage conditions", Canadian Geotechnical Journal, Vol. 38, pp. 1113-1126.

Chapuis, R.P., L'Écuyer, M., and Aubertin, M., (1993), "Field permeability tests in mine tailings", 46th Canadian Geotechnical Conference, Saskatoon, pp. 51-59.

Charlie, W.A., Doering, D.O., Durnford, D.S. and Martin, J.P., (1983),"Dewatering tailings impoundments: Interior drains", Proceedings of the Seventh Pan-American Conference on Soil Mechanics and Foundation Engineering, Canadian Geotechnical Society, Vancouver, pp. 807-817.

Conlin, B.H., (1987) "A review of the performance of mine tailings impoundments under earthquake loading conditions", Earthquake Geotechnique, Vancouver Geotechnical Society.

Crespo, R., (1993), "Modélisation par éléments finis des écoulements à traves les ouvrages de retenue et de confinement des résidus miniers" M.Sc.A. thesis, École Polytechnique de Montréal, Montréal.

Daniel, D.E., (1984), "Predicting hydraulic conductivity of clay liners", Journal of Geotechnical Engineering, ASEC, Vol. 110, No. 2, pp. 233-254.

Davies, J.L. and Chudobiac, W.J., (1975), "In-situ meters for measuring relative permitivity of soils, Pap. 75-1A, Geol. Surv. Can., Ottawa, pp.75-79.

Davies, M.P.and Martin, T.E., (2000), "Upstream constructed tailings dams - A review of the basics", Tailings and Mine Waste '00, Balkema, Rotterdam, pp. 21-55.

Davies, M.P., Martin, T.E. and Lightall, P.C., (2000), "Tailings dam stability – essential ingredients for success", Chapter 40 in Slope Stability in Surface Mining, SME, pp.365-378.

de Groot, M.B., Henzen, F.T., Masterbergen, D.R. and Stefess, H., (1988), "Slopes and densities of hydraulically placed sands", Hydraulic Fill Structures, Geotechnical Special Publication No. 21, ASCE, pp. 32-50.

Devinny, J.S., Everett, L.G., Lu, J.C.S. and Stollar, R.L., (1989), "Subsurface migration of hazardous wastes", VNR Environmental Engineering Series, New York, pp. 40-115.

East, D.R. and Ransone, J.W., (1988), "Testing of the Homestake mine tailings deposit", Proceedings of the Second International Conference on Case Histories in Geotechnical Engineering, St-Louis, pp. 495-502.

Elsbury, B.R., Daniel, D.E., Sraders, G.A., and Anderson, D.C., (1990), "Lessons learned from compacted clay liner", Journal of Geotechnical Engineering, Vol. 11, pp.1641-1660.

Elzeftawy, A. and Cartwright, K., (1981), "Evaluating the saturated and snsaturated sydraulic conductivity of soils", Permeability and Groundwater Contaminant Transport,

ASTM STP 746, T.F. Zimmie and C.O. Riggs Eds., American Society for Testing and Materials, pp. 168-181.

Elzeftawy, A. and Mansell, R.S., (1975), "Hydraulic conductivity calculations for unsaturated steady-state and transient-state flow in sand", Soil Science Society of America Proceedings, Vol. 39, No. 4., pp. 599-603.

Fala, O., Aubertin, M., Bussière, B., and Chapuis, R.P., (2002), "Analyse numérique des écoulements non saturés dans des haldes à stériles, Proceedings of the 55th Canadian Geotechnical and 3rd Joint IAH-CNC and CGS Groundwater Specialty Conferences, Niagara Falls, pp. 489-496.

Ferré, P.A., Redman, J.D., Rudolf, D.L. and Kachanoski, R.G., (1998), "The dependence of the electrical conductivity measured by time domain reflectometry on water content of a sand", Water Resources Research, Vol. 34, No. 5, pp. 1207-1213.

Fetter, C.W., (1992), "Contaminant hydrogeology", Macmillan, Toronto, pp. 163-201.

Finn, W.D.L., (1980), "Seismic response of tailings dams", Design and Construction of Tailings Dams, Ed. David Wilson, Colorado School of Mines, Colorado, pp. 77-98.

Fleureau, J.M. and Taibi, S., (1995), "Water-air permeabilities of unsaturated soils", Proceedings of the First International Conference on Unsaturated Soils, Balkema, Paris, pp. 479-484.

Fourie, A., (1988), "Beaching and permeability properties of tailings", Hydraulic Fill Structures, Geotechnical Special Publication No. 21, ASCE, pp. 142-154

Fourie, A.B. and Papageorgiou, G., (2001), "Defining an appropriate steady state line for Merriespruit gold tailings", Canadian Geotechnical Journal, Vol. 38, pp. 695-706.

Fourie, A.B., Blight, G.E. and Papageorgiou, G., (2001), "Static liquefaction as a possible explanation for the Merriespruit tailings dam failure", Canadian Geotechnical Journal, Vol. 38, pp. 707-719.

Fourie, A.B., Hofmann, B.A., Mikula, R.J., Lord, E.R.F. and Robertson, P.K., (2001), Partially saturated tailings sand below the phreatic surface", Géotechnique, Vol. 51, No. 7, pp. 577-585.

Frechette, R.J., (1994), "Construction of access ramps and reclamation covers upon tailings impoundment surfaces", Tailings and Mine Waste '94, Balkema.

Fredlund, D.G. and Rahardjo, H., (1993), "Soil mechanics for unsaturated soils", John Wiley & Sons, Toronto, 517 pp.

Fredlund, D.G. and Xing, A., (1994), "Equations for the soil-water characteristic curve", Canadian Geotechnical Journal, Vol. 31, pp. 521-532.

Fredlund, D.G., (1997), "An introduction to unsaturated soil mechanics", ASCE, Geotechnical Special Publication No. 68, New York, pp. 1-37.

Fredlund, M., Fredlund, D.G., and Wilson, W.G. (1997), "Prediction of the soil-water characteristic curve from grain-size distribution and volume-mass properties" Proceedings of the Third Brazilian Symposium on Unsaturated Soils, Rio de Janeiro, Brazil.

Fredlund, D.G., Xing, A. and Huang, S., (1994), "Predicting the permeability function for unsaturated soils using the soil-water characteristic curve", Canadian Geotechnical Journal, Vol. 31, pp. 533-545.

Fredlund, M.D., Wilson, G.W. and Fredlund, D.G., (1998), "Estimation of hydraulic properties of an unsaturated soil using a knowledge-based system", Proceedings of the

Second International Conference on Unsaturated Soils, Beijing, China, Vol. 1, International Academic Publishers, pp. 549-556.

Freeze, R.A. and Cherry, J.A., (1979), "Groundwater", Prentice Hall, Toronto, 604 pp.

Gardner, W.R., (1958), "Some steady state solutions of the unsaturated moisture flow equation with application to evaporation from a water table", Soil Science, 85(4):228-232

Gonzalez, P.A., and Adams, B.J., "Mine tailings disposal: I. Laboratory characterization of tailings", Dept. Of Civil Eng., University of Toronto, pp. 1-14.

Griffin, P.M., Smith, E.S., Von Loebenstein, J.G. and Edwards, R., (1983), "Perez Caldera tailings dams - A case history", Proceedings of the Seventh Pan-American Conference on Soil Mechanics and Foundation Engineering, Canadian Geotechnical Society, Vancouver, pp. 751-761.

Grozic, J.L., Robertson, P.K. and Morgenstern, N.R., (1999), "The behaviour of loose gassy sand", Canadian Geotechnical Journal, Vol. 36, pp. 482-492.

Gupta, S.C. and Larson, W.E., (1979), "Estimating soil water retention characteristics from particle size distribution, organic matter percent, and bulk density", Water Resources Research, 15(6):325-339.

Hamilton, J.M., Daniel, D.E. and Olson, R.E., (1979), "Measurement of hydraulic conductivity of partially saturated soils", Permeability and Groundwater Contaminant Transport, ASTM Spec. Tech. Pub. 746, Eds. Zimmie/Riggs, pp. 182-196.

Harper, T.G., McLeod, H.N. and Davies, M.P., (1992), "Seismic assessment of tailings dams", Civil Engineering, December, pp.64-66.

Harr, M.E., (1991), "Groundwater and seepage", Dover Publications, New York.

Holland, D.F., Yitayew, M. and Warrick, A.W., (2000), "Measurement of subsurface unsaturated hydraulic conductivity", Journal of irrigation and drainage engineering, Jan-Feb, pp. 21-27.

Houston, W.N. and Houston, S.L., (1995), "Infiltration studies for unsaturated soils", In Proceedings of the First International Conference on Unsaturated Soils - Paris, Vol. 2, pp.869-875.

ICOLD, (1994), "Tailings Dams – Design of Drainage; Review and recommendations", Bulletin 97.

ICOLD, (1995), "Tailings Dams and Seismicity; Review and recommendations", Bulletin 98.

ICOLD, (1995), "Tailings Dams – Transport, Placement and Decantation; Review and recommendations", Bulletin 101.

ICOLD, (1996), "Tailings Dams – Monitoring of Tailings Dams; Review and recommendations", Bulletin 104.

ICOLD, (2001), "Tailings Dams – Risk of Dangerous Occurences; Lessons learnt from practical experiences", Bulletin 121.

Ishihara, K., (1985), "Stability of natural deposits during earthquakes", Proceedings of the Eleventh International Conference on Soil Mechanics and Foundation Engineering, Balkema, Boston, 321 pp.

Keshian JR, B. and Rager, R., (1988), "Geotechnical properties of hydraulically placed uranium mill tailings", Hydraulic Fill Structures, ASCE Geotechnical Special Publication No. 21, pp. 227-253.

Kézdi, A., (1974), "Handbook of soil mechanics", Elsevier Scientific Publishing Company, New York, pp. 137-164.

Klohn, E.J., (1979), "Seepage control for tailings dams", reprinted from MINE DRAINAGE, the proceedings of the first International Mine Drainage Symposium, Denver, Colorado, Miller Freeman Publications

Klohn, E.J., (1986), "Dam Safety and Tailings Dam Design", Proceedings of Dam Safety Seminar, Edmonton, Alberta, BiTech Publishers Ltd., pp. 129-154.

Klute, A., (1972), "The determination of the hydraulic conductivity and diffusity of unsaturated soils", Soil Science, Vol. 113, No. 4, pp. 264-276.

Klute, A. and Dirksen, C., (1986), "Hydraylic conductivity and diffusivity: laboratory methods", Methods of Soil Analysis, Part 1 –Physical and Mineralogical Methods, 2nd Ed., A. Klute, Ed., Soil Science Society of America, Madison, WI, pp. 687-729.

Krause, A.J., (1997), "Regulatory and technical tailings design considerations in Chile", Tailings and Mine Waste '99, Balkema, Rotterdam, pp. 21-55.

Leoni, G.L.M., Almeida, M.D.S.S, Fernandes, H.M., (2004), "Computational modelling of final covers for uranium mill tailings impoudments", Journal of Hazardous Materials, Vol. 110, No. 1-3, pp. 139-149.

Lightall, P.C., Martin, T. and Davies, M.P., (2000), "Design and construction of tailings dams – A millenium update", source unavailable

Linsley, R.K., Kohler, M.A. , and Paulhus, J.L.H., (1975), "Hydrology for engineers - Second edition", McGraw-Hill, New York, 482 pp.

Lipinski, M.J. and Golebiewska, A., (2000), "A study of granulation distribution in a beach of tailings dam", Tailings and Mine Waste '00, Balkema, Rotterdam, pp. 159-168.

Lo, R. (1980), "Seismic investigation of sand-fill tailings dams", Design and Construction of Tailings Dams, Ed. David Wilson, Colorado School of Mines, Colorado, pp. 170-186.

Mabula, M.P., (1995), "Mechanics of water movement in solids - A re-examination of basic principals", Ph.D. Thesis, University of Witwatersrand, Johannesburg, South Africa.

Martin, T.E. and McRoberts, E.C, (1998), "Safety audits of upstream tailings dam in Latin America", 51st Canadian Geotechnical Conference, Edmonton, pp. 133-140.

Martin, T.E. and McRoberts, E.C, (1999), "Some considerations in the stability analysis of upstream tailings dams", Tailings and Mine Waste '99, Balkema, Rotterdam, pp. 287-302.

Martin, T.E., (1999), "Characterization of pore pressure conditions in upstream tailings dams", Tailings and Mine Waste '99, Balkema, Rotterdam, pp. 303-313.

Martins, R., "Dam safety and protection of human lives", source unavailable.

McWorther, D.B. and Nelson, J.D., (1979), "Unsaturated flow beneath tailings impoundments", Journal of the Geotechnical Engineering Division, ASCE, Vol. 105, No. GT11, Nov., pp. 1317-1334.

Meerdink, J.S., Benson, C.H. and Khire, M.V., (1996), "Unsaturated hydraulic conductivity of two compacted barrier soils", Journal of Geotechnical Engineering, ASCE, pp. 565-576.

Morgenstern, N.R., (1985), "Geotechnical aspects of environmental control", Proceedings of the Eleventh International Conference on Soil Mechanics and Foundation Engineering, San Francisco, Balkema, Rotterdam, pp. 155.

Mualem, Y., (1976), "A new model for predicting the hydraulic conductivity of unsaturated porous media", Water Resources Research, 12: 593-622.

Nimmo, J., Rubin, J., and Hammermeister, D., (1992), "Unsaturated flow in a centrifugal field: measurment of hydraulic conductivity and testing of Darcy's Law", Water Resource Research, Vol. 23, No. 1, pp. 124-134.

O'Connor, K.M. and Dowding, C.H., (1999), "Geomeasurements by pulsing TDR cables and probes", CRC Press, New York, 402 pp.

O'Connor, K.M., Poulter, D.A. and Znidarcic, D., (2000), "Tailings management using TDR technology", Tailings and Mine Waste '00, Balkema, Rotterdam, pp. 451-460.

Olson, R.E. and Daniel, D.E., (1981), "Measurement of the hydraulic conductivity of fine-grained soils", Permeability and Groundwater Contaminant Transport, ASTM STP 746, T.F.Zimmie and C.O. Riggs, Eds., American Society for Testing and Materials, pp. 18-64.

Pierce, S.J., Yadon, D.M., Miller, D.J. and Jewell, A.C., (1994), "Geotechnical aspects of dam safety improvements for two water treatment detention ponds - Warm springs ponds operable unit, Montana, USA", Tailings and Mine Waste '94, Balkema, Rotterdam.

Poulos, S.J., Castro, G. and France, J.W., (1985), "Liquefaction evaluation procedure", Journal of Geotechnical Engineering, ASCE, pp. 772-792.

Qui, Y. and Sego, D.C., (2001), "Laboratory properties of mine tailings", Canadian Geotechnical Journal, Vol. 38, pp. 183-190.

Rassam, D.W. and Williams, D.J., (1999), "A numerical study of steady state evaporative conditions applied to mine tailings", Canadian Geotechnical Journal, Vol. 36, pp. 640-650.

Rassam, D.W., (2002), "Variation of evaporative and shear strength parameters along a tailings delta", Canadian Geotechnical Journal, Vol. 39, pp. 32-45.

Rawls, W.J. and Brakensiek, D.L., (1985), "Prediction of soil water properties for hydrologic modelling", Watershed managemenent in the Eighties, E.B. Jones and T.J.Ward (Eds), ASCE Convention, Denver, CO, April 30-May 1, pp.293-299.

Richards, S. and Weeks, L., (1953), "Capillary conductivity values from moisture yield and tension measurements on soil columns", Proceedings of Soil Science of America, Vol. 17, pp. 206-209.

Robinski, E.I., (1999), "Tailings dam failures need not be disasters - The thickened tailings disposal (TTD) system", CIM Bulletin, Vol.92, No.1028, pp. 140-142.

Robinson, D.A., Bell, J.P. and Batchelor, C.H., (1994), "Influence of iron minerals on the determination of soil water content using dielectric techniques", Journal of Hydrology, Vol. 161, pp. 169-180.

Rodgers, M. and Mulqueen, J., (2006), "Field-saturated hydraulic conductivity of unsaturated soils from falling-head well", Agricultural Water Management, Vol. 79, No. 2, pp. 160-176.

Rosenshein, J. and Gordon, D.B., (1984), "Groundwater hydraulics", American Geophysical Union, Washington

Sassa, K., Fukuoka, H., Scarascia-Mugnozza, G. and Evans, S., (1996), "Earthquake-induced-landslides: Distribution, motion and mechanisms", Special Issue of Soils and Foundations, pp. 53-64.

Scheinost, A.C, Sinowski, W. and Auerswald, K., (1996), "Regionalization of soil water retention curves in a highly variable soilscape", Developing a new pedotransfer function, Geoderma, 78: 129-143.

Schiffman, R.L., Vick, S.G. and Gibson, R.E., (1988), "Behaviour and properties of hydraulic fills", Hydraulic Fill Structures, Geotechnical Special Publication No. 21, ASCE, pp. 166-202.

Seed, H.B. and Idriss, I.M., (1971), "Simplified procedure for evaluating soil liquefaction potential", Journal of the Soils Mechanics and Foundations Division, ASCE, Vol. 97, No. SM9, pp. 1249-1273.

Seed, R.B. and Harder, L.F., (1990), "SPT-based analysis of cyclic pore pressure generation and undrained residual strength", H.Bolton Seed Memorial Symposium Proceedings, Ed. J. Michael Duncan, pp. 351-376.

Shuai, F. and Fredlund, D.G., (2000), "Use of a new thermal conductivity sensor to measure soil suction", Geotechnical Special Publication No. 99, ASCE, pp. 1-12.

Shuai, F., Clements, C., Ryan, L. and Fredlund, D.G., (2000), "Some factors that influence soil suction measurements using a thermal conductivity sensor", submitted to 2001 Annual Transportation Research Board Meeting in Washington, DC.

Singh, V.P., (1992), "Elementary hydrology", Prentice Hall, New Jersey, pp. 207-210.

SoilVision 3.04. 1999. Software Package for Modelling the Engineering Behaviour of Unsaturated Soils. Soil Vision Systems Ltd.

Strachan, C., (1994), "Covering tailings - Some theoretical and practical aspects", Tailings and Mine Waste '94, (proceedings of the first international conference on tailings and mine waste '94), Balkema, Rotterdam, pp.189-192.

Strachan, C., (2001), "Tailings dam performance from USCOLD incident-survey data", Mining Engineering, Vol. 53, No. 3, pp.49-53.

Swanson, D.A., Savci, G., Danziger, G., Mohr, R.N. and Weiskopf, T., (1999), "Predicting the soil-water characteristics of mine soils", Tailings and Mine Waste '99, Balkema, Rotterdam, pp. 345-349.

Szymanski, A., (1999), "Analysis of subsoil deformations", Embankments on organic soils, Edited by J.Hartlen and W.Wolski, Amsterdam, New York, Elsevier Science

Tindall, J.A. and Kunkel, J.R., (1999), "Unsaturated zone hydrology for scientists and engineers", Prentice-Hall, New Jersey.

Tinjum, J., Benson, C. and Blotz, L., (1996), "Soil-water characteristic curves for compacted clays", Journal of Geotechnical and Geoenvironmental Engineering, ASCE.

Tokimatsu, K. and Seed, H.B., (1987), "Evaluation of settlement in sands due to earthquake shaking", Journal of Geotechnical Engineering, ASCE, Vol.113, No.8, pp. 861.

Topp, G.C. and Davies, J.L., (1985), "Time domain reflectometry (TDR) and its application to irrigation scheduling", Advances in irrigation, Vol. 3, Academic Press, pp.107-127.

Trichês, G. and Pedroso, R.S., (2002), "Using time domain reflectometry to determine moisture contents in unsaturated soils", Proceedings of the third international conference on unsaturated soils, Recife, Brazil, Vol. 1, pp. 357-361.

Tronsco, J.H., (1983), "Seismic pore water pressures in tailings dams", Proceedings of the Seventh Pan-American Conference on Soil Mechanics and Foundation Engineering, Canadian Geotechnical Society, Montreal, pp. 641-655.

Troncoso, J., (1988), "Evaluation of seismic behaviors of hydraulic fill structures", Hydraulic Fill Structures, ASCE Special Pub., No. 21, pp.475-491.

Troncoso, J., (1990), "Failure risks of abandonned tailings dams", Proceedings of International Symposium on Safety and Rehabilitation of Tailings Dams, ICOLD.

Tyler, S.W. and Wheatcraft, S.W., (1989), "Application of fractal mathematics to soil water retention estimation", Soil Science Society American Journal, V.53, No.4, pp.987-996.

Uginchus, A.A., (1966), "Seepage through earth dams", Israel Program for Scientific Translations, Jerusalem.

Ulrich, B.F. and Hughes, J.M.O., (1994), "SPT/CPT correlations for mine tailings", Tailings and Mine Waste '94, Balkema, pp. 215-223.

U.S. Environmental Protection Agency, (1994), "Design and evaluation of tailings dams" Office of Solid Waste Branch, Washington, Technical Report EPA530-R-94-038.

van Genuchten, M.T., (1980), "A closed form equation for predicting the hydraulic conductivity of unsaturated soils", Soil Science Society of America Journal, 44: 892-898.

Vanapalli, S. K., Fredlund, D. G. and Pufahl, D. E., (1999), "The influence of soil structure and stress history on the soil-water characteristics of a compacted till", Geotechnique, Vol. 49, pp.143-159.

Vanapalli, S.K. and Lobbezoo, J.P., (2002), "A normalized function for predicting the coefficient of permeability of unsaturated soils", Proceedings of the Third International Conference on Unsaturated Soils, Brazil, Vol.2, pp.839-844.

Vereecken, H., Maes, J., Feyen, J. and Darius, P., (1989), "Estimating the soil moisture retention characteristics from texture, bulk density, and carbon content", Soil Science, V.148, No.6.

Vick, S.G. and Watts, B.D., (1994), "Risk and reliability in ground engineering", Institution of Civil Engineers, Thomas Telford, London, pp. 241-253.

Vick, S.G., (1983), "Planning, design and analysis of tailings dams", Wiley, Toronto, Canada.

Vick, S.G., (1990), "Risk-based approach to seismic stability and inundation hazard for upstream tailings dams", International Symposium on Safety and Rehabilitation of Tailings Dams, ICOLD, Sydney, pp. 53-62.

Wardwell, R.E., Findlay, R.C. and Muzzy, M.M., (1988), "Seepage effects on sedimentation of fly ash slurry", Hydraulic Fill Structures, Geotechnical Special Publication No. 21, ASCE, pp. 389-409.

Wedage, A.M.P., Morgenstern, N.R., and Chan, D.H., (1998), "Simulation of time-dependent movements in Syncrude tailings dyke foundation, Canadian Geotechnical Journal, Vol. 35. pp. 284-298.

Williams, D.J., and Morris, P.H., (1988), "Properties of slurried coal tailings", Hydraulic Fill Structures, Geotechnical Special Publication No. 21, ASCE, pp. 410-429.

www.falconbridge.com

Yoshimi, Y., Tanaka, K., and Tokimatsu, K., (1989), "Liquefaction resistance of a partially saturated sand", Soils and Foundations, Vol. 39, No. 3, pp.157-162.

Yoshimine, M., Robertson, P.K. and Wride (Fear), C.E., (1999), "Undrained shear strength of clean sands to trigger flow liquefaction", Canadian Geotechnical Journal, Vol.36, pp. 891-906.

Zapata, C.E, Houston, W.N., Houston, S.L., and Walsh, K.D., (2000), "Soil-water characteristic curve variability", Geotechnical Special Publication No. 99, ASCE, pp. 84-124.

Zegelin, S.J., White, I. and Jenkins, D.R., (1989), "Improved field probes for soil-water content and electrical conductivity measurement using time domain reflectometry, Water Resources Research, Vol. 25, No. 11, pp.2367-2376.

Zimmie, T.F. and Riggs, C.O., (1979), "Permeability and groundwater contaminant transport", ASTM Special Technical Publication 746, Philadelphia.

# Appendix A: Shop Drawings

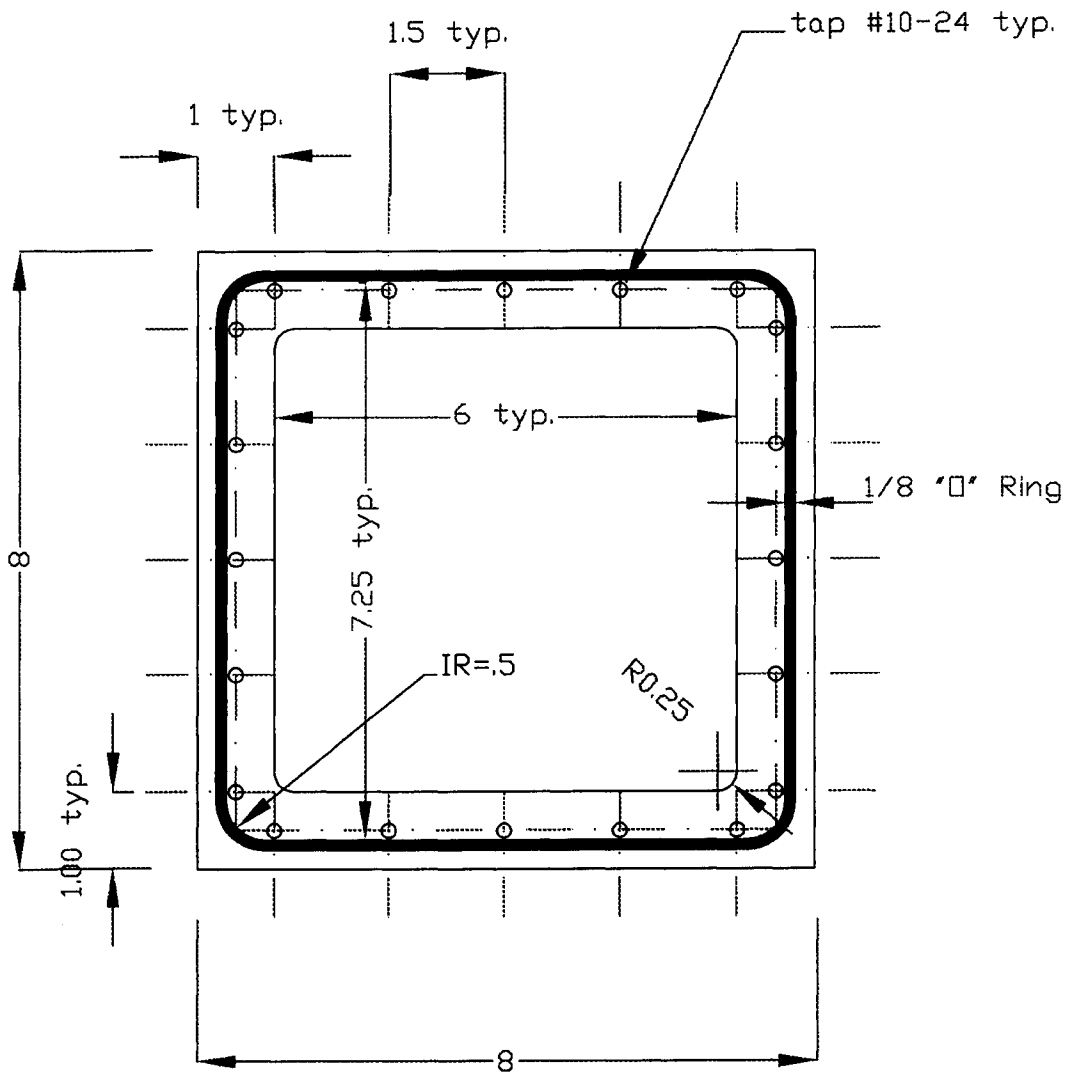


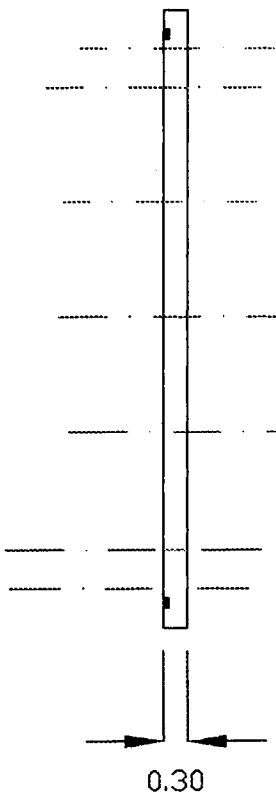


University of Ottawa
Université d'Ottawa

PROJECT :
Instantaneous Profile Setup

PART :
Stone Seal

MATERIAL :
Aluminium

QUANTITY :
1

NOTE :

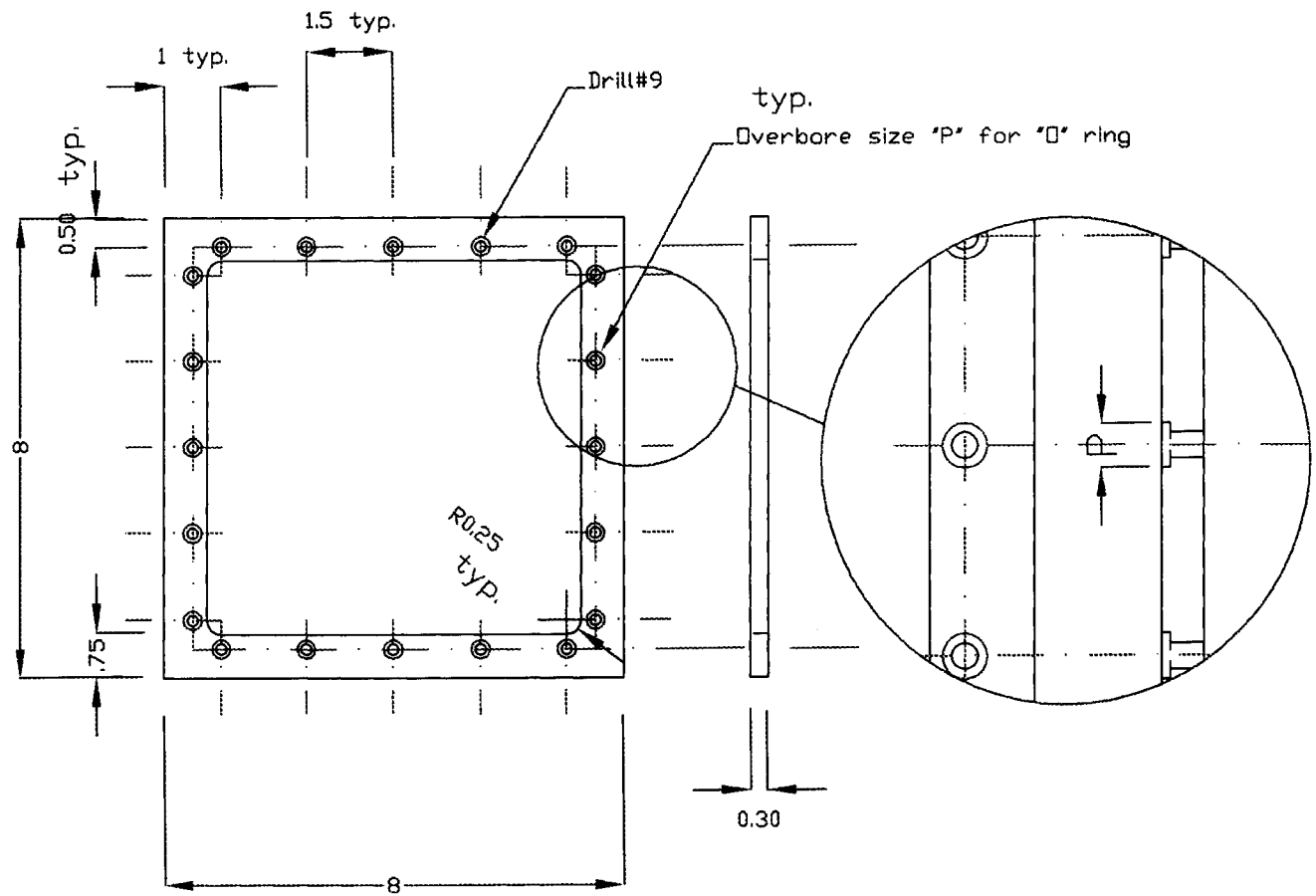


University of Ottawa
Université d'Ottawa

PROJECT :

Instantaneous
Profile Setup

PART :

Stone Collar

MATERIAL :

Aluminium

QUANTITY :

1

NOTE :

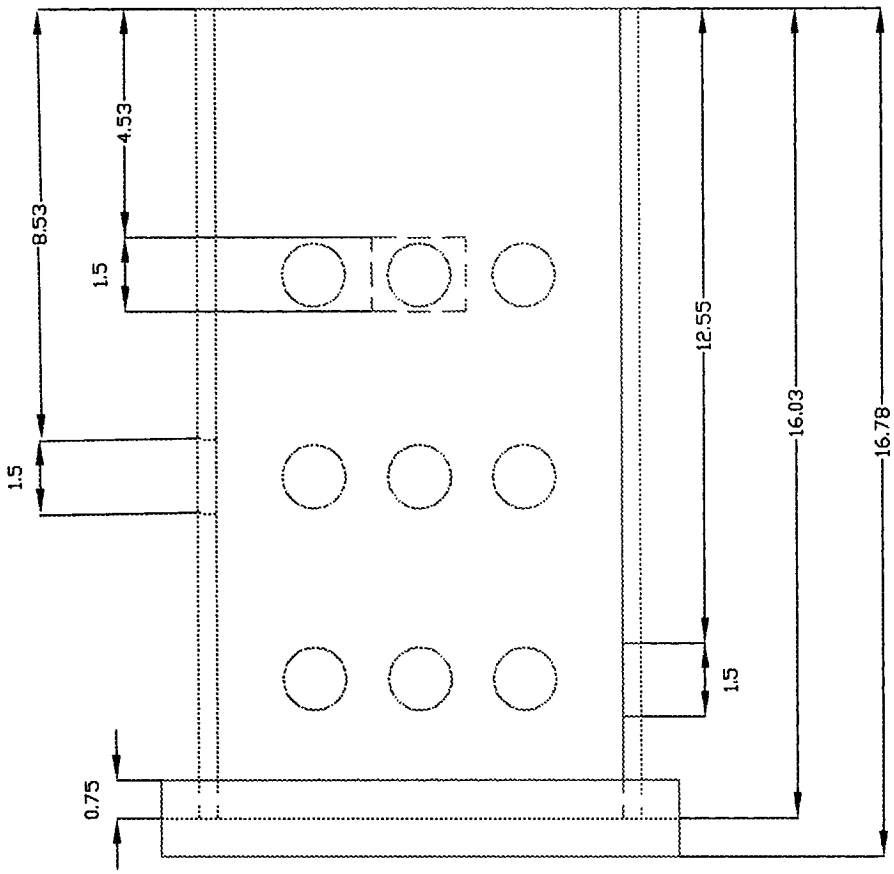


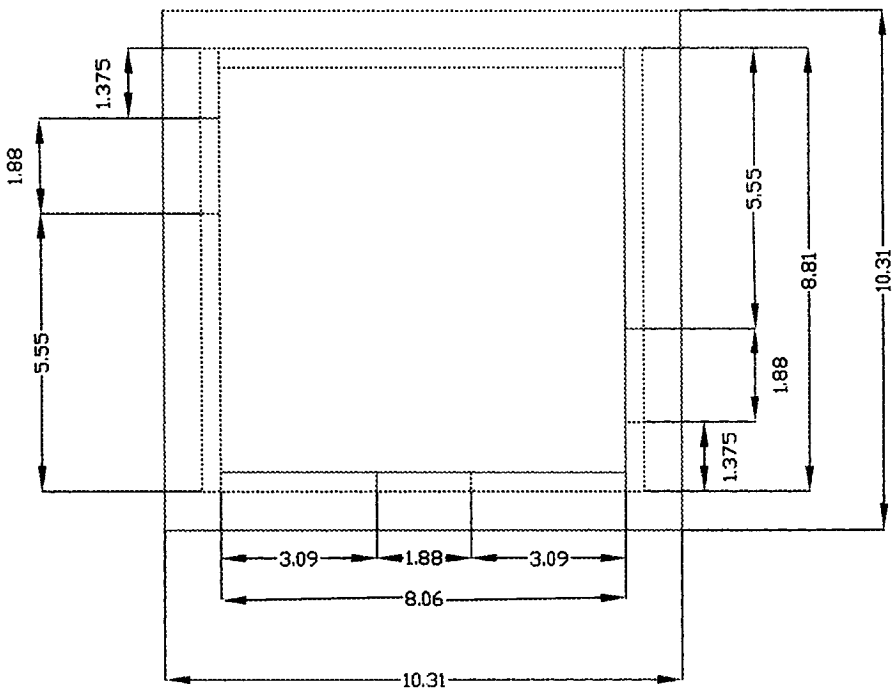


University of Ottawa
Université d'Ottawa

PROJECT :

Instantaneous
Profile Setup

PART :

Permeameter

MATERIAL :

Plexi-glass

QUANTITY :

1

NOTE :

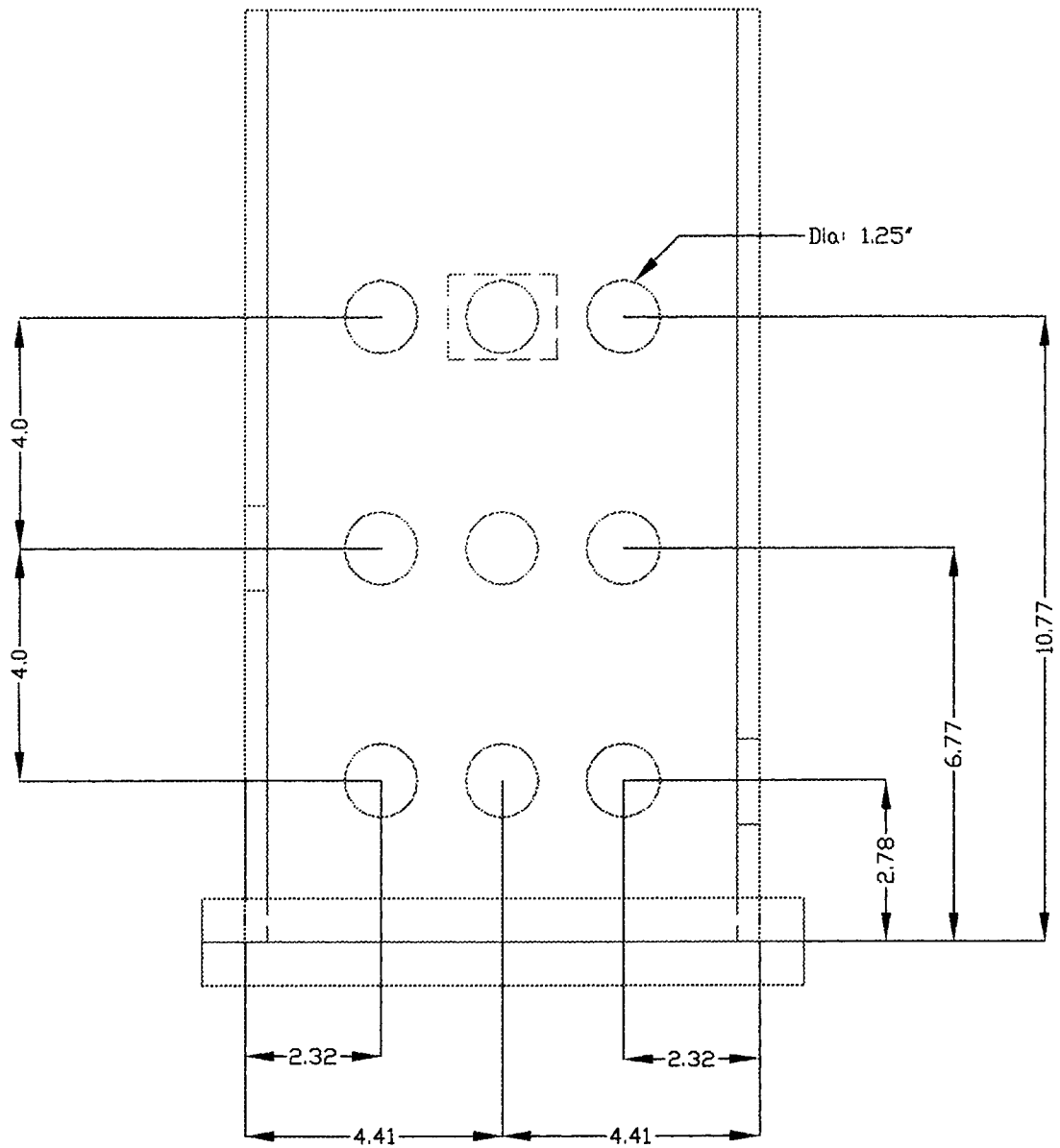


University of Ottawa
Université d'Ottawa

PROJECT :

Instantaneous Profile Setup

PART :

Holes for Samplers

MATERIAL :

Plexi-glass

QUANTITY :

9 (holes)

NOTE :

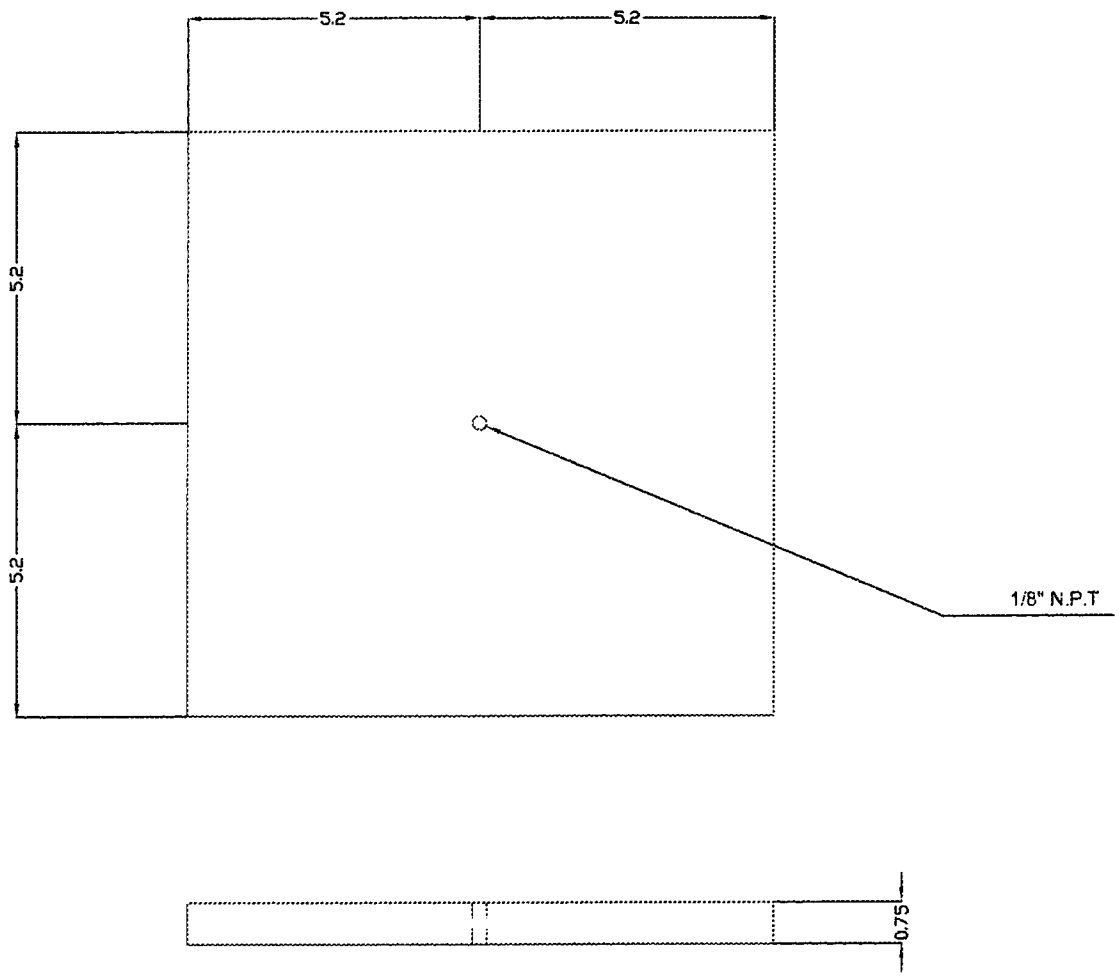


University of Ottawa
Université d'Ottawa

PROJECT :

Instantaneous
Profile Setup

PART :

Base plate

MATERIAL :

Plexi-glass

QUANTITY :

1

NOTE :

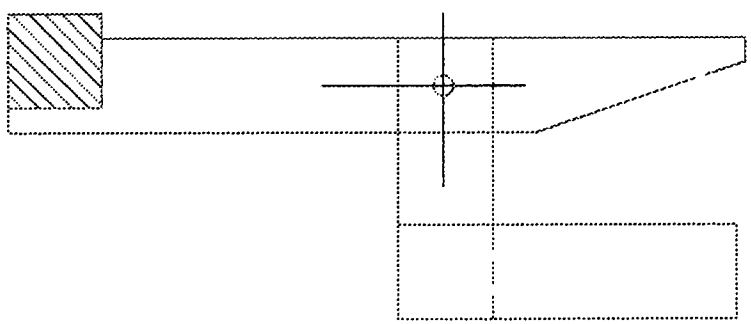

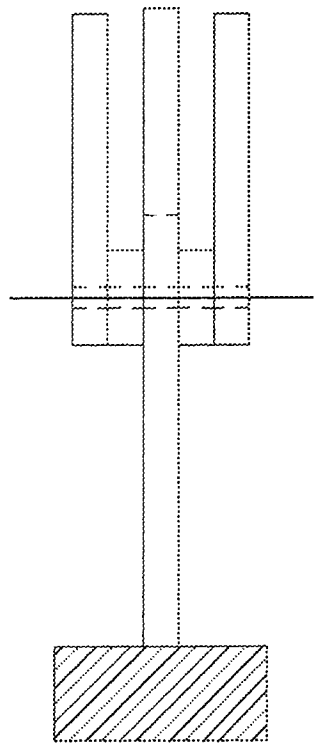

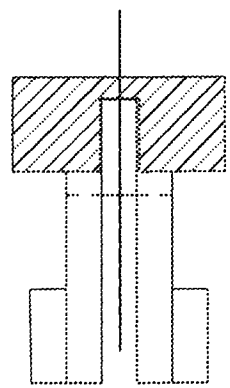

University of Ottawa
Université d'Ottawa

PROJECT :

Instantaneous
Profile Setup

PART :
Top Counterweight
Bracket

MATERIAL :

Plexi-glass

QUANTITY :

3

NOTE :

Assembly Drawing

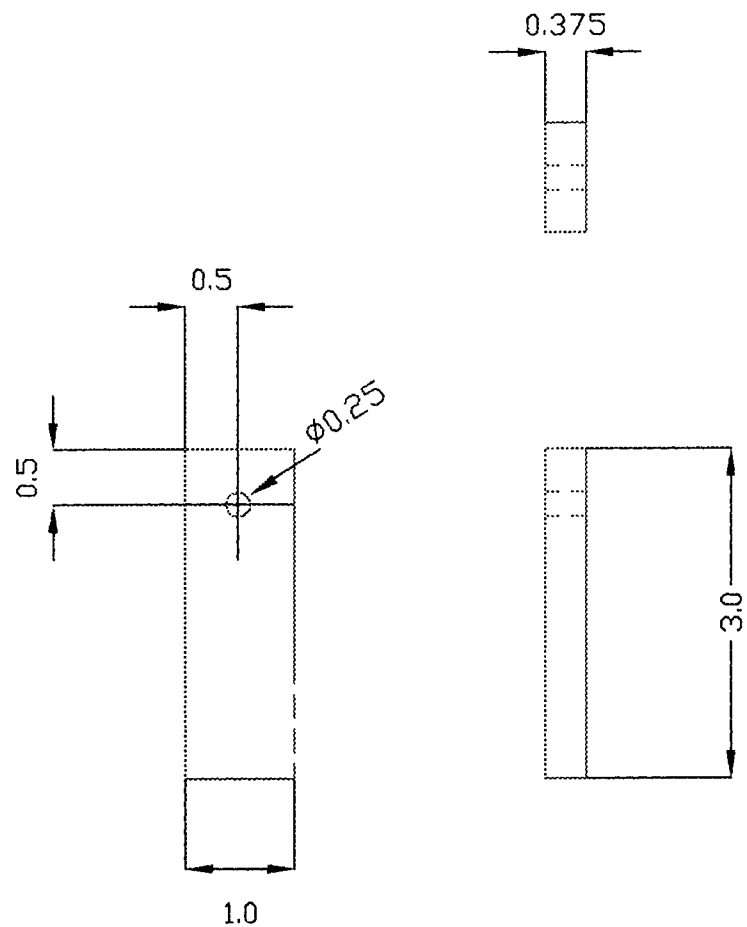


University of Ottawa
Université d'Ottawa

PROJECT :

Instantaneous
Profile Setup

PART :

T-CTW-A

MATERIAL :

Plexi-glass

QUANTITY :

6

NOTE :

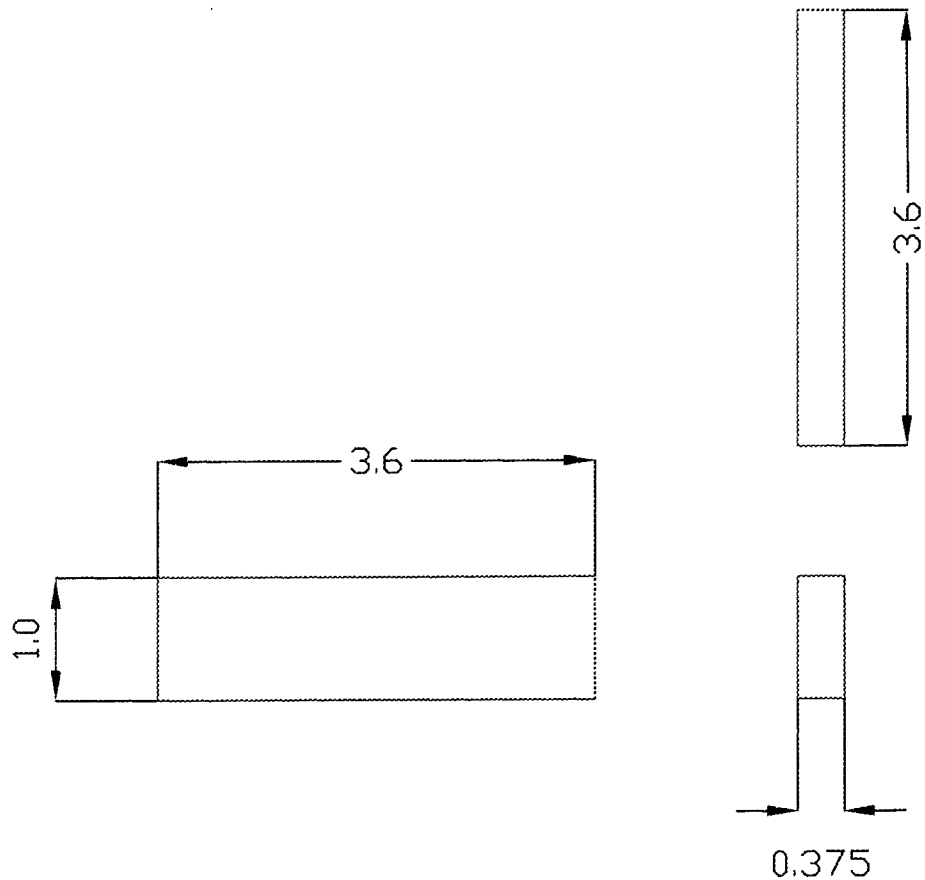


University of Ottawa
Université d'Ottawa

PROJECT :

Instantaneous
Profile Setup

PART :

T-CTW-B

MATERIAL :

Plexi-glass

QUANTITY :

6

NOTE :

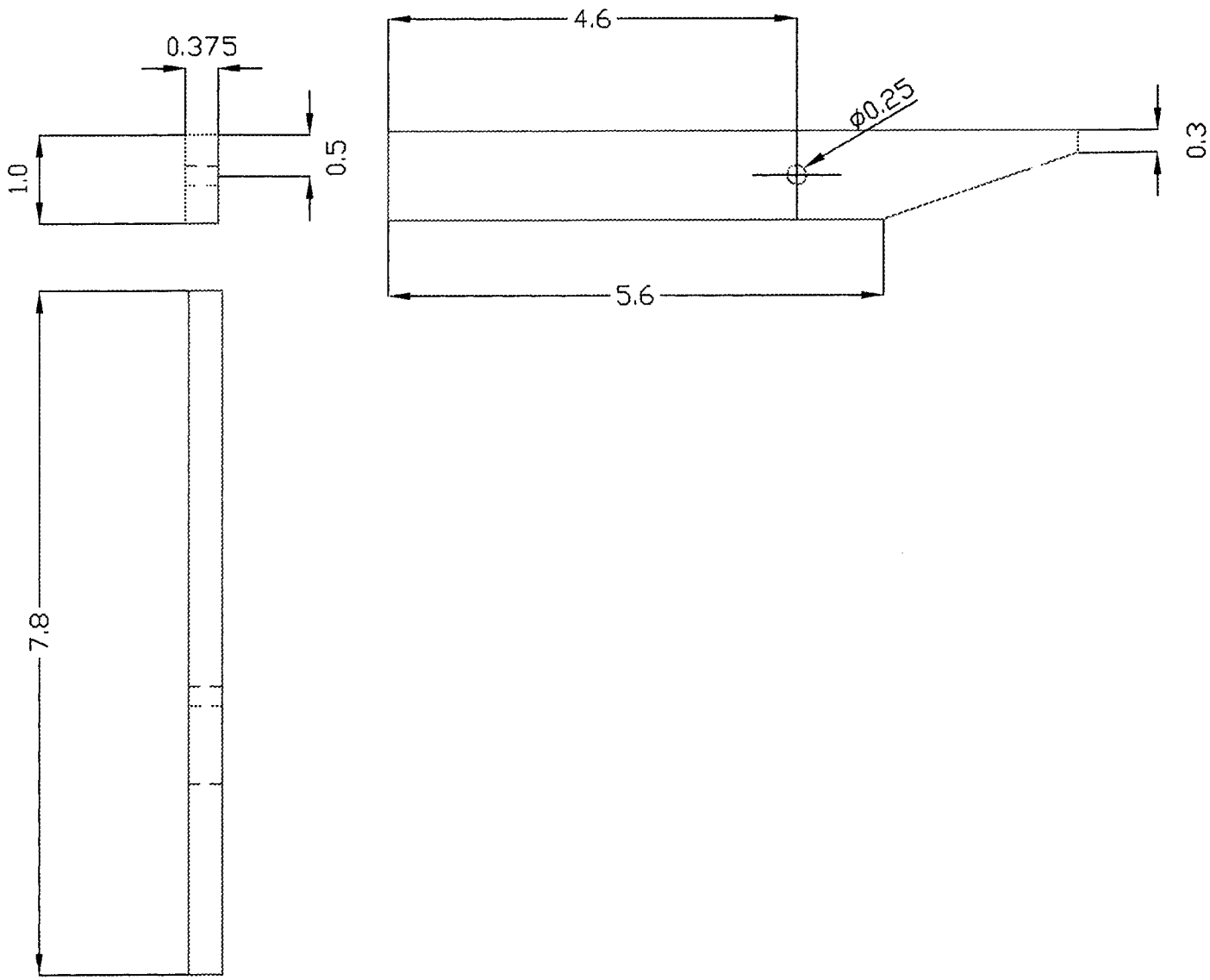


University of Ottawa
Université d'Ottawa

PROJECT :

Instantaneous
Profile Setup

PART :

T-CTW-C

MATERIAL :

Plexi-glass

QUANTITY :

3

NOTE :

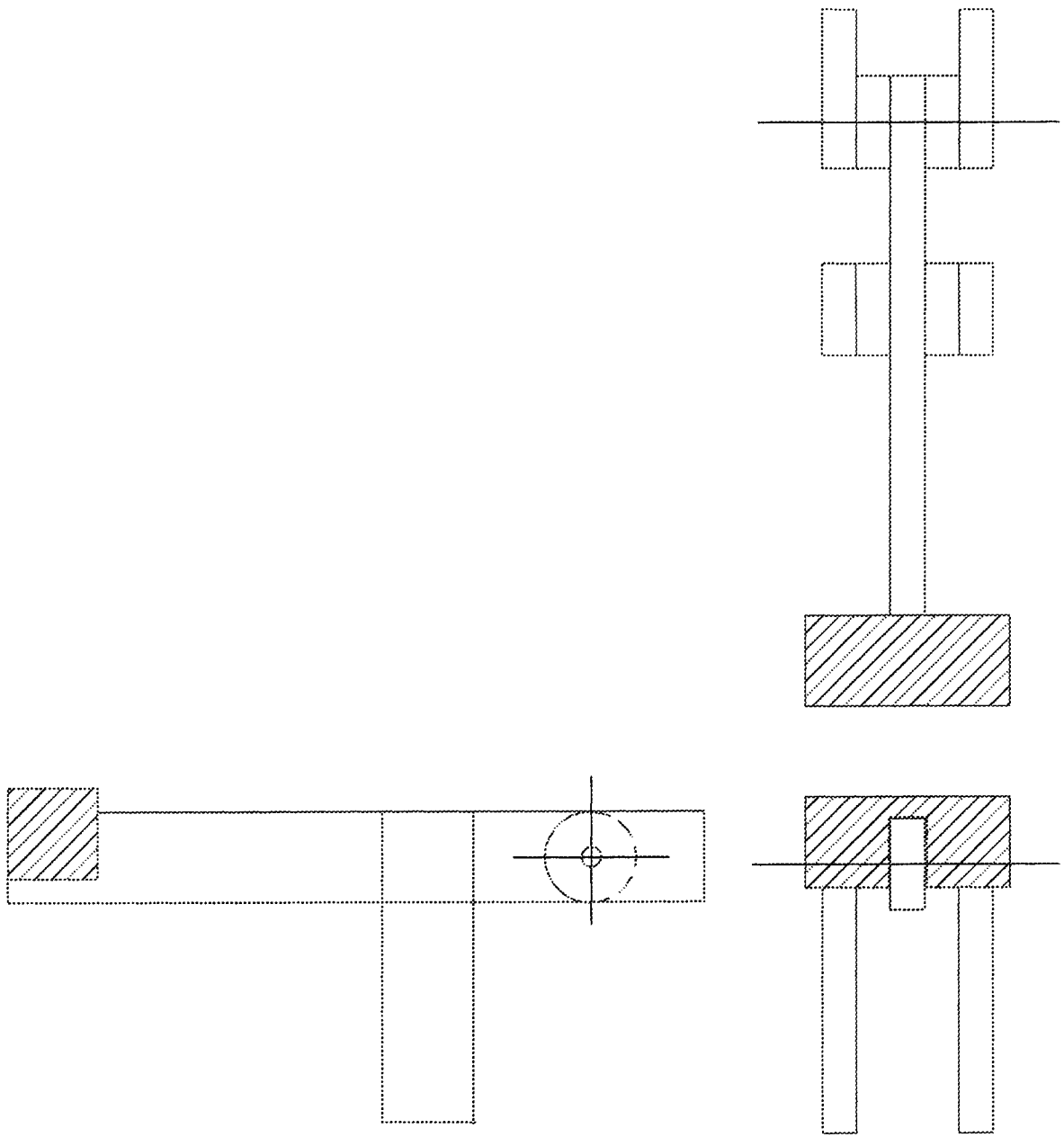

University of Ottawa
Université d'Ottawa

PROJECT :

Instantaneous
Profile Setup

PART :
Bottom Counterweight
Bracket

MATERIAL :

Plexi-glass

QUANTITY :

3

NOTE :

Assembly Drawing

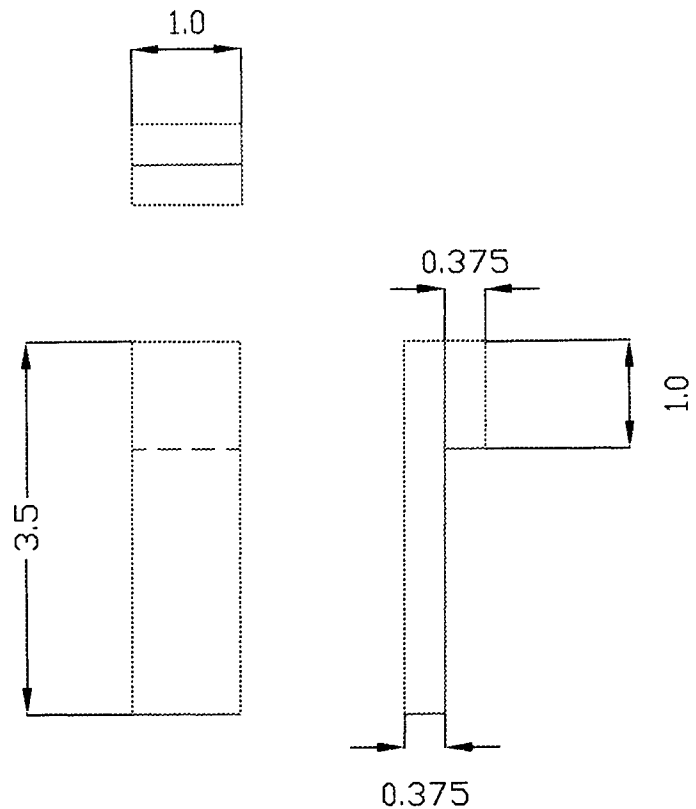


University of Ottawa
Université d'Ottawa

PROJECT :

Instantaneous
Profile Setup

PART :

B-CTW-A

MATERIAL :

Plexi-glass

QUANTITY :

6

NOTE :

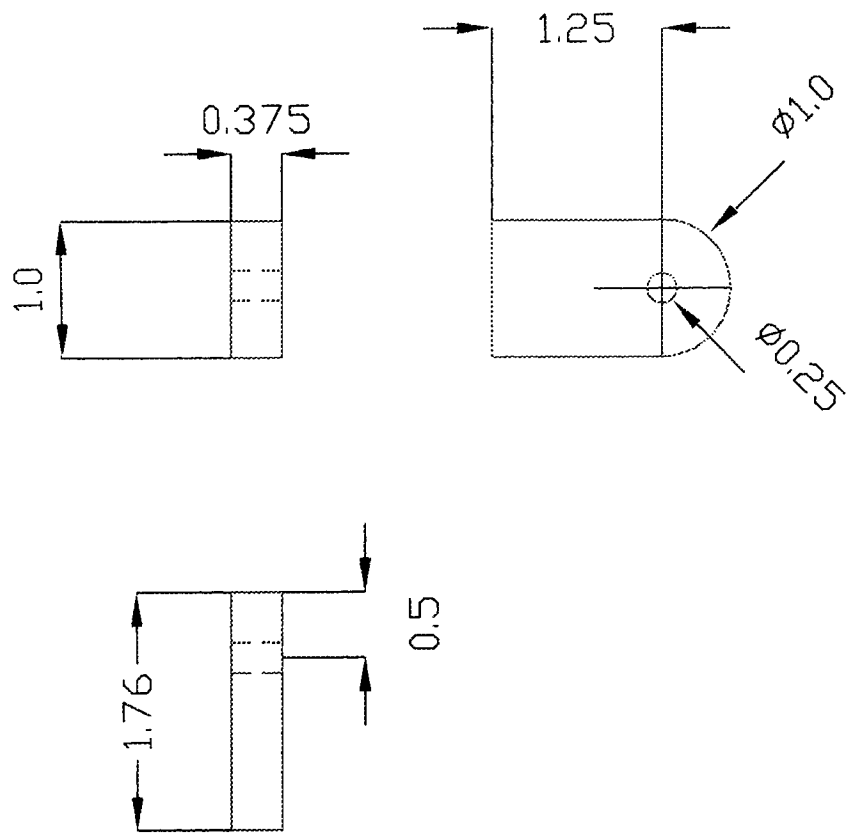


University of Ottawa
Université d'Ottawa

PROJECT :

Instantaneous
Profile Setup

PART :

B-CTW-B

MATERIAL :

Plexi-glass

QUANTITY :

6

NOTE :

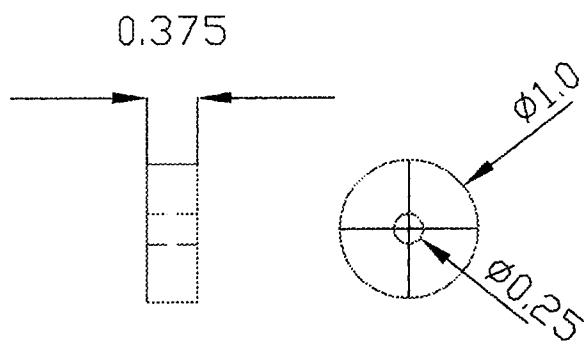


University of Ottawa
Université d'Ottawa

PROJECT :

Instantaneous
Profile Setup

PART :

B-CTW-C

MATERIAL :

Plexi-glass

QUANTITY :

6

NOTE :

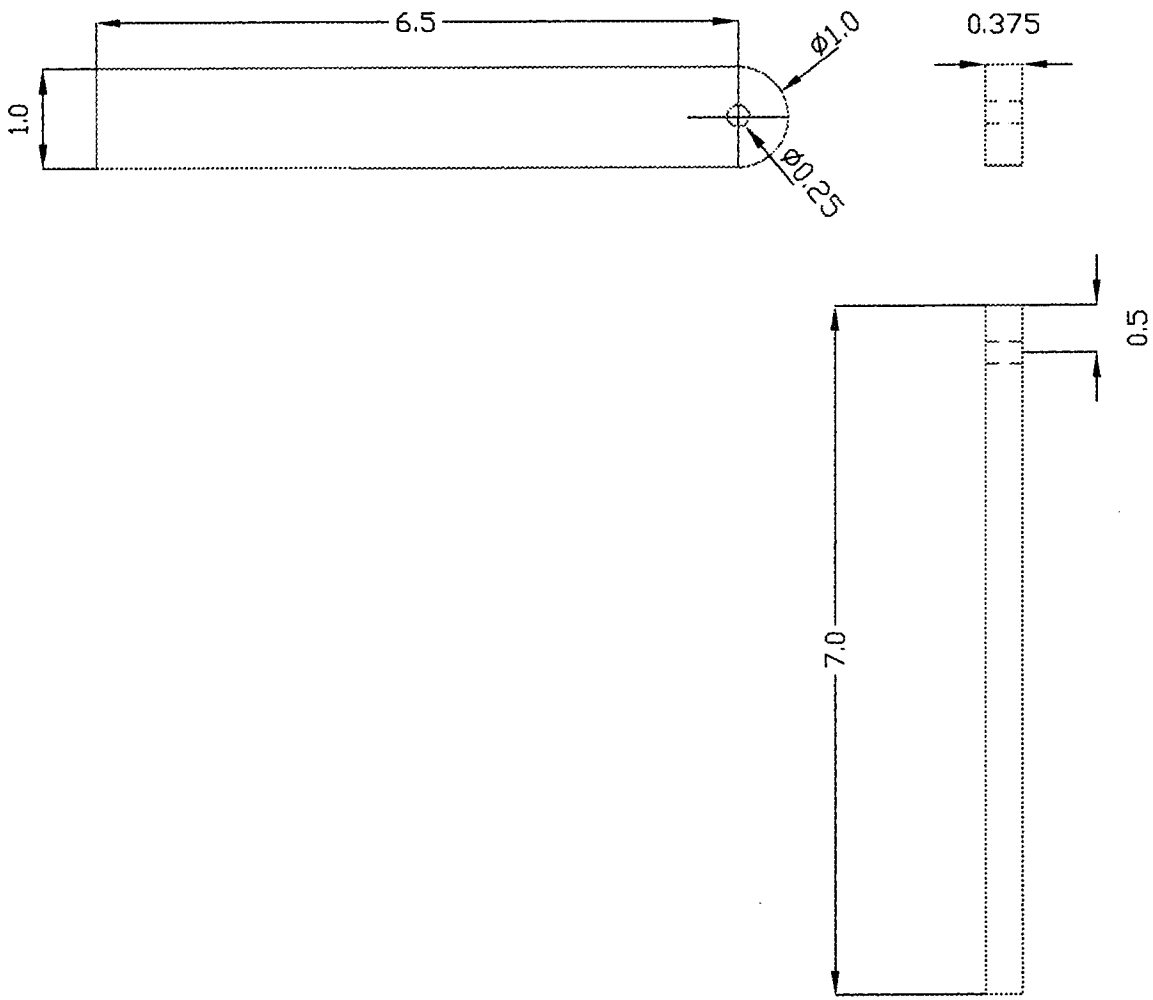


University of Ottawa
Université d'Ottawa

PROJECT :

Instantaneous
Profile Setup

PART :

B-CTW-D

MATERIAL :

Plexi-glass

QUANTITY :

3

NOTE :

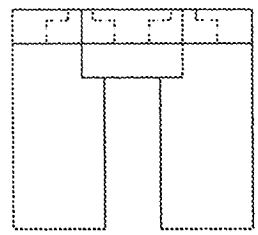

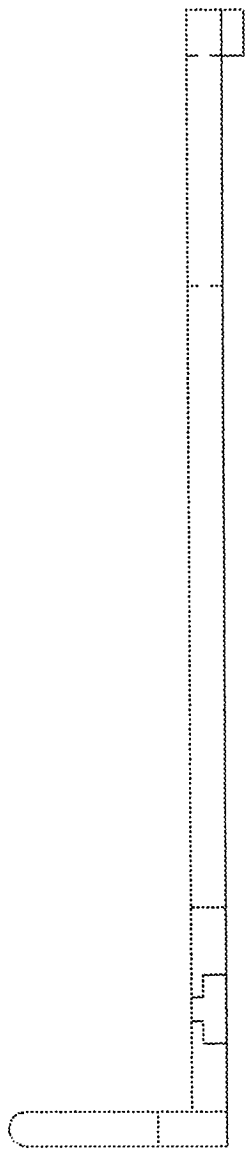

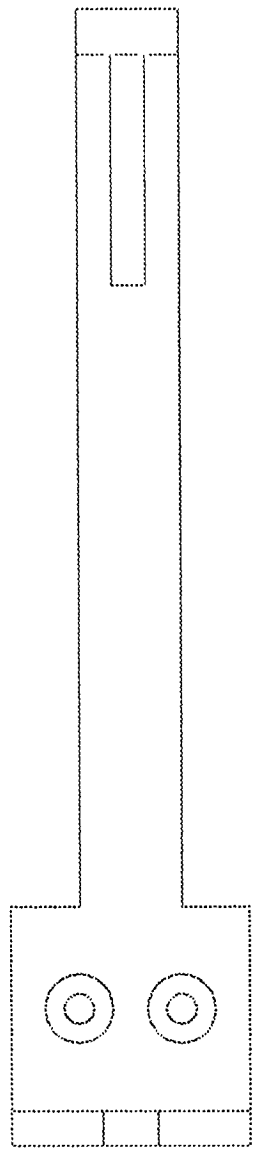

University of Ottawa
Université d'Ottawa

PROJECT :

Instantaneous
Profile Setup

PART :

Sliders

MATERIAL :

Plexi-glass

QUANTITY :

NOTE :

Assembly Drawing

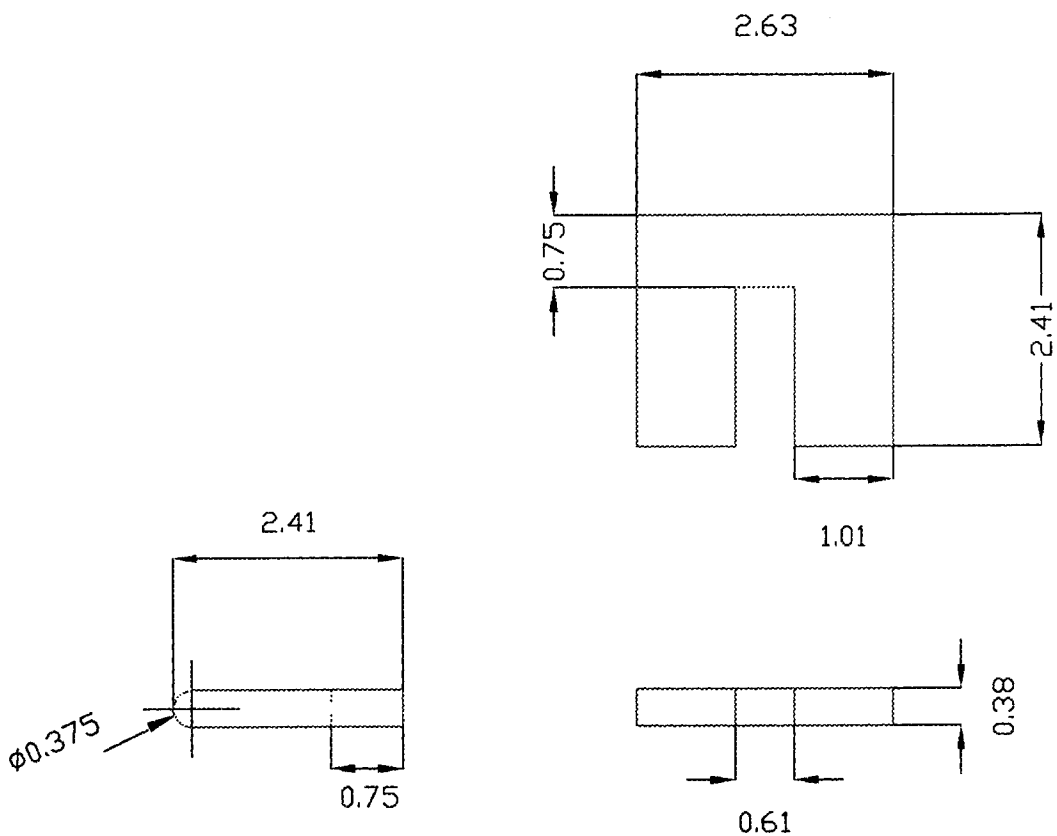


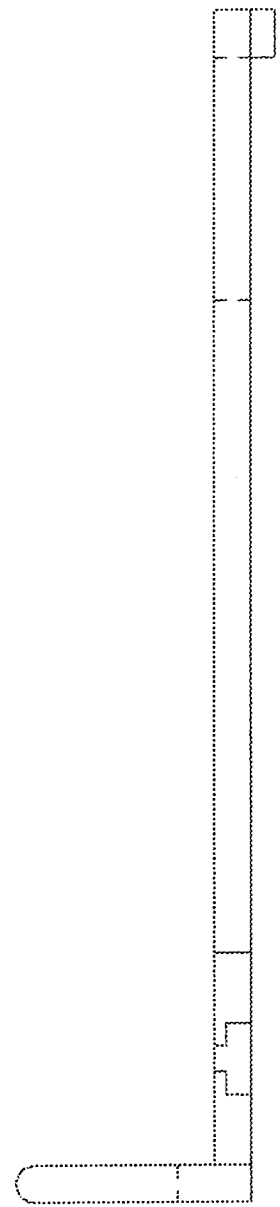

University of Ottawa
Université d'Ottawa

PROJECT :

Instantaneous
Profile Setup

PART :

Seat

MATERIAL :

Plexi-glass

QUANTITY :

3

NOTE :

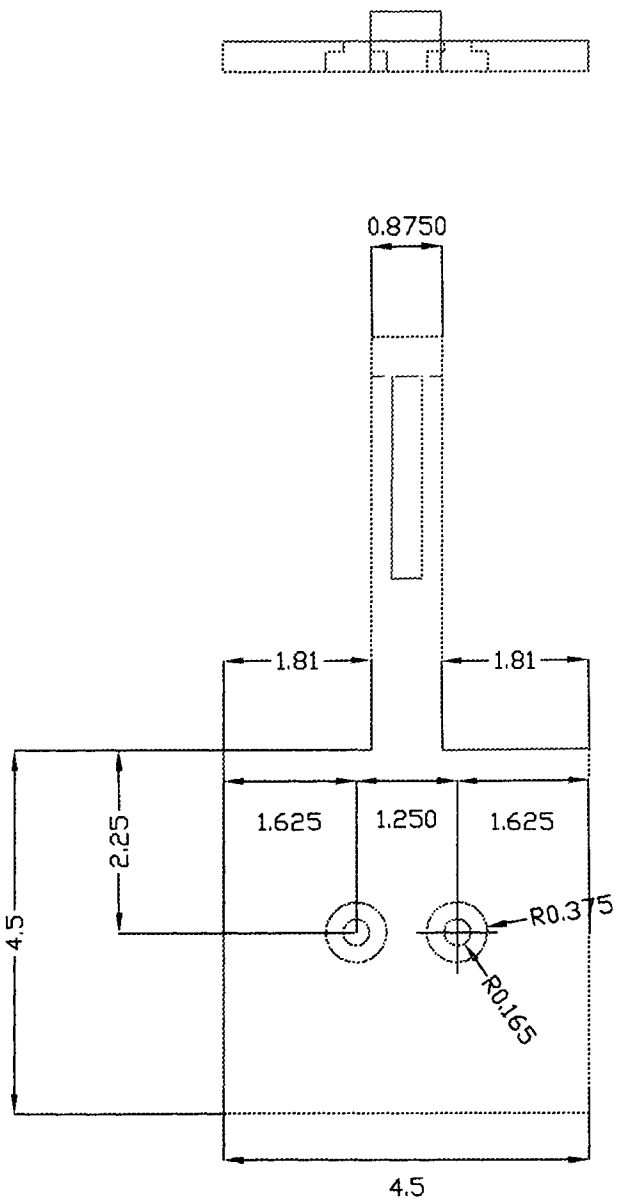


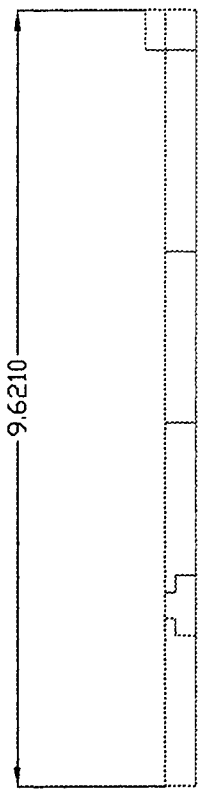


University of Ottawa
Université d'Ottawa

PROJECT :

Instantaneous Profile Setup

PART :

Slider 1

MATERIAL :

Plexi-glass

QUANTITY :

1

NOTE :

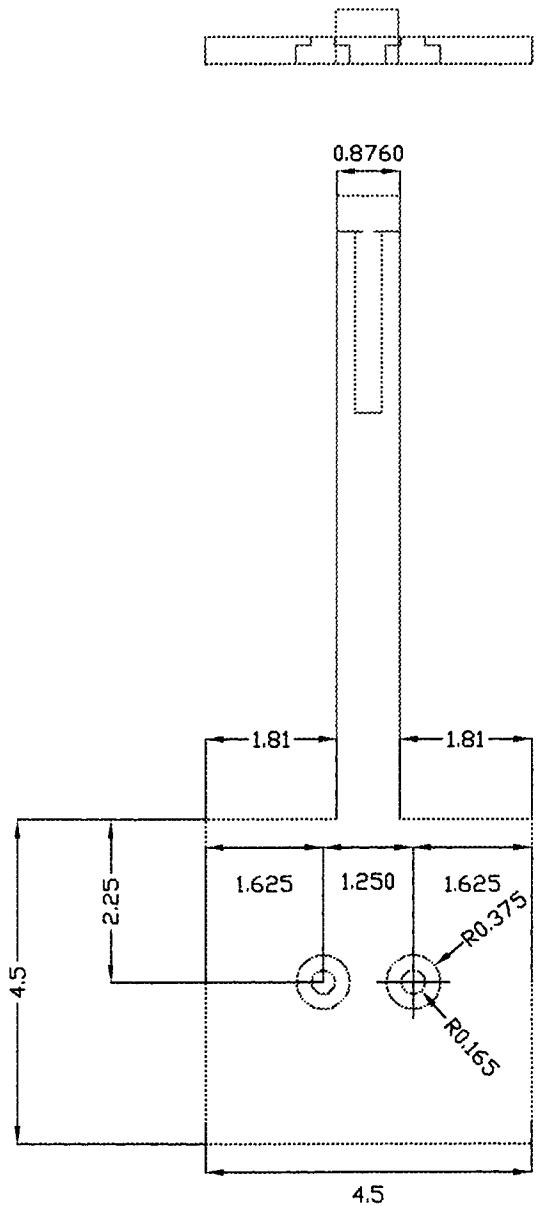


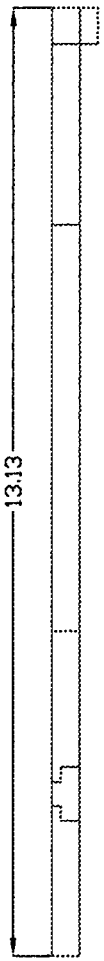


University of Ottawa
Université d'Ottawa

PROJECT :

Instantaneous
Profile Setup

PART :

Slider 2

MATERIAL :

Plexi-glass

QUANTITY :

1

NOTE :

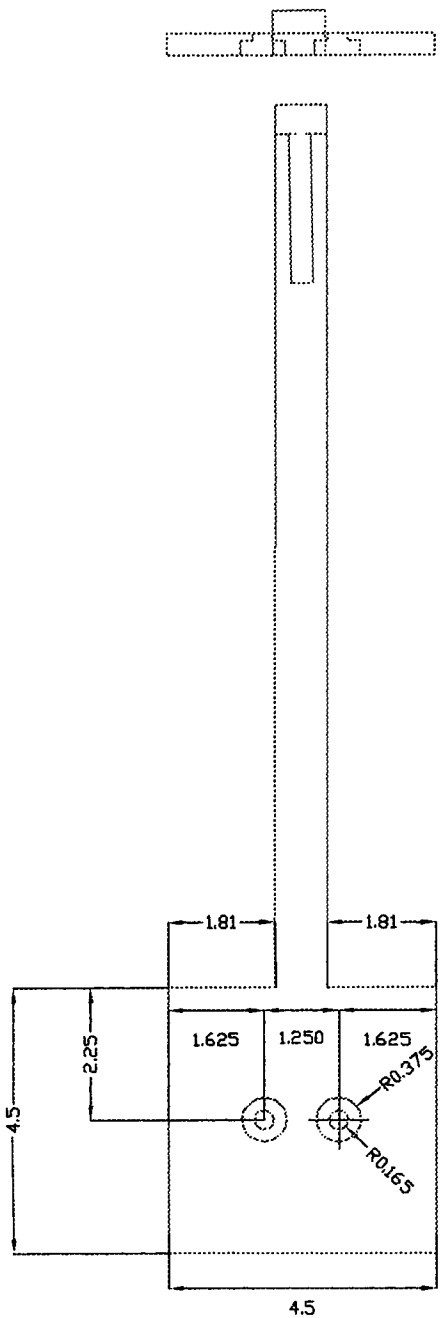


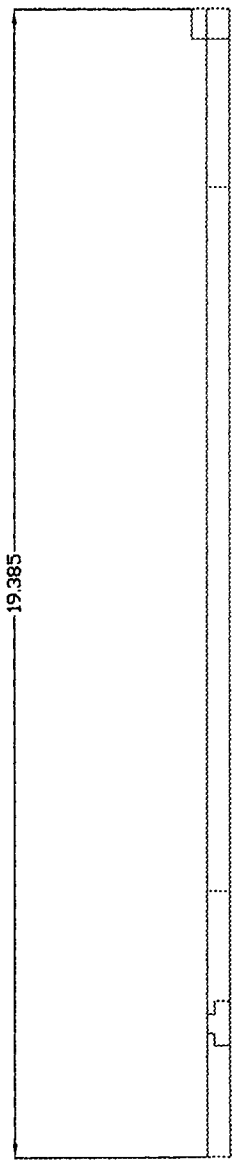


University of Ottawa
Université d'Ottawa

PROJECT :

Instantaneous
Profile Setup

PART :

Slider 3

MATERIAL :

Plexi-glass

QUANTITY :

1

NOTE :

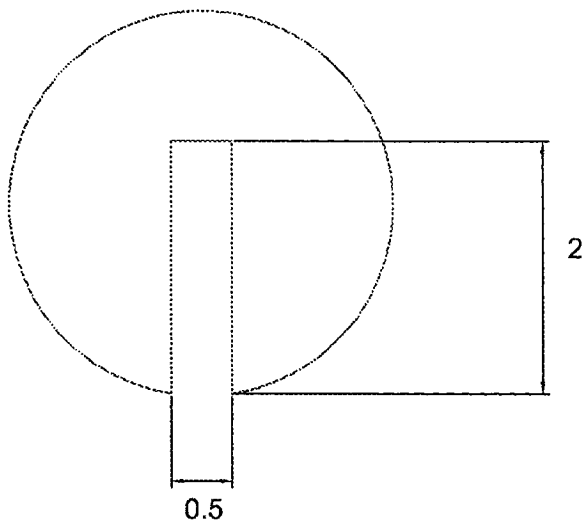


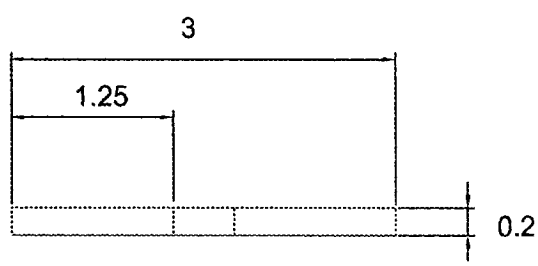


University of Ottawa
Université d'Ottawa

PROJECT :

Instantaneous Profile Setup

PART :

0.20" Counterweight

MATERIAL :

Brass

QUANTITY :

1

NOTE :

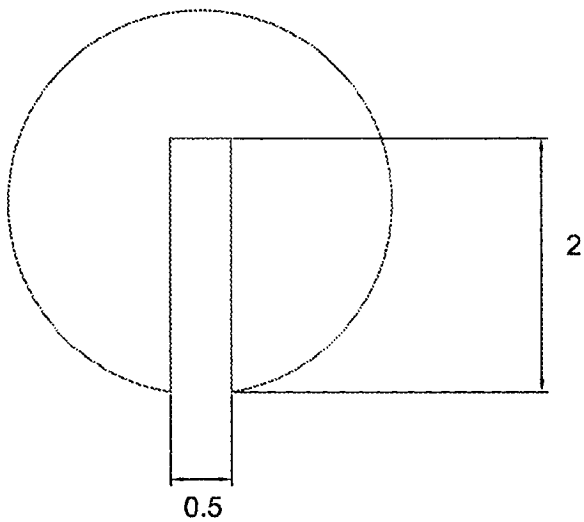


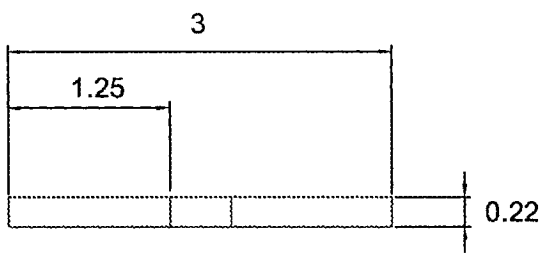


University of Ottawa
Université d'Ottawa

PROJECT :

Instantaneous
Profile Setup

PART :

0.22" Counterweight

MATERIAL :

Brass

QUANTITY :

1

NOTE :

University of Ottawa
Université d'Ottawa

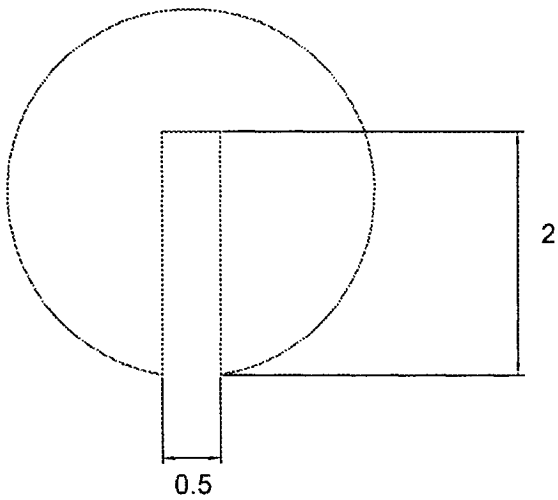


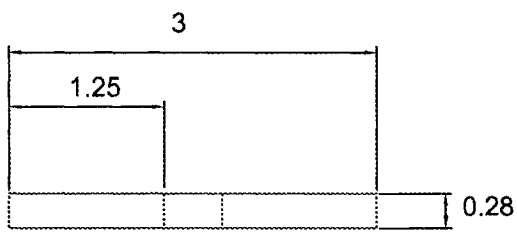


PROJECT :

Instantaneous Profile Setup

PART :

0.28" Counterweight

MATERIAL :

Brass

QUANTITY :

1

NOTE :

University of Ottawa
Université d'Ottawa

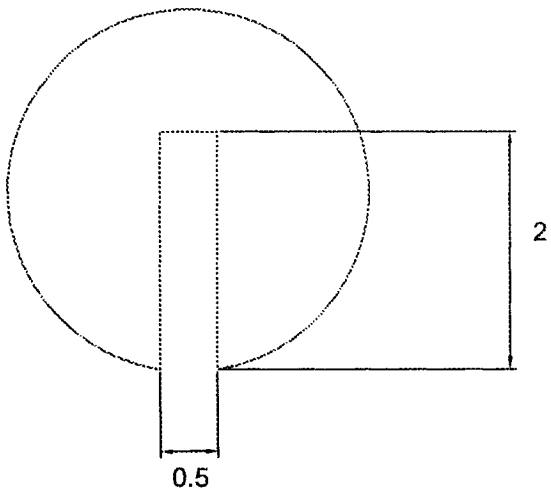


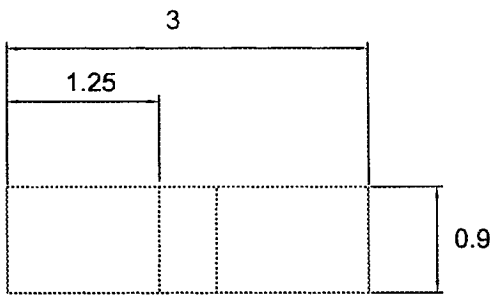


PROJECT :

Instantaneous
Profile Setup

PART :

0.90" Counterweight

MATERIAL :

Brass

QUANTITY :

1

NOTE :

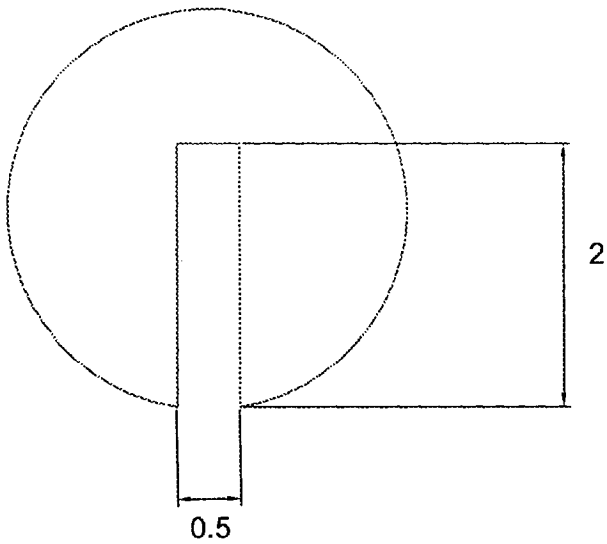


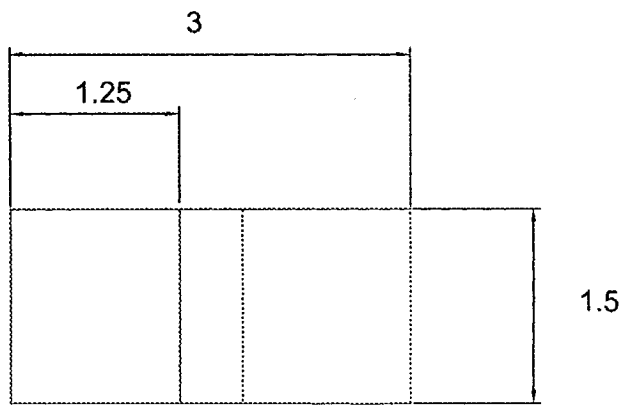


University of Ottawa
Université d'Ottawa

PROJECT :

Instantaneous
Profile Setup

PART :

1.50" Counterweight

MATERIAL :

Brass

QUANTITY :

1

NOTE :

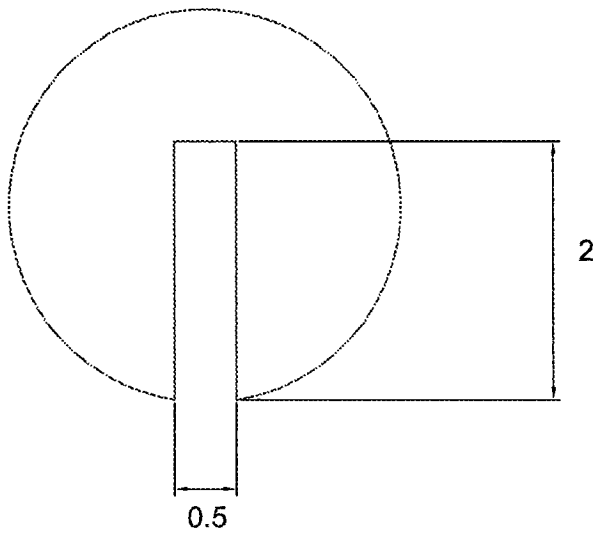


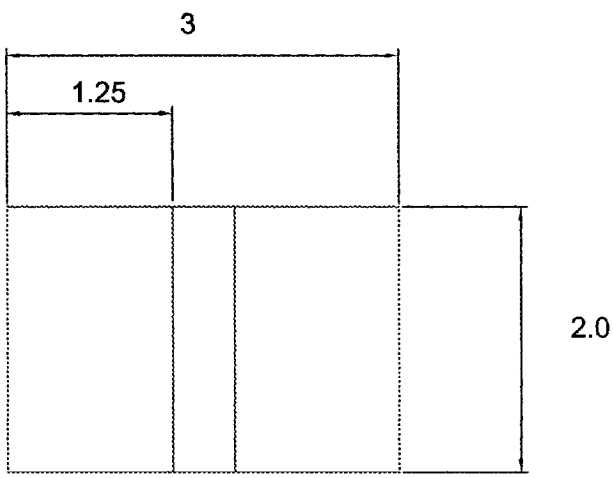


University of Ottawa
Université d'Ottawa

PROJECT :

Instantaneous
Profile Setup

PART :

2.00" Counterweight

MATERIAL :

Brass

QUANTITY :

1

NOTE :

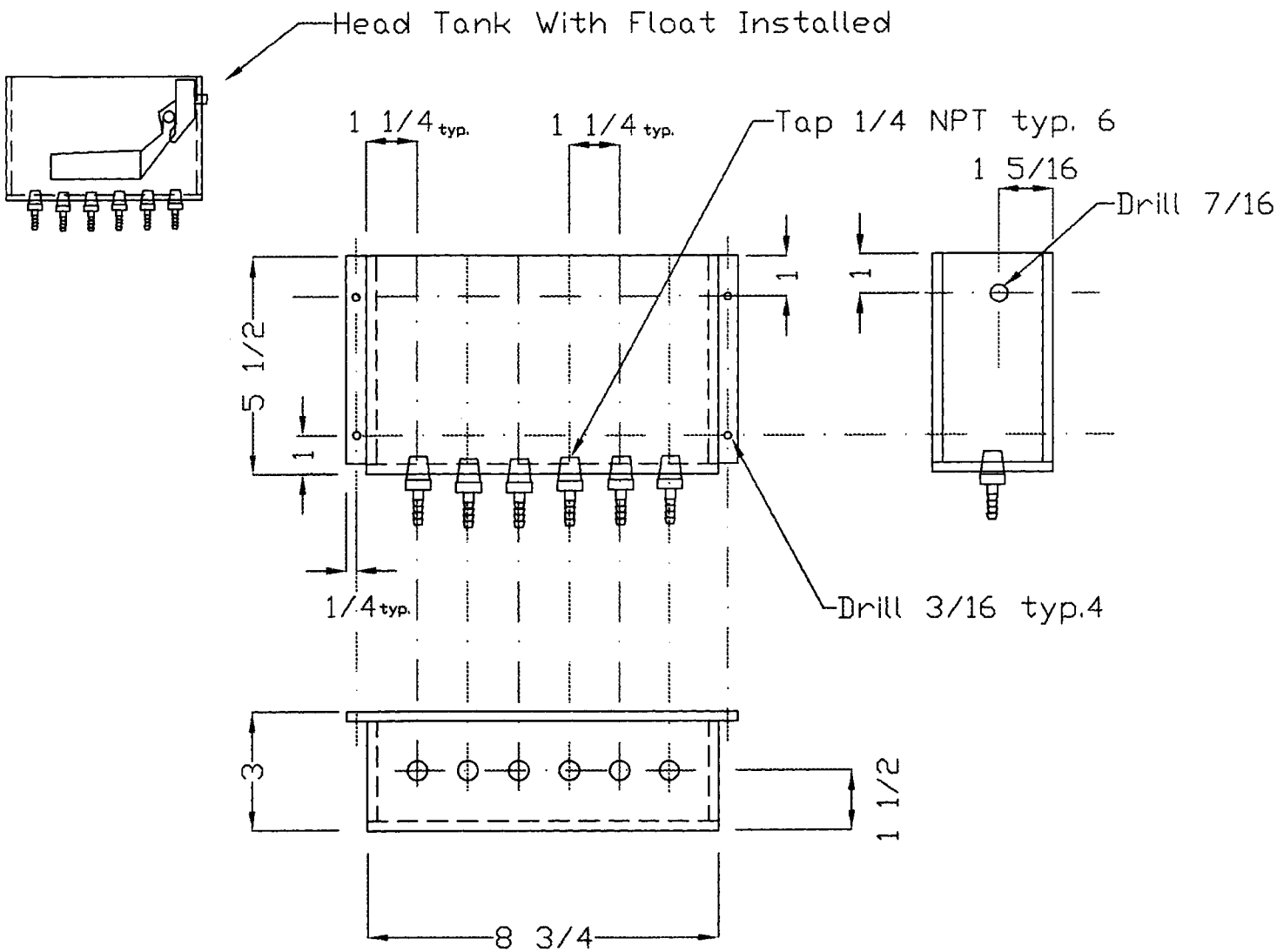


University of Ottawa
Université d'Ottawa

PROJECT :
Permeameter

PART :
Reservoir

MATERIAL :
Plexi-glass

QUANTITY :
1

NOTE :

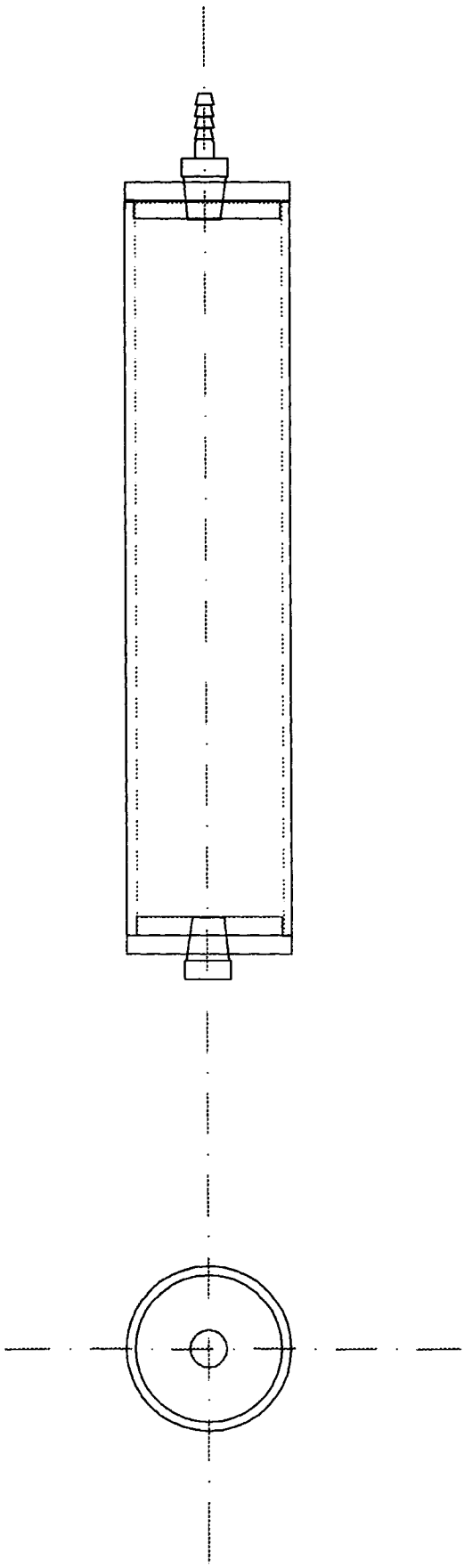

University of Ottawa
Université d'Ottawa

PROJECT :

Permeameter

PART :

Discharge Tube

MATERIAL :

Plexi-glass

QUANTITY :

6

NOTE :

Assembly Drawing

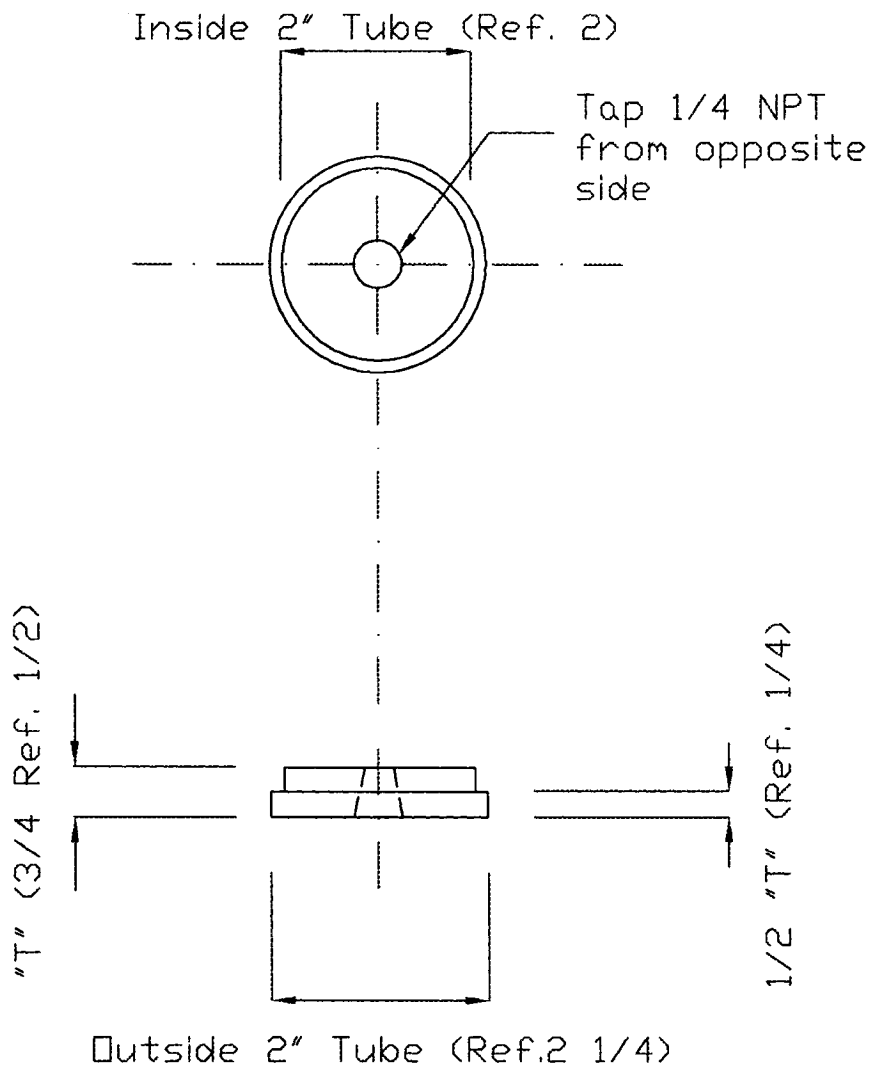


University of Ottawa
Université d'Ottawa

PROJECT :
Permeameter

PART :
Discharge Tube Cap

MATERIAL :
Plexi-glass

QUANTITY :
12

NOTE :

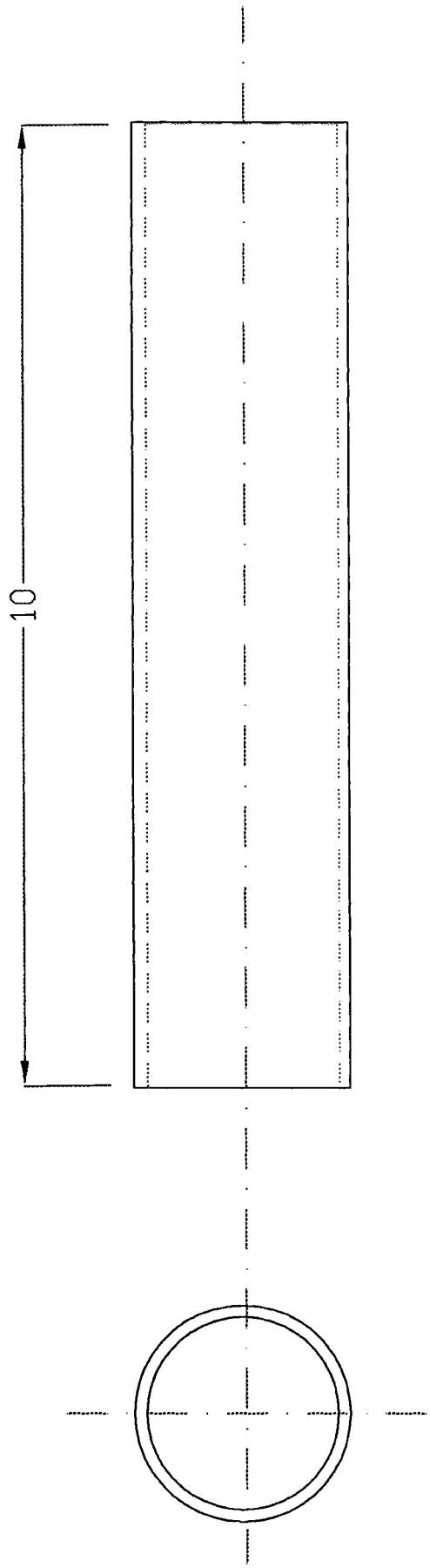


University of Ottawa
Université d'Ottawa

PROJECT :

Permeameter

PART :

Discharge Tube

MATERIAL :

Plexi-glass

QUANTITY :

6

NOTE :

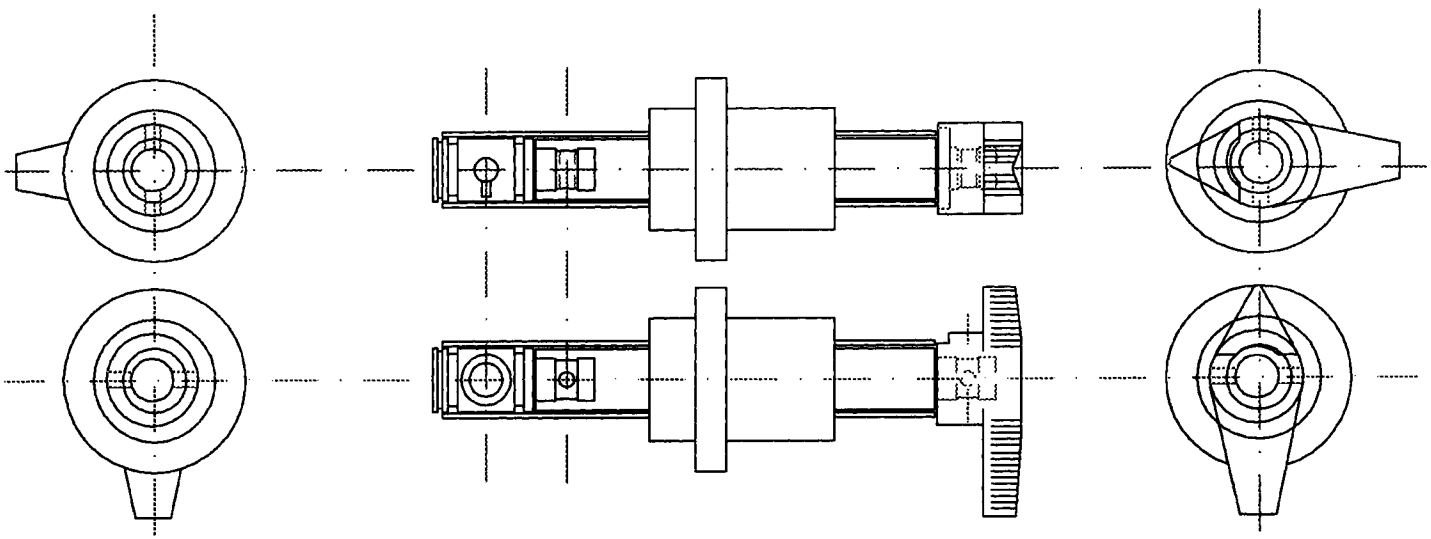

University of Ottawa
Université d'Ottawa

PROJECT :
Instantaneous Profile Setup

PART :
Sampler

MATERIAL :
Various

QUANTITY :
9

NOTE :
Assembly Drawing

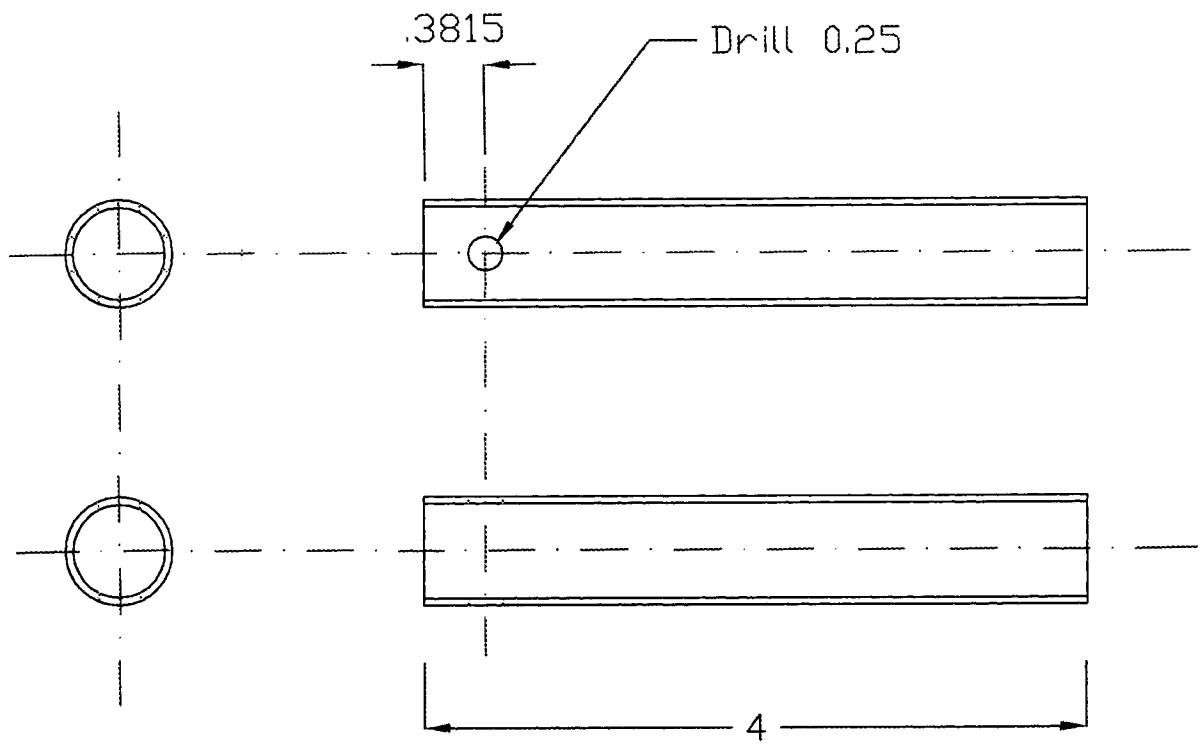


University of Ottawa
Université d'Ottawa

PROJECT :
Instantaneous Profile Setup

PART :
Sampler Outer Tube

MATERIAL :
Copper

QUANTITY :
9

NOTE :

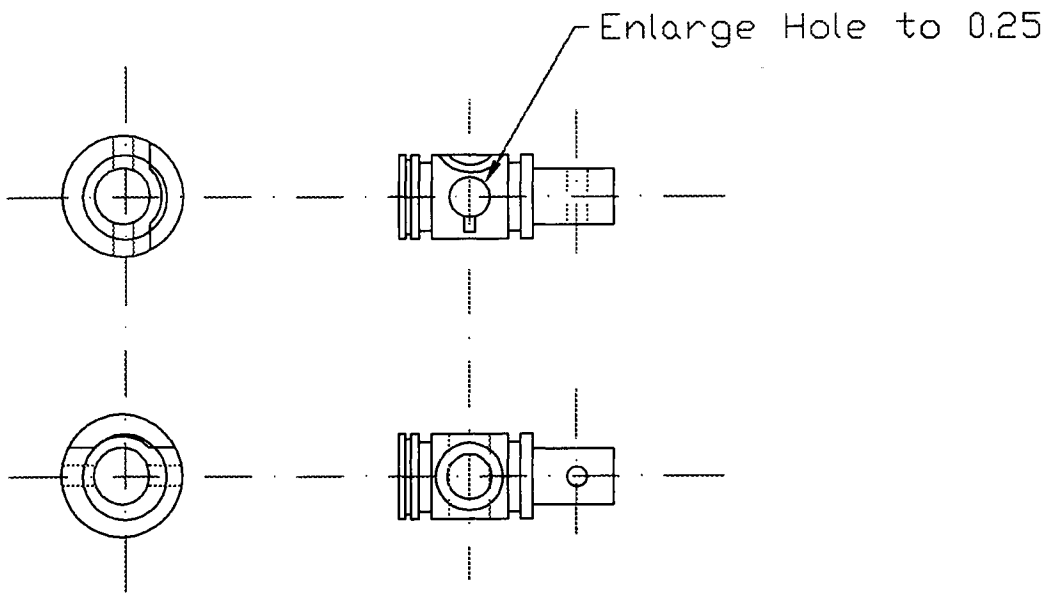


University of Ottawa
Université d'Ottawa

PROJECT :

Instantaneous
Profile Setup

PART :

Sampler Plug

MATERIAL :

Brass

QUANTITY :

9

NOTE :

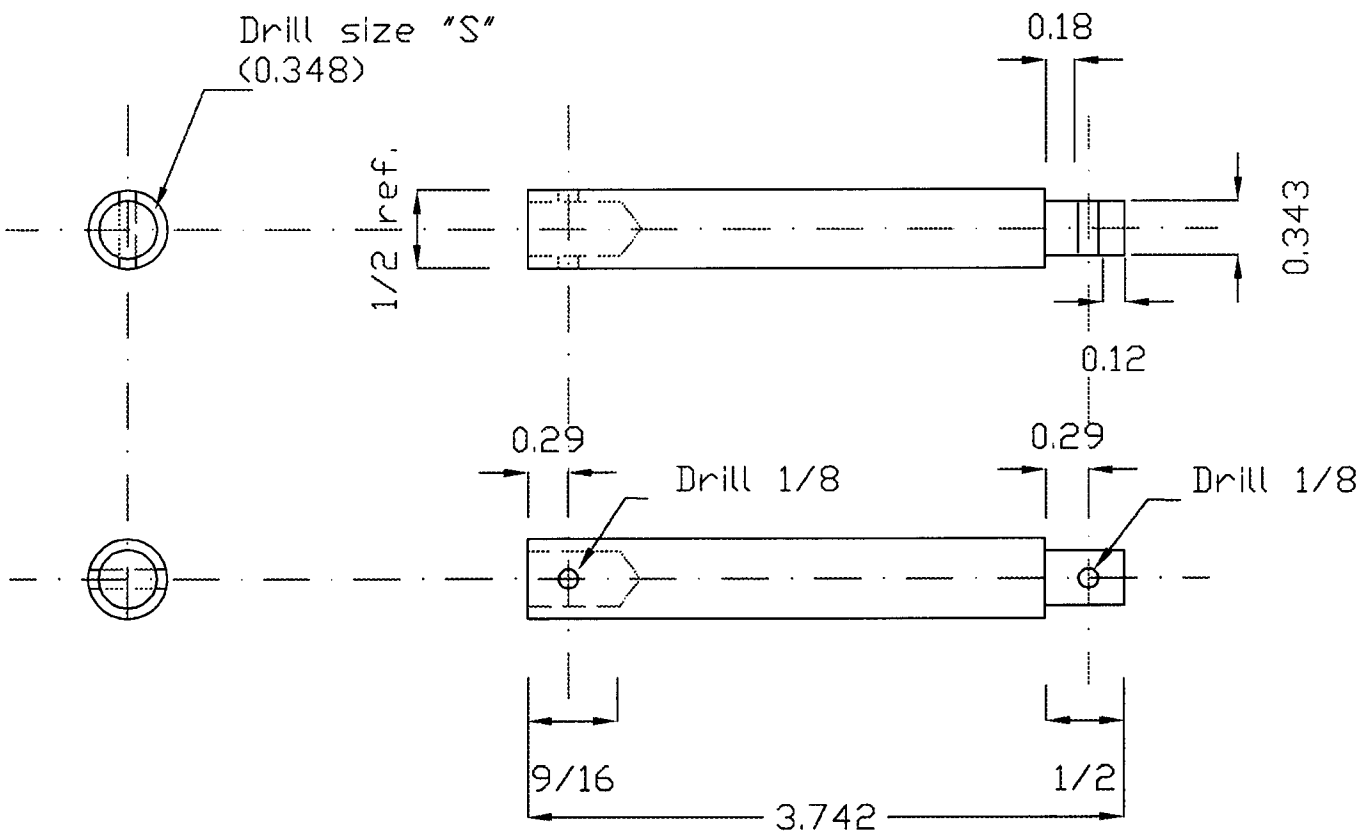


University of Ottawa
Université d'Ottawa

PROJECT :
Instantaneous Profile Setup

PART :
Sampler Extension

MATERIAL :
Aluminum

QUANTITY :
9

NOTE :

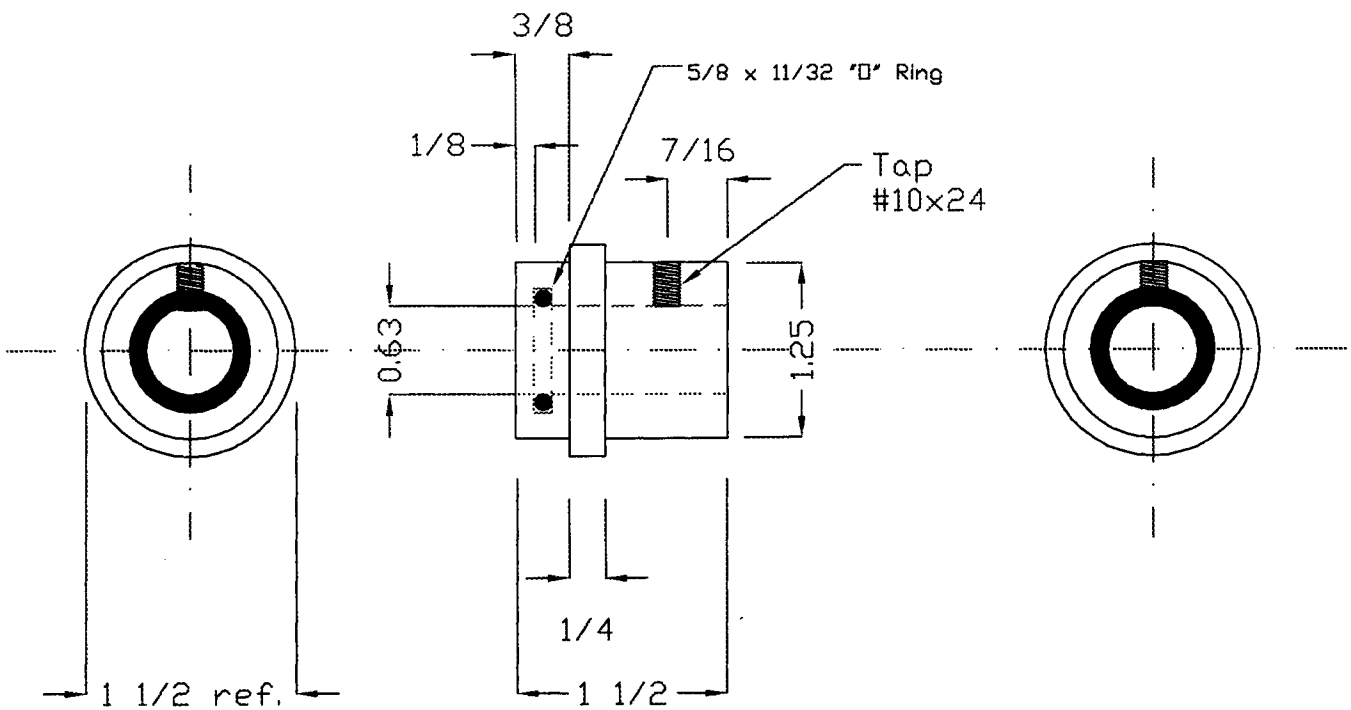


University of Ottawa
Université d'Ottawa

PROJECT :

Instantaneous
Profile Setup

PART :

Sampler Bushing

MATERIAL :

Plexi-glass

QUANTITY :

9

NOTE :

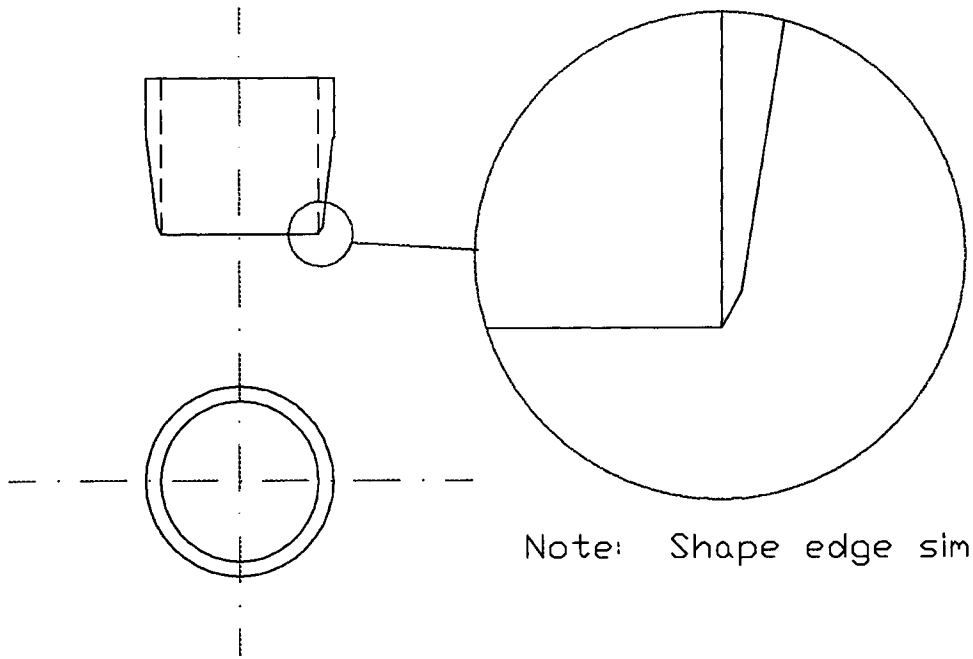

Note: Shape edge simillar to sketch

University of Ottawa
Université d'Ottawa

PROJECT :
Permeameter

PART :
Cutting Shoe

MATERIAL :
ABS

QUANTITY :
2

NOTE :

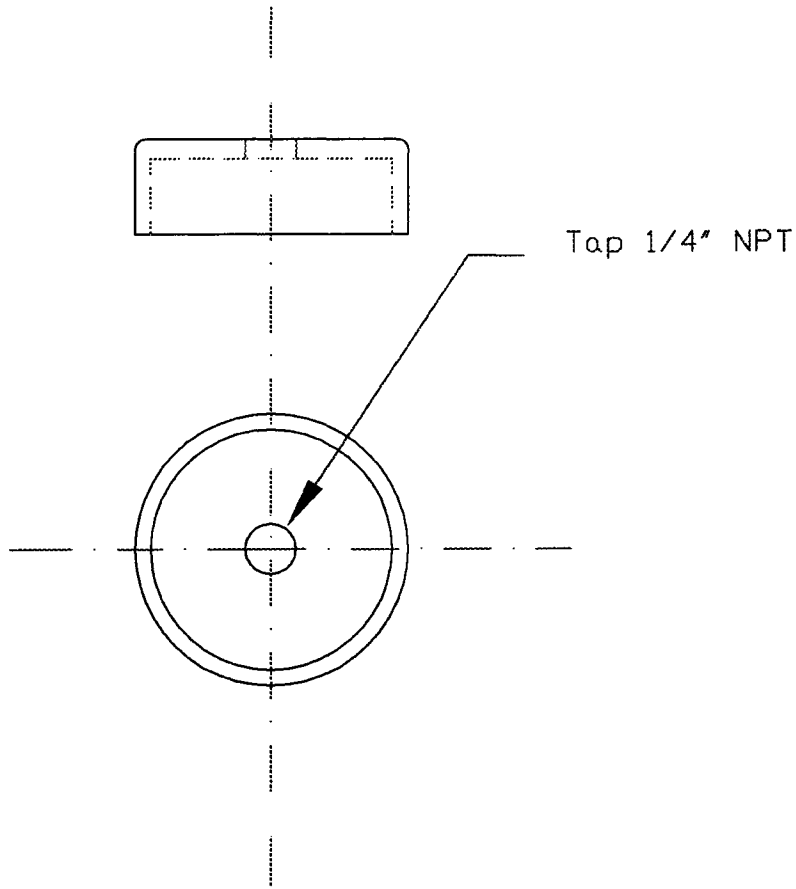


University of Ottawa
Université d'Ottawa

PROJECT :
Permeameter

PART :
Cap

MATERIAL :
ABS

QUANTITY :
16

NOTE :

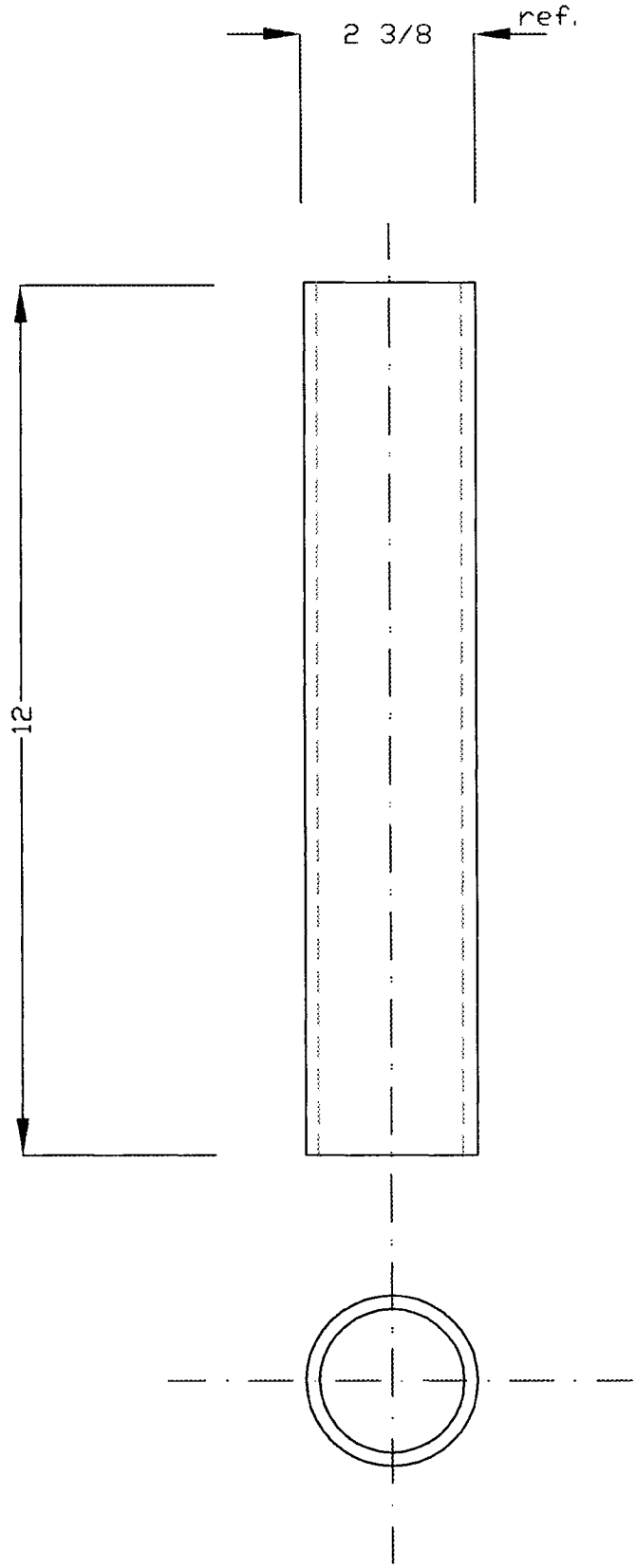


University of Ottawa
Université d'Ottawa

PROJECT :
Permeameter

PART :
Body

MATERIAL :
ABS

QUANTITY :
8

NOTE :